AN ABSTRACT OF THE THESIS OF

Nicolas Matus Casanova for the degree of Master of Science in Civil Engineering presented on September 7, 2018

Title: Performance of High-Strength Steel Reinforcement in Shear Friction Applications.

Abstract approved:

_____

David Trejo Andre R. Barbosa

The use of high strength steel reinforcement has the potential to provide economic and constructability benefits when used in reinforced concrete structures. However, more research is needed to justify and confidently allow its use. Current design provisions limit the nominal yield strength of reinforcing steel bars to 60 ksi (420 MPa) for many bridge design applications. This thesis presents results from a laboratory testing program designed to evaluate the performance of concrete interface shear reinforced with ASTM A706 Grade 60 (420 MPa), ASTM A706 Grade 80 (550 MPa), ASTM A615 Grade 100 (690 MPa), and ASTM A1035 Grade 120 (830 MPa) reinforcing steel bars. Results are reported on the influence of reinforcing steel bar size, reinforcing steel bar spacing, shear interface surface preparation, and nominal concrete strength on shear friction performance. This thesis provides a summary of previous research regarding shear friction theory, a description of the test specimen design, and an overview of the materials used. Results indicate that using high strength steel reinforcing bars did not have a significant impact on the peak loads reached, however they did allow the development of greater post-peak sustained loads due to dowel action in the post-peak stage of the test response. Significant variation was observed when analyzing the effect of surface preparation. Additionally, in some cases, an exposed aggregate surface preparation enhanced the aggregate interlock and

allowed it to contribute to the post-peak shear capacity. Overall, the results presented indicate that an increase in allowable nominal yield strength to 80 ksi (550 MPa) maintains a conservative design per AASHTO and ACI 318-14 code provisions.

Performance of High-Strength Steel Reinforcement in Shear Friction Applications

by
Nicolas Matus Casanova

A THESIS

submitted to

Oregon State University

in partial fulfillment of
the requirements for the
degree of

Master of Science

Presented September 7, 2018
Commencement June 2019

Master of Science thesis of Nicolas Matus Casanova presented on September 7, 2018

APPROVED:

Co-Major Professor, representing Civil Engineering

Co-Major Professor, representing Civil Engineering

Head of the School of Civil and Construction Engineering

Dean of the Graduate School

I understand that my thesis will become part of the permanent collection of Oregon State University libraries. My signature below authorizes release of my thesis to any reader upon request.

Nicolas Matus Casanova, Author

ACKNOWLEDGEMENTS

First and foremost, I would like to thank my advisors Dr. Andre Barbosa and Dr. David Trejo for taking a chance on me and providing me the opportunity to join their research group as a graduate research assistant. I would also like to thank Dr. Arijit Sinha and Dr. John Parmigiani for taking the time to serve on my thesis committee. Their valuable input is greatly appreciated.

Thank you to the Oregon Department of Transportation for providing the funding for this project.

I would like to thank James Batti and Jeff Gent for their assistance in constructing and testing the specimens. Special thanks to Dr. Christopher Higgins for providing valuable assistance throughout my time spent at the Structures Lab. Students who assisted on the project include: Pavan Vaddey, Gokul Vasudevan, Sharoo Shrestha, Luke Thompson, Hunter Anderson, Lance Parson, Spencer Maunu, Ignace Mugabo, Brian DeMeza, Aiyad Alshimaysawee, Zeping Liu, Nicholas Hannan, Kirsten Fox, Luis Chaparro, and Keenan Blanchfill. The assistance of Dana Ainsworth on all things financial and Cindy Olson on various aspects of the project, is duly noted.

Finally, I want to thank my parents, Ivan Matus and Florencia Casanova, my sister, Catalina Casanova for their unwavering love and support. Without them I would not be the person I am today. A special thanks to my amazing girlfriend, Ariel Rice, for her love, patience, and support throughout this process. I do not know how I could have done this without her.

CONTRIBUTION OF AUTHORS

Dr. Andre R. Barbosa is the principal investigator for this research project. Dr. David Trejo is the co-principal investigator of this research project. Both Dr. David Trejo and Dr. Andre R. Barbosa are co-authors of this thesis.

TABLE OF CONTENTS

Page

TABLE OF CONTENTS (Continued)

Page

LIST OF FIGURES

LIST OF FIGURES (Continued)

Figure Page

LIST OF FIGURES (Continued)

Figure Page

LIST OF FIGURES (Continued)

Figure Page

LIST OF FIGURES (Continued)

Figure Page

LIST OF FIGURES (Continued)

Figure Page

LIST OF FIGURES (Continued)

LIST OF FIGURES (Continued)

Figure Page

LIST OF FIGURES (Continued)

Figure Page

LIST OF FIGURES (Continued)

Figure Page

LIST OF FIGURES (Continued)

Figure Page

LIST OF FIGURES (Continued)

Figure Page

LIST OF TABLES

LIST OF TABLES (Continued)

Table Page

LIST OF TABLES (Continued)

Table Page

LIST OF TABLES (Continued)

Table Page

LIST OF TABLES (Continued)

Table Page

LIST OF TABLES (Continued)

LIST OF TABLES (Continued)

Table Page

LIST OF TABLES (Continued)

Table Page

LIST OF TABLES (Continued)

Table Page

1.0 INTRODUCTION

High strength steel (HSS) reinforcing bars are commercially available, but limited research has been performed to justify and provide confidence for its use. When used in reinforced concrete elements, HSS reinforcing bars have the potential to provide economic and constructability benefits. However, the lack of laboratory testing results on the performance of HSS reinforcing bars in concrete elements is a cause for concern. Because of this, current design code provisions, such as AASHTO LRFD Bridge Design Specifications and ACI 318-14, limit the nominal yield strength of reinforcing steel bars to 60 ksi (420 MPa) for many bridge design applications. Previous research has reported that using nominal yield strength larger than 60 ksi (420 MPa) in shear interfaces results in unconservative estimates of the shear interface capacity of the specimens (Zeno 2009, Harries et al. 2012, Barbosa et al. 2017). More recent research has reported that AASHTO LRFD could potentially increase the limit of nominal yield strength values up to 80 ksi (550 MPa), but results were mixed and depended on other variables not tested in the original Barbosa et al. (2017) publication.

1.1 OBJECTIVE OF THE RESEARCH

The objective of this research is to evaluate and define the performance of HSS reinforcing bars in shear friction applications. The thesis focuses on the use of ASTM A706 Grade 80 (550 MPa), ASTM A615 Grade 100 (690 MPa), and ASTM A1035 Grade 120 (830 MPa) reinforcing steel bars, since these are representative of the range of strengths expected in future bridge design and construction. To successfully implement the use of HSS reinforcement to current design provisions for reinforced concrete structures, it is critical to understand and define its performance. A total of forty-five (45) push-off specimens were designed and tested at the Structural Engineering Research Laboratory at Oregon State University to gain more insight into the effects of reinforcing steel bar grade, shear interface surface preparation,

reinforcing steel bar spacing, reinforcing steel bar size, and nominal concrete strength in concrete interface shear behavior.

1.2 OUTLINE OF THE RESEARCH REPORT

This thesis consists of seven chapters. Chapter 1 provides an introduction, objectives of the research, and a brief description of each chapter. Chapter 2 presents a literature review of previous research regarding shear friction theory, code review regarding current design code provisions, experimental research, and research with full-scale composite beam specimens. Chapter 3 presents the experimental program and specimen design. It provides descriptions of the test specimen dimensions, reinforcement layout, experimental test matrix, and test setup and procedures. Chapter 4 is an overview of the materials used in this research, including specifications and standards considered for reinforcing steel bars and concrete mixtures used. Additionally, this chapter provides results from testing performed on reinforcing steel bars, beyond the ones that were selected for the construction of the push-off test specimens, and concrete cylinders of the push-off test specimens that were constructed and tested. Chapter 5 presents experimental results and discussion on the tested specimens focusing on the effects of high-strength reinforcing steel on shear friction, including the influence of reinforcing steel bar grade, reinforcing steel bar spacing, and reinforcing steel bar size. In addition, a summary of results and main findings are provided from the results obtained for these parameters related to the HSS reinforcement. Chapter 6 presents experimental results and discussion for test specimens focusing on the effects of surface preparation and nominal concrete strength on shear friction. In addition, a summary of results and main findings are provided. Finally, chapter 7 presents the main conclusions obtained.

2.0 LITERATURE REVIEW

This chapter presents a review of the literature on concrete-concrete shear interface behavior. Shear friction theory in concrete-concrete interfaces is presented first. A review of the research with push-off test specimens is then presented before research results from full-scale composite beam specimens is presented. Finally, current code equations for predicting in-service performance are reviewed.

Shear friction is defined in this document as the resistance to displacement of an interface of two elements when acted upon by a shear force. The force is considered to be parallel to a given plane at an existing or potential crack location, an interface between dissimilar materials, an interface between two concretes cast at different times, or the interface between different elements of the cross section (AASHTO 2015). Examples are corbels, bearing shoes, ledger beam bearings, and connections between precast concrete elements (Mansur et al. 2008).

2.1 SHEAR FRICTION THEORY

Shear friction theory is used to predict the strength of concrete-to-concrete interfaces under longitudinal shear stresses. It assumes that friction arising from the roughness of the concrete-to-concrete interface controls the shear force transfer mechanism. Figure 2.1 shows the saw-tooth model used to represent this theory. It is important to note that shear friction theory can be applied when a relative displacement between both concrete faces exists. Harries et al. (2012) described shear friction as a “wedging action” arising from the displacement between rough concrete interfaces, referring to an influential Birkeland and Birkeland (1966) document. This movement forces a crack to open in the direction perpendicular to the shear interface. As the crack opening increases, the reinforcing steel will engage, thus creating a clamping force acting perpendicularly to the shear interface.

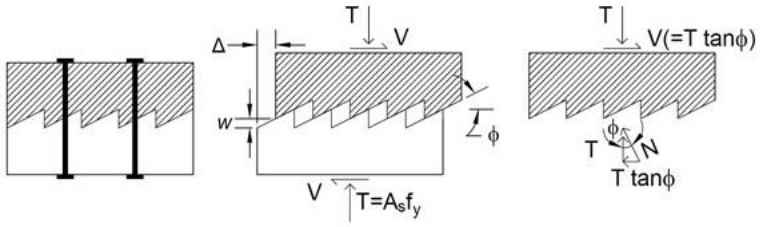

Figure 2.1: Shear friction reinforcement analogy (adapted from Birkeland and Birkeland 1966)

Santos and Julio (2012) reported that the four main parameters included in the shear friction model are adhesion (chemical bond), cohesion (aggregate interlock), friction, and dowel action, similar to those described in Zilch and Reinecke (2000). The parameters that make up the shear capacity can be separated into the following three load carrying mechanisms: (1) adhesion and cohesion, τ_a, (2) aggregate interlock shear friction, τ_{sf}, and (3) dowel action of the shear reinforcement, τ_{sr}. Figure 2.2 shows the influence of these three load-carrying mechanisms as a function of the relative displacement between concrete-to-concrete shear interfaces. As reported in Santos and Julio (2012), the roughness of the concrete surface has a significant impact on the concrete-to-concrete bond strength. This effect of the surface roughness is considered in code design equations as a combination of a cohesion coefficient and friction coefficient. Santos and Julio (2014) reports that even though it is well known that the load transfer mechanism in concrete-to-concrete interfaces depends on cohesion, friction, and dowel action, current design codes do not consider the dowel action mechanism.

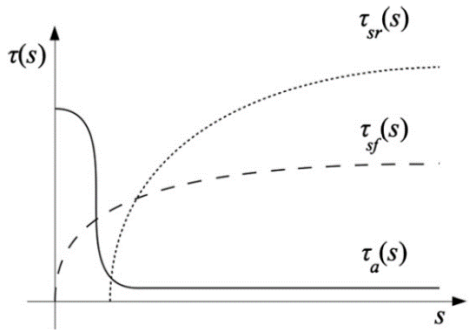

Figure 2.2: Load transfer mechanisms (adapted from Zilch and Reinecke 2000)

As shown in Figure 2.2, when the relative displacement, *s*, between two concrete interfaces is low, the main load carrying mechanism is the adhesion and cohesion between concrete interfaces, τ_a. During this stage, the bond between the two concrete surfaces is unbroken and will exhibit its highest resistance when little to no cracks are visible across the interface. Both concrete strength and concrete-to-concrete interface roughness are factors influencing the bond between these concrete surfaces. The characteristics of the roughened concrete surface may also influence the shear capacity.

The second load carrying mechanism shown in Figure 2.2 is the shear-friction mechanism. As the relative displacement between the concrete interfaces increases, the aggregates will interact and force the crack between the concrete surfaces to increase. This causes the interface separation to further widen, thus engaging the reinforcing bars crossing the concrete-to-concrete interface. The opening at the interface generates a clamping force and increases the friction forces across the interface. The combination of the clamping force and the effect of the surface roughness result in aggregate interlock. The strength and size of the aggregates and roughened surface at this interface, and the clamping force provided by the reinforcing bars are factors that will influence the magnitude of the aggregate interlock mechanism. Harries et al. (2012) reported that the crack width across the interface is critical in the interface shear friction behavior and that the crack width must be large enough to cause the reinforcing steel to strain. As a result of this, the crack width is directly proportional to clamping force. As crack width increases, the cohesion generated at the interface by the roughened surface is reduced and therefore the crack width is inversely proportional to the cohesion component of shear friction.

Kim et al. (2010) determined that aggregate type is a critical factor influencing aggregate interlock. The authors reported that larger aggregate interlock was observed in concrete mixtures containing river ravel compared to concrete mixtures containing limestone aggregate, for both self-consolidating concrete (SCC) and conventional concrete (CC) mixtures. The authors reported that the friction coefficients μ, for the CC mixtures is 0.30. Figure 2.3 shows the observed behavior of the crack width-

normal stress relationship and the crack width-crack slip relationship for mixture SR48/32.3, which corresponds to a self-consolidated concrete [S] mixture with river gravel [R], 48 MPa [48] release strength, and 32.3% coarse aggregate volume. The normal stress and crack slip increase as crack width increases.

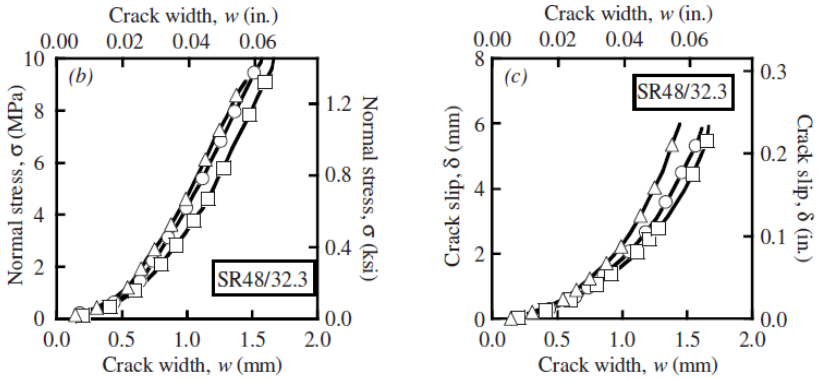

Figure 2.3: Typical plots of measured parameters (Kim et al. 2010)

The last load carrying mechanism shown in Figure 2.2 is the shear reinforcement dowel action. The relative displacement between concrete interfaces will cause the reinforcement crossing the interface to be subjected to shear, in what is usually referred to as dowel action. Figure 2.4 illustrates three different dowel modes described in Park and Paulay (1975): flexure, shear, and kinking. The moment resistance of the reinforcing bar resists flexure dowel action, while the shear resistance of the reinforcing bar resists shear dowel action. Kinking is resisted by tensile resistance at an angle between the two plastic hinges, therefore creating both horizontal and vertical resistance. Each of these mechanisms may require substantial slip on the interface for the dowel action to engage significantly.

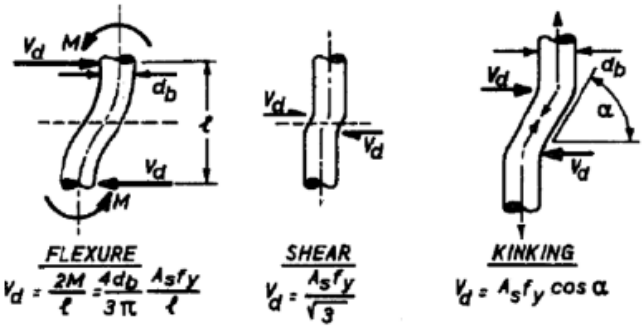

Figure 2.4: Three mechanisms of dowel action (Park and Paulay 1975)

Walraven and Reinhardt (1981) reported that for small crack widths dowel action is not a contributing load carrying mechanism, as can be seen in Figure 2.5. This indicates that cohesion and aggregate interlock are the main load carrying mechanisms at small crack widths. However, as the contribution of aggregate interlock is reduced due to increasing crack width, dowel action becomes the main contributor to the interface shear strength. This is consistent with results from Zilch and Reinecke (2000), as shown in Figure 2.2.

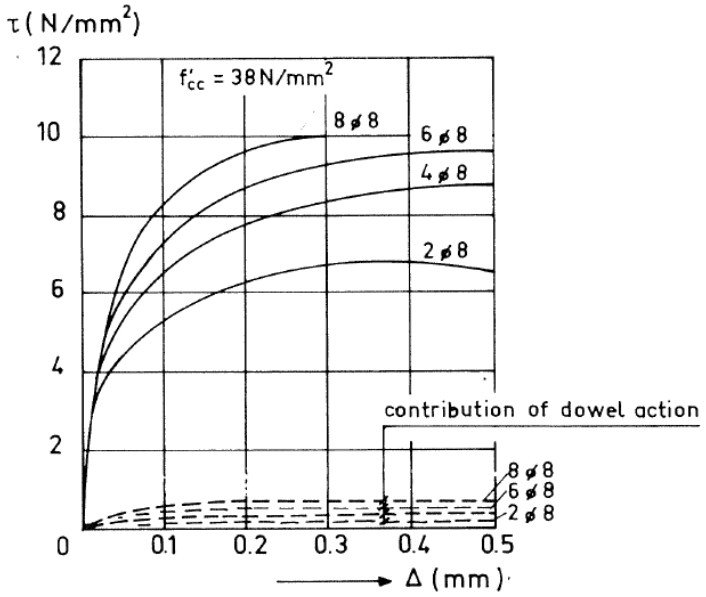

Figure 2.5: Contribution of dowel action to the total shear stress in a crack (Walraven and Reinhardt 1981)

2.2 CODE REVIEW

This section reviews the main codes used in the United States of America including the AASHTO (2014) standard design specification, ACI 318-14 design specification, PCI Design Handbook, and FIB Model Code 2010.

2.2.1 American Association of State Highway and Transportation Officials (AASHTO) Design

The equations in AASHTO (2014) Section 5.8.4.1 are presented in Equation (2-1) through Equation (2-5). Equation (2-1) consists of two terms. The first term refers to the contribution from cohesion and/or aggregate interlock through the use of a cohesion coefficient, *c*. The second term refers to the contribution of the net normal clamping force through a friction coefficient, μ.

$$V_{ni} = cA_{cv} + \mu\left(A_{vf}\, f_y + P_c\right) \quad \textbf{(2-1)}$$

The nominal shear resistance, V_{ni}, shall not be greater than the lesser of:

$$V_{ni} \le K_1 f_c' A_{cv} \quad \textbf{(2-2)}$$

$$V_{ni} \le K_2 A_{cv} \quad \textbf{(2-3)}$$

In which

$$A_{cv} = b_{vi} L_{vi} \quad \textbf{(2-4)}$$

Where

c = cohesion factor specified in Article 5.8.4.3 (ksi [MPa]);

A_{cv} = area of concrete considered to be engaged in interface shear transfer (in.^{2} [mm^2]);

μ = friction factor specified in Article 5.8.4.3;

A_{vf} = area of interface reinforcement crossing the shear plane (in.^{2} [mm^2]);

f_y = yield stress of reinforcement but design value not to exceed 60 ksi (420 MPa);

P_c = permanent net compressive force normal to the shear plane; if force is tensile, Pc is taken equal to 0.0 (kip [kN]);

b_{vi} = interface width considered to be engaged in shear transfer (in. [mm]);

L_{vi} = interface length considered to be engaged in shear transfer (in. [mm]);

f_c' = specified 28-day compressive strength of the weaker concrete on either side of the interface (ksi [MPa]);

K_1 = fraction of concrete strength available to resist shear specified in Article 5.8.4.3;

K_2 = limiting interface shear resistance specified in Article 5.8.4.3 (ksi [MPa]).

Equation (2-2) is implemented to prevent crushing or shearing of aggregate along the shear plane. Equation (2-3) is implemented to account for the sparseness of available experimental data. AASHTO (2014) states that the interface shear resistance is limited to 60 ksi, due to an overestimation of interface shear capacity when higher values are used, even though limited number of tests have been carried out.

AASHTO (2014) Section 5.8.4.4 requires a minimum area of interface reinforcement across the interface given by:

$$A_{vf} \geq \frac{0.05A_{cv}}{f_y} \quad \textbf{(2-5)}$$

Factors for Equation 2-2 to 2-4 are listed in AASHTO (2014) Section 5.8.4.3 and in Table 2.1.

Table 2.1: Cohesion and friction factors from AASHTO Section 5.8.4.3.

Interface Preparation	***c*, ksi (MPa)**	***μ***	***K*1**	***K*2, ksi (MPa)**
Cast-in-place concrete slab on clean concrete girder surfaces, free of laitance with surface roughened to an amplitude of 0.25 in. (6.35 mm).	0.28 (1.93)	1.0	0.30	1.8 (12.4)
Normal-weight concrete placed monolithically.	0.40 (2.76)	1.4	0.25	1.5 (10.3)
Normal-weight concrete placed against a clean concrete surface, free of laitance, with surface intentionally roughened to an amplitude of 0.25 in. (6.35 mm).	0.24 (1.65)	1.0	0.25	1.5 (10.3)
Concrete placed against a clean concrete surface, free of laitance, but not intentionally roughened.	0.075 (0.52)	0.6	0.20	0.8 (5.52)

The minimum interface shear reinforcement, A_{vf}, need not exceed the lesser of the amount determined using Equation (2-5) and the amount needed to resist $1.33V_{ni}/\phi$ (ϕ

from AASHTO 2014, Article 5.5.4.2.1) as determined using Equation (2-1). This is intended as an overstrength factor as the minimum is waived or lowered if the shear resistance without reinforcing steel exceeds $1.33V_{ni}/\phi$. Additionally, the minimum reinforcement provisions specified shall also be waived for girder/slab interfaces with surface roughened to an amplitude of 0.25 in. where the factored interface shear stress, v_{ni} of AASHTO (2014) Equation 5.8.4.2-1 is less than 0.210 ksi, and all vertical (transverse) shear reinforcement required by AASHTO (2014) Article 5.8.2.5 is extended across the interface and adequately anchored in the slab.

2.2.2 American Concrete Institute (ACI) Design Specifications

The horizontal shear capacity specified in the American Concrete Institute (ACI) 318-14 Section 16.4.4 is presented in Equation (2-6) through Equation (2-11). Equation (2-6) consists of two terms. The first term assumes a cohesion factor of 260 psi multiplied by the area being investigated. The second term refers to the contribution of the reinforcing steel to the horizontal shear strength multiplied by a factor of 0.6, all multiplied by the area being investigated. The requirements for a surface intentionally roughened to 0.25 in. amplitude are based on tests discussed in Kaar et al. (1960), Saemann and Washa (1964), and Hanson (1960).

$$V_{nh} = \lambda\left(260 + 0.6\frac{A_v f_{yt}}{b_v s}\right)b_v d \qquad \textbf{(2-6)}$$

where

λ = modification factor for lightweight concrete from Section 19.2.4;
f_{yt} = specified yield strength of transverse steel reinforcement (psi [MPa]);
A_v = area of shear reinforcement within spacing s, (in.^{2} [mm^2]);
b_v = width of shear interface (in. [mm]);
s = center-to-center spacing of transverse reinforcement (in. [mm]);
d = distance from the top face of the beam to the centroid of the tensile longitudinal reinforcement (in. [mm]).

ACI 318-14 does not have a limit of 60 ksi (420 MPa) for the yield stress of reinforcing steel, which is the case in AASHTO (2014). However, it does have an upper limit for V_{nh}, as shown in Equation (2-7).

$$V_{nh} \le 500 b_v d \tag{2-7}$$

If this limit is surpassed, V_{nh} shall be calculated per ACI 318-14 Section 22.9, shown in Equation (2-8), which limits the yield stress of reinforcing to 60 ksi (420 MPa), and the coefficient of friction μ determined per to ACI 318-14 Table 22.9.4.2.

$$V_n = \mu A_{vf} f_y \tag{2-8}$$

In addition to the upper limit presented in Equation (2-7), a minimum area of shear reinforcement within spacing s, $A_{v,min}$, shall be provided in accordance to ACI 318-14 Section 16.4.6, shown in Equation (2-9), for concrete placed against hardened concrete intentionally roughened to a full amplitude of approximately 0.25 in. and concrete placed against hardened concrete not intentionally roughened.

$$A_{v,\min} = \max\left\{0.75\sqrt{f_c'}\frac{b_w s}{f_y}; 50\frac{b_w s}{f_y}\right\} \tag{2-9}$$

When concrete contact surfaces are clean and free of laitance, and concrete is placed against hardened concrete not intentionally roughened and minimum area of shear reinforcement is provided, V_{nh} has an upper limit as shown in Equation (2-10).

$$V_{nh} \le 80 b_v d \tag{2-10}$$

For normal-weight concrete placed either monolithically or placed against an intentionally roughened concrete surface as specified in ACI 318-14 Section 16.4.4, V_n shall comply with Equation (2-11).

$$V_n < \min\begin{cases} 0.2 f_c' A_c \\ \left(480 + 0.08 f_c'\right) A_c \\ 1600 A_c \end{cases} \tag{2-11}$$

2.2.3 PCI Handbook

The PCI Handbook in Section 5.3.6 states that shear friction shall be calculated according to ACI 318-14 Section 22.9, as shown in Equation (2-8). In scenarios where load reversal does not occur, the use of an effective shear-friction coefficient μ_e is permitted when the concept is applied to monolithic or concrete with roughened surfaces.

$$\mu_e = \frac{1000\lambda A_{vf}\mu}{V_n} \quad \textbf{(2-12)}$$

where

λ = factor for use with lightweight concrete (see PCI Section 5.3.3);
A_{vf} = area of shear reinforcement perpendicular to the assumed crack plane, (in.^{2} [mm^2]);
μ = shear-friction coefficient (value in PCI Table 5.3.1);
V_n = nominal interface shear resistance.

2.2.4 FIB Model Code 2010

The FIB Model Code 2010 states that the main parameters determining the actual load bearing capacity observed in tests (large scale and small scale) are interface roughness, cleanliness of surface, concrete strength and quality, eccentricity/inclination of shear force, strong bond/pre-cracking/de-bonding before testing, and ratio of reinforcement crossing the interface. The overall shear resistance results from the following main mechanisms:

- Mechanical interlocking and adhesive bonding,
- Friction due to:
  - External compression forces perpendicular to the interface,
  - Clamping forces due to reinforcement and/or connectors,
- Dowel action of reinforcement and/or connectors crossing the interface.

FIB Model Code 2010 describes two indicators to quantify the surface roughness of concrete, the mean roughness parameter, R_m, and the mean peak-to-valley height parameter R_z. Figure 2.6 illustrates these concepts. The mean roughness parameter represents the average deviation of the profile from a mean line and it is calculated as shown in Equation (2-13)

$$R_m = \frac{1}{l}\int_0^l \left| y(x) - \bar{y} \right| \cdot dx \approx \frac{1}{n}\sum_{i=1}^{n} \left| y_i - \bar{y} \right|$$
$$\bar{y} = \frac{1}{l}\int_0^l y(x) \cdot dx \approx \frac{1}{n}\sum_{i=1}^{n} y(x) \qquad \textbf{(2-13)}$$

The mean peak-to-valley height represents the average difference between peak and valley measurements within a certain number of assessment lengths as shown in Equation (2-14).

$$R_z = \frac{1}{n} \cdot \sum_{i=1}^{n} R_{zi} \qquad \textbf{(2-14)}$$

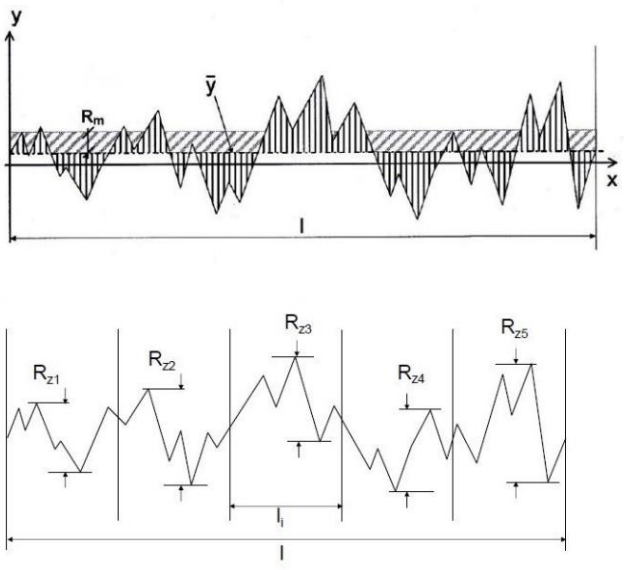

Figure 2.6: Average roughness, R_m, and mean peak-to-valley height, R_z (FIB Model Code 2010)

The design limit for interface shear (no reinforcing steel crossing the interface):

$$\tau_{Rdi} = c_a \cdot f_{ctd} + \mu \cdot \sigma_n \leq 0.5 \cdot \nu \cdot f_{cd} \quad \textbf{(2-15)}$$

where

c_a = coefficient for adhesive bond;
μ = coefficient of friction;
σ_n = lowest compressive stress resulting from a normal force acting on the interface;
f_{ctd} = design value for concrete tensile strength;
f_{cd} = design value of f_c

If reinforcement is required to cross the interface, the design limit is:

$$\tau_{Rdi} = c_r \cdot f_{ck}^{1/3} + \mu \cdot \sigma_n + \kappa_1 \cdot \rho \cdot f_{yd} \cdot \left(\mu \cdot \sin\alpha + \cos\alpha\right) + \kappa_2 \cdot \rho \cdot \sqrt{f_{yd} \cdot f_{cd}} \leq \beta_c \cdot \nu \cdot f_{cd} \quad \textbf{(2-16)}$$

where

c_r = coefficient for aggregate interlock effect at rough interfaces;
f_{ck} = characteristic value of the compressive strength of concrete;
f_{yd} = reinforcing steel tensile design yield strength;
κ_1 = interaction coefficient for tensile force activated in the reinforcement;
κ_2 = interaction coefficient for flexural resistance;
ρ = ratio of reinforcement steel crossing the interface;
α = angle of inclination of reinforcing steel crossing the interface;
β_c = coefficient for the strength of the compression strut;
ν = effectiveness factor for the concrete.

The surface roughness categories and coefficients are presented in Table 2.2.

Table 2.2: Coefficients for different surface roughness as presented in FIB Model Code (2010)

Surface roughness	Example	R_t, in. (mm)	c_a	c_r	κ_1	κ_2	β_c	μ	
								$f_{ck} \geq 20$	$f_{ck} \geq 35$
Very rough	High pressure water jetting, indented	≥ 0.12 (3)	0.5	0.2	0.5	0.9	0.5	0.8	1.0
Rough	Sand blasted, high pressure water blasted, etc.	< 0.06 (1.5)	0.4	0.1	0.5	0.9	0.5	0.7	
Smooth	Untreated, slightly roughened	≥ 0.06 (1.5)	0.2	0	0.5	1.1	0.4	0.6	
Very smooth	Cast against steel formwork	Not measurable	0.025	0	0	1.5	0.3	0.5	

There is a limit set on the tensile force in the reinforcement due to simultaneous bending and/or reduced anchorage of bars, and also because shear failure can occur at low slip values.

$$\kappa_1 = \frac{\sigma_s}{f_y} \leq 1.0 \qquad \textbf{(2-17)}$$

The ultimate shear stress resulting from different single mechanisms can be expressed as shown in Equation (2-19).

2.3 EXPERIMENTAL RESEARCH

This section provides a summary of the literature where shear experimental research was conducted with push-off test specimens. Table 2.3 provides an overview of the published research and identifies test and experimental parameters identified by each reference to assess interfacial shear. The table is in chronological order. A description of each study is provided.

Hofbeck et al. (1969) investigated the shear transfer strength of reinforced concrete specimens with and without cracking along the shear plane. The objective of the study was to determine the influence of pre-existing cracks in the shear plane on the shear transfer strength, to determine the influence of strength, size, and arrangement of reinforcement on the shear transfer strength, and to examine the possible contribution of the dowel action on shear transfer strength. Test results indicated that a pre-existing crack along the shear interface increased the slip and reduced the

ultimate shear strength when compared with uncracked specimens. The reduction in ultimate shear strength decreased as the reinforcement ratio increased. Additionally, test specimens reinforced with higher strength steel bars reported higher shear transfer strength, except for the specimen with the highest reinforcement ratio. The authors concluded that shear-friction theory provided a reasonable and conservative estimate of shear transfer strength in pre-cracked normal weight concrete assuming.

Mattock et al. (1976) tested push-off specimens, both uncracked and pre-cracked, using lightweight concrete to develop shear transfer design recommendations. The types of aggregate used were naturally occurring gravel and sand, rounded lightweight aggregate, crushed angular lightweight aggregate, and sanded lightweight aggregate. Test results indicated that diagonal tension cracks in uncracked specimens began to appear at shear stresses of 400 psi (2.76 MPa) to 700 psi (4.8 MPa). No diagonal cracks formed in pre-cracked specimens. The authors noted that the ultimate shear capacity increased for larger reinforcement ratio values. The authors reported a lower shear transfer strength for concrete specimens with lightweight aggregate when compared with specimens containing normal-weight gravel aggregate and sand concrete mixtures.

Kahn and Mitchell (2012) tested fifty push-off specimens with uncracked, pre-cracked, and cold joint interfaces. The objective of the study was to extend the existing provisions presented in ACI 318-99 to high-strength concrete. Concrete design strengths in the specimens were 4 ksi (27.6 MPa), 7 ksi (48.3 MPa), 10 ksi (68.9 MPa), and 14 ksi (96.5 MPa), and the reinforcement ratio varied from 0.37% to 1.47%. The authors recommended the yield stress, f_y, be taken as 60 ksi (420 MPa) rather than using the measured yield stress. This recommendation is due to the results of normal-weight and high-strength concretes showing lower scatter and reaching larger capacities when compared to the ACI 318 design equation values. The authors concluded that the current ACI 318 provisions were conservative in estimating interface shear strength for high-strength concrete. They recommend f_y be taken as 60 ksi (420 MPa) to limit the slip along the smooth cracks in high-strength concrete. An upper limit of shear stress of 20% was proposed.

Table 2.3: Reference parameters for push-off test specimens

Reference	Specimen size, in. (mm)	Number of specimens	Bar Size, in. (mm)	Steel ratio, ρ, %	Yield Stress, f_y, ksi (MPa)	Design Concrete Strength, f_c', ksi (MPa)
Hofbeck et al. (1969)	21.5 x 10 x 5 (546 x 254 x 127)	38	1/8 (3.2), #2 (6.4 mm), #3 (#10M), #4 (#13M), #5 (#16M)	0.00% -2.64%	48.0-66.1 (331-456)	4 (27.6)
Mattock et al. (1976)	22 x 12 x 12 (559 x 305 x 305)	62	#3 (#10M)	0.00%-3.79%	47.7-53.6 (328.9-369.6)	2.5 (17.2), 6.0 (41.4)
Kahn and Mitchell (2002)	24 x 12 x 10 (610 x 305 x 254)	50	#3 (#10M)	0.37%-1.47%	69.5 (479.2), 83.0 (572.3)	6.8 (46.9), 17.9 (123.4)
Scholz et al. (2007)/ Wallenfelsz (2006)	48 x 18 x 16 (1219 x 457 x 406)	26	#4 (#13M), #5 (#16M)	0.10%, 0.16%	73 (503.3)	4.3-6.0 (29.6-41.4)
Mansur et al. (2008)	29.5 x 15.75 x 5.9 (750 x 400 x 150)	19	0.315 in. (8 mm), #3 (#10M)	0.45%-2.67%	43.5 (300)	10.6 (73.1), 12.3 (84.8), 13.8 (95.1), 15.4 (106.2)
Scott (2010)	50 x 18 x 16 (1270 x 457 x 406)	36	#4 (#13M), #5 (#16M), #6 (#19M)	0.00%, 0.10%, 0.5%, 1.2%	60 (410)*	5.7-6.2 (39.3-42.7)
Trejo and Kim (2011)	48 x 18 x 16 (1219 x 457 x 406)	8	#4 (#13M), #5 (#16M)	0.10%	62 (428)	5.9-7.5 (40.7-51.7)
Harries et al. (2012)	44 x 24 x 10 (1118 x 610 x 254)	8	#3 (#10M), #4 (#13M)	0.41%, 0.75%	61.5 (424.0)-140.0 (965.3)	5 (34.5)
Shaw and Sneed (2014)	24 x 12 x 5.5 (610 x 305 x 140)	36	#3 (#10M)	1.33%	66.2 (456)	5, 8 (34, 55)
Sneed et al. (2016)	24 x 12 x 5.5 (610 x 305 x 140)	52	#3 (#10M)	0.009% 0.013% 0.017% 0.022%	72.2 (498)	4.4-5.6 (30.3-38.6)
Barbosa et al. (2017)	44 (52) x 24 x 24 (1118 (1321) x 610 x 610)	20	#4 (#13M) #5 (#16M)	0.42% 0.65%	64.5 (445)-89 (614)	4.2-5.2 (29.0-35.9)
Li et al. (2017)	33 x 18 x 12 (24) (838 x 457 x 305 (610))	16	#5 (#16M)	0.22% 0.43% 0.86%	72 (496) 140 (965)	5.0-7.5 (34.5-51.7)

*Actual yield stress not reported. Nominal yield stress stated.

Kahn and Mitchell (2012) tested fifty push-off specimens with uncracked, pre-cracked, and cold joint interfaces. The objective of the study was to extend the existing provisions presented in ACI 318-99 to high-strength concrete. Concrete design strengths in the specimens were 4 ksi (27.6 MPa), 7 ksi (48.3 MPa), 10 ksi (68.9 MPa), and 14 ksi (96.5 MPa), and the reinforcement ratio varied from 0.37% to 1.47%. The authors recommended the yield stress, f_y, be taken as 60 ksi (420 MPa) rather than using the measured yield stress. This recommendation is due to the results of normal-weight and high-strength concretes showing lower scatter and reaching larger capacities when compared to the ACI 318 design equation values. The authors concluded that the current ACI 318 provisions were conservative in estimating interface shear strength for high-strength concrete. They recommend f_y be taken as 60 ksi (420 MPa) to limit the slip along the smooth cracks in high-strength concrete. An upper limit of shear stress of 20% was proposed.

Wallenfelsz (2006) and Scholz et al. (2007) assessed the horizontal shear strength of a deck panel to prestressed concrete beam connection. Figure 2.7 provides a schematic of the horizontal push-off tests described in both publications. Figure 2.8 shows three cases of the typical load versus slip testing results. Figure 2.8(a) presents the case where the horizontal shear resistance of the shear connector is lower than the cohesion shear resistance. The shear-slip response is characterized by a sharp drop in shear load after the interface cracks, followed by a sustained load phase. Figure 2.8(b) presents the case where the steel shear connectors resistance is approximately equal to the cohesion resistance. The shear-slip response is characterized by a small drop in shear load after cracking, followed by a sustained growth phase. Figure 2.8(c) presents the case where the steel shear connector resistance is higher than the cohesion resistance. The shear-slip response is characterized by an initial slope change after cracking occurs which represents the load transferring from cohesion to the shear connectors. The load continues to grow until peak load is reached, at which point the shear connectors begin to yield. Results indicated that the resistance provided by shear friction did not occur until cracking begins, which occurred when the adhesion bond was broken. This observation led the authors to recommended

modifications of the current equation in AASHTO (2014), described in the next section, by separating the two components.

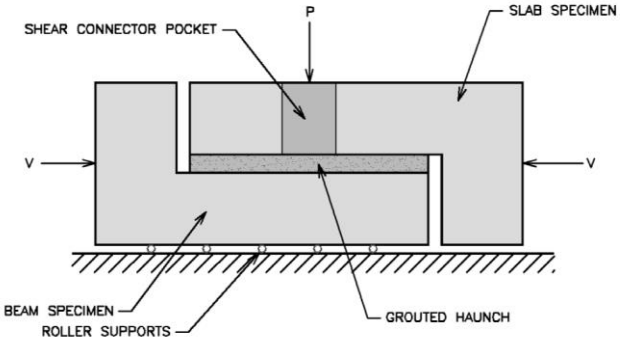

Figure 2.7: Horizontal push-off test (Wallenfelsz 2006)

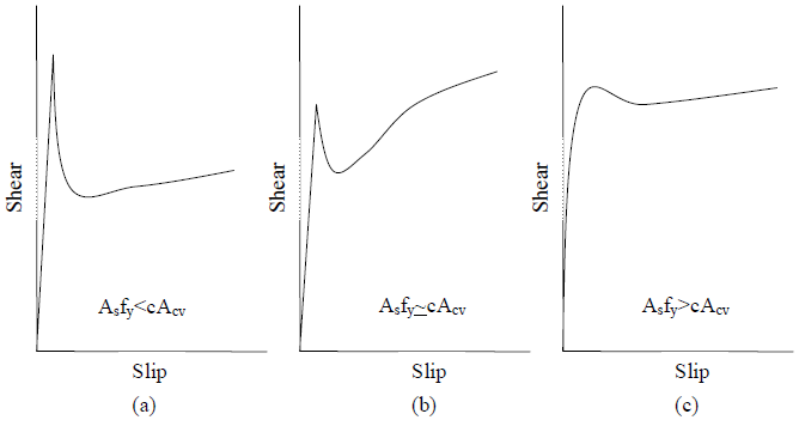

Figure 2.8: Typical Load versus. Slip Plots (Wallenfelsz 2006)

Mansur et al. (2008) conducted tests on 19 pre-cracked push-off specimens. The two major parameters considered in the research were the compressive strength of the concrete, f'_c, and the reinforcement parameter, $\rho_v f_y$, through the shear interface. Figure 2.9 shows the typical load-deformation response of the test specimens. It is characterized by the four (4) events shown in Figure 2.9. Results indicated that an increase in the concrete strength increased the stiffness of Branch I, increased the load achieved in the Branch I, and also increased the peak shear stress (strength). Results also indicated that an increase in the reinforcement parameter, $\rho_v f_y$, generated changes in response similar to when the concrete strength was increased. The authors noted

that a balanced reinforcement parameter and concrete strength parameter could be achieved to result in higher shear resistance values.

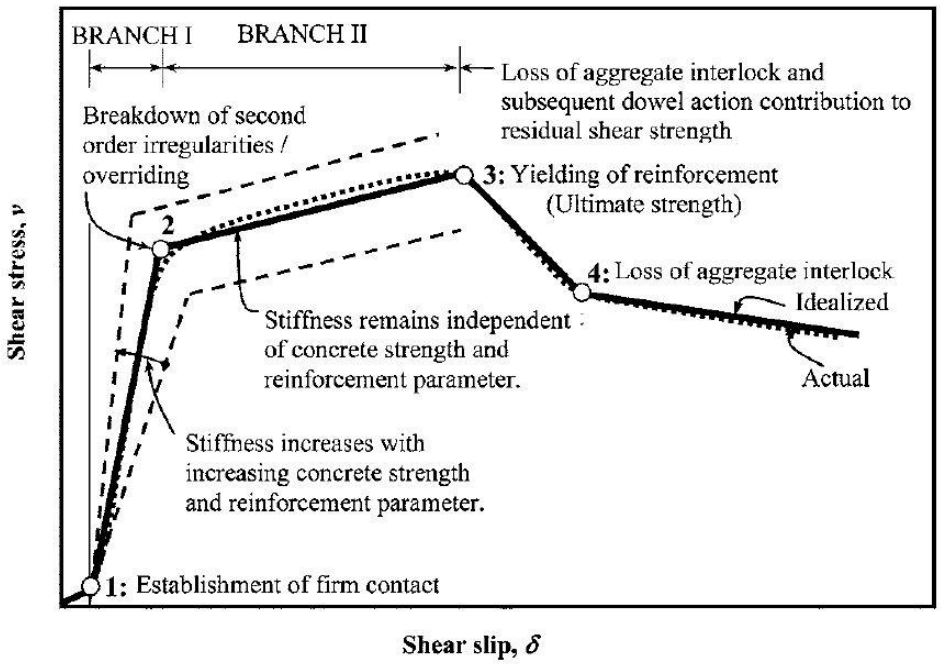

Figure 2.9: Response in terms of slip/separation under increasing load (Mansur et al. 2008)

Scott (2010) evaluated the accuracy of the current AASHTO LRFD provisions in predicting horizontal shear strength of precast girders and cast-in-place decks for both normal weight and lightweight concrete. The experimental program included testing thirty-six push-off specimens. The tests investigated the steel reinforcement ratio and the combination of deck and girder concrete. From the results of the push-off tests, the author concluded that the AASHTO (2007) provisions were conservative in predicting interface horizontal shear strength for a precast concrete girder and cast-in-place concrete deck. The authors noted that if higher values of reinforcement area crossing the shear interface were used, the strain values in the reinforcement either right before or right after cracking were lower than with lower reinforcement area. However, the reinforcement still reached strain levels that suggested yielding. The author noted that the modifications proposed in Wallenfelsz (2006) provided a better fit to their test data.

Trejo and Kim (2011) conducted 24 push-off tests to assess the shear transfer behavior of the girder-haunch-deck systems. Results indicated that there were five different stages of a typical failure mode, as shown in Figure 2.10. These stages included: (1) adhesion loss, where interface slips at constant load, V_{loss}; (2) engagement of shear key components; (3) peak load shear key failure, V_{peak}; (4) dowel action of connectors or beginning of sustained load; and (5) system failure.

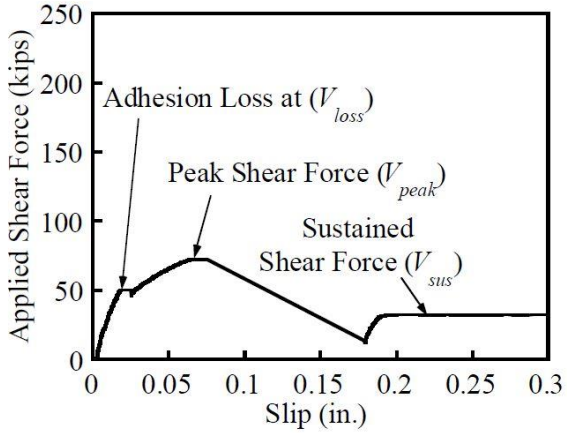

Figure 2.10: Typical failure mode and the plot of the system (Trejo and Kim 2011)

Harries et al. (2012) and Zeno (2009) summarized a research program developed to study the shear interface behavior when using with high-strength reinforcing steel bars across the interface. The objective of the research was to compare the behavior of the horizontal shear capacity of specimens containing ASTM A615 and ASTM A1035 reinforcing steel. The experimental program included push-off test specimens with 60 ksi (420 MPa) and 100 ksi (690 MPa) reinforcing steel with reinforcement steel ratios varying from 0.40 to 0.75%. The bar sizes were #3 (#10M) and #4 (#13M) bars, and the concrete-to-concrete surface was prepared with a 1/4 in. (6.35 mm) amplitude roughness and cleared of laitance before the second layer was cast. Results from the testing showed that three of the four specimens reinforced with ASTM A615 Grade 60 (420 MPa) reinforcing steel reached the design values determined per AASHTO (2007). On the other hand, none of the specimens reinforced with ASTM A1035 Grade 100 (690 MPa) specimens reached the design values when using 100

ksi (690 MPa) to compute the shear capacity. However, when f_y was limited to 60 ksi (420 MPa), the A1035 specimens did reach the design values per AASHTO (2007).

Test results reported by Zeno (2009) indicate that the shear-friction mechanism occurs in stages, as shown in Figure 2.11. The author reported that the concrete component had the highest contribution to the load transfer mechanism before cracking occurred. After cracking, the contribution of the reinforcing steel bars ("steel component" in the figure) increased. These results indicate that the load transfer through the concrete and reinforcing steel bars of the shear-friction mechanisms do not act simultaneously, as suggested by the shear-friction equation in AASHTO (2014).

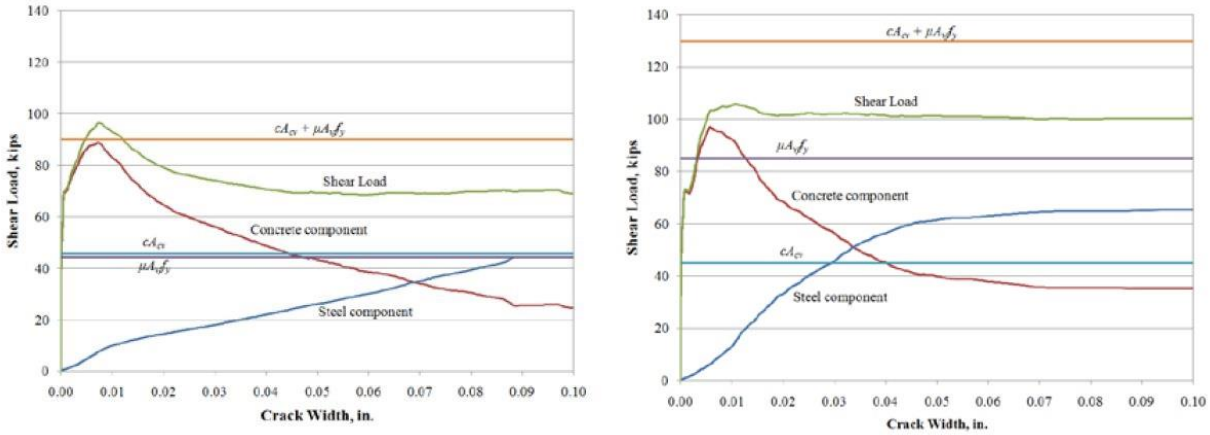

Figure 2.11: Components of shear-friction shear load versus crack width for specimens with reinforcing steel bars consisting of (a) A615 #3 (#10M), and (b) A1035 #3 (#10M) (Zeno 2009)

Figure 2.12 to Figure 2.15 can be used to summarize the main observations in the research described in Harries et al. (2012). Figure 2.12 shows results of shear load versus average shear displacement. The strain measurements are shown in Figure 2.14. The authors reported that the shear-friction capacity did not increase considerable with the use of ASTM A1035 Grade 100 (690 MPa) reinforcing steel. The researchers concluded that this occurred because the specimens reached the ultimate load before the reinforcing steel yielded. Based on these findings, the authors recommend the clamping force should be considered as a function of the steel modulus rather than the yield strength.

Figure 2.13 and Figure 2.15 show the linearized results of shear load versus average shear displacement behavior and strains, respective, where the three stages can be clearly identified:

1. Stage 1: this stage covers the behavior before cracking occurs. It is characterized by a linear shear load versus shear displacement behavior in all the specimens. During this stage, the applied load is resisted by the concrete component, controlled by the concrete-to-concrete bond between the two surfaces.

2. Stage 2: this stage covers the behavior from cracking to reaching the ultimate capacity. It is characterized by softening, observed in the change of slope. During this stage, the applied load is resisted by the friction originated from the interface surface roughness. Due to the low values of strain reached in the reinforcing steel bars crossing the interface, the clamping force across the interface is still low and does not have a considerable contribution to resisting the applied load.

3. Stage 3: this stage covers the post ultimate behavior. It is characterized by a sustained load carrying capacity in the ASTM A1035 Grade 100 (690 MPa) specimens. The ASTM A615 Grade 60 (420 MPa) specimens exhibited a faster degradation of the post ultimate load carrying capacity.

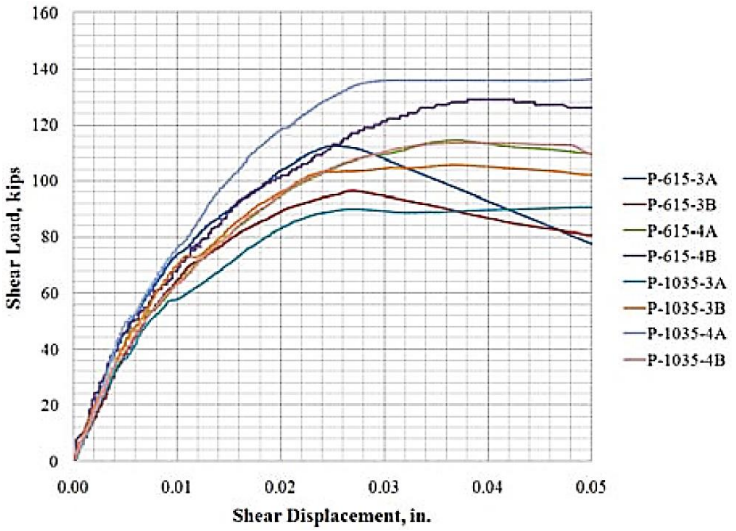

Figure 2.12: Shear load versus shear displacement showing the described stages of the shear friction mechanism (Zeno 2009)

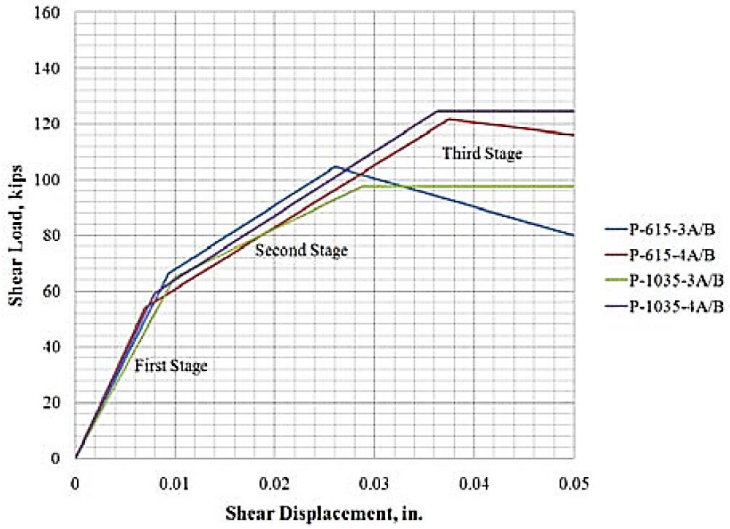

Figure 2.13: Linearization of shear load versus shear displacement showing the described stages of the shear friction mechanism (Zeno 2009)

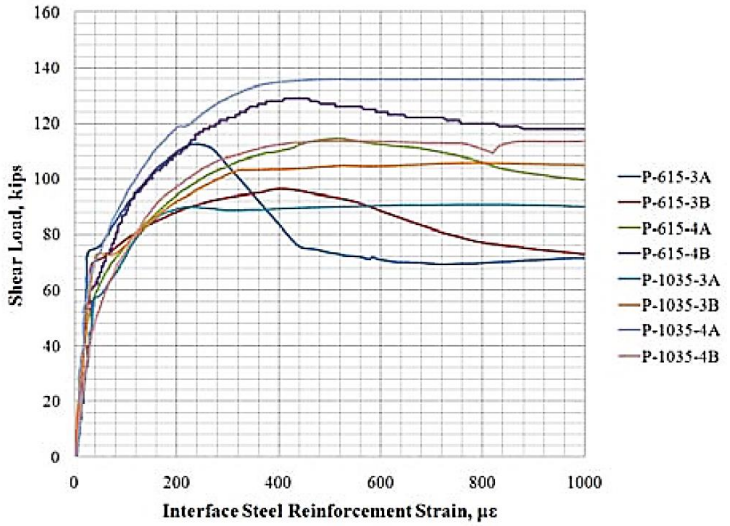

Figure 2.14: Shear load versus average interface steel strain showing described stages of the shear friction mechanism (Zeno 2009)

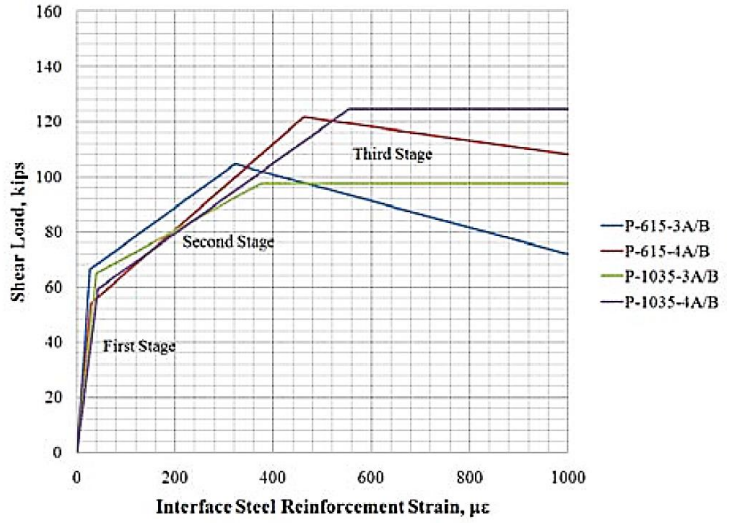

Figure 2.15: Linearization of shear load versus average interface steel strain showing described stages of the shear friction mechanism (Zeno 2009)

In summary, Harries et al. (2012) concluded that the design values calculated per AASHTO (2007) were only reached by specimens reinforced with ASTM A615 Grade 60 (420 MPa) reinforcing steel. The results showed that increasing the yield stress of the reinforcing steel did not increase the peak load capacity due to the reinforcing bars not reaching their yielding strain before reaching the peak load, as indicated by the strain measurements collected via strain gages. However, the peak load did increase with a higher bar size. This was attributed to a higher interface stiffness resulting from a higher reinforcing bar area.

Shaw and Sneed (2014) researched the direct shear transfer across an interface of lightweight aggregate concretes cast at different times. The experimental program consisted in testing 36 push-off test specimens with test variables such as concrete type, concrete compressive strength, and surface preparation. Shear strengths obtained from the experimental tests were compared to PCI Design Handbook and ACI 318-11 code provisions. The authors reported that concrete type had no influence on the shear strength of the test specimens, however, concrete compressive strength had a significant impact on shear strength of the test specimens. The authors noted that PCI and ACI 318-11 provided conservative estimates of shear strengths for the sand-lightweight and all-lightweight cold-joint test specimens. The authors noted that additional research is needed to assess the impact of the reinforcement ratio in shear strength for all-lightweight and sand-lightweight concrete cold-joint test specimens.

Sneed et al. (2016) compiled a database of shear friction test results from previous research performed with push-off test specimens subjected to monotonic loading without external normal forces. The authors compared the database results to PCI Design Handbook and ACI 318-14 shear friction design provision in order to validate these provisions. Test variables considered were concrete type, lightweight aggregate material, shear interface surface preparation, reinforcement ratio, and crack interface condition. The authors reported that values of V_{test}/V_{calc} indicate that the effective shear friction coefficient, μ_e, approach presented in PCI is more accurate than the conventional shear friction coefficient, μ, approach presented in both PCI and ACI 318-14 for normal weight, sand-lightweight, and all-lightweight concrete with monolithic uncracked, monolithic precracked, and cold-joint roughened interface conditions. PCI and ACI 318-14 conventional shear friction coefficient, μ, approach provides a conservative shear friction capacity estimation for cold-joints with a smooth interface preparation for sand light-weight and all-lightweight concrete. The authors recommend removing the modification factor λ used to calculate the coefficient of friction, μ, in order to obtain more accurate shear friction capacity estimations.

The second phase of Sneed el al. (2016) entailed an experimental program with 52 push-off test specimens and test variables such as concrete type, lightweight-aggregate material, surface preparation, reinforcement ratio, and crack interface condition. The authors reported that cold-joint specimens with a roughened interface reached a larger ultimate shear stress than cold-joint specimens with a smooth interface. Additionally, the ultimate shear stress reached by the cold-joint specimens with a smooth interface appeared to be independent of concrete type. The authors reported that the use of λ in the coefficient of friction, μ, approach presented in PCI and ACI 318-14 are conservative for all lightweight-aggregate specimens. The authors recommend the use of the effective coefficient of friction, μ_e, approach presented in PCI.

Barbosa et al. (2017) investigated the effect of high-strength steel (HSS) reinforcement on concrete-to-concrete shear interface capacity. Four sets of five push-off test specimens were used with reinforcing steel ratios varying from 0.42 to 0.64%, #4 (#13M) and #5 (#16M) bar sizes, and reinforcing steel grade 60 (420 MPa) and grade 80 (550 MPa), per ASTM A615 and A706. All the specimens were designed to have similar peak shear loads per AASHTO (2014). The authors concluded that the specimens reinforced with #5 (#16M) reinforcing bars showed an increase in shear friction resistance when HSS was used. However, the same change was not observed in the specimens reinforced with #4 (#13M) reinforcing bars. Figure 2.16 shows the average interface shear force versus reinforcing steel strain for all the specimens tested. The specimen label 4G60 corresponds to the reinforcing steel bar size [4], and the reinforcing steel bar grade [G60]. All the specimens show linear behavior until approximately 50 microstrain, where a substantial change in slope is observed. This change in slope occurs at a higher load for specimens reinforced with #4 (#13M) reinforcing bars. The authors attributed this difference to the lower concrete area present in the #5 bar specimens, thus having less contribution from concrete-to-concrete cohesion. For specimens reinforced with grade 60 (420 MPa) reinforcing steel, the specimens reinforced with #4 (#13M) reinforcing bars reached the nominal yield strain after the peak interface shear load was reached.

However, the specimens reinforced with #5 (#16M) reinforcing bars reached the nominal yield strain prior to reaching the peak load.

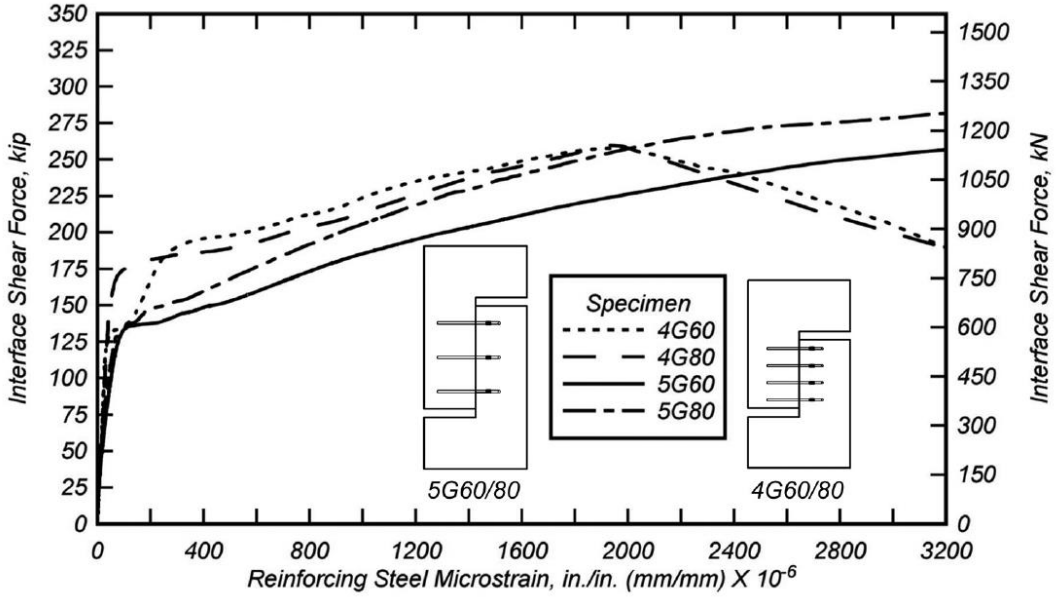

Figure 2.16: Average (over all specimens tested per group) interface shear force versus reinforcing steel strain for all specimens (Barbosa et al. 2017)

Figure 2.17 shows a plot of data points normalized by the concrete strength versus the reinforcement ratio normalized by concrete strength and Young's modulus of the reinforcing steel. The specimens reinforced with #4 (#13M) bars, with both grade 60 (420 MPa) and grade 80 (550 MPa) reinforcing steel, did not reach their yield stress until reaching the ultimate capacity; therefore, the authors concluded that the clamping force can be described as a function of the elastic modulus instead of the yield strength (Harries et al. 2012). The thick line represents the design equation proposed by AASHTO (2015), with a maximum value limited by the shear value corresponding to $K_1 A_{cv} f_c'$ per AASHTO (2015). The cohesion and friction coefficients, c and μ, respectively, were obtained through linear interpolation between the case of a surface roughened to 1/4 in. (6.35 mm) and the case of a surface not intentionally roughened, as there is no case in AASHTO (2015) for directly accounting for the surface roughened to 1/8 in. (3.175 mm) The authors pointed out that all the data points collected were above the line defined by AASHTO (2015), thus indicating that the design equation is conservative. The data points are also

above the line defined by the design equation using f_y = 80 ksi (550 MPa), which indicates that allowing the use of this stress would still be considered conservative. It is worth noting, however, that the vertical axis in Figure 2.17 is normalized by the concrete strength and not only the interface shear area, which is used in AASHTO (2015) to characterize the cohesion factor used in the equations.

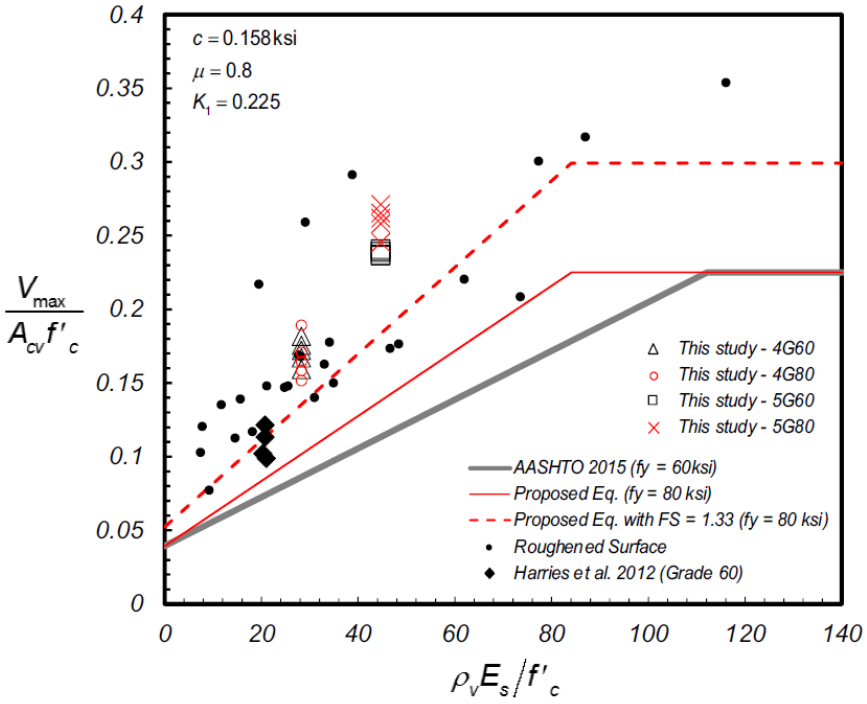

Figure 2.17: Experimental normalized peak shear stress versus normalized reinforcement stiffness across the interface (Barbosa et al. 2017)

Li et al. (2017) tested sixteen small-scale push-off test specimens to study how horizontal shear transfer between precast and cast-in-place concrete surfaces were influenced by surface preparation, bond breakers (epoxy and roofing felt), and interface reinforcement properties (yield strength, reinforcement amount, and means of anchorage). Three different surface preparations were tested: (1) fully roughened surface with 1/4 in. (6.35 mm) groves, (2) troweled surface, and (3) middle 6 in. (152.4 mm) or 12 in. (304.8 mm) of the surface roughened with 1/4 in. (6.35 mm) groves. Two debonding agents were used: (1) epoxy, which was applied to the concrete of the bottom piece after initial set and again prior to casting of the top piece, and (2) roofing felt. Two types of reinforcing steel were used: (1) normal-

strength (ASTM A615/A615M-16 Grade 60 [420 MPa]), and (2) high-strength (ASTM A1035/A1035M-16 Grade 120 [830 MPa]). Two types of spacing were used: (1) 6 in. (152.4 mm) spacing for specimens with two pairs of interface reinforcement bars, and (2) specimens with a single interface reinforcement bar placed at the center of the 12-inch-long (304.8 mm) interface. All interface reinforcement bars used were #5 (#16M) reinforcing bars. Reinforcing steel ratios varied from 0.22 to 0.86%.

Results from the Li et al. (2017) experimental program indicated that surface preparation and interface area had a large influence over the peak strength. The highest peak strength was achieved by specimens with fully roughened surfaces, followed by middle surface roughened specimens, and troweled and debonded specimens. Figure 2.18 illustrates this observation where the higher initial stiffness, in terms of force versus slip, can be observed in specimens with fully roughened surfaces. Specimen labels consist of five terms: (1) surface preparation (R is rough, T is troweled, RM is rough middle); (2) specimen width (12 in. [304.8 mm], 24 in. [609.6 mm]); (3) bond breaker (NB is no bond breaker, F is roofing felt, E is epoxy); (4) shear reinforcement spacing (12 in. [304.8 mm] means one pair of #5 [#16M] bars, 6 in. [152.4 mm] means two pairs of #5 [#16M] bars); and (5) reinforcement parameters (NR is normal-strength hooked, HR is high-strength hooked, HB is high-strength headed). The large drop in force after the peak force is reached led to a sustained load behavior controlled by dowel action in the reinforcement. As expected, the peak force in partially roughened specimens was lower than the peak force in fully roughened specimens. However, when compared in terms of stress (force divided by the area of roughened concrete), partially roughened specimens had higher first cracking and peak strength than comparable fully roughened specimens. The authors concluded that shear transfer performance should be considered in terms of stress. Figure 2.19 illustrates that an essentially bilinear behavior was observed in specimens with a partially roughened surface and fully roughened surface, representing the behavior before and after cracking of the interface. In this study, the contributions of cohesion and reinforcement to peak strength were estimated working under the assumption that shear strength can be expressed as the sum of both contributors. The values obtained for cohesion were approximately double and equal

to values recommended in AASHTO Specification for roughened and troweled surfaces, respectively. The contribution of normal strength steel was estimated at $1.1A_sf_y$, where the coefficient of 1.1 is larger than the coefficient recommended by AASHTO Specifications (1.0 and 0.6 for roughened and troweled surfaces). Post-testing observations showed that the failure plane was primarily located in the side with lower strength concrete. This observation led the authors to conclude that the lower concrete strength should be used when calculating shear strength.

Results in Li et al. (2017) indicated that the use of high-strength reinforcing steel did not transform into a significant effect on stiffness, cracking strength, peak strength and post-peak strength. In comparison, the increase of reinforcement area had a more important impact. The authors concluded that additional studies are required due to the small number of specimens tested.

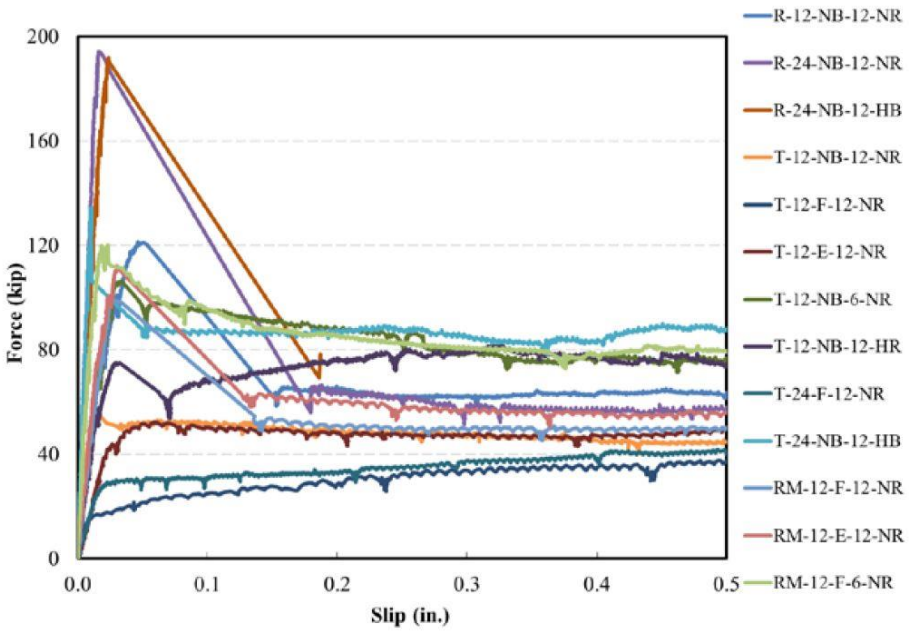

Figure 2.18: Force versus slip (Li et al. 2017)

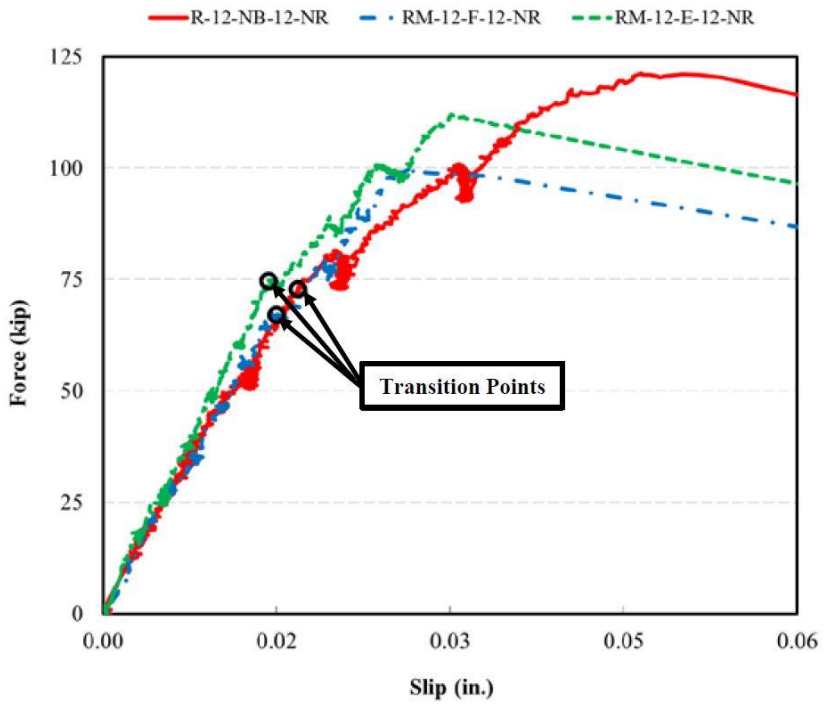

Figure 2.19: Force versus slip zoomed region up to 0.06 in. slip (Li et al. 2017)

Soltani and Ross (2017) created a database of experiments carried out to evaluate the interface shear transfer on uncracked reinforced concrete specimens. Data from 774 tests was studied and gathered into a database with the objective of evaluating the accuracy of the interface shear transfer provisions per AASHTO LRFD Bridge Design Specifications, Eurocode 2, and CSA A23.3. The authors filtered the data to create code-specific databases for the three mentioned code provisions. The authors found that all codes evaluated are conservative, although the degree of conservatism varied depending on design variables such as concrete compressive strength, steel reinforcement ratio across the interface, and test specimen dimensions. The results of the analysis showed that when strength reduction factors are not considered, unconservative results were observed in 8.2%, 1.6%, and 7.6% of the specimens for AASHTO LRFD, Eurocode 2, and CSA A23.3, respectively. When strength reduction factors are considered, the percentage of unconservative results observed were 1.8%, 1.6%, and 2.3%, for AASHTO LRFD, Eurocode 2, and CSA A23.3, respectively. The authors determined that AASHTO LRFD provisions presented a decrease in level of conservatism as concrete compressive strength decreased,

Eurocode 2 presented an inverse relationship between level and conservatism and the interface reinforcement index (ρf_y), and CSA A23.3 presented the most alarming observation as 69% of the specimens heavily reinforced (ρf_y > 1305 psi (9 MPa)) showed unconservative strength ratios.

2.4 RESEARCH WITH FULL-SCALE COMPOSITE BEAM SPECIMENS

This section provides a summary of research performed on full-scale composite beam tests. Table 2.4 provides an overview of the published research and identifies test and experimental parameters provided by each reference.

Seamann and Washa (1964) researched the strength of the joint between precast concrete beams and cast-in-place concrete slabs. The experimental program involved testing 42 beams to provide insight into the following test variables: (1) concrete interface roughness; (2) joint position with respect to the neutral axis; (3) length of shear span; (4) reinforcing ratio across the interface; (5) shear key effect; and (6) concrete strength. The authors reported that the ultimate shear strength increased as the concrete surface roughness increased from smooth to intermediate roughness. The ultimate shear strength also increased when the reinforcement ratio of reinforcement steel bars crossing the interface increased. On the other hand, the ultimate shear strength was approximately equal between beams with intermediate rough surface and beams with shear keys. Additionally, the authors reported that the ultimate shear strength presented a subtle increase when concrete strength increased from 3 ksi (20.7 MPa) to 5.5 ksi (37.9 MPa).

Loov and Patnaik (1994) investigated the behavior of “rough” joints in composite concrete beams and their capacity to develop interface shear for different reinforcing steel ratios. The experimental program involved testing 16 composite concrete beams with two main test variables: clamping stress, and concrete strength. The joint preparation was described as “well compacted having a rough surface, clean and free of laitance, with coarse aggregate protruding but firmly fixed in the matrix” (*Loov and Patnaik 1994*). All beams were designed to fail in horizontal shear. The authors

recommended a parabolic equation for shear resistance based on the test results and it combines the effect of concrete strength and clamping stress. The authors proposed an equation that represents the test results more accurately compared to the design equation in ACI Code in 1963.

Patnaik (2001) studied the behavior of shear friction behavior of composite concrete beams with smooth interfaces. The experimental program consisted in testing 18 rectangular-shaped section beams and six T-shaped section beams with a smooth interface. Test variables include interface width, (d/s) ratio, and clamping stress, among other. The author reported that concrete strength and depth of the tensile reinforcing steel to spacing of the horizontal shear reinforcing steel ratio (d/s) had no significant influence on the horizontal shear strength. The author concluded that the ACI 318 provisions for horizontal shear in composite concrete beams is conservative.

Kahn and Slapkus (2004) evaluated the AASHTO (1998) and ACI 318-02 horizontal shear strength design provisions for the use of high-strength concrete at the interface created by a precast concrete beam and a cast-in-place deck. The experimental program consisted in testing six composite beams with precast webs with nominal strength 12 ksi (83 MPa). Test variables were concrete strength, and transverse reinforcement ratio. The authors reported results that indicated that AASHTO (1998) and ACI 318-02 provisions for horizontal shear are conservative for static loads. The authors recommend that current design provisions for shear friction and for interface shear in composite beams can be extended to high-strength concrete.

Kovach (2008) researched the horizontal shear stress of composite concrete beams without horizontal shear ties. The experimental program consisted in two phases totaling in thirty-two test specimens. The test variables considered were roughness of the composite interface surface finish and concrete strength of the slab. The author concluded that interface roughness has a significant on the horizontal shear capacity, therefore it is important to properly roughen the interface surface. It is important to note that the author mentioned some issues that may arise from push-off tests. Even though the point load applied to the test specimen is aligned in a way to avoid causing

eccentricities, these occur and result in an overturning moment causing the loaded element to pull away near the loaded edge. Stress concentrations can arise depending on the accuracy and correct alignment of the test setup, which can lead to non-conservative estimates of horizontal shear capacity.

Table 2.4: Reference parameters for the full scale composite beam specimens

Reference	Specimen size, in. (mm)	Number of specimens	Bar Size	Reinforcement ratio, ρ, %	Yield Stress, f_y, ksi (MPa)	Concrete Quality, f'c, ksi (MPa)
Seamann and Washa (1964)	96, 144, 240 x 17 x 15 (2438, 3658, 6096 x 432 x 381)	42	#3 (#10M), #4 (#13M)	0.00-1.07%	42.6 (293.7), 53.7 (370.2)	3 (20.7), 4.5 (31.0), 5.5 (37.9)
Loov and Patnaik (1994)	118.1 x 15.75 x 13.78 (2999.7 x 400 x 350)	16	#3 (#10M)	0.10-1.89%	59.0-63.5 (407-438)	2.8-7.5 (19.3-51.7)
Patnaik (2001)	Rectangular Beams: 106.3 x 13.78 x 9.84 (2700 x 350 x 250) T-Section Beams: 126.0 x 13.78 x 15.75 (3200 x 350 x 400)	18	0.22 in. (5.6 mm), 0.25 in. (6.4 mm), 0.34 in. (8.7 mm), 0.35 in. (8.9 mm), 0.56 in. (14.1 mm)	0.05-1.05%	49.3-102.1 (339.9-704.0)	2.5-5.0 (17-34.8)
Kahn and Slapkus (2004)	120 x 16.5 x 15.5 (3048 x 419 x 394)	6	#3 (#10M)	0.19-0.37%	80.7 (556)	7.3 (50.3), 11.3 (77.9)
Kovach (2008)	130 x 12 x 11.5 (3302 x 305 x 292)	35	N/A	0.00%	N/A	3 (20.7), 6 (41.4)
Fang et al. (2018)	94.5 x 15.7 x 13.8 (2400 x 400 x 300)	12	#3 (#10M)	0.00-0.698%	50 (345.86)	7.3 (50)

Fang et al. (2018) researched the interface shear behavior of normal weight and lightweight concrete composite T-beams compared to AASHTO and ACI design code

provisions. An experimental program was developed where 12 T-beams were tested with the variables of interface preparation, clamping stress, and lightweight slab concrete strength. The authors found that most composite beams failed at the horizontal shear interface in which the main test variables influencing the horizontal shear capacity were the interface preparation and clamping stress. The authors determined that AASHTO and ACI design code provisions predicted the interface shear capacity conservatively. The authors proposed a new equation to predict a more accurate interface shear capacity for different types of concrete with both smooth and rough shear interface preparations.

2.5 SUMMARY

This chapter consisted of reviewing available information related with shear friction theory and the effect of surface roughness and high-strength reinforcing steel. This comprehensive literature review compiled information on shear friction behavior and load transfer mechanisms, experimental programs using push-off test specimens and the equations in the main design specifications used in the United States.

Previous research has shown that before the peak shear capacity is reached the controlling parameters in concrete-to-concrete interfaces are cohesion and aggregate interlock. Aggregate interlock is influenced by surface roughness, clamping force, and aggregate size. After the peak shear capacity is reached, dowel action becomes the controlling parameter.

Limited research has been performed on specimens containing high strength steel and research is needed to gain a better understanding of its behavior in shear friction applications (Zeno 2009, Harries et al. 2012). Results from these experimental programs show that the shear interface capacity of the specimens can be overestimated when a yield strength higher than 60 ksi is used. Barbosa et al. (2017) reported results that indicated that as long as the reinforcing bars crossing the interface yields, a stress higher than 60 ksi (420 MPa) may be used to calculate the shear friction resistance. However, a group of test specimens from the same project reported that when the reinforcing bars did not yield the results are in agreement with

findings reported by Harries et al. (2012). Barbosa et al. (2017) determined that the reinforcement bar size and spacing may have an important effect over the results obtained. Surface preparation was not considered as a test variable in Harries et al. (2012) or Barbosa et al. (2017), therefore there is limited information on the influence it has over the behavior of shear friction interfaces.

3.0 EXPERIMENTAL PROGRAM AND SPECIMEN DESIGN

3.1 INTRODUCTION

Although high strength steel (HSS) reinforcement is commercially available today, its use is still limited. Currently, AASHTO limits the design yield stress of horizontal shear concrete interface reinforcing bars to 60 ksi (420 MPa). Some research on the application of HSS reinforcement bars in bridges (Trejo et al. 2014, Barbosa et al. 2017) has been performed but limited research has been done on the application of HSS reinforcement in concrete horizontal shear interface connections (Zeno 2009, Harries et al. 2012, Barbosa et al. 2017).

The objective of this study is to provide new data on the behavior of concrete cold joint interface connections reinforced with ASTM A706 Grade 80 ksi (550 MPa), ASTM A615 Grade 100 ksi (690 MPa), and ASTM A1035 – 16b Grade 120 ksi (830 MPa) reinforcing steel subjected to horizontal shear loading. To do this, specimens were designed based on ODOT (2014) BR300 standard drawing. These specimens simulated a girder-deck connection. Testing of these specimens provided data on the performance of horizontal shear interface connections reinforced with HSS reinforcement. Additional test variables not considered in previous research, such as interface preparation, reinforcing steel bar size, reinforcing steel bar spacing, and nominal concrete strength, are included to provide further insight into the behavior of concrete cold joint interface connections.

3.2 EXPERIMENTAL DESIGN

An experimental program was developed to assess the performance of A706 Grade 60 ksi, (420 MPa), A706 Grade 80 ksi (550 MPa), ASTM A615 Grade 100 ksi (690 MPa), ASTM A1035 – 16b Grade 120 ksi (830 MPa) reinforcing steel performance in shear friction applications. This experimental program included testing forty-five push-off test specimens separated into five groups depending on the test parameter being tested in each specimen. All 45 specimens were designed using ODOT (2014)

section 1.17.8.2, which refers to AASHTO (2014) 5.8.4 for design. The test variables included grade of reinforcing steel, interface preparation, bar spacing, bar size, and concrete nominal strength.

Figure 3.1 shows the naming convention for the specimens. The experimental test matrix is shown in Table 3.1.

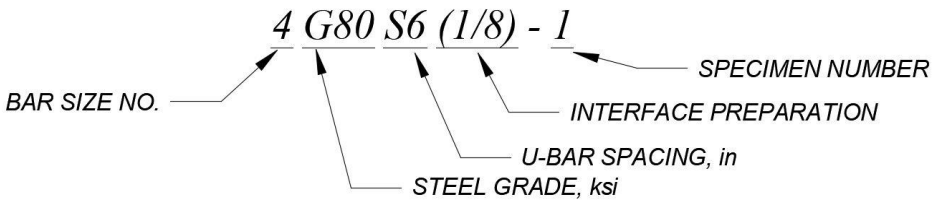

Figure 3.1: Naming convention of the push-off test specimen series.

Table 3.1 Experimental test matrix.

(a) Influence of Reinforcing Grade

Reinforcement Type	Grade, ksi	Nominal f_c', ksi	Interface Preparation	Rebar Spacing in.	Rebar Size	# of Specimens	Specimen Group Label
A706	**60**	**5**	**1/8" IR**	**6**	**#4**	**3**	**4G60S6(1/8)**
A706	**80**	**5**	**1/8" IR**	**6**	**#4**	**3**	**4G80S6(1/8)**
A615	**100**	**5**	**1/8" IR**	**6**	**#4**	**3**	**4G100S6(1/8)**
A1035	**120**	**5**	**1/8" IR**	**6**	**#4**	**3**	**4G120S6(1/8)**

(b) Influence of Interface Preparation

Reinforcement Type	Grade, ksi	Nominal f_c' ksi	Interface Preparation	Rebar Spacing, in.	Rebar Size	# of Specimens	Specimen Group Label
A706	**80**	**5**	**As Cast**	**6**	**#4**	**3**	**4G80S6(AC)**
A706	80	5	1/8" IR	6	#4	See 1(a)	4G80S6(1/8)
A706	**80**	**5**	**1/4" IR**	**6**	**#4**	**3**	**4G80S6(1/4)**
A706	**80**	**5**	**EA**	**6**	**#4**	**3**	**4G80S6(EA)**

(c) Influence of Bar Spacing

Reinforcement Type	Grade, ksi	Nominal f_c' ksi	Interface Preparation	Rebar Spacing, in.	Rebar Size	# of Specimens	Specimen Group Label
A706	**80**	**5**	**1/8" IR**	**4**	**#4**	**3**	**4G80S4(1/8)**
A706	80	5	1/8" IR	6	#4	See 1(a)	4G80S6(1/8)
A706	**80**	**5**	**1/8" IR**	**12**	**#4**	**3**	**4G80S12(1/8)**

(d) Influence of Reinforcing Bar Size

Reinforcement Type	Grade, ksi	Nominal f_c' ksi	Interface Preparation	Rebar Spacing, in.	Rebar Size	# of Specimens	Specimen Group Label
A706	80	5	As Cast	6	#4	See 1(b)	4G80S6(AC)
A706	**80**	**5**	**As Cast**	**6**	**#5**	**3**	**5G80S6(AC)**
A706	80	5	1/8" IR	6	#4	See 1(a)	4G80S6(1/8)
A706	**80**	**5**	**1/8" IR**	**6**	**#5**	**3**	**5G80S6(1/8)**
A706	80	5	1/4" IR	6	#4	See 1(b)	4G80S6(1/4)
A706	**80**	**5**	**1/4" IR**	**6**	**#5**	**3**	**5G80S6(1/4)**
A706	80	5	EA	6	#4	See 1(b)	4G80S6(EA)
A706	**80**	**5**	**EA**	**6**	**#5**	**3**	**5G80S6(EA)**

(e) Influence of Nominal Concrete Strength

Reinforcement Type	Grade, ksi	Nominal f_c' ksi	Interface Preparation	Rebar Spacing, in.	Rebar Size	# of Specimens	Specimen Group Label
A706	**80**	**3**	**1/8" IR**	**6**	**#4**	**3**	**4G80S6F3(1/8)**
A706	80	5	1/8" IR	6	#4	See 1(a)	4G80S6(1/8)
A706	**80**	**6**	**1/8" IR**	**6**	**#4**	**3**	**4G80S6F6(1/8)**

Total # of specimens (a) + (b) + (c) + (d) + (e) = 45 tests

Legend: Reinforcing steel grade – 60 ksi, 80 ksi, 100 ksi, 120 ksi. Nominal concrete strength – 3 ksi, 5 ksi, 6 ksi. IR – Intentionally roughened; *As Cast*: surface was leveled and not intentionally roughened; 1/8" IR: surface roughened to an amplitude of 1/8 in.; 1/4" IR: surface roughened to an amplitude of 1/4 in.; EA: Euclid Chemical Surface Retarder Formula S was utilized to expose the aggregate of the surface resulting in a surface roughened up to an amplitude of 1/4 in. Rebar spacing – 4 in., 6 in., 12 in. Rebar size – #4, #5.

Figure 3.2 shows the layout of the push-off test specimen with the deck (top) and girder (bottom) halves of the push-off test specimen, which are illustrated in the figure and referred to in this report as side 2 and side 1, respectively. The specimen presented in the figure is one that was constructed with three (3) U-Bars and 6 in. (152.4 mm) spacing between U-Bars, respectively.

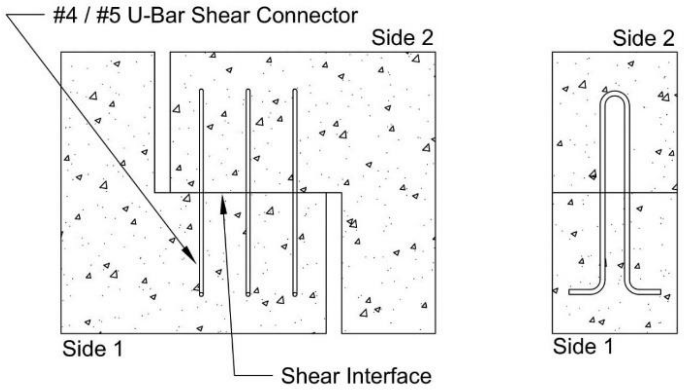

Figure 3.2: Simplified elevation schematic of push-off test specimen containing 3 U-bars to show side 2 (top), side 1 (bottom), reinforcing steel bars, and shear interface.

In the experimental design the actuator selected had a capacity limit (500 kips [2224 kN]), and to limit the probability of exceeding the actuator capacity during testing, an area of 2 in. (50.8 mm) by 20 in. (508 mm) was debonded on the interface of each specimen. Ultra-high-molecular-weight polyethylene (UHMW) strips with dimensions 2 in. (50.8 mm) by 20 in. (508 mm) by 0.25 in. (6.35 mm) were used to create the debonded area. Figure 3.3 shows the debonded area of the specimens along with the overall dimensions of the test specimens and the direction of the applied load.

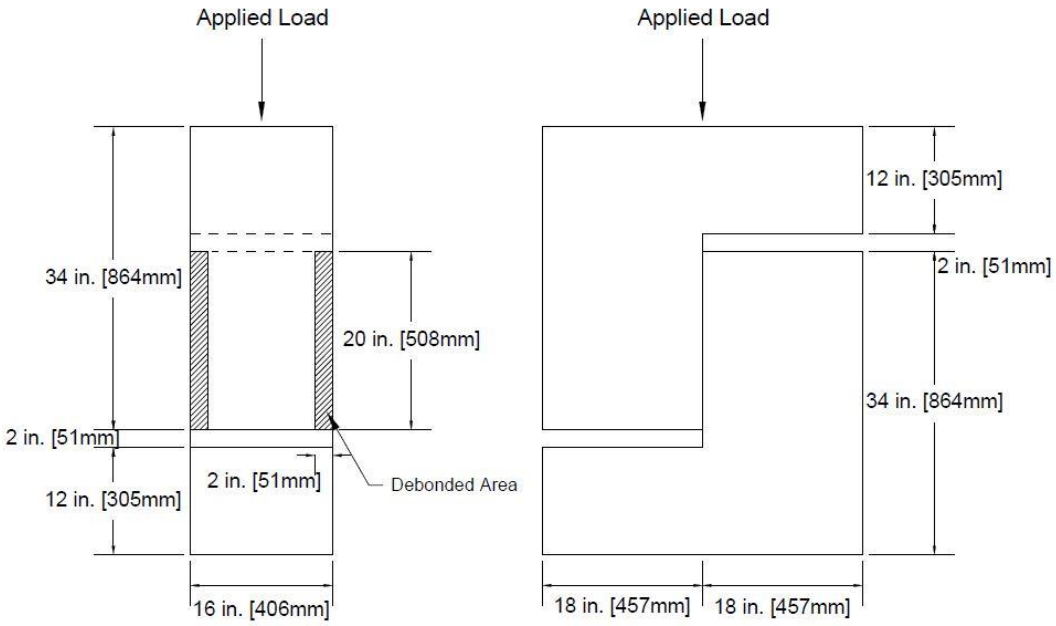

(a) (b)

Figure 3.3: (a) Front view elevation, (b) side view elevation. “Debonded area is shaded”.

3.3 PUSH-OFF TEST SPECIMENS DESIGN

Push-off test specimens were designed using ODOT (2014) section 1.17.8.2, which refers to AASHTO (2014) Section 5.8.4. A Strut-and-Tie model was developed to design the steel reinforcement layout, not including the U-bars crossing the shear interface. Detailed design procedure is shown in Appendix B.

3.3.1 Interface Shear Capacity Design

The interface shear capacity for all test specimens was calculated per AASHTO (2014) Section 5.8.4. Mathcad sheets were developed for each specimen group depending on the characteristics such as reinforcing steel bar grade, shear interface surface preparation, reinforcing steel bar spacing, reinforcing steel bar size, and nominal concrete strength. The Mathcad sheets are presented in Appendix B.

Out of all the specimens listed in Table 3.1, the maximum interface shear force of 410 kips (1824 kN) Thus, the experimental peak load is estimated to be 500 kips (2224 kN) assuming an over strength factor of 2.0 is used.

3.3.2 Interface Preparation

Four (4) different interface preparations were implemented to aid in the study of the influence of interface preparation on shear friction: (i) As Cast: surface was leveled and not intentionally roughened; (ii) surface roughened to an amplitude of 1/8 in. (3.175 mm); (iii) surface roughened to an amplitude of 1/4 in. (6.35 mm); and (iv) Exposed aggregate: Euclid Chemical Concrete Surface Retarder Formula S was utilized to expose the aggregate of the surface resulting in a surface roughened up to an amplitude of 1/4 in. (6.35 mm).

3.3.3 Reinforcing Steel Layout

Figure 3.4 shows the reinforcing steel layout for all specimen types. The differences between specimens are in the size, grade, and spacing of the reinforcing steel U-bars crossing the interface. The U-bars terminate in 90-degree standard hooks that satisfy AASHTO (2014) Section 5.10.2.1 and all bend diameters satisfy AASHTO (2014) Table 5.10.2.3-1. All other reinforcing steel (other than the reinforcement that crossed the interface) met ASTM A706 Grade 60 ksi (420 MPa). Stirrups were designed to be #4 (#13M) bars. Longitudinal reinforcing steel was designed to be #6 (#19M) bars. All longitudinal bars terminate with 90-degree hooks. All transverse stirrups end with 135-degree hooks. Figure 3.5 shows a section view of specimens constructed with three #4 (#13M) bars.

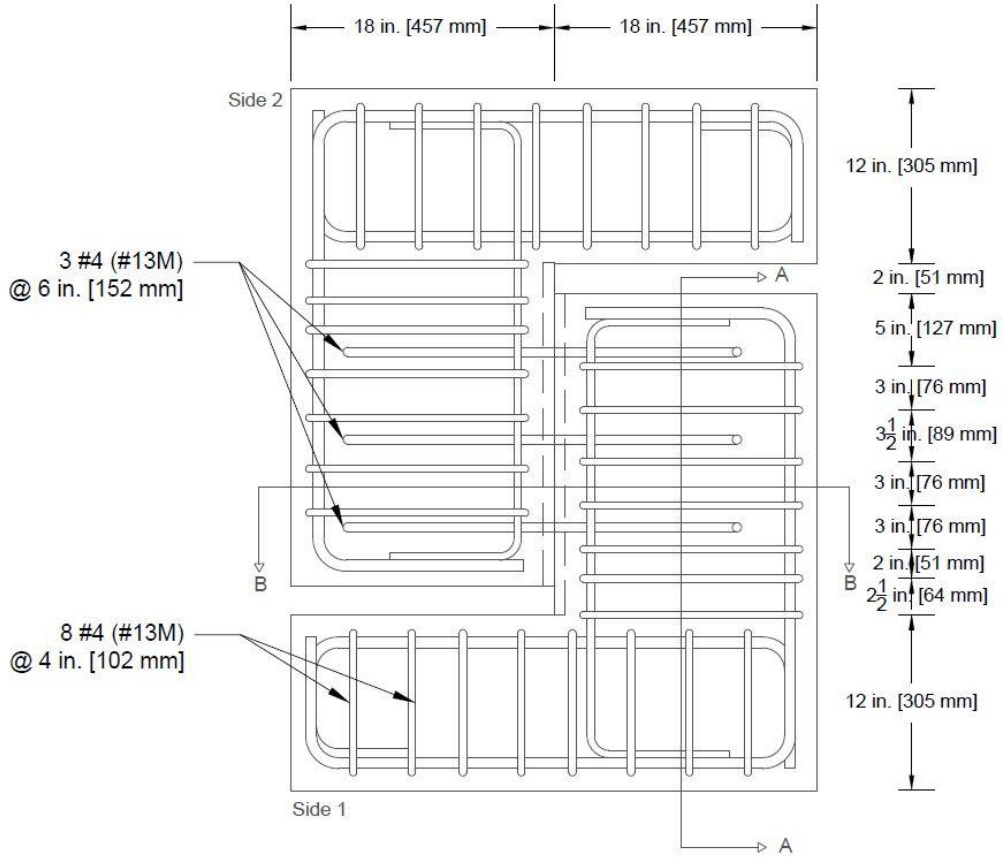

Figure 3.4: Steel layout for a specimen containing three #4 U-bars spaced at 6 in. (152 mm).

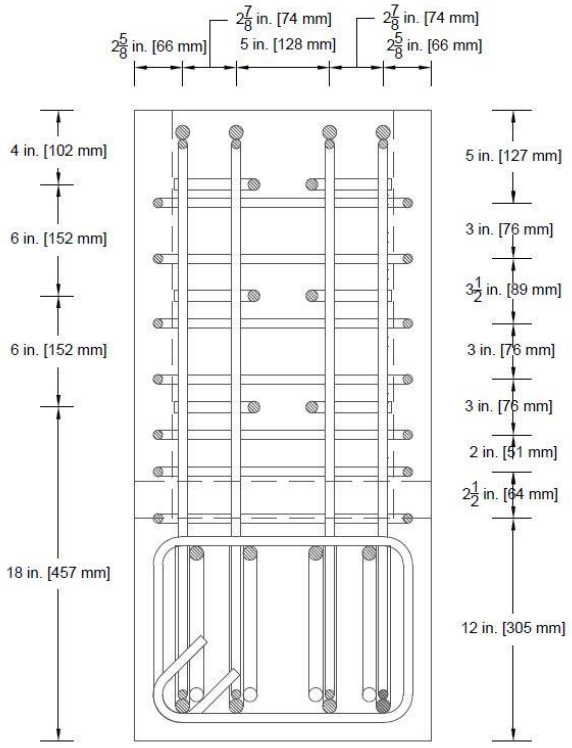

Figure 3.5: Section A-A steel layout for a specimen containing three #4 U-bars spaced at 6 in. (152 mm).

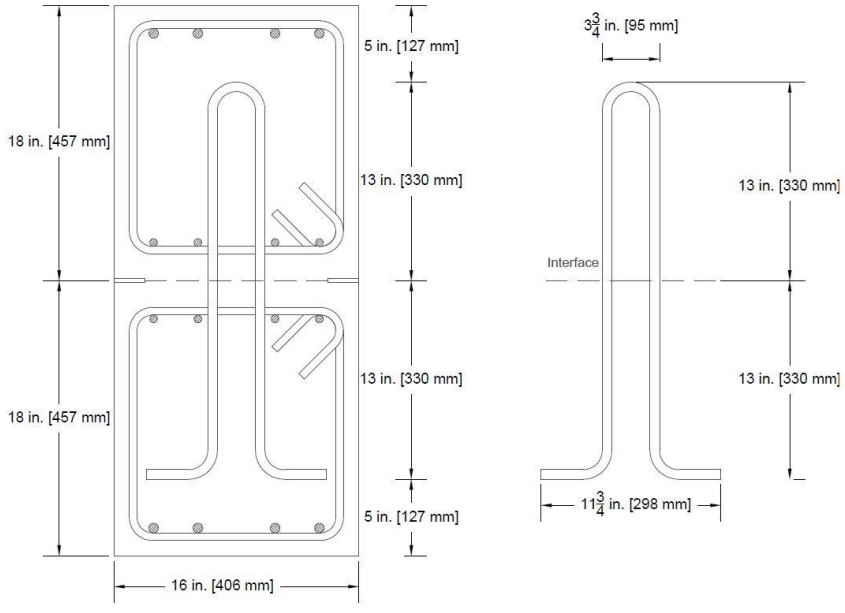

Figure 3.6: Section B-B steel layout for a specimen containing three #4 U-bars spaced at 6 in. (152 mm).

3.4 PUSH-OFF TEST PROCEDURES

The following section discusses the push-off test setup, instrumentation, and testing procedures. Setup procedures, instrumentation for stress and displacement measurement, and rate of loading during the test are presented.

3.4.1 Push-off Test Setup

Figure 3.7 shows an overall view of the specimen and Figure 3.8 shows a photograph of the test setup. Appendix E shows isometric views of the test specimen setups. These figures illustrate the actuator, test specimen, top roller and plates, base plates, roller supports, actuator displacement transducer (LVDT), and reaction frame. Elevation views are shown in Figure 3.9 and Figure 3.10.

Each test was initiated by placing the test specimen in the center of two 4 in. wide steel plates resting on top of the main load transfer base steel plates. It was important to ensure that the specimen interface shear plane was aligned with the load path of the actuator, thus minimizing local stresses due to an eccentric load. A laser level was used to maximize alignment accuracy by aligning the center of the actuator with the specimen interface shear plane. Once the specimen was aligned in the direction parallel to the shear interface, the rollers supports were adjusted to hold the specimen in place. To align the specimen in the direction perpendicular to the shear interface the roller supports on the south side of the specimen were adjusted. Once the rollers were temporarily in place, the specimen was lowered into position. After the test specimen was in position, the reaction frame on the north side was set into place with the overhead crane. The roller guides on all sides were adjusted to be within 0.125 in. (3.2 mm) of the specimen on each side, with the exception of the top roller on the north side reaction frame which was set 2 in. (51 mm) to allow the top side to move, and therefore for cracks to form across the interface being tested, during the tests. Once all the rollers were in place, the top load transfer plates were placed and aligned with the axis of the actuator. External instrumentation was put into place, then all instrumentation was connected, using wire splicers, to the DAQ.

The actuator was placed on manual displacement and lowered to be 0.125 in. (3.2 mm) above the top loading plate. The test rate was then set to 0.001 in./sec (0.0254 mm/sec). The actuator was lowered and stopped when an initial force of 0.5 kip (2.2 kN) was reached to ensure the top plate is tight in place. The pumps were turned off momentarily to adjust the LVDT measuring actuator displacement. This ensured the LVDT would capture the testing displacements within the actuator stroke length limits.

The sensors data started being logged once the pumps were turned back on. The loading rate was set to 0.001 in./sec (0.0254 mm/sec) and the test was initiated in displacement control. The test was paused at the moment when the actuator force is approximately 20 kip (89 kN) to ensure all sensors were working properly. Testing was then continued until a displacement of 0.5 in. (13 mm) was reached, after which the test rate was set to 0.005 in./s (0.127 mm/s). The test ended when the 2 in. (51 mm) gap between the top and bottom sides of the specimen was closed, or when all the reinforcing steel U-bars across the interface ruptured.

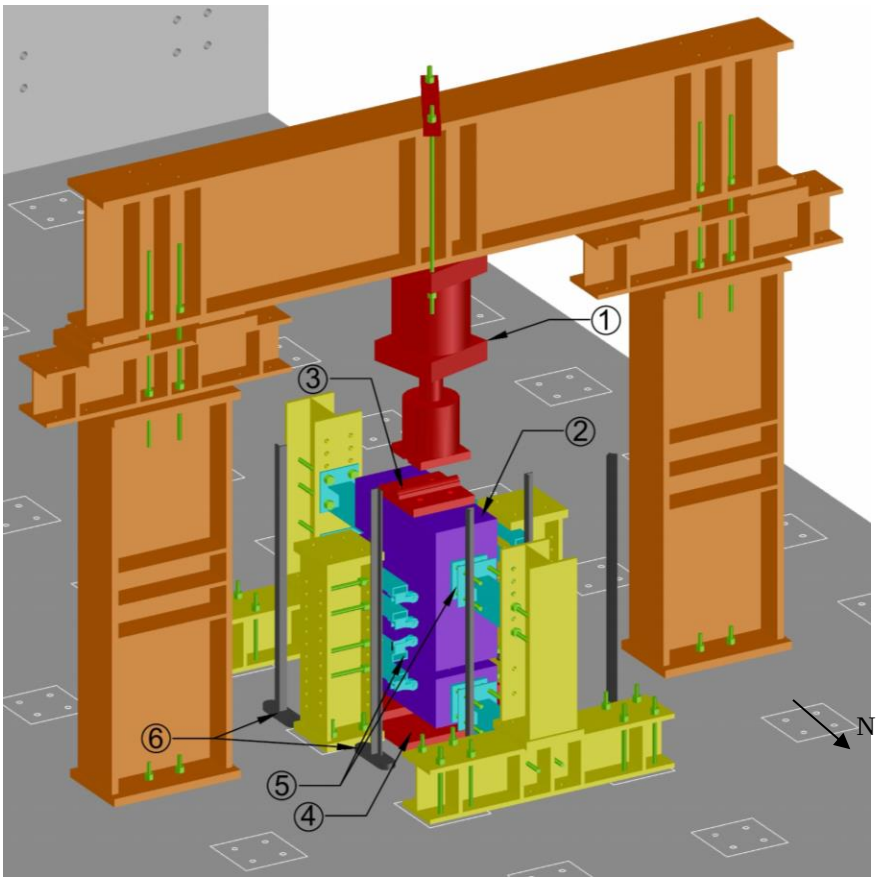

Figure 3.7 General overview of the test setup.

Legend – 1:Actuator; 2: test specimen; 3:roller plate; 4: base plate; 5: roller support for safety (gap provided between rollers and specimen); 6: LVDT sensor supports.

Figure 3.8: Photograph of specimen before testing.

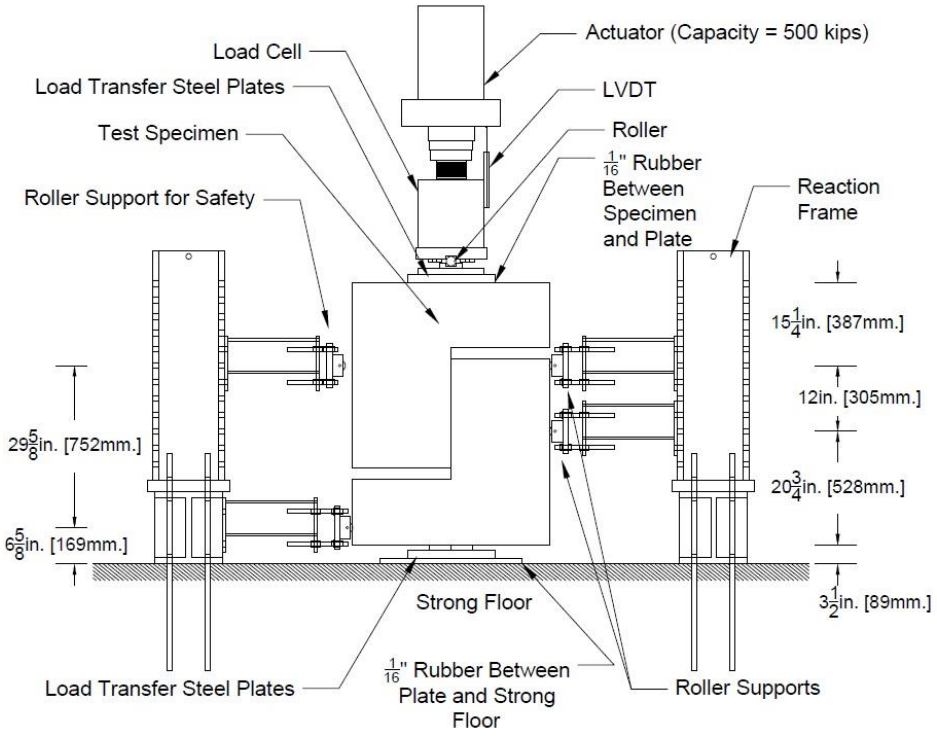

Figure 3.9: North-south elevation view of test setup.

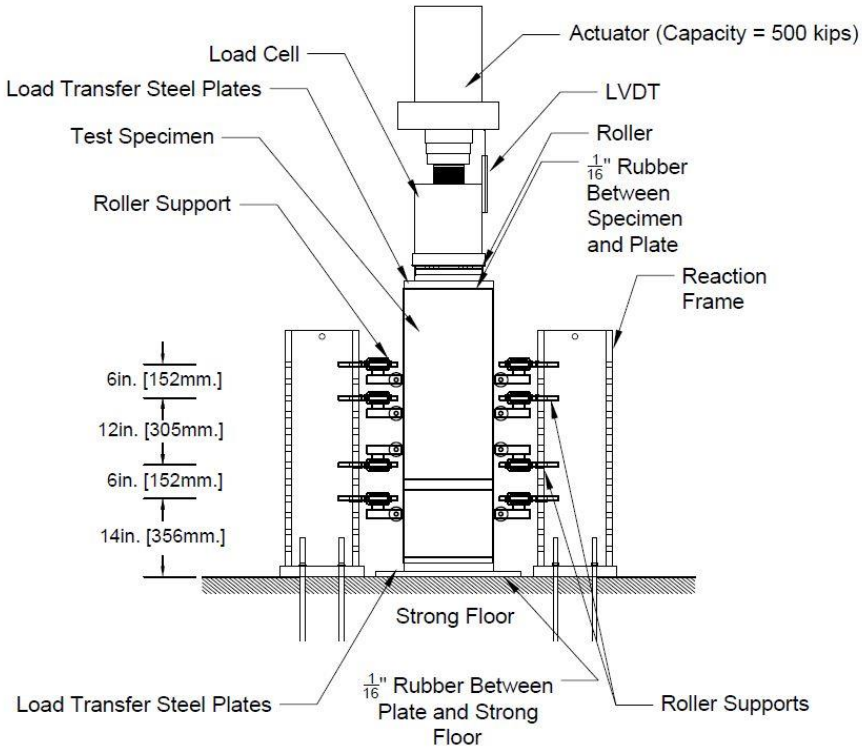

Figure 3.10: East-west elevation view of test setup.

3.5 INSTRUMENTATION

Instrumentation was used to monitor the movement of the test specimen and the strains of the U-bars during testing. Figure 3.11 shows the external instrumentation used and Table 3.2 lists the external instrumentation used with the corresponding measurement that was targeted. The vertical displacement of the top L-shape was measured with two (2) string potentiometers (label 1) attached on the face of the specimen and 8 in. (203 mm) from the vertical alignment of the shear interface. The shear interface separation was measured with two (2) Duncan pots (label 2). The tip of the Duncan pot plungers rested on UHMW plastic plates to minimize friction. The base movement was measured using four (4) Duncan pots (labels 3 and lower label 5) placed at 2 in. (51 mm) from the side edge and bottom edge. Two (2) 6 in. (152 mm) LVDTs (label 4) were used to measure the vertical movement of the top L-shape. Their measurements were used to determine if there was rotation of the top L-shape. The plunger of the LVDTs rested on top of UHMW plastic strips to minimize friction. Four (4) Duncan pots were attached 3 in. (76 mm) from the top face to measure potential lateral movement of the top L-shape. One (1) string potentiometer was used to measure the reaction frame beam displacement (label 6). The actuator displacement was measured by an LVDT attached to the actuator (label 7). Prior to the first test, all instruments were calibrated with a Mitutoyo Absolute Digimatic Height Gage (Series 570).

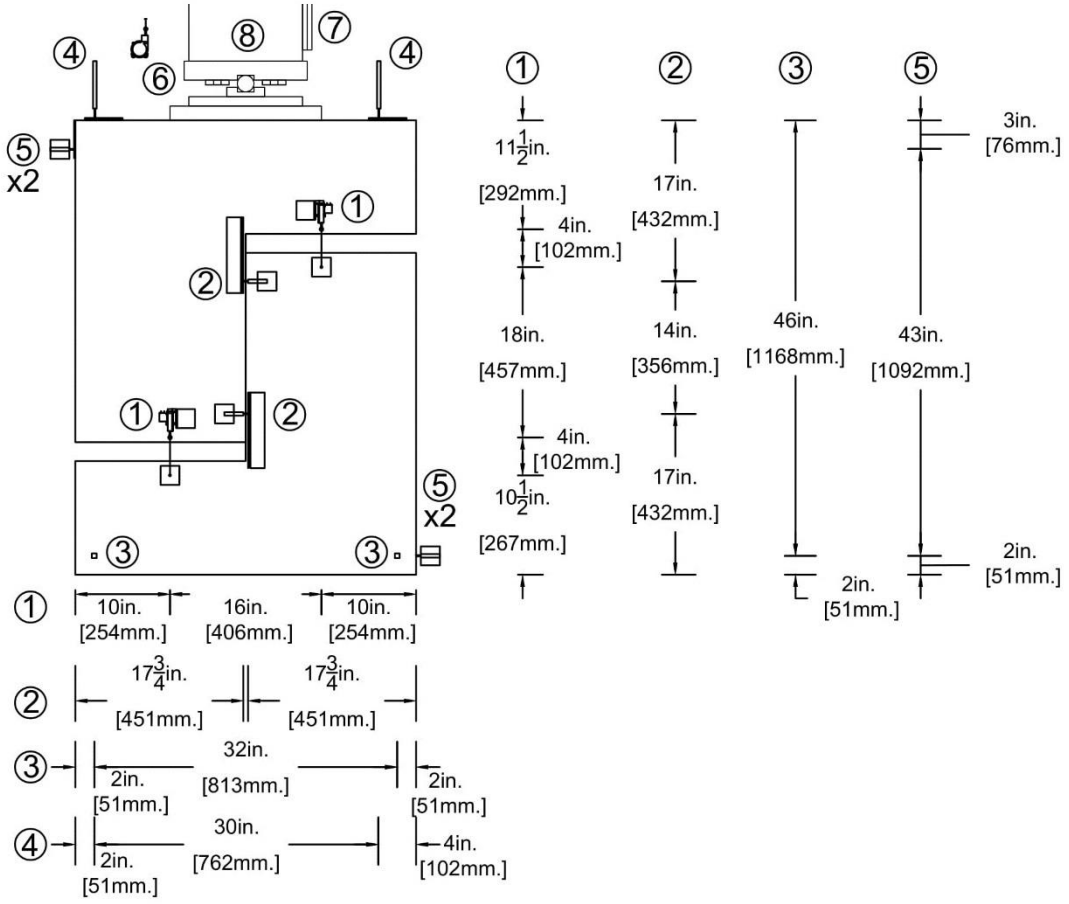

Figure 3.11: North-south external instrumentation elevation view.

Table 3.2: Summary of instrumentation.

Instrumentation	Objective	Figure 3.11 label
4 Duncan pots (1.5” stroke)	Specimen base movement	3 & 5
4 Duncan pots (1.5” stroke)	Specimen top lateral movement	5
2 LVDT’s (6” stroke)	Specimen top vertical movement	4
2 String pots (2” stroke)	Shear interface vertical movement	1
2 Duncan pots (1.5” stroke)	Shear interface horizontal movement	2
1 Actuator	Applied shear load	8
1 LVDT (12” stroke)	Actuator displacement	7
1 string pot (2” stroke)	Reaction frame beam displacement	6

Internal instrumentation used consisted of strain gauges placed on the reinforcing bars crossing the shear interface for all specimens. Strain gauges were placed at 3 in. (76 mm) from the interface on both legs of every U-bar to ensure data collection after

initiation of cracking of the concrete interface. An additional strain gauge was placed at 1 in. (25 mm) on one U-bar. All strain gauges were placed on the inside of the 90° bend of the reinforcing steel U-bars. Strain gauges were labeled s1 to s5, s1 to s7, and s1 to s9 in specimens constructed with two, three, and four reinforcing steel U-bars, respectively. Table 3.3, Table 3.4, and Table 3.5 present descriptions of the strain gauge labels and locations for specimens constructed with two, three, and four reinforcing steel U-bars, respectively. Figure 3.12, Figure 3.13, and Figure 3.14 present an illustration of the location of the reinforcing steel U-bars in the specimen, the location of the strain gauges on each bar in the specimen, and a front view of the reinforcing steel U-bar showing the strain gauges located at 1 in. (25 mm) and 3 in. (76 mm) on the reinforcing steel U-bar for specimens constructed with two, three, and four reinforcing steel U-bars, respectively.

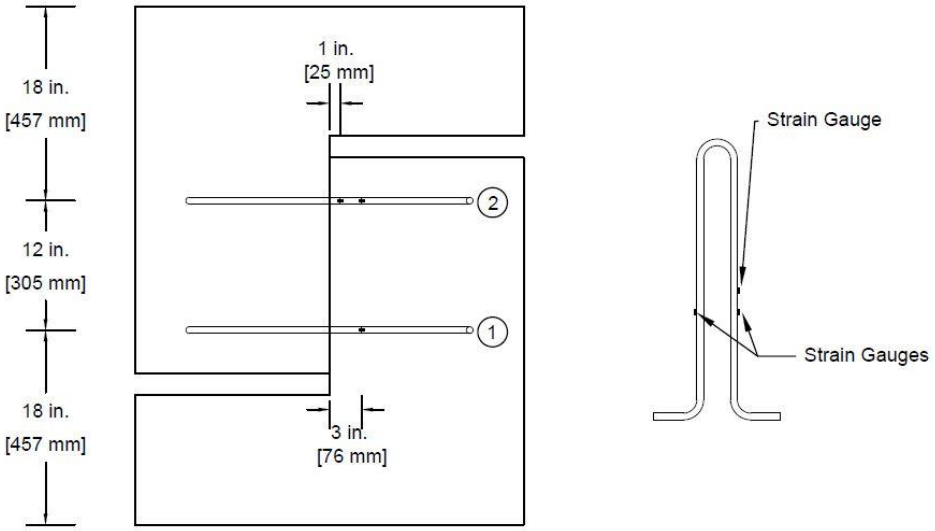

(a) (b)

Figure 3.12: (a) Internal instrumentation elevation for specimens constructed with 2 reinforcing steel U-bars; (b) U-bar.

Table 3.3: Strain gauge labels for specimens containing 2 reinforcing steel U-bars.

Strain gauge label	Bar Number	Side	Distance from interface, in. (mm)
s_1	1	West	3 (76)
s_2	2	West	3 (76)
s_3	2	West	1 (25)
s_4	1	East	3 (76)
s_5	2	East	3 (76)

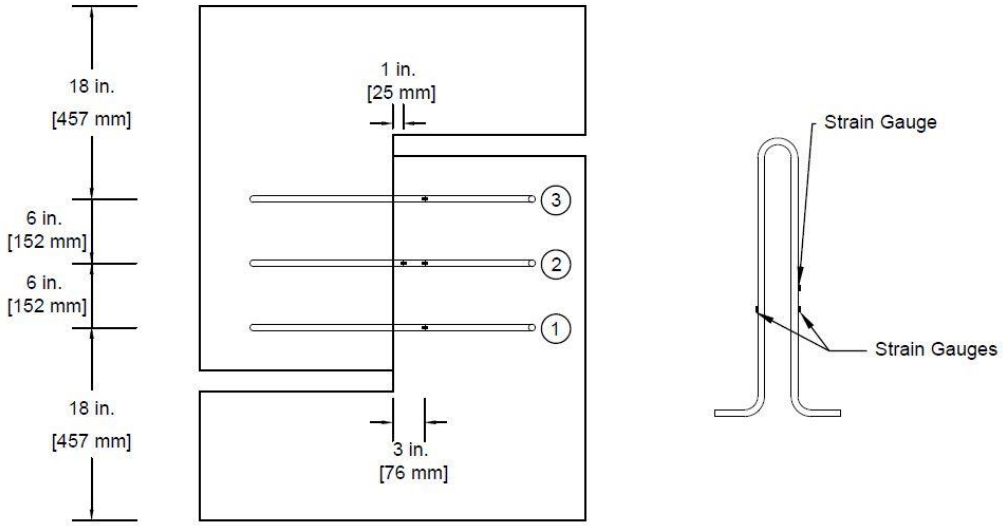

(a) (b)

Figure 3.13: (a) Internal instrumentation elevation for specimens constructed with 3 reinforcing steel U-bars; (b) U-bar

Table 3.4: Strain gauge labels for specimens containing 3 reinforcing steel U-bars.

Strain gauge label	Bar Number	Side	Distance from interface, in. (mm)
s_1	1	West	3 (76)
s_2	2	West	3 (76)
s_3	3	West	3 (76)
s_4	2	West	1 (25)
s_5	1	East	3 (76)
s_6	2	East	3 (76)
s_7	3	East	3 (76)

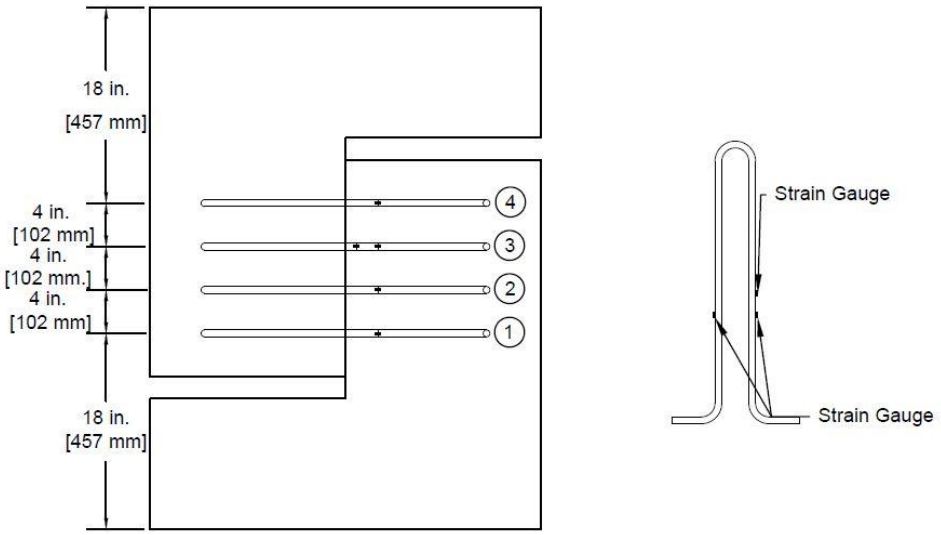

(a) (b)

Figure 3.14: (a) Internal instrumentation elevation for specimens constructed with 4 reinforcing steel U-bars; (b) U-bar.

Table 3.5: Strain gauge labels for specimens containing 4 reinforcing steel U-bars.

Strain gauge label	Bar Number	Side	Distance from interface, in. (mm)
s_1	1	West	3 (76)
s_2	2	West	3 (76)
s_3	3	West	3 (76)
s_4	4	West	3 (76)
s_5	3	West	1 (25)
s_6	1	East	3 (76)
s_7	2	East	3 (76)
s_8	3	East	3 (76)
s_9	4	East	3 (76)

(a) (b)

Figure 3.15: Strain gauges applied to reinforcing steel U-bar (a) view of strain gauge with initial protective coating and (b) view of U-bars with strain gauges after these were installed.

3.6 CONSTRUCTION PROCEDURE

The push-off test specimens were fabricated in the Structural Engineering Research Laboratory at Oregon State University. The test specimens were cast in two concrete placements. The construction sequence and procedures used are summarized below.

1. Installation of strain gauges on U-bars as shown in Figure 3.15;

2. Construction and assembly of formwork as shown in Figure 3.16. Formwork for side 1 was placed on a leveled surface, squared, and strapped;

3. Assembly of reinforcing steel L-cages. Stirrup locations were measured and marked. Rebar tie wire was used to tie steel cages. A construction square was used to ensure the cages were square. As specimens were symmetrical, both side 1 and side 2 had the same L-shape cage configuration. Example specimen cages are shown in Figure 3.17;

4. Placement of the L-cages in the formwork. The L-shape cage was placed into formwork with plastic spacer guides as shown in Figure 3.18. Loose ties and other objects were cleaned out of the formwork before casting;

5. Placement of reinforcing steel U-bars. Plywood pieces marked with the correct reinforcing bar spacing were placed under the U-bars to ensure that they were normal to the interface and at the designed spacing, as shown in Figure 3.19;

6. Casting of side 1. Concrete was cast and consolidated, struck level with the surface, and interfaces finished accordingly. For the initial curing phase, burlap and plastic were placed over the concrete immediately after casting and wetted once in the morning and once in the evening. Plastic sheets were placed immediately after casting. Wetting of the specimen started on the day after casting and went on for three days. After three days, the burlap and plastic were removed. Cast specimens are shown in Figure 3.20;

7. Assembly and placement of Side 2 L-cages. L-shape cages for side 2 were assembled and placed on top of side 1, as shown in Figure 3.21;

8. Placement of Side 2 formwork. The second set of formwork was installed, and plastic spacers were used to ensure the correct cover is achieved as shown in Figure 3.22.

9. Casting of Side 2. Concrete was cast and consolidated and struck level with the top of the formwork. Curing followed the same procedure explained in step 6. After three days, the burlap and plastic were removed.

10. The formwork was removed 7 days later. The specimens were all labelled immediately after formwork was removed. Figure 3.23 shows a test specimen after formwork removal.

Figure 3.16: Formwork construction.

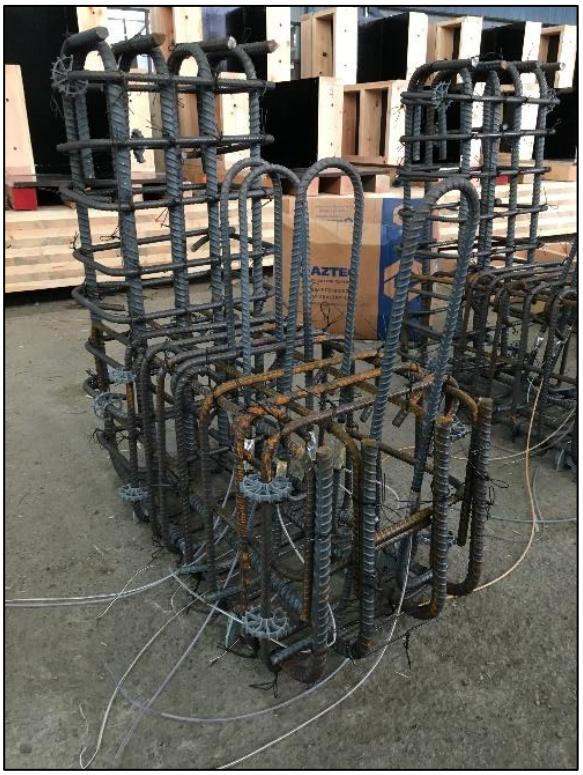

Figure 3.17: Cage for a specimen containing #4 (#13M) reinforcing bars across the interface.

Figure 3.18: Cage is inserted into formwork.

Figure 3.19: The L-shape half of a specimen containing #4 (#13M) U-bars at the correct location.

Figure 3.20: Cast specimens after the concrete pour of side 1.

Figure 3.21: Top L-shaped cage placed on top of specimen.

Figure 3.22: Top L-shaped cage placed inside formwork.

Figure 3.23: Constructed specimens after formwork removal.

3.7 POST-PROCESSING OF EXPERIMENTAL RESULTS

The results of the force-displacement, force-crack width, and force-strain response for each push-off test specimen are reported in the following sections. The displacement of the shear interface was measured to gain a better understanding of the effect of concrete cohesion, aggregate interlock, and dowel action at the different stages of deformation. The strain in the reinforcing steel U-bars is measured because it was useful in computing the clamping force generated by the reinforcing steel U-bars, which has a direct effect on aggregate interlock. Crack width is an important parameter to measure due to its relation to the concrete-to-concrete cohesion component and the clamping force generated by the reinforcing steel U-bars. Crack width has an inverse relation to the cohesion component, in other words the cohesion component degrades as crack width increases. In contrast, the clamping force in the reinforcing steel U-bars will increase as crack width increases. Section 3.5 provides a detailed explanation of the instrumentation used to measure these parameters.

The typical force-displacement response of a push-off test specimen can be seen in Figure 3.24. There are five important points to highlight from the response, which are: (i) Δ_{cr}, V_{cr}: loss of cohesion identified as described in this section; (ii) V_{ult}, Δ_{ult}: peak interface shear load and corresponding displacement, respectively; (iii) $V_{sus,min}$: minimum sustained interface shear force during post-peak response; (iv) $V_{sus,max}$: maximum sustained interface shear force during post-peak response; and (v) V_b, Δ_b: interface shear force and displacement at the moment the first bar fractures, respectively. The tabulated values for each important point of interest are obtained from the response curves of each individual specimen.

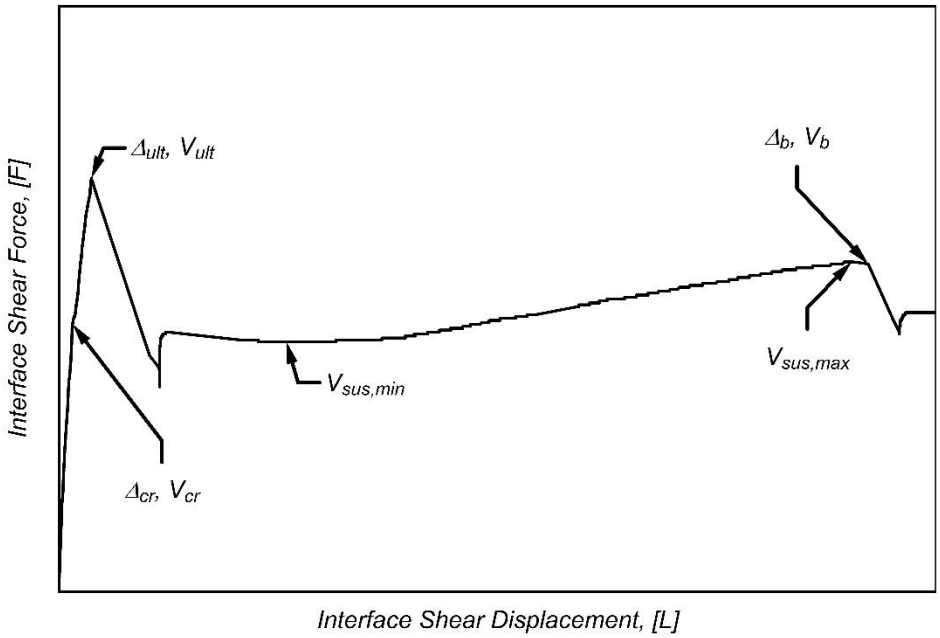

Figure 3.24: Typical force-displacement response of push-off tests and definition of notable parameters.

A standardized method was developed to determine the cracking interface shear force at the point of loss of cohesion, V_{cr}. Figure 3.25 presents a graph illustrating the standardized method for a typical test specimen force-strain response. The standardized method consists of the following four steps: (1) the interface shear force versus reinforcing steel microstrain relationship is plotted. The reinforcing steel microstrain used corresponds to readings from the strain gauge located at 1 in. (25.4 mm) from the interface, as it provides the closest measurement of the strain on the reinforcing steel bar; (2) the values of the interface shear force versus reinforcing steel microstrain curve between $0.1\varepsilon_y$ and $0.2\varepsilon_y$ are isolated to be used to develop a curve fit. These limits were chosen due to their proximity to the inflection point identifying the reduction of stiffness that results from the loss of cohesion, and because they are both within the limits of the reinforcing steel bars being well engaged and linear-elastic behavior of the reinforcing steel bar; (3) the value of the cracking interface shear force at the point of loss of cohesion, V_{cr}, is taken as the y-intercept of the resulting linear fit; and, (4) the corresponding cracking displacement at the point of loss of cohesion, Δ_{cr}, is determined as the interface shear displacement

corresponding to the cracking interface shear force load in the interface shear force versus interface shear displacement response.

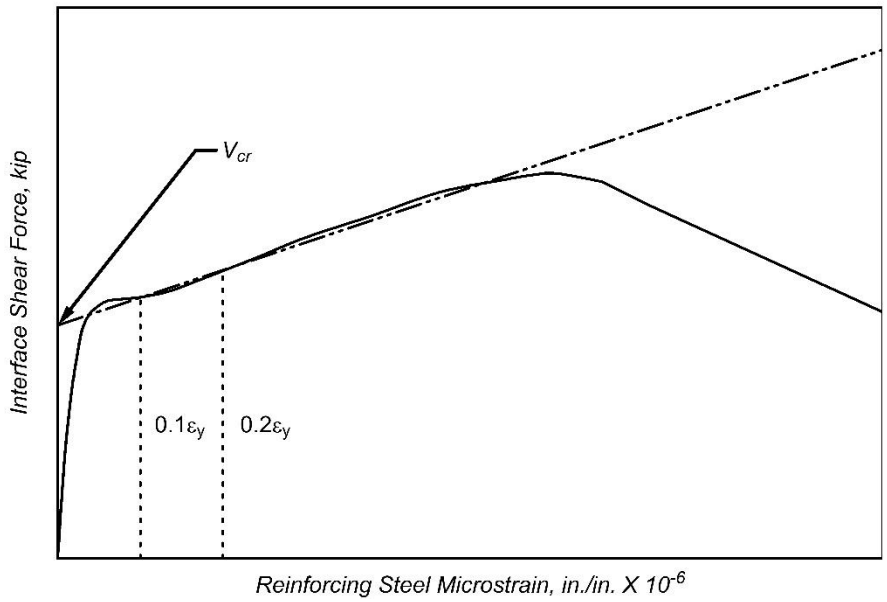

Figure 3.25: Illustration of the points used to determine the point of loss of cohesion.

4.0 MATERIALS

4.1 REINFORCING STEEL

Test specimens were constructed using three types of reinforcing steel U-bars (ASTM A615, ASTM A706, and ASTM A1035) and four grades (60 ksi (420 MPa), 80 ksi (550 MPa), 100 ksi (690 MPa), and 120 ksi (830 MPa)). For ASTM A706 Grade 80, two bar sizes were used, #4 (#13M) and #5 (#16M). For all other grades #4 (#13M) bars were used. All of the reinforcing U-bars were provided by Cascade Steel located in McMinnville, Oregon. U-bars were cut and bent at Oregon State University. Farwest Steel, Eugene, Oregon provided and bent all other specimen reinforcing bars used to construct the specimen rebar cages.

Table 4.1 shows the bar sizes and mechanical properties of the reinforcing bar as reported by the manufacturers. Table 4.2 shows the chemical composition of the reinforcing steel bars tested from the steel certification provided by the manufacturers.

Table 4.3 shows the results from tensile testing from testing performed at Oregon State University. The tensile testing followed ASTM E8/E8M-13a (ASTM 2013). Three (3) specimens were tested for each size and grade of reinforcing steel. All specimens were marked by a metal punch and tested in a 250 kN INSTRON universal testing machine (UTM) Model 5985 at an 8-in. (203.2 mm) grip-to-grip length, per the specifications defined in ASTM A615/A615M-16 (ASTM 2016a), ASTM A706/A706M-16 (ASTM 2016b), and ASTM A1035/A1035-16b (ASTM 2016c). A 3 in. (76 mm) grip length on both ends of the specimen was maintained for all tests. All specimens were tested at a constant displacement rate of 0.0003 in./sec (0.00762 mm/sec) until rupture. A static axial clip-on extensometer that meets the requirements of ASTM E83-16 (ASTM 2016d) was hooked at the center of the specimen for strain measurements. The UTM force, the UTM displacement, and the extensometer output were recorded at 100 millisecond intervals. The extensometer was removed at a strain value of 0.08 for the ASTM 706 Grade 60 (420 MPa), the ASTM 615 Grade 80 (550 MPa), the ASTM 706 Grade 80 (550 MPa), and the ASTM 615 Grade 100 (690 MPa)

specimens. For ASTM 1035 (CRX4100 and CRX9100) specimens, the extensometer was removed at a strain value of 0.03 and 0.06, respectively. A curve-fitting technique was used to establish relationship between the extensometer strain and the UTM displacement-computed-strain measured prior to extensometer removal. Using the fitted function, the post extensometer-removal strains were extrapolated based on the displacement of the UTM head recorded during the test.

Table 4.3 provides a summary of tensile test results, including the elastic modulus, yield point stress and strain and percentage elongation over an 8-inch gauge length for the specimens tested. The yield stress was determined using both (1) the 0.2% offset method and (2) the 'Extension Under Load' (EUL) method, as described in ASTM E8/E8M-13a (ASTM 2013). A strain value of 0.0035 in/in (mm/mm) strain was chosen for the EUL method. For the elastic modulus, data falling in the stress range of 20 ksi (140 MPa) to 60 ksi (420 MPa) were considered for the elastic modulus calculations of ASTM 706 Grade 60 (420 MPa) steel reinforcing bars, while for all other grades, the stress range of 20 ksi (140 MPa) to 80 ksi (550 MPa) was considered in the estimation of the Young's modulus. It is important to note that ASTM A1035-16b Type CM Grade 100 (690 MPa) reinforcing steel, as described in the steel mill data, met the tensile properties requirements for a Grade 120 denomination per standard ASTM A1035/A1035M-16b, even though the mill data denominates it as Grade 100, as results show in Table 4.3. Therefore, this material was referred to as A1035/A1035M-16b Grade 120 (830 MPa) reinforcing steel. Table 4.4 lists the stress and strain values at the onset of strain hardening, peak tensile point and rupture points. These are needed to characterize the main points defining the stress-strain curves. Figure 4.1 through Figure 4.8 show the stress-strain curves of each of the bar types and sizes.

Table 4.1: Mechanical and physical properties of reinforcing steel bars (mill data).

Product ID	Grade	Rebar Size	Heat #	Yield strength, ksi (MPa)	Tensile strength, ksi (MPa)	Elong. % 8 in. (0.2 m)*
#4 706/60	ASTM A706-16 Grade 60	#4 (#13M)	195517	67.5 (465)	95 (655)	18
#5 706/60		#5 (#16M)	211217	67 (462)	94.5 (652)	16
#4 615/80	ASTM A615-16 Grade 80	#4 (#13M)	013517	89.5 (617)	125 (862)	11
#5 615/80		#5 (#16M)	220817	87.5 (603)	121 (834)	12
#4 706/80	ASTM A706-16 Grade 80	#4 (#13M)	062517	91 (627)	116 (800)	14
#5 706/80		#5 (#16M)	042517	89.5 (617)	116 (800)	13
#4 615/100	ASTM A615-16 Grade 100	#4 (#13M)	511215	103 (710)	131 (903)	12
#5 615/100		#5 (#16M)	503615	108 (745)	141 (972)	9.5
#4 CRX4100	ASTM A1035-16b Type CM Grade 100**	#4 (#13M)	179817	119 (820)	160 (1103)	9
#5 CRX4100		#5 (#16M)	059417	136 (938)	165 (1138)	9
#4 CRX9100	ASTM A1035-16b Type CS Grade 100**	#4 (#13M)	166016	133 (917)	170 (1172)	11
#5 CRX 9100		#5 (#16M)	165916	131 (903)	164 (1131)	10

*According to ASTM A706.

** Meets tensile properties requirements for Grade 120 denomination per subsequent reinforcing bar tensile test results summary shown in Table 4.3.These were therefore relabeled as Grade 120.

Table 4.2: Chemical composition of reinforcing steel bars (mill data).

Product ID	C	Mn	P	S	Si	Cu	Ni	Cr	V	Mo	Sn	N_2	CE*
#4 706/60	0.28	1.22	0.03	0.02	0.23	0.24	0.06	0.17	0.03	0.02	0.02	-	0.5
#5 706/60	0.28	1.28	0.02	0.02	0.23	0.24	0.08	0.13	0.03	0.02	0.01	-	0.52
#4 615/80	0.44	1.27	0.02	0.02	0.26	0.28	0.08	0.16	-	0.02	0.02	-	0.67
#5 615/80	0.43	1.22	0.02	0.02	0.28	0.29	0.07	0.16	-	0.02	-	-	0.66
#4 706/80	0.27	1.33	0.20	0.01	0.24	0.28	0.05	0.16	-	0.01	0.02	-	0.51
#5 706/80	0.27	1.35	0.02	0.02	0.24	0.28	0.06	0.15	-	0.11	-	-	0.51
#4 615/100	0.34	1.34	0.02	0.02	0.25	0.27	0.09	0.12	0.17	0.02	0.02	-	0.57
#5 615/100	0.37	1.34	0.30	0.02	0.27	0.22	0.07	0.14	-	0.15	-	-	0.60
#4 CRX4100	0.10	1.33	0.01	0.01	0.35	0.18	0.06	4.15	0.01	0.02	0.01	0.01	0.74
#5 CRX4100	0.09	0.87	0.01	0.01	0.36	0.14	0.04	4.68	0.01	0.01	0.01	0.01	0.71
#4 CRX9100	0.11	0.58	0.01	0.01	0.39	0.14	0.10	9.54	0.03	0.01	0.01	0.02	1.17
#5 CRX9100	0.09	0.58	0.01	0.01	0.39	0.16	0.10	9.42	0.03	0.02	0.01	0.02	1.14

*CE is defined as the Carbon Equivalent by ASTM A706/A706M-14, Standard Specification for Deformed and Plain Low-Alloy Steel Bars for Concrete Reinforcement.

Table 4.3: Reinforcing steel bar tensile test results summary.

Product ID	Elastic Modulus ksi (MPa)	Yield point (0.2% offset)		Yield point (0.0035 EUL)		Tensile strength point		Ultimate strain		% Elong in 8 in. (203 mm)
		Stress, ksi (MPa)	Strain, in./in. (-)	Stress, ksi (MPa)	Strain, in./in. (-)	Stress, ksi (MPa)	Strain, in./in. (-)	Stress, ksi (MPa)	Strain, in./in. (-)	
#4 706/60	28964 (199700)	64.04 (442)	0.0043	64.08 (442)	0.0035	92.42 (637)	0.121	65.74 (453)	0.157	17.23
#5 706/60	28296 (195094)	65.15 (449)	0.0043	65.15 (449)	0.0035	94.56 (652)	0.112	71.87 (496)	0.170	15.79
#4 615/80	29254 (201699)	85.95 (593)	0.0049	95.88 (661)	0.0035	120.9 (833)	0.091	93.86 (647)	0.132	12.71
#5 615/80	30131 (207746)	85.63 (590)	0.0048	85.74 (591)	0.0035	121.5 (837)	0.092	110.4 (761)	0.126	11.72
#4 706/80	28203 (194453)	88.63 (611)	0.0052	88.37 (609)	0.0035	114.3 (788)	0.098	83.42 (575)	0.135	13.51
#5 706/80	27704 (191012)	88.94 (613)	0.0053	89.11 (614)	0.0035	113.5 (783)	0.103	98.18 (677)	0.143	15.03
#4 615/100	29188 (201244)	103.9 (717)	0.0056	97.73 (674)	0.0035	132.5 (914)	0.085	115.0 (793)	0.103	11.52
#5 615/100	29865 (205912)	105.0 (724)	0.0055	102.0 (703)	0.0035	137.7 (950)	0.081	122.2 (843)	0.104	11.91
#4 CRX4100	28451 (196163)	126.6 (873)	0.0064	92.10 (635)	0.0035	159.7 (1101)	0.041	95.47 (658)	0.086	6.79
#5 CRX4100	31168 (214896)	131.8 (908)	0.0062	101.5 (700)	0.0035	163.0 (1124)	0.060	99.13 (683)	0.091	7.25
#4 CRX9100	29575 (203913)	134.3 (926)	0.0066	100.4 (692)	0.0035	176.1 (1214)	0.054	115.8 (798)	0.093	8.04
#5 CRX9100	27219 (187668)	125.9 (868)	0.0065	92.57 (638)	0.0035	164.3 (1133)	0.056	111.8 (771)	0.096	8.92

Table 4.4: Reinforcing steel bar strain hardening results summary.

Product ID	Grade, ksi (MPa)	Strain hardening point	
		Stress, ksi (MPa)	Strain, in./in. (mm/mm)
#4 706/60	ASTM A706-16 Grade 60	64.02 (441)	0.011
#5 706/60		65.24 (450)	0.006
#4 615/80	ASTM A615-16 Grade 80	85.69 (591)	0.009
#5 615/80		86.04 (593)	0.007
#4 706/80	ASTM A706-16 Grade 80	88.07 (607)	0.011
#5 706/80		88.32 (609)	0.012
#4 615/100	ASTM A615-16 Grade 100	104.45 (720)	0.009
#5 615/100		105.39 (727)	0.007
#4 CRX4100	ASTM A1035-16b Type CM Grade 120	71.45 (493)	0.002
#5 CRX4100		82.41 (568)	0.003
#4 CRX9100	ASTM A1035-16b Type CS Grade 120	87.94 (606)	0.003
#5 CRX9100		84.33 (581)	0.003

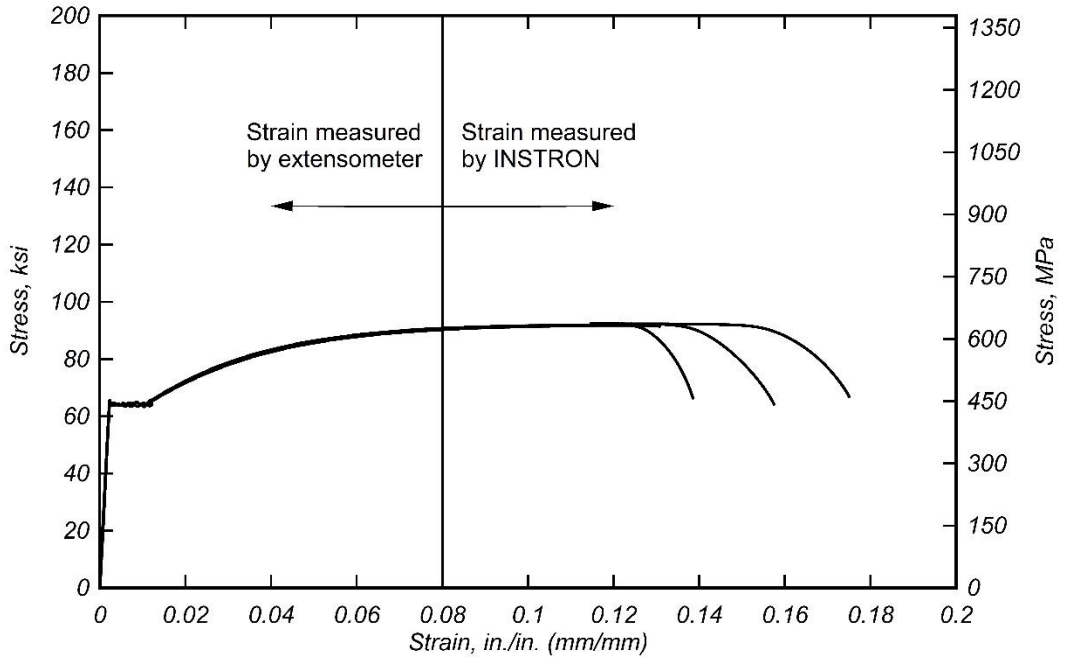

Figure 4.1: Stress-strain plot of #4 (#13M) A706 Grade 60 reinforcing steel bar.

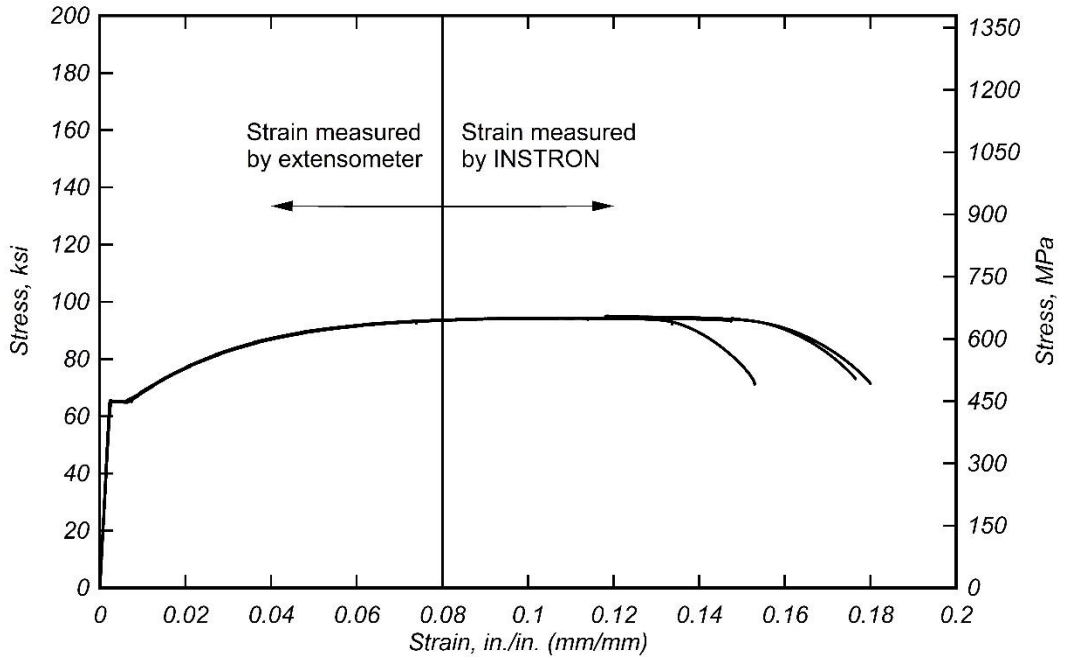

Figure 4.2: Stress-strain plot of #5 (#16M) A706 Grade 60 reinforcing steel bar.

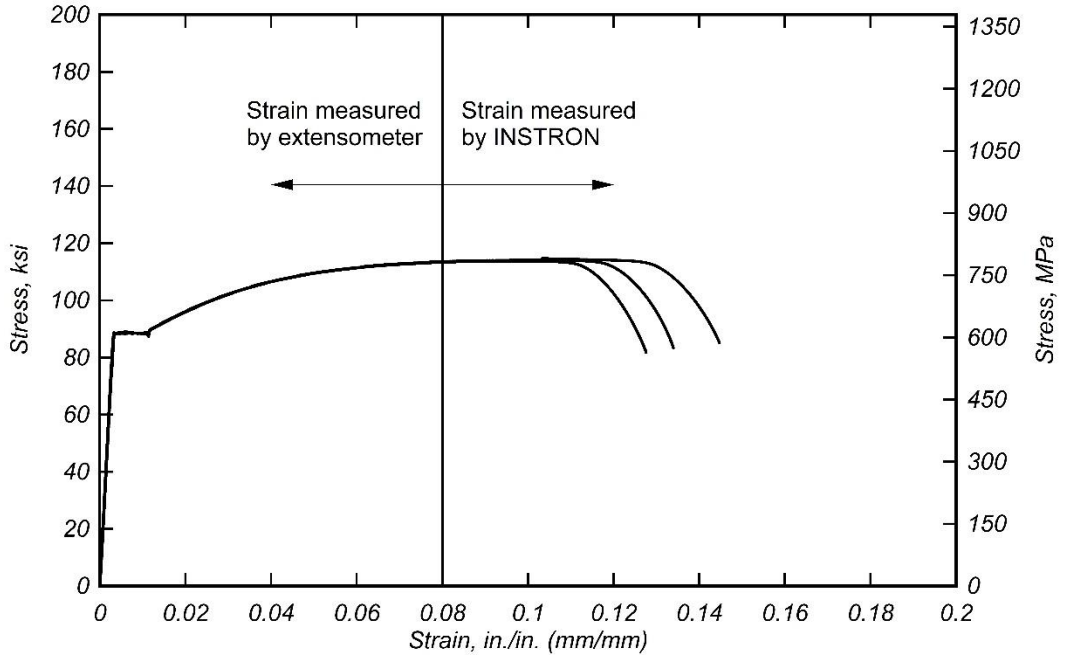

Figure 4.3: Stress-strain plot of #4 (#13M) A706 Grade 80 reinforcing steel bar.

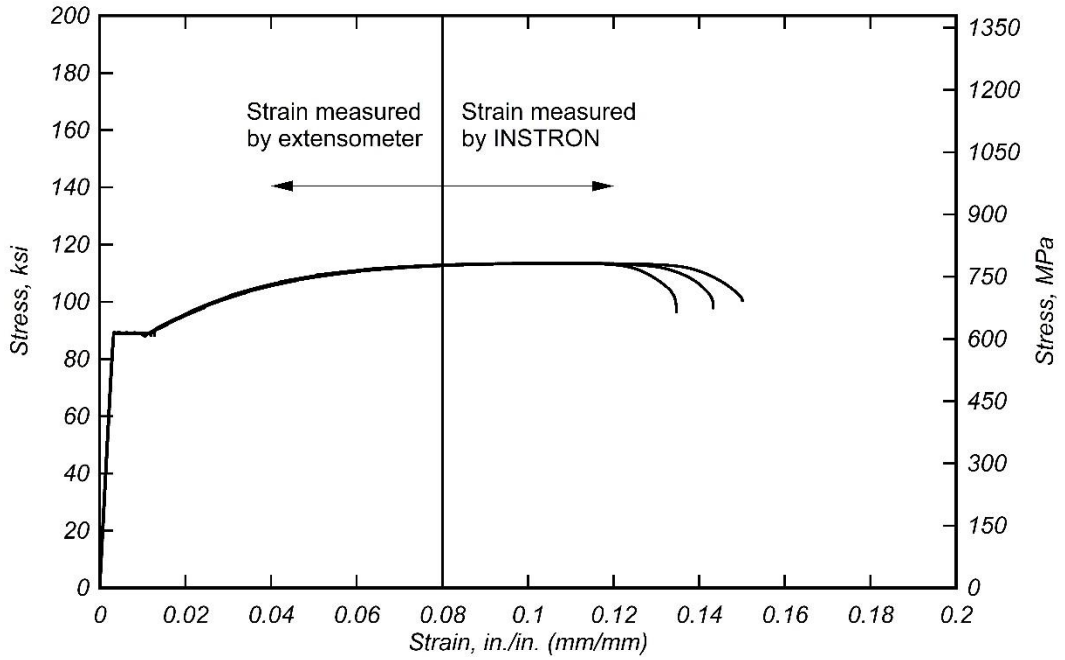

Figure 4.4: Stress-strain plot of #5 (#16M) A706 Grade 80 reinforcing steel bar.

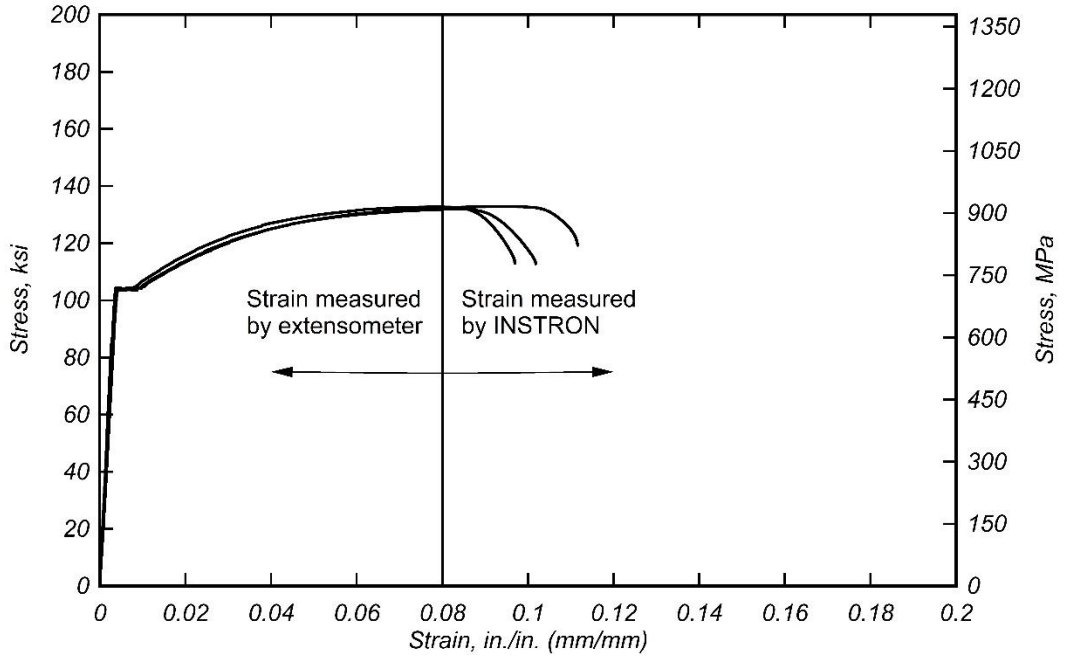

Figure 4.5: Stress-strain plot of #4 (#13M) A615 Grade 100 reinforcing steel bar.

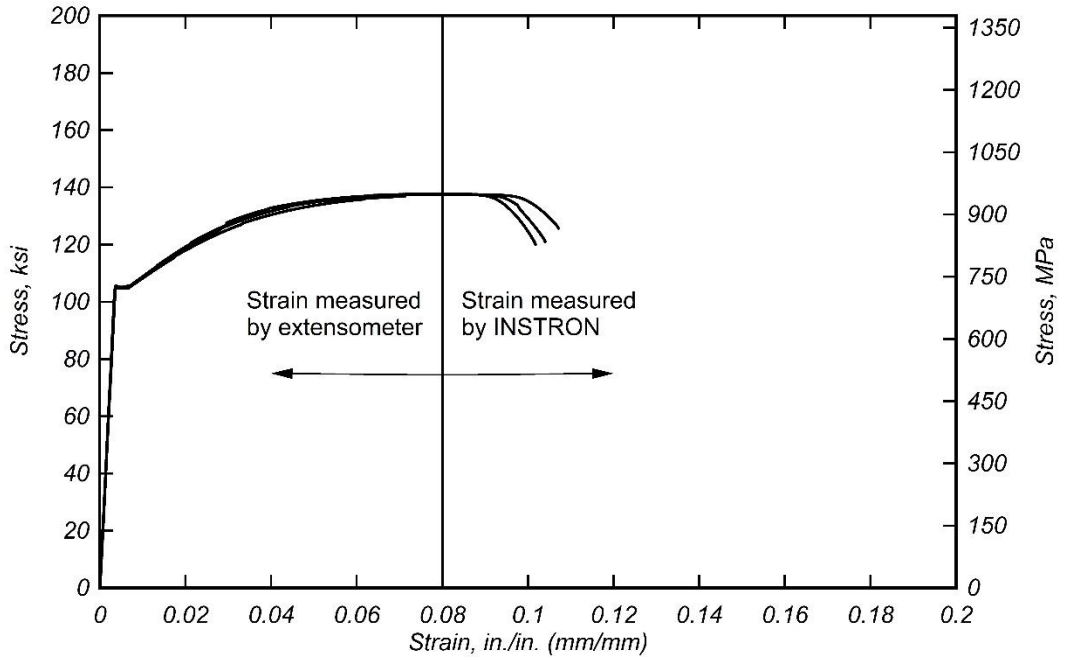

Figure 4.6: Stress-strain plot of #5 (#16M) A615 Grade 100 reinforcing steel bar.

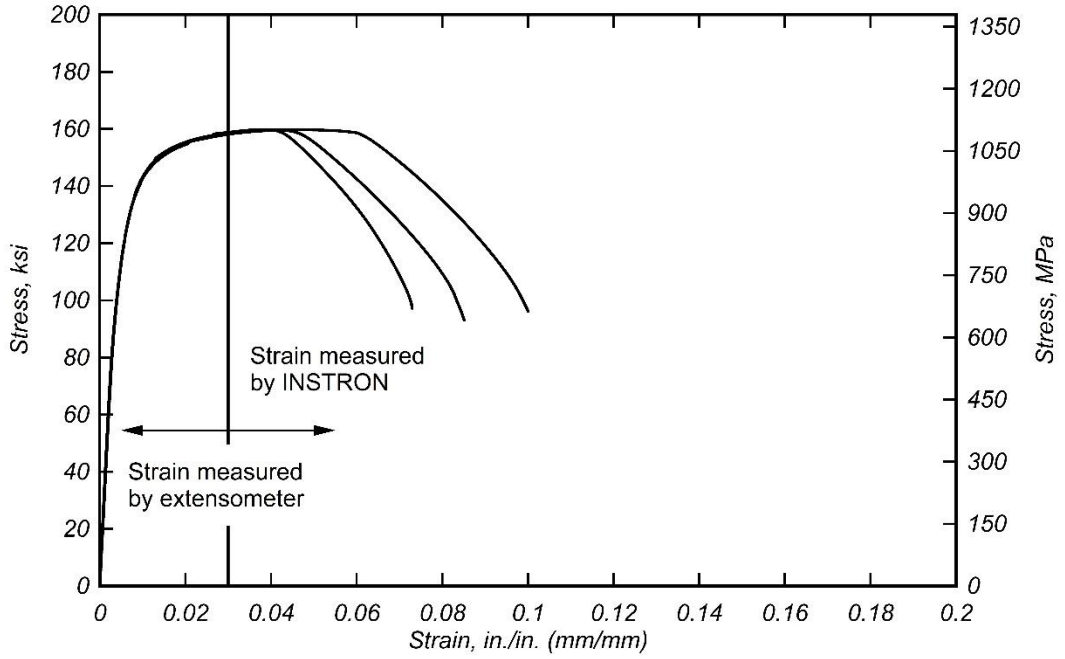

Figure 4.7: Stress-strain plot of #4 (#13M) A1035 CM Grade 120 reinforcing steel bar.

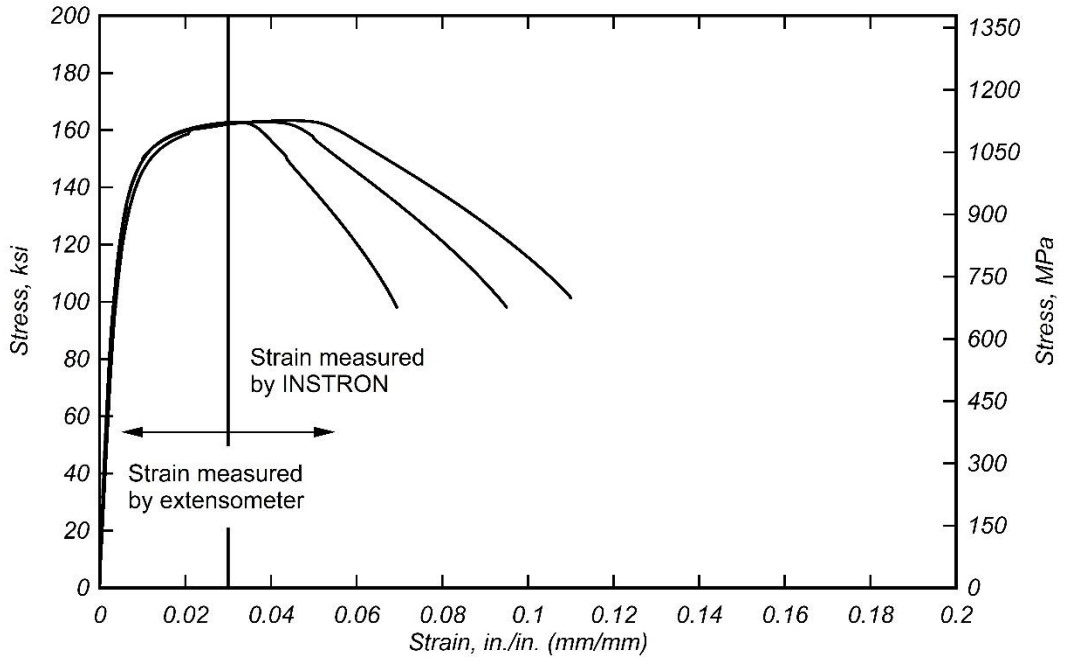

Figure 4.8: Stress-strain plot of #5 (#16M) A1035 CM Grade 120 reinforcing steel bar.

4.2 CONCRETE

For each specimen, the push-off test specimens were cast on two different cast dates. The same concrete mixture proportions were used for both casts. The maximum aggregate size was 3/8 in. (9.52 mm) for all mixtures. Table 4.5 shows the concrete mixture proportions for different mixtures used in the study. All of the concrete used in this study was provided by Knife River Corporation. The concrete was mixed at the batch plant and delivered by truck. The 28-day design/nominal compression strength for Mix #1, Mix #2, and Mix #3 were 5000 psi (35 MPa), 6000 psi (40 MPa), and 3000 psi (20 MPa), respectively.

Table 4.5: Concrete mixture proportions per cubic yard.

Mix #	Design/ nominal f_c', psi (MPa)	W/(C+P)	Coarse agg. lbs (kg)*	Fine agg. lbs (kg)	Cement, lbs (kg)	Slag, lbs (kg)	Fly ash, lbs (kg)	Water, lbs (kg)	Ad. Mix. 1 (WRDA-64), oz (g)	Ad. Mix. 2 (V-MAR3), oz (g)
1	5000 (35)	0.388	1250 (567)	1479 (671)	695 (315)	-	80 (36)	300.6 (135.3)	31 (879)	-
2	6000 (40)	0.438	1100 (499)	1692 (767)	590 (268)	115 (52)	-	309 (139)	24.7 (700)	-
3	3000 (20)	0.525	1200 (544)	1840 (835)	525 (238)	-	-	275.6 (124)	21 (595)	21 (595)

*Maximum aggregate size of 3/8 in. (9.5 mm).
Legend: W/(C+P) – Water to Cement Ratio.

Table 4.6 shows the slump and the 28-day mean compressive strengths of concrete. The slump was evaluated using ASTM Standard C143-12. Concrete cylinder samples were cast in accordance to ASTM C31/31M-12, Standard Practice for Making and Curing Concrete Test Specimens in the field and were 4 in. (102 mm) diameter by 8 in. (203 mm) tall cylinders. Twenty-four hours after the concrete cast, cylinders were stripped from the molds and stored in the casting area, close to the push-off test specimens. Cylinders were tested for compressive strength following ASTM C39/39M-12a, Standard Test Method for Compressive Strength of Cylindrical Concrete Specimens. For each cast, 3-day, 7-day, 28-day, and test-day compression cylinder tests were performed. Before testing, both sides of the cylinder were ground to minimize variance in the test data. Using OriginLab software, non-linear curves were fit for the compressive strength test data for each mixture. The empirical equations generated from the non-linear regression fits were used to estimate compressive strength values at different test times. This is done to minimize the variability induced in the ultimate shear strength of push-off test specimens by the compressive strength of concrete.

The compressive strength at the time of testing for each push-off specimen is presented in Table 4.7. Each row corresponds to one specimen group where the compressive strength values at the time of testing for the bottom and top casts are presented for the three identical specimens conforming each specimen group. Note that Mix #1 with a nominal concrete strength of 5 ksi (35 MPa) presented

compressive strengths at the time of testing of 5.6 ksi (38 MPa) and above. On the other hand, Mix #2 with a nominal concrete strength of 6 ksi (40 MPa) presented compressive strength at the time of testing of 4.7 ksi (32.4 MPa). Mix #3 with a nominal concrete strength of 3 ksi (20 MPa) presented compressive strength at the time of testing of 2.8 ksi (19.5 MPa).

Table 4.6: Concrete fresh concrete slump and mean compressive strengths.

Mix #	Cast Date	Nominal concrete strength, psi (MPa)	Slump, in. (mm)	28-day mean compressive strength, psi (MPa)
1	07/21/2017	5000 (34.47)	7.75 (197)	6849 (47.5)
1	08/04/2017	5000 (34.47)	6.50 (165)	6778 (46.7)
1	09/12/2017	5000 (34.47)	7.25 (184)	6718 (46.3)
1	10/25/2017	5000 (34.47)	4.25 (108)	6037 (41.6)
1	12/05/2017	5000 (34.47)	7.50 (191)	5540 (38.2)
2	12/06/2017	6000 (41.37)	7.50 (191)	4040 (27.9)
3	12/07/2017	3000 (20.68)	7.00 (179)	3203 (22.1)
1	12/14/2017	5000 (34.47)	6.50 (165)	5661 (39.0)
2	12/15/2017	6000 (41.37)	6.25 (159)	4471 (30.8)
3	12/15/2017	3000 (20.68)	6.75 (171)	2519 (17.4)
1	04/12/2018	5000 (34.47)	7.50 (191)	6261 (43.2)
1	05/03/2018	5000 (34.47)	6.00 (152)	5815 (40.1)

Table 4.7: Concrete compressive strength at time of shear specimen testing.

Specimen label	Adopted value f'_c, psi (MPa)
4G80S12(1/8)	6190 (42.68)
4G80S4(1/8)	6190 (42.68)
4G80S6(EA)	5977 (41.21)
4G80S6(1/4)	6190 (42.68)
4G80S6(1/8)	6190 (42.68)
4G80S6(AC)	6190 (42.68)
4G60S6(1/8)	5954 (41.05)
4G100S6(1/8)	5954 (41.05)
5G80S6(AC)	5954 (41.05)
5G80S6(1/8)	5954 (41.05)
5G80S6(EA)	5609 (38.68)
5G80S6(1/4)	5954 (41.05)
4G120S6(1/8)	5977 (41.21)
4G80S6F6(1/8)	4701 (32.41)
4G80S6F3(1/8)	2823 (19.46)

5.0 EFFECT OF HIGH-STRENGTH REINFORCING STEEL ON SHEAR FRICTION

5.1 INTRODUCTION

This chapter presents test results from push-off test specimens with a focus on the effect of high-strength reinforcing steel on shear friction. The effects analyzed in this section are: (1) influence of reinforcing steel grade, (2) influence of reinforcing steel bar spacing, and (3) influence of reinforcing steel bar size. The details of each push-off test specimen discussed in this chapter can be found in the test matrix presented in Table 3.1, section (a), (c), and (d). The discussion in this chapter focuses on results for interface shear force versus interface shear displacement, interface shear force versus strain, and interface shear force versus crack width. The methods implemented for data collection and the instrumentation utilized are presented in Section 3.5. The typical force-displacement response of a push-off test specimen is shown in Figure 3.24.

5.2 INFLUENCE OF REINFORCING STEEL GRADE

This section focuses on the influence of reinforcing steel grade. All specimens discussed in this section have an interface preparation of 1/8 in. (3.175 mm) interface roughness, contain three (3) #4 (#13M) reinforcing steel U-bars spaced at 6 in. (152.4 mm), and have a nominal concrete strength of 5000 psi (35 MPa). Since the variable of interest in this discussion is the reinforcing steel grade, the experimental results and discussion focuses on test specimens containing Grade 60 ksi (420 MPa), Grade 80 ksi (550 MPa), Grade 100 ksi (690 MPa), and Grade 120 (830 MPa) reinforcing steel U-bars labeled 4G60S6(1/8), 4G80S6(1/8), 4G100S6(1/8), and 4G120S6(1/8), respectively. Details of the specimens such as bar size, bar spacing, and interface preparation can be found in section (a) of Table 3.1; drawings showing dimensions of the specimens, as well as location of the reinforcing steel U-bars are presented in Chapter 3. Properties of the reinforcing steel and concrete used are presented in Section 4.1 and Section 4.2, respectively.

5.2.1 Interface Shear Force versus Interface Shear Displacement

Figure 5.1 to Figure 5.4 show the interface shear force versus interface shear displacement relationship curves for the three specimens making up each specimen group constructed with Grade 60 (420 MPa), Grade 80 (550 MPa), Grade 100 (690 MPa), and Grade 120 (830 MPa) reinforcing steel U-bars. The corresponding specimen group labels are 4G60S6(1/8), 4G80S6(1/8), 4G100S6(1/8), and 4G120S6(1/8), respectively. Table 5.1 to Table 5.4 show values of the main characteristic points of the test results for the specimens. The tabulated values were computed as an average value of the three specimens per group for each characteristic point.

From inspection of Figure 5.1 to Figure 5.4, it can be observed that all tested specimens present similar behavior with a linear initial response until the cracking interface shear load, V_{cr}, is reached, followed by a subtle reduction of stiffness caused by the loss of cohesion, even though the V_{cr} value is slightly different for all specimens. Following this point, V_{cr}, the stiffness remains roughly constant until the peak load is reached. As the displacement increases the reinforcing steel U-bars crossing the shear interface are engaged and generate a clamping force that holds both pieces of the test specimen together. After the peak load, the shear interface undergoes a significant slip accompanied by a reduction in interface shear force. This big drop in interface shear force is due to the sudden failure of the aggregate interlock mechanism and it is also related to the stiffness and strain energy released by the test setup. Beyond this level of displacement, the response is controlled by the dowel action mechanism, as cohesion is lost, and aggregate interlock is significantly reduced as the crack width gradually increases. However, as reinforcing steel bars engage with increased displacement, a steady increase in shear load until first bar fracture is observed, indicating a hardening phase as the dowel action mechanism develops.

Figure 5.2 presents the interface shear force versus interface shear displacement relationship for specimen group 4G80S6(1/8). In this figure, it can be observed that specimen 4G80S6(1/8)-2 presents a significantly higher peak load. The load at cracking, however, is similar to that shown by the other specimens. This indicates that

the reason for reaching a higher peak load may be due to the variability originating from roughening the surface to an amplitude of 1/8 in. (3.175 mm), in this case causing the aggregate interlock mechanism to have a higher impact on the force-displacement response. Similarly, in Figure 5.4 it can be seen that specimen 4G120S6(1/8)-2 also reaches a significantly higher peak load. This behavior may be explained by the variability originating from the interface roughening process.

Table 5.5 summarizes the average values of the three specimens in each group. From the table, it can be seen that the average peak load values, V_{ult}, for specimen groups 4G60S6(1/8), 4G80S6(1/8), 4G100S6(1/8), and 4G120S6(1/8) are 196.34 kip (873.38 kN), 238.70 kip (1061.8 kN), 213.33 kip (948.92 kN), and 229.88 kip (1022.5 kN), respectively, with COV values ranging from 2% to 19%. Thus, when comparing the average peak load, it can be seen that increasing the grade of reinforcing steel U-bars increases the average peak load slightly, but the average peak load remains essentially the same for the Grade 80, Grade 100, and Grade 120 specimens. The variability in Δ_{ult} is much higher with COV values ranging from 14% to 27%. It can be seen that increasing the grade of reinforcing steel U-bars tends to increase the interface shear load at cracking, V_{cr}. Specimens 4G120S6(1/8) showed a 14% higher average V_{cr} and 50% higher average Δ_{cr} compared to 4G60S6(1/8) specimens.

The post-peak phase of the average interface shear force versus interface shear displacement response is also affected by the grade of reinforcing steel. First, as it can be observed in Table 5.5, the post-peak sustained strength increases with increasing reinforcing steel grade. The post-peak sustained strength at first bar fracture, V_b, values for the 4G60S6(1/8) specimens are the lowest [123.65 kip (550.01 kN)], and are highest for the 4G120S6(1/8) specimens [213.37 kip (949.10 kN)]. Even though the increase in strength is observable with increase in reinforcing steel grade, the 4G80S6(1/8) and 4G100S6(1/8) specimens present very similar average sustained loads reaching V_b values of 148.87 kip (662.19 kN) and 169.42 kip (753.63 kN), respectively. In contrast with the differences in average interface shear force at first bar fracture, V_b, the average displacement at first bar fracture, Δ_b, for all specimens range between 1.018 in. (25.85 mm) and 1.082 in. (27.48 mm), with the exception of

the 4G100S6(1/8) specimens which had an average Δ_b value of 0.918 in. (23.32 mm). The energy dissipated until first bar fracture, E_b, which is calculated as the area under the interface shear force versus interface shear displacement curve until first bar fracture, is a parameter where significant differences can be observed. The average E_b is the highest in 4G120S6(1/8) specimens with 16.85 kip-ft (22.85 kJ) and lowest in 4G60S6(1/8) specimens with 10.25 kip-ft (13.90 kJ). This corresponds to a 64% increase in work done by the 4G120S6(1/8) specimens over the 4G60S6(1/8) specimens. Overall, these results indicate the dowel action mechanism controls the response and it is characterized by a steady increase in strength and stiffness with increased strength of the reinforcing steel bars.

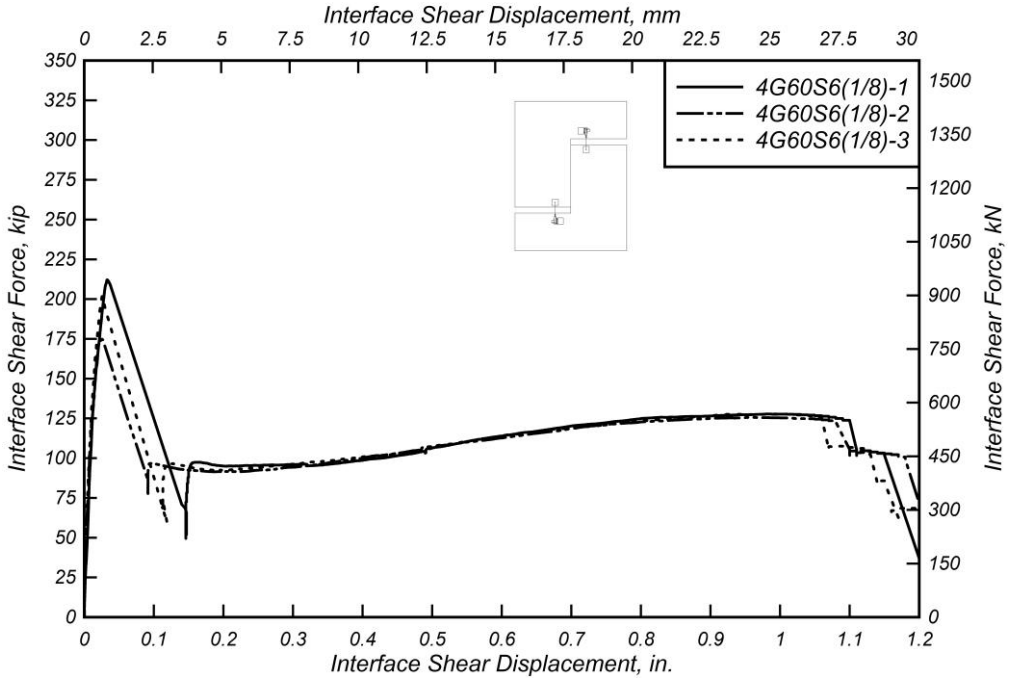

Figure 5.1: Interface shear force versus interface shear displacement for 4G60S6(1/8) specimens.

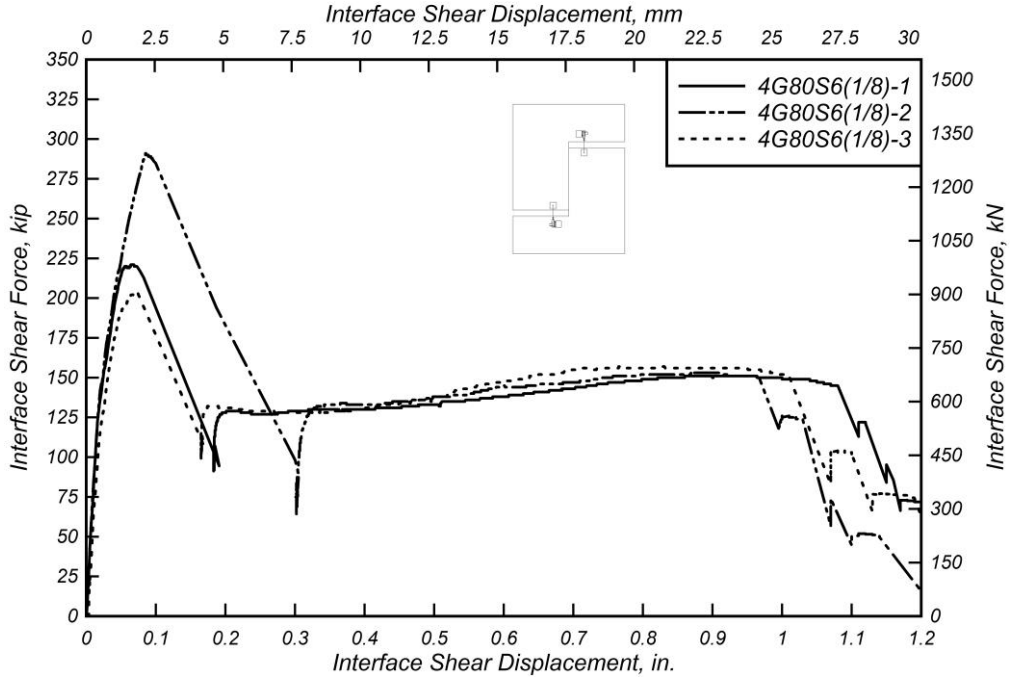

Figure 5.2: Interface shear force versus interface shear displacement for 4G80S6(1/8) specimens.

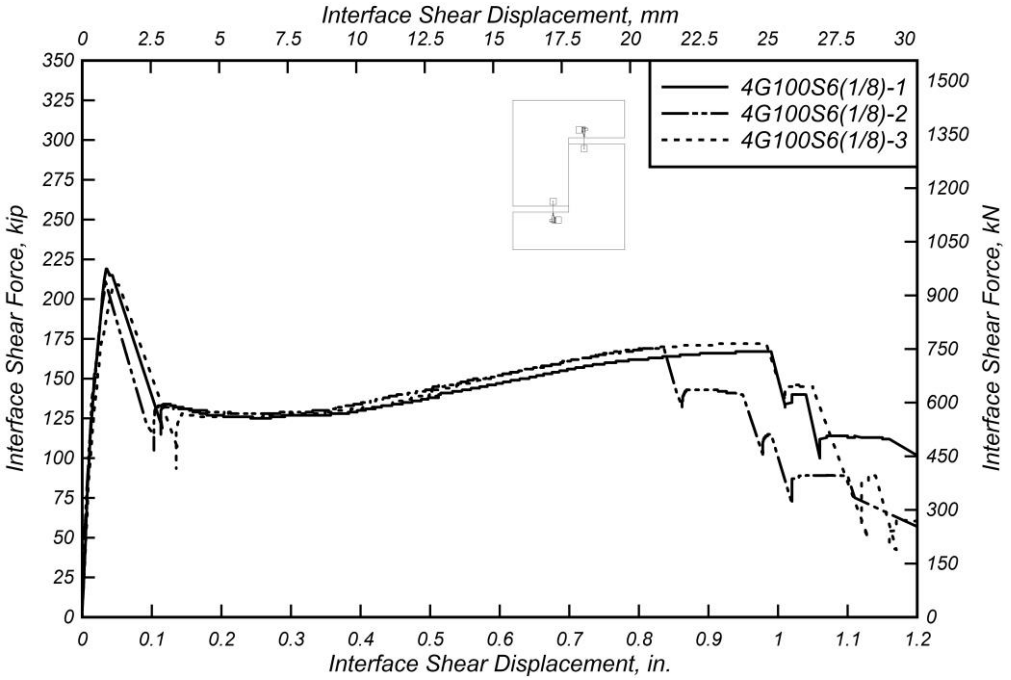

Figure 5.3: Interface shear force versus interface shear displacement for 4G100S6(1/8) specimens.

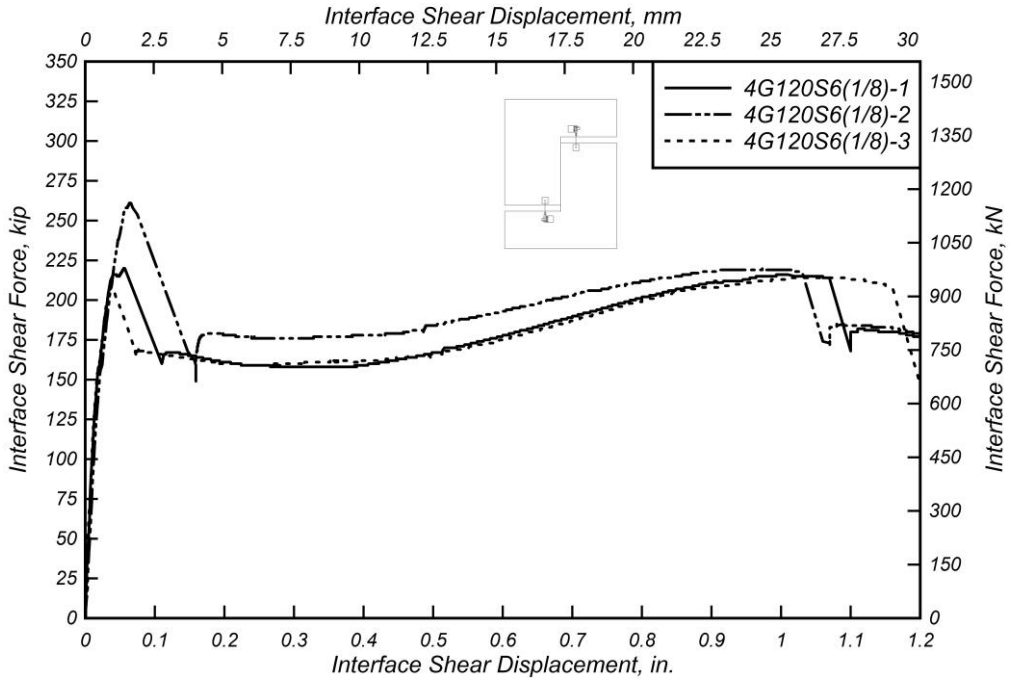

Figure 5.4: Interface shear force versus interface shear displacement for 4G120S6(1/8) specimens.

Table 5.1: Specimen 4G60S6(1/8) shear test results.

Spec	Δ_{ult}, in. (mm)	V_{ult}, kip (kN)	σ_{ult}, ksi (MPa)	$V_{sus,min}$, kip (kN)	$V_{sus,max}$, kip (kN)	Δ_{cr}, in. (mm)	V_{cr}, kip (kN)	Δ_{b}, in. (mm)	V_b, kip (kN)	E_b, kip-ft (kJ)
4G60S6 (1/8)-1	0.033 (0.84)	212.19 (943.9)	0.884 (6.10)	94.96 (422.4)	127.78 (568.4)	0.013 (0.33)	134.80 (599.6)	1.096 (27.8)	123.45 (549.1)	10.64 (14.43)
4G60S6 (1/8)-2	0.025 (0.64)	174.84 (777.7)	0.729 (5.02)	91.47 (406.9)	125.80 (559.6)	0.010 (0.26)	121.30 (539.6)	1.081 (27.5)	122.83 (546.4)	10.06 (13.64)
4G60S6 (1/8)-3	0.026 (0.66)	202.00 (898.5)	0.842 (5.80)	92.43 (411.2)	127.78 (568.4)	0.007 (0.19)	102.10 (454.2)	1.056 (26.8)	124.66 (554.5)	10.05 (13.63)
Mean	0.028 (0.71)	196.34 (873.4)	0.818 (5.64)	92.95 (413.5)	127.12 (565.5)	0.010 (0.26)	119.40 (531.1)	1.078 (27.4)	123.65 (550.0)	10.25 (13.90)
Median	0.026 (0.66)	202.00 (898.5)	0.842 (5.80)	92.43 (411.2)	127.78 (568.4)	0.010 (0.26)	121.30 (539.6)	1.081 (27.5)	123.45 (549.1)	10.06 (13.64)
STDEV	0.004 (0.11)	19.31 (85.9)	0.081 (0.56)	1.803 (8.02)	1.143 (5.09)	0.003 (0.07)	16.43 (73.10)	0.020 (0.51)	0.931 (4.14)	0.339 (0.459)
COV	16%	10%	10%	2%	1%	28%	14%	2%	1%	3%

Table 5.2: Specimen 4G80S6(1/8) shear test results.

Spec	Δ_{ult}, in. (mm)	V_{ult}, kip (kN)	σ_{ult}, ksi (MPa)	$V_{sus,min}$, kip (kN)	$V_{sus,max}$, kip (kN)	Δ_{cr}, in. (mm)	V_{cr}, kip (kN)	Δ_{b}, in. (mm)	V_b, kip (kN)	E_b, kip-ft (kJ)
4G80S6 (1/8)-1	0.065 (1.65)	221.21 (984.0)	0.922 (6.36)	126.72 (563.7)	151.44 (673.6)	0.015 (0.37)	112.5 (500.4)	1.079 (27.4)	145.00 (645.0)	12.92 (17.52)
4G80S6 (1/8)-2	0.085 (2.16)	290.99 (1294)	1.212 (8.36)	132.37 (588.8)	152.83 (679.8)	0.016 (0.40)	119.00 (529.3)	0.962 (24.4)	150.57 (669.8)	12.73 (17.26)
4G80S6 (1/8)-3	0.070 (1.78)	203.91 (907.0)	0.850 (5.86)	127.94 (569.1)	156.60 (696.6)	0.016 (0.41)	96.81 (430.6)	1.012 (25.7)	151.03 (671.8)	12.19 (16.53)
Mean	0.073 (1.86)	238.70 (1062)	0.995 (6.86)	129.01 (573.9)	153.62 (683.4)	0.016 (0.40)	109.44 (486.8)	1.018 (25.9)	148.87 (662.2)	12.61 (17.10)
Median	0.070 (1.78)	221.21 (984.0)	0.922 (6.36)	127.94 (569.1)	152.83 (679.8)	0.016 (0.40)	112.50 (500.4)	1.012 (25.7)	150.57 (669.8)	12.73 (17.26)
STDEV	0.010 (0.26)	46.10 (205.1)	0.1921 (1.32)	2.973 (13.2)	2.670 (11.88)	0.001 (0.02)	11.41 (50.74)	0.059 (1.49)	3.357 (14.93)	0.377 (0.512)
COV	14%	19%	19%	2%	2%	5%	10%	6%	2%	3%

Table 5.3: Specimen 4G100S6(1/8) shear test results.

Spec	Δ_{ult}, in. (mm)	V_{ult}, kip (kN)	σ_{ult}, ksi (MPa)	$V_{sus,min}$, kip (kN)	$V_{sus,max}$, kip (kN)	Δ_{cr}, in. (mm)	V_{cr}, kip (kN)	Δ_{b}, in. (mm)	V_b, kip (kN)	E_b, kip-ft (kJ)
4G100 S6(1/8) -1	0.035 (0.89)	218.87 (973.6)	0.912 (6.29)	125.08 (556.4)	166.89 (742.4)	0.016 (0.40)	139.70 (621.4)	0.944 (24.0)	166.65 (741.3)	12.08 (16.37)
4G100 S6(1/8) -2	0.033 (0.84)	211.69 (941.6)	0.882 (6.08)	127.77 (568.4)	169.47 (753.8)	0.014 (0.34)	136.00 (605.0)	0.836 (21.2)	169.47 (753.8)	10.09 (13.68)
4G100 S6(1/8) -3	0.048 (1.22)	209.42 (931.6)	0.873 (6.02)	125.56 (558.5)	172.28 (766.3)	0.011 (0.27)	95.16 (423.3)	0.974 (24.7)	172.15 (765.8)	12.19 (16.53)
Mean	0.039 (0.98)	213.33 (948.9)	0.889 (6.13)	126.14 (561.1)	169.55 (754.2)	0.013 (0.35)	123.62 (549.9)	0.918 (23.3)	169.42 (753.6)	11.45 (15.53)
Median	0.035 (0.89)	211.69 (941.6)	0.882 (6.08)	125.56 (558.5)	169.47 (753.8)	0.014 (0.34)	136.00 (605.0)	0.944 (24.0)	169.47 (753.8)	12.08 (16.37)
STDEV	0.008 (0.21)	4.933 (21.9)	0.021 (0.14)	1.435 (6.38)	2.696 (11.99)	0.002 (0.06)	24.72 (109.9)	0.073 (1.84)	2.750 (12.23)	1.182 (1.602)
COV	21%	2%	2%	1%	2%	18%	20%	8%	2%	10%

Table 5.4: Specimen 4G120S6(1/8) shear test results.

Spec	Δ_{ult}, in. (mm)	V_{ult}, kip (kN)	σ_{ult}, ksi (MPa)	$V_{sus,min}$, kip (kN)	$V_{sus,max}$, kip (kN)	Δ_{cr}, in. (mm)	V_{cr}, kip (kN)	Δ_{b}, in. (mm)	V_b, kip (kN)	E_b, kip-ft (kJ)
4G120 S6(1/8) -1	0.056 (1.42)	220.21 (979.1)	0.917 (6.32)	158.00 (702.8)	215.99 (960.8)	0.013 (0.33)	126.00 (560.5)	1.066 (27.1)	213.49 (949.7)	16.18 (21.94)
4G120 S6(1/8) -2	0.065 (1.65)	261.45 (1163)	1.089 (7.51)	175.75 (781.8)	219.51 (976.4)	0.017 (0.43)	130.50 (580.5)	1.026 (26.1)	218.05 (969.9)	16.75 (22.71)
4G120 S6(1/8) -3	0.037 (0.94)	208.06 (925.5)	0.867 (5.98)	158.79 (706.3)	214.24 (953.0)	0.016 (0.42)	152.00 (676.1)	1.154 (29.3)	208.56 (927.7)	17.61 (23.88)
Mean	0.053 (1.34)	229.88 (1023)	0.958 (6.60)	164.18 (730.3)	216.58 (963.4)	0.015 (0.39)	136.17 (605.7)	1.082 (27.5)	213.37 (949.1)	16.85 (22.85)
Median	0.056 (1.42)	220.12 (979.1)	0.917 (6.32)	158.79 (706.3)	215.99 (960.8)	0.016 (0.42)	130.50 (580.5)	1.066 (27.1)	213.49 (949.7)	16.75 (22.71)
STDEV	0.014 (0.36)	28.00 (124.6)	0.117 (0.80)	10.03 (44.61)	2.684 (11.94)	0.002 (0.06)	13.90 (61.81)	0.066 (1.66)	4.746 (21.11)	0.720 (0.976)
COV	27%	12%	12%	6%	1%	14%	10%	6%	2%	4%

Table 5.5: Summary of averages of specimen groups analyzing influence of reinforcing steel grade.

Spec	Δ_{ult}, in. (mm)	V_{ult}, kip (kN)	σ_{ult}, ksi (MPa)	$V_{sus,min}$, kip (kN)	$V_{sus,max}$, kip (kN)	Δ_{cr}, in. (mm)	V_{cr}, kip (kN)	Δ_{b}, in. (mm)	V_b, kip (kN)	E_b, kip-ft (kJ)
4G60S6 (1/8)	0.028 (0.71)	196.34 (873.4)	0.818 (5.64)	92.95 (413.5)	127.12 (565.5)	0.010 (0.26)	119.40 (531.1)	1.078 (27.4)	123.65 (550.0)	10.25 (13.90)
4G80S6 (1/8)	0.073 (1.86)	238.70 (1062)	0.995 (6.86)	129.01 (573.9)	153.62 (683.4)	0.016 (0.40)	109.44 (486.8)	1.018 (25.9)	148.87 (662.2)	12.61 (17.10)
4G100S 6 (1/8)	0.039 (0.98)	213.33 (948.9)	0.889 (6.13)	126.14 (561.1)	169.55 (754.2)	0.013 (0.34)	123.62 (549.9)	0.918 (23.3)	169.42 (753.6)	11.45 (15.53)
4G120S 6 (1/8)	0.053 (1.34)	229.88 (1023)	0.958 (6.60)	164.18 (730.3)	216.58 (963.4)	0.015 (0.39)	136.17 (605.7)	1.082 (27.5)	213.37 (949.1)	16.85 (22.85)

5.2.2 Interface Shear Force versus Strain

Figure 5.5 to Figure 5.8 show the interface shear force versus reinforcing steel strain response for specimen groups 4G60S6(1/8), 4G80S6(1/8), 4G100S6(1/8), and 4G120S6(1/8). In these figures, it can be observed that the behavior for all specimens is linear until the cracking shear force, V_{cr}, is reached at the point of nominal loss of cohesion. These figures also show that the strain in the reinforcing steel U-bars begins to increase at a much higher rate after cracking occurs, which indicates that this region of the response corresponds to an instant at which transition between controlling shear force transfer mechanisms from cohesion to aggregate interlock. Beyond this point, a reduction in stiffness is observed, and the stiffness remains

essentially unchanged until peak load is reached. It is important to note that at peak load none of the measurements from the strain gauges located on the U-bars indicated that the specimens had reached their respective nominal yield strain.

The post-peak behavior is where the difference between test specimen groups becomes more apparent. In this post-peak behavior stage, the force-strain response is characterized by an initial softening phase that precedes a hardening phase. The 4G60S6(1/8) specimens display a rapid shear force capacity reduction and the lowest average maximum sustained interface shear load at 127.12 kip (565.46 kN). In contrast, the 4G120S6(1/8) specimens exhibit a smooth post-peak transition into the sustained load stage with the highest average maximum sustained interface shear load at 215.12 kip (956.88 kN). It is important to note that even though at the peak load none of the specimens reached their respective nominal yield strain, results indicate that the U-bars exceeded the yield strain limit in this stage of the response.

Table 5.6 to Table 5.9 present the strain measurements at peak load, V_{ult}, for all the strain gauges contained in each test specimen. Table 5.10 lists the average strain gauges measurements. It is important to note that many strain gauge readings present high COV values, thus indicating the innate variability of the distribution of strain within the test specimen. Additionally, there were several strain gauges that were damaged before the peak load was reached, which limits the additional analysis that can be performed with these strain gauge data.

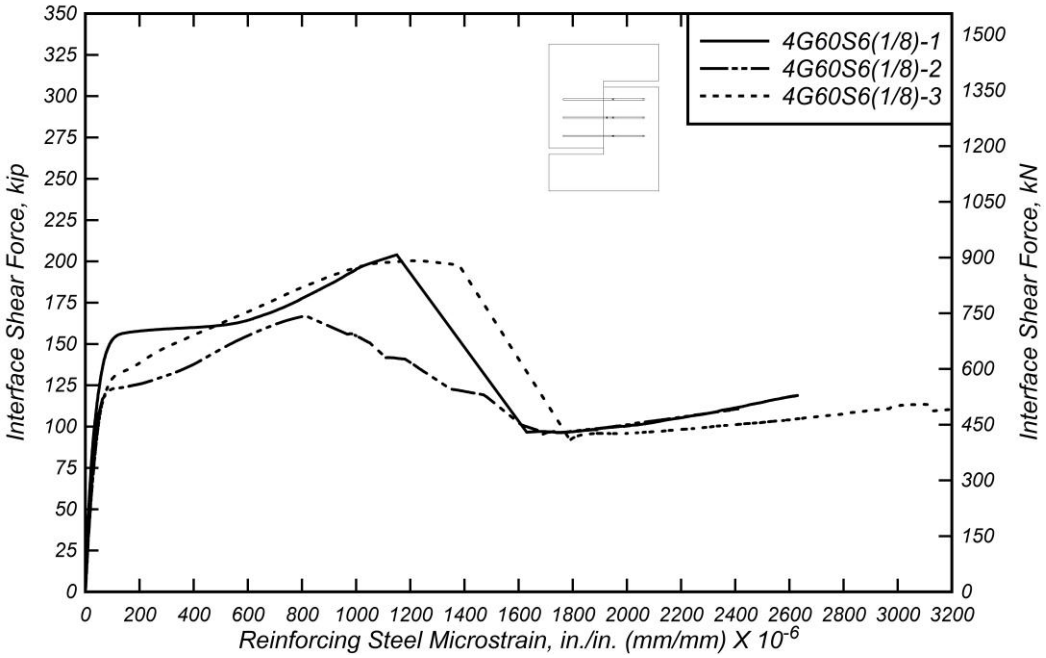

Figure 5.5: Interface shear force versus average reinforcing steel microstrain for 4G60S6(1/8) specimens.

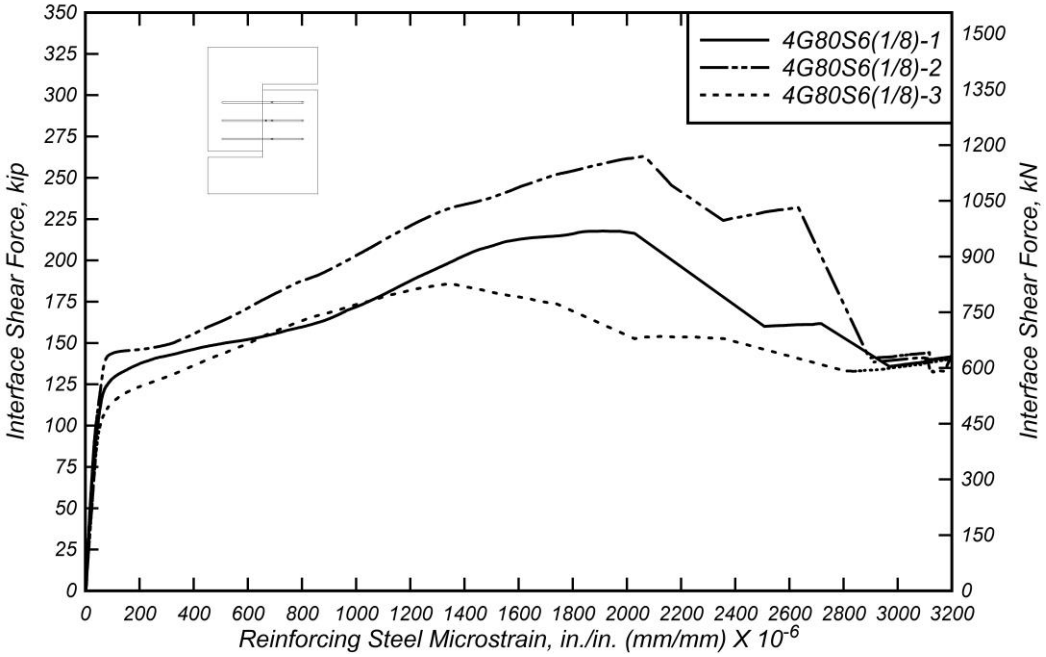

Figure 5.6: Interface shear force versus average reinforcing steel microstrain for 4G80S6(1/8) specimens.

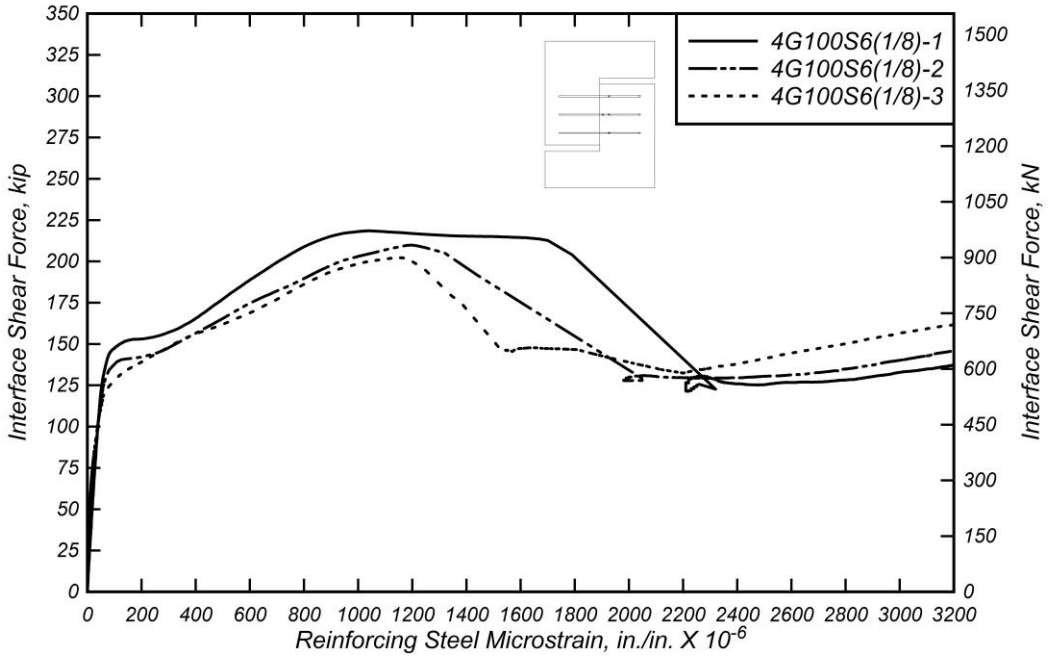

Figure 5.7: Interface shear force versus average reinforcing steel microstrain for 4G100S6(1/8) specimens.

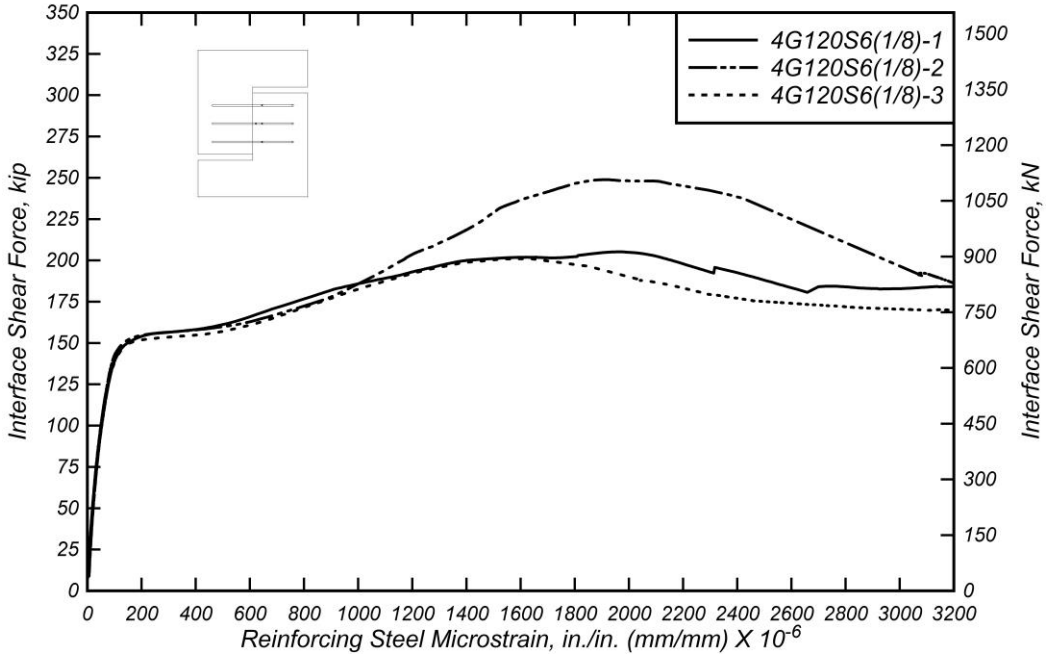

Figure 5.8: Interface shear force versus average reinforcing steel microstrain for 4G120S6(1/8) specimens.

Table 5.6: Specimen 4G60S6(1/8) strain gauge readings at peak interface shear force.

Spec	s_1, in./in. (mm/mm)	s_2, in./in. (mm/mm)	s_3, in./in. (mm/mm)	s_4, in./in. (mm/mm)	s_5, in./in. (mm/mm)	s_6, in./in. (mm/mm)	s_7, in./in. (mm/mm)
4G60S6 (1/8)-1	0.0010	-	0.0014	0.0018	-	0.0013	0.0014
4G60S6 (1/8)-2	0.0007	0.0009	0.0013	0.0011	-	0.0011	0.0011
4G60S6 (1/8)-3	0.0010	0.0011	0.0013	0.0016	-	0.0012	N/A
Mean	0.0009	0.0010	0.0013	0.0015	-	0.0012	0.0012
Median	0.0010	0.0010	0.0013	0.0016	-	0.0012	0.0012
STDEV	0.0002	0.0001	0.0001	0.0003	-	0.0001	0.0002
COV	17%	12%	7%	22%	-	9%	16%

Table 5.7: Specimen 4G80S6(1/8) strain gauge readings at peak interface shear force.

Spec	s_1, in./in. (mm/mm)	s_2, in./in. (mm/mm)	s_3, in./in. (mm/mm)	s_4, in./in. (mm/mm)	s_5, in./in. (mm/mm)	s_6, in./in. (mm/mm)	s_7, in./in. (mm/mm)
4G80S6 (1/8)-1	-	-	0.0019	-	0.0025	0.0018	-
4G80S6 (1/8)-2	-	-	-	-	0.0030	0.0025	0.0017
4G80S6 (1/8)-3	-	0.0022	-	0.0026	-	0.0018	0.0012
Mean	-	0.0022	0.0019	0.0026	0.0028	0.0021	0.0015
Median	-	0.0022	0.0019	0.0026	0.0028	0.0018	0.0015
STDEV	-	-	-	-	0.0004	0.0004	0.0004
COV	-	-	-	-	13%	19%	26%

Table 5.8: Specimen 4G100S6(1/8) strain gauge readings at peak interface shear force.

Spec	s_1, in./in. (mm/mm)	s_2, in./in. (mm/mm)	s_3, in./in. (mm/mm)	s_4, in./in. (mm/mm)	s_5, in./in. (mm/mm)	s_6, in./in. (mm/mm)	s_7, in./in. (mm/mm)
4G100S6 (1/8)-1	0.0010	-	0.0012	0.0015	0.0010	0.0011	-
4G100S6 (1/8)-2	0.0011	-	0.0017	-	0.0010	0.0012	0.0012
4G100S6 (1/8)-3	0.0012	-	0.0011	0.0020	0.0010	-	0.0011
Mean	0.0011	-	0.0013	0.0018	0.0010	0.0012	0.0011
Median	0.0011	-	0.0012	0.0018	0.0010	0.0012	0.0011
STDEV	0.0001	-	0.0003	0.0003	0.0000	0.0001	0.0001
COV	8%	-	26%	19%	0%	11%	9%

Table 5.9: Specimen 4G120S6(1/8) strain gauge readings at peak interface shear force.

Spec	s_1, in./in. (mm/mm)	s_2, in./in. (mm/mm)	s_3, in./in. (mm/mm)	s_4, in./in. (mm/mm)	s_5, in./in. (mm/mm)	s_6, in./in. (mm/mm)	s_7, in./in. (mm/mm)
4G120S6 (1/8)-1	0.0016	0.0033	0.0019	0.0029	0.0013	0.0031	0.0020
4G120S6 (1/8)-2	0.0021	0.0022	0.0027	0.0026	0.0015	0.0019	0.0023
4G120S6 (1/8)-3	0.0011	0.0017	0.0013	0.0021	0.0022	0.0015	0.0015
Mean	0.0016	0.0024	0.0020	0.0025	0.0017	0.0022	0.0020
Median	0.0016	0.0022	0.0019	0.0026	0.0015	0.0019	0.0020
STDEV	0.0005	0.0008	0.0007	0.0004	0.0004	0.0008	0.0004
COV	31%	33%	34%	16%	26%	39%	21%

Table 5.10: Summary of average strain readings at peak interface shear force of specimen groups analyzing influence of reinforcing steel grade.

Spec	s_1, in./in. (mm/mm)	s_2, in./in. (mm/mm)	s_3, in./in. (mm/mm)	s_4, in./in. (mm/mm)	s_5, in./in. (mm/mm)	s_6, in./in. (mm/mm)	s_7, in./in. (mm/mm)
4G60S6(1/8)	0.0009	0.0010	0.0013	0.0015	-	0.0012	0.0012
4G80S6(1/8)	-	0.0022	0.0019	0.0026	0.0028	0.0021	0.0015
4G100S6(1/8)	0.0011	-	0.0013	0.0018	0.0010	0.0012	0.0011
4G120S6(1/8)	0.0016	0.0024	0.0020	0.0025	0.0017	0.0022	0.0020

5.2.3 Interface Shear Force versus Crack Width

Figure 5.9 to Figure 5.12 show the interface shear force vs crack width response for all 4G60S6(1/8), 4G80S6(1/8), 4G100S6(1/8), and 4G120S6(1/8) test specimens. Each figure shows the force-crack width response for all three test specimens in each group. The overall characteristics of the response are very similar within each test specimen group. In the initial stages of the test, crack width is negligible due to the concrete-to-concrete cohesion bond controlling the response and limiting shear interface displacements. After cracking occurs, the crack width grows causing cohesion to degrade and aggregate interlock begins to control until the peak load is reached. At peak load, the main identifiable trend is crack width increases as reinforcing steel U-bar grade increases, with the exception of the 4G80S6(1/8) specimens.

Table 5.11 to Table 5.14 present crack width values at points of interest in the response for each specimen group. From these tables, it can be seen that crack width

values at peak load, w_{ult}, and crack width values at first bar fracture, w_b, present a high variability with COV ranging from 12% to 33% and 14% to 28%, respectively. On the other hand, the values of peak load, V_{ult}, and load at first bar fracture, V_b, present lower variability with COV ranging from 2% to 19% and 1% to 2%, respectively.

Table 5.15 presents a summary of the average results for all four specimen groups. The average crack width at peak load, w_{ult}, is 0.0106 in. (0.2692 mm), 0.0152 in. (0.3857 mm), and 0.0207 in. (0.5262 mm), in specimen groups 4G60S6(1/8), 4G100S6(1/8), and 4G120S6(1/8), respectively, while the average crack width at peak load in specimen group 4G80S6(1/8) is 0.0297 in. (0.7532 mm), which is significantly higher than the other specimen groups. These results indicate that while using higher strength steel does translate into higher capacity, the bond characteristics of the different reinforcing steel grades may play a role at these levels of loading. Thus, even though the use of high-strength reinforcing steel tends to increase the clamping force, its use may also induce larger crack widths which tends to reduce the contributions of the aggregate interlock mechanism to the interface shear force.

The post-peak behavior presents significant differences in behavior between specimen groups. Specimens in group 4G120S6(1/8) exhibit an average crack width at first bar fracture of 0.1112 in. (2.824 mm) at the sustained load of 216.58 kip (963.40 kN). Specimens in group 4G60S6(1/8) have average crack widths at first bar fracture of 0.1110 in. (2.820 mm), which is similar to the one obtained for the 4G120S6(1/8) specimens, even though the post-peak sustained load was significantly lower [127.12 kip (565.46 kN)]. Specimen groups 4G80S6(1/8) and 4G100S6(1/8) present very similar post-peak crack width response, with the 4G80S6(1/8) having an average crack width at first bar fracture of 0.2039 in. (5.178 mm), while the 4G100S6(1/8) specimens exhibited an average crack width at first bar fracture of 0.1813 in. (4.605 mm). This shows that for every case in which the reinforcing steel U-bars used were higher than grade 60, the average sustained load capacity increased without causing a reduction in crack width.

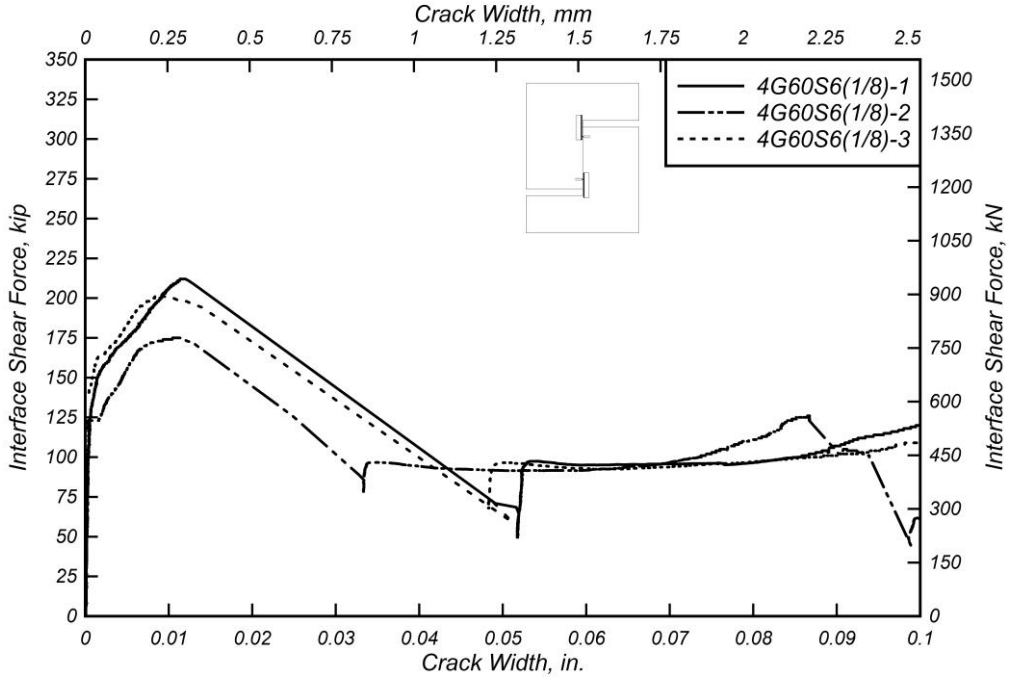

Figure 5.9: Interface shear force versus crack width for 4G60S6(1/8) specimens.

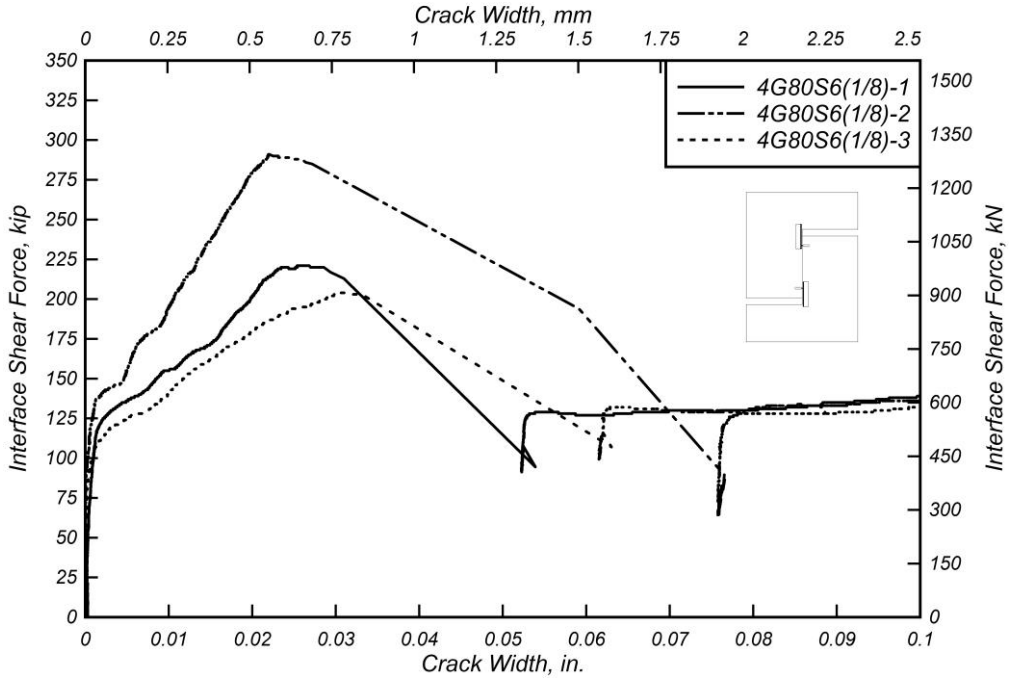

Figure 5.10: Interface shear force versus crack width for 4G80S6(1/8) specimens.

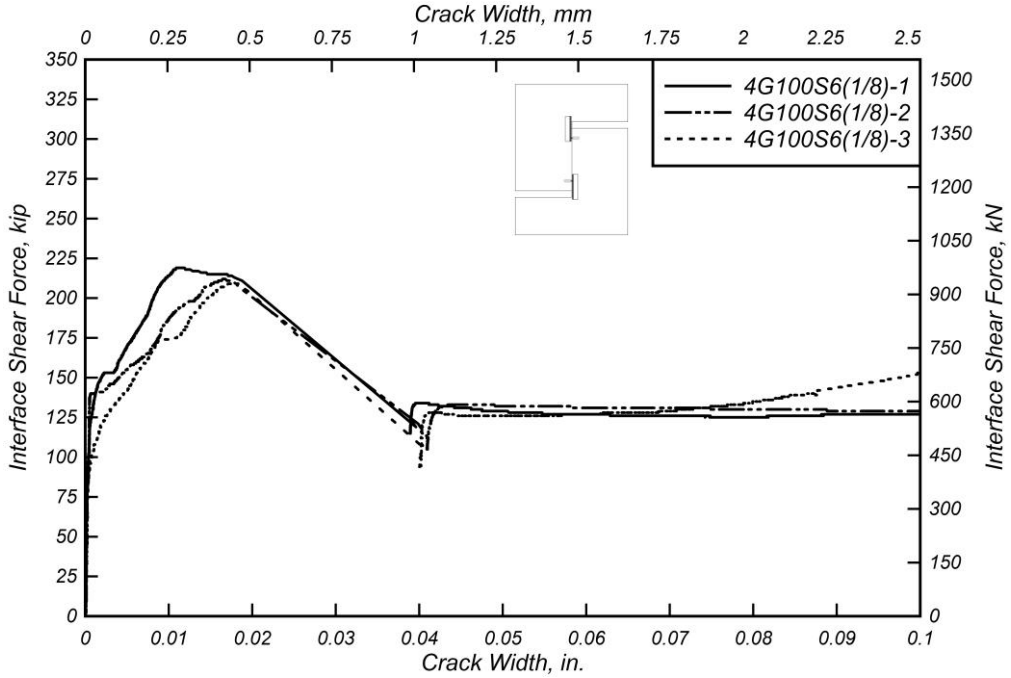

Figure 5.11: Interface shear force versus crack width for 4G100S6(1/8) specimens.

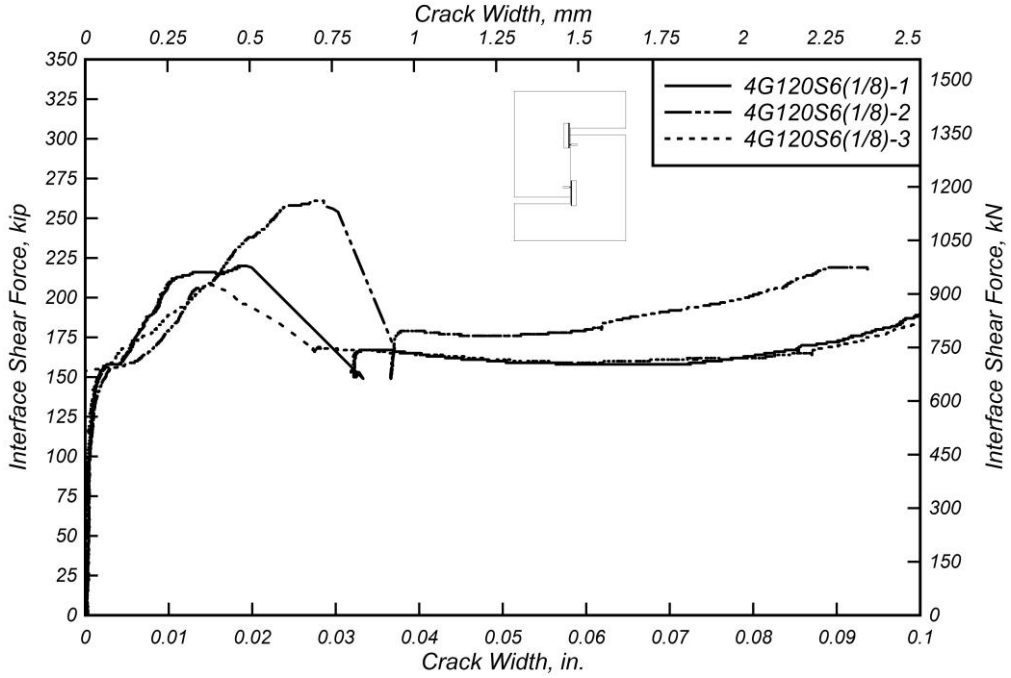

Figure 5.12: Interface shear force versus crack width for 4G120S6(1/8) specimens.

Table 5.11: Specimen 4G60S6(1/8) crack width measurements.

Specimen	w_{ult}, in. (mm)	V_{ult}, kip (kN)	w_b, in. (mm)	V_b, kip (kN)
4G60S6(1/8)-1	0.0117 (0.2972)	212.19 (943.87)	0.1184 (3.007)	123.45 (549.13)
4G60S6(1/8)-2	0.0112 (0.2845)	174.84 (777.73)	0.0867 (2.202)	122.83 (546.37)
4G60S6(1/8)-3	0.0089 (0.2261)	202.00 (898.54)	0.1280 (3.251)	124.66 (554.52)
Mean	0.0106 (0.2692)	196.34 (873.38)	0.1110 (2.820)	123.65 (550.01)
Median	0.0112 (0.2845)	202.00 (898.54)	0.1184 (3.007)	123.45 (549.13)
STDEV	0.0015 (0.0379)	19.31 (85.88)	0.0216 (0.5490)	0.9307 (4.140)
COV	14%	10%	19%	1%

Table 5.12: Specimen 4G80S6(1/8) crack width measurements.

Specimen	w_{ult}, in. (mm)	V_{ult}, kip (kN)	w_b, in. (mm)	V_b, kip (kN)
4G80S6(1/8)-1	0.0256 (0.6510)	221.21 (983.98)	0.1732 (4.398)	145.00 (645.01)
4G80S6(1/8)-2	0.0327 (0.8314)	290.99 (1294.4)	0.2602 (6.610)	150.57 (669.77)
4G80S6(1/8)-3	0.0306 (0.7771)	203.91 (907.04)	0.1782 (4.526)	151.03 (671.81)
Mean	0.0297 (0.7532)	238.70 (1061.8)	0.2039 (5.178)	148.87 (662.20)
Median	0.0306 (0.7771)	221.21 (983.98)	0.1782 (4.526)	150.57 (669.77)
STDEV	0.0036 (0.0926)	46.10 (205.07)	0.0489 (1.242)	3.354 (14.92)
COV	12%	19%	24%	2%

Table 5.13: Specimen 4G100S6(1/8) crack width measurements.

Specimen	w_{ult}, in. (mm)	V_{ult}, kip (kN)	w_b, in. (mm)	V_b, kip (kN)
4G100S6(1/8)-1	0.0111 (0.2828)	218.87 (973.60)	0.2369 (6.017)	166.65 (741.29)
4G100S6(1/8)-2	0.0166 (0.4207)	211.69 (941.64)	0.1669 (4.239)	169.47 (753.84)
4G100S6(1/8)-3	0.0179 (0.4537)	209.42 (931.53)	0.1401 (3.558)	172.15 (765.78)
Mean	0.0152 (0.3857)	213.33 (948.93)	0.1813 (4.605)	169.42 (753.63)
Median	0.0166 (0.4207)	211.69 (941.64)	0.1669 (4.239)	169.47 (753.84)
STDEV	0.0036 (0.0906)	4.936 (21.96)	0.0500 (1.269)	2.753 (12.25)
COV	23%	2%	28%	2%

Table 5.14: Specimen 4G120S6(1/8) crack width measurements.

Specimen	w_{ult}, in. (mm)	V_{ult}, kip (kN)	w_b, in. (mm)	V_b, kip (kN)
4G120S6(1/8)-1	0.0186 (0.4737)	220.12 (979.16)	0.1179 (2.995)	213.49 (949.65)
4G120S6(1/8)-2	0.0284 (0.7212)	261.45 (1163.0)	0.0937 (2.379)	218.05 (969.94)
4G120S6(1/8)-3	0.0151 (0.3835)	208.06 (925.50)	0.1220 (3.099)	208.56 (927.72)
Mean	0.0207 (0.5262)	229.88 (1022.5)	0.1112 (2.824)	213.37 (949.10)
Median	0.0186 (0.4737)	220.12 (979.16)	0.1179 (2.995)	213.49 (949.65)
STDEV	0.0069 (0.1750)	28.00 (124.54)	0.0153 (0.3889)	4.746 (21.11)
COV	33%	12%	14%	2%

Table 5.15: Summary of crack width readings for specimens analyzing influence of reinforcing steel grade.

Specimen	w_{ult}, in. (mm)	V_{ult}, kip (kN)	w_b, in. (mm)	V_b, kip (kN)
4G60S6(1/8)	0.0106 (0.2692)	196.34 (873.38)	0.1110 (2.820)	123.65 (550.01)
4G80S6(1/8)	0.0297 (0.7532)	238.70 (1061.8)	0.2039 (5.178)	148.87 (662.20)
4G100S6(1/8)	0.0152 (0.3857)	213.33 (948.93)	0.1813 (4.605)	169.42 (753.63)
4G120S6(1/8)	0.0207 (0.5262)	229.88 (1022.5)	0.1112 (2.824)	213.37 (949.10)

5.3 INFLUENCE OF BAR SPACING

This section presents the experimental results and discussion for test specimens built with reinforcing steel U-bars spaced at 4 in. (101.6 mm), 6 in. (152.4 mm), and 12 in. (304.8 mm), labeled 4G80S4(1/8), 4G80S6(1/8), and 4G80S12(1/8), respectively. All specimens discussed in this section have an interface preparation of 1/8 in. (3.175 mm) interface roughness, contain #4 (#13M) Grade 80 ksi (550 MPa) reinforcing steel U-bars, and a nominal concrete strength of 5000 psi (35 MPa). Details of the specimens such as bar size, bar spacing, and interface preparation can be found in section (c) of Table 3.1, while drawings showing dimensions, as well as location of the reinforcing steel U-bars are shown in Chapter 3.

5.3.1 Interface Shear Force versus Interface Shear Displacement

Figure 5.13 and Figure 5.14 show the interface shear force versus interface shear displacement curves for the three specimens within each test specimen group containing reinforcing steel U-bars spaced at 4 in. (101.6 mm), and 12 in. (304.8 mm), labeled as 4G80S4(1/8), and 4G80S12(1/8), respectively. The interface shear force versus interface shear displacement response for specimen group with reinforcing steel U-bars of 6 in. (152.4 mm), labeled as 4G80S6(1/8) can be observed in Figure 5.2. In Figure 5.13 and Figure 5.14 it can be observed that in general, the peak load increased as the spacing between reinforcing steel crossing the interface decreased. In Figure 5.13 it can be seen that specimen 4G80S4(1/8)-3 shows a significantly lower interface shear load at cracking and peak load compared to the other specimens in the group. These results indicate that the behavior displayed by this test specimen may be due to a weak concrete-to-concrete bond created at the shear interface. Figure 5.14 shows that specimen 4G80S12(1/8)-1 reaches a significantly lower peak load, but it reaches a similar interface shear load at cracking compared to the other specimens in the group. These results indicate that the behavior observed in specimen 4G80S12(1/8)-1 may be caused by the variability originating from the shear interface preparation of 1/8 in. (3.175 mm) interface roughness. Table 5.16 and Table 5.17 show values of the main points of study discussed in Figure 5.13 and Figure 5.14. Results in these tables and figures indicate that the behavior of all tested specimens is similar beginning with a linear force-displacement response until initial cracking occurs at V_{cr}. The COV for V_{cr} range from 9% to 23%, meanwhile the COV for Δ_{cr} range from 5% to 19%. After cracking, the slope is slightly reduced as the load continues to grow until peak load, V_{ult}, is reached. The respective COV range from 16% to 28%, meanwhile the COV for Δ_{ult} range from 8% to 23%. Following the peak load, the force-displacement response presents a rapid loss of interface shear load accompanied by a rapid increase in interface shear displacement. The post-peak response is characterized by a steady increase in interface shear load and interface shear displacement until first bar fracture.

Table 5.18 shows a summary of the average values for the three specimens in each group. Analysis of the values in table indicates that there is a correlation between peak interface shear capacity and spacing of reinforcing steel U-bars. Specimens with less spacing between reinforcing steel U-bars presented higher average peak interface shear loads. The average peak interface shear loads for 4G80S4(1/8), 4G80S6(1/8), and 4G80S12(1/8) specimens are 238.56 kip (1061.2 kN), 238.70 kip (1061.8 kN), and 160.46 kip (713.78 kN), respectively. This indicates that there is a 49% increase in capacity when the spacing is reduced from 12 in. (304.8 mm) to 4 in. (101.6 mm). These results indicate that reinforcing steel U-bars have a significant impact on interface shear force capacity, even though the capacity remained essentially the same when reducing the spacing from 6 in. (152.4 mm) to 4 in. (101.6 mm). On the other hand, the results do not show a clear influence on the interface shear force at cracking, V_{cr}, which is expected because cohesion controls the initial response prior to cracking. After cracking, the reinforcing steel U-bars begin to engage and strain readings from the strain gauges grow generating the clamping force necessary for aggregate interlock to engage. Specimens with smaller spacing between reinforcing steel U-bars have more reinforcing steel area, and therefore can generate a higher clamping force.

From Table 5.18 it can be inferred that the post-peak sustained load increases as spacing between reinforcing steel U-bars is reduced. The maximum average post-peak sustained loads at first bar fracture, V_b, are 196.79 kip (875.38 kN), 148.87 kip (662.19 kN), and 99.40 kip (442.17 kN) for specimens 4G80S4(1/8), 4G80S6(1/8), and 4G80S12(1/8), respectively. These values are expected, as dowel action is the controlling mechanism in post-peak behavior and it is directly related to area of reinforcing steel present across the interface. The displacements at first bar fracture, Δ_b, do not show any evidence of being influenced by the spacing between reinforcing steel bars as they are 0.998 in. (25.36 mm), 1.018 in. (25.85 mm), and 0.917 in. (23.28 mm) for 4G80S4(1/8), 4G80S6(1/8), and 4G80S12(1/8) specimens, respectively.

The energy dissipated by the specimens until first bar fracture, E_b, is calculated as the area under the force-displacement curve. This parameter increases as the spacing between reinforcing steel bars is reduced. The 4G80S4(1/8) specimens had the highest average E_b at 14.39 kip-ft (19.51 kJ), followed by the 4G80S6(1/8) specimens at 12.61 kip-ft (17.10 kJ). The 4G80S12(1/8) specimens had the lowest average E_b at 7.245 kip-ft (9.823 kJ). This is expected as the specimens exhibit higher peak loads and higher sustained loads as reinforcing steel U-bar spacing is reduced.

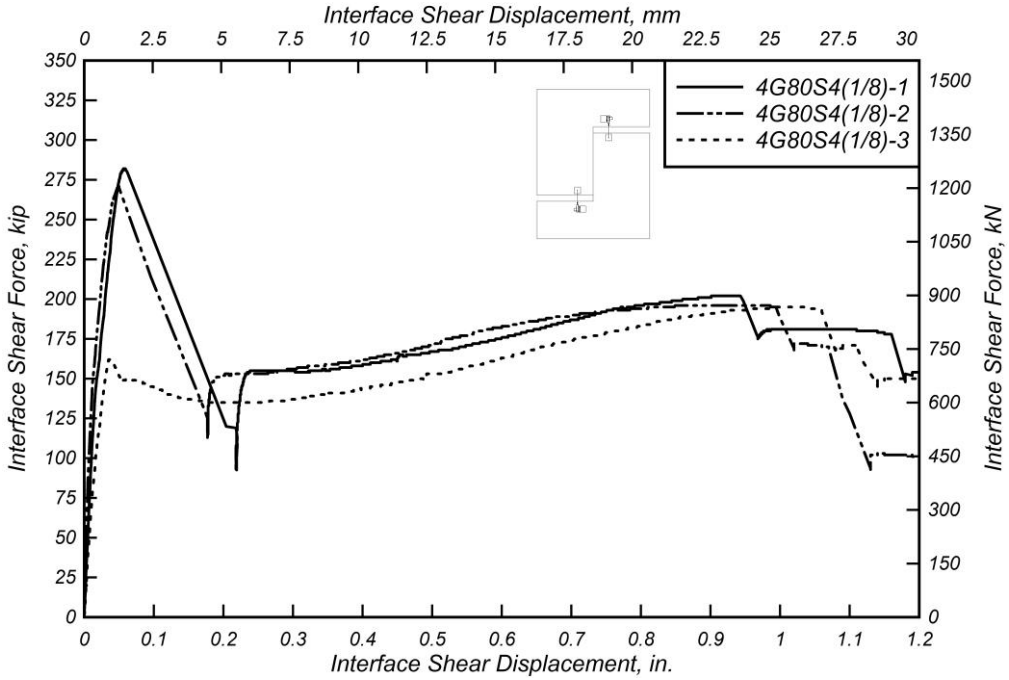

Figure 5.13: Interface shear force versus interface shear displacement for 4G80S4(1/8) specimens.

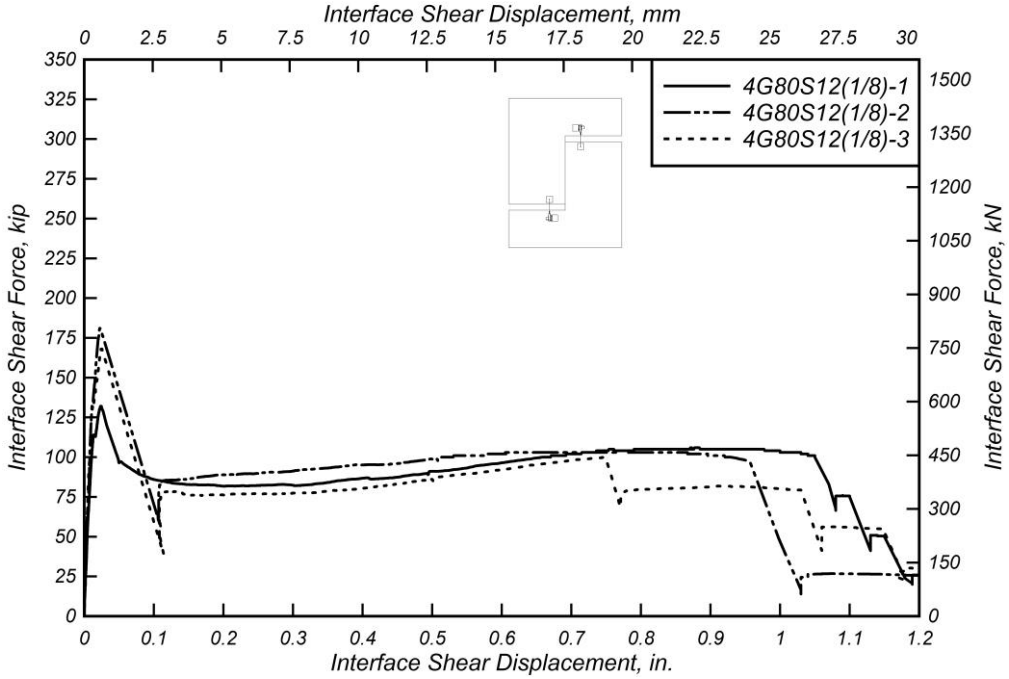

Figure 5.14: Interface shear force versus interface shear displacement for 4G80S12(1/8) specimens.

Table 5.16: Specimen 4G80S4(1/8) shear test results.

Spec	Δ_{ult}, in. (mm)	V_{ult}, kip (kN)	σ_{ult}, ksi (MPa)	$V_{sus,min}$, kip (kN)	$V_{sus,max}$, kip (kN)	Δ_{cr}, in. (mm)	V_{cr}, kip (kN)	Δ_{b}, in. (mm)	V_b, kip (kN)	E_b, kip-ft (kJ)
4G80S4 (1/8)-1	0.058 (1.47)	282.25 (1256)	1.176 (8.11)	154.23 (686.1)	202.29 (899.8)	0.015 (0.39)	138.40 (615.6)	0.943 (24.0)	202.22 (899.5)	14.09 (19.11)
4G80S4 (1/8)-2	0.049 (1.25)	271.13 (1206)	1.130 (7.79)	152.46 (678.2)	196.16 (872.6)	0.011 (0.27)	135.80 (604.1)	0.994 (25.3)	194.67 (865.9)	14.94 (20.26)
4G80S4 (1/8)-3	0.036 (0.91)	162.30 (722.0)	0.676 (4.66)	134.63 (598.9)	194.84 (866.7)	0.014 (0.36)	88.34 (393.0)	1.058 (26.9)	193.49 (860.7)	14.13 (19.15)
Mean	0.048 (1.21)	238.56 (1061)	0.994 (6.85)	147.11 (654.4)	197.76 (879.7)	0.013 (0.34)	120.85 (537.6)	0.998 (25.4)	196.79 (875.4)	14.39 (19.51)
Median	0.049 (1.25)	271.13 (1206)	1.130 (7.79)	152.46 (678.2)	196.16 (872.6)	0.014 (0.36)	135.80 (604.1)	0.994 (25.3)	194.67 (866.0)	14.13 (19.15)
STDEV	0.011 (0.28)	66.28 (294.8)	0.276 (1.90)	10.84 (48.22)	3.975 (17.68)	0.003 (0.06)	28.18 (125.4)	0.058 (1.46)	4.737 (21.07)	0.479 (0.650)
COV	23%	28%	28%	7%	2%	19%	23%	6%	2%	3%

Table 5.17: Specimen 4G80S12(1/8) shear test results.

Spec	Δ_{ult}, in. (mm)	V_{ult}, kip (kN)	σ_{ult}, ksi (MPa)	$V_{sus,min}$, kip (kN)	$V_{sus,max}$, kip (kN)	Δ_{cr}, in. (mm)	V_{cr}, kip (kN)	Δ_{b}, in. (mm)	V_b, kip (kN)	E_b, kip-ft (kJ)
4G80 S12 (1/8)-1	0.024 (0.61)	132.13 (587.7)	0.551 (3.80)	81.75 (363.6)	105.65 (470.0)	0.013 (0.34)	114.40 (508.9)	1.045 (26.5)	101.23 (450.3)	8.27 (11.21)
4G80 S12 (1/8)-2	0.022 (0.56)	181.29 (806.4)	0.755 (5.21)	84.94 (377.8)	103.55 (460.6)	0.010 (0.25)	122.50 (544.9)	0.956 (24.3)	96.99 (431.4)	7.96 (10.79)
4G80 S12 (1/8)-3	0.026 (0.66)	167.97 (747.2)	0.700 (4.83)	75.94 (337.8)	99.90 (444.4)	0.012 (0.29)	135.90 (604.5)	0.749 (19.0)	99.99 (444.8)	5.51 (7.469)
Mean	0.024 (0.61)	160.46 (713.8)	0.669 (4.61)	80.88 (359.8)	103.03 (458.3)	0.012 (0.29)	124.27 (552.8)	0.917 (23.3)	99.40 (442.2)	7.25 (9.823)
Median	0.024 (0.61)	167.97 (747.2)	0.700 (4.83)	81.75 (363.6)	103.55 (460.6)	0.012 (0.29)	122.50 (544.9)	0.956 (24.3)	99.99 (444.8)	7.96 (10.79)
STDEV	0.002 (0.05)	25.43 (113.1)	0.106 (0.73)	4.563 (20.30)	2.910 (12.94)	0.002 (0.04)	10.86 (48.30)	0.152 (3.86)	2.180 (9.70)	1.51 (2.049)
COV	8%	16%	16%	6%	3%	15%	9%	17%	2%	21%

Table 5.18: Summary of averages of specimen groups analyzing influence of reinforcing steel bar spacing.

Spec	Δ_{ult}, in. (mm)	V_{ult}, kip (kN)	σ_{ult}, ksi (MPa)	$V_{sus,min}$, kip (kN)	$V_{sus,max}$, kip (kN)	Δ_{cr}, in. (mm)	V_{cr}, kip (kN)	Δ_{b}, in. (mm)	V_b, kip (kN)	E_b, kip-ft (kJ)
4G80S4 (1/8)	0.048 (1.21)	238.56 (1061)	0.994 (6.85)	147.11 (654.4)	197.76 (879.7)	0.013 (0.34)	120.85 (537.6)	0.998 (25.4)	196.79 (875.4)	14.39 (19.51)
4G80S6 (1/8)	0.073 (1.86)	238.70 (1062)	0.995 (6.86)	129.01 (573.9)	153.62 (683.4)	0.016 (0.40)	109.44 (486.8)	1.018 (25.9)	148.87 (662.2)	12.61 (17.10)
4G80S12 (1/8)	0.024 (0.61)	160.46 (713.8)	0.669 (4.61)	80.88 (359.8)	103.03 (458.3)	0.012 (0.29)	124.27 (552.8)	0.917 (23.3)	99.40 (442.2)	7.25 (9.823)

5.3.2 Interface Shear Force versus Strain

The interface shear force versus reinforcing steel strain relationship for 4G80S4(1/8) and 4G80S12(1/8) specimen groups are presented in Figure 5.15 and Figure 5.16. Figure 5.6 shows the interface shear force versus reinforcing steel strain relationship for specimen group 4G80S6(1/8). All tested specimens present a similar behavior in the initial stages, whereby the force-strain response is linear until the cracking shear force, V_{cr}, is reached. At this point the stiffness (slope) is reduced and the strain in the reinforcing steel U-bars begins to increase at a higher rate, which indicates that the reinforcing steel U-bars engage most once cohesion is lost.

As seen in Figure 5.15, strain in specimen 4G80S4(1/8)-3 begins to grow rapidly at a much lower load compared to the other specimens in the group. This result may suggest that the cohesion bond at the shear interface was significantly weaker, which can be attributed to the variability originating from creating the 1/8 in. (3.175 mm) interface preparation. Figure 5.16 shows that strain in specimen 4G80S12(1/8)-1 begins to grow rapidly at a shear load slightly lower than the other specimens in the group. However, it does reach peak load at significantly lower strains. These results indicate that the behavior observed may be related to the aggregate interlock mechanism, possibly weakened by the variability originating from creating the 1/8 in. (3.175 mm) interface preparation.

The force-strain response begins to show differences in the post-cracking stage, where specimens in group 4G80S12(1/8) present a much lower post-cracking stiffness until the peak load, V_{ult}. After the peak load is reached there is a steep drop in interface shear load followed by a sustained load as strain continues to grow. This steep drop is significantly different from the force-strain response of specimen groups 4G80S4(1/8) and 4G80S6(1/8), which display a smooth softening curve leading to the sustained load phase. The abrupt loss of capacity in the 4G80S12(1/8) specimens indicates that the larger the spacing of the reinforcing steel bars across the interface the more brittle the interface shear response becomes.

Table 5.19 and Table 5.20 list the strain measurements at peak load for the strain gauges contained in each test specimen. Table 5.21 summarizes the average strain gauge readings of strain gauges in the same location for all test specimens within each group. Values in the mentioned tables indicate that specimen group 4G80S6(1/8) reached higher strains at peak load. Note that in the mentioned tables, the strain gauges that were damaged before reaching peak load are labeled "-". Table cells containing "N/A" indicate that the corresponding strain gauges was not installed. Refer to Section 3.5 for strain gauges configurations.

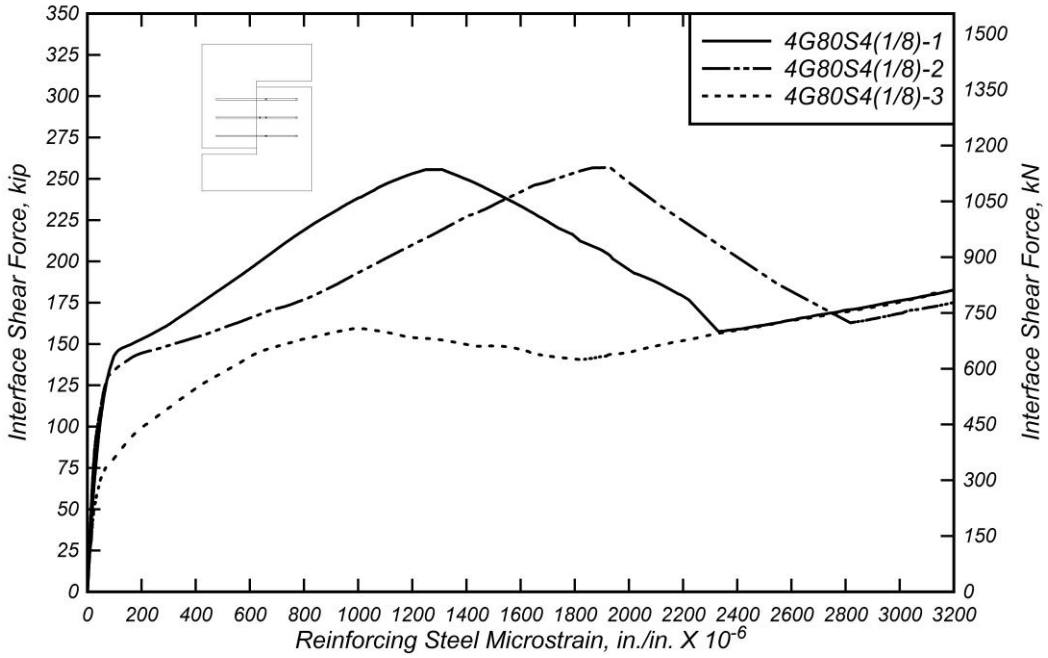

Figure 5.15: Interface shear force versus average reinforcing steel microstrain for 4G80S4(1/8) specimens.

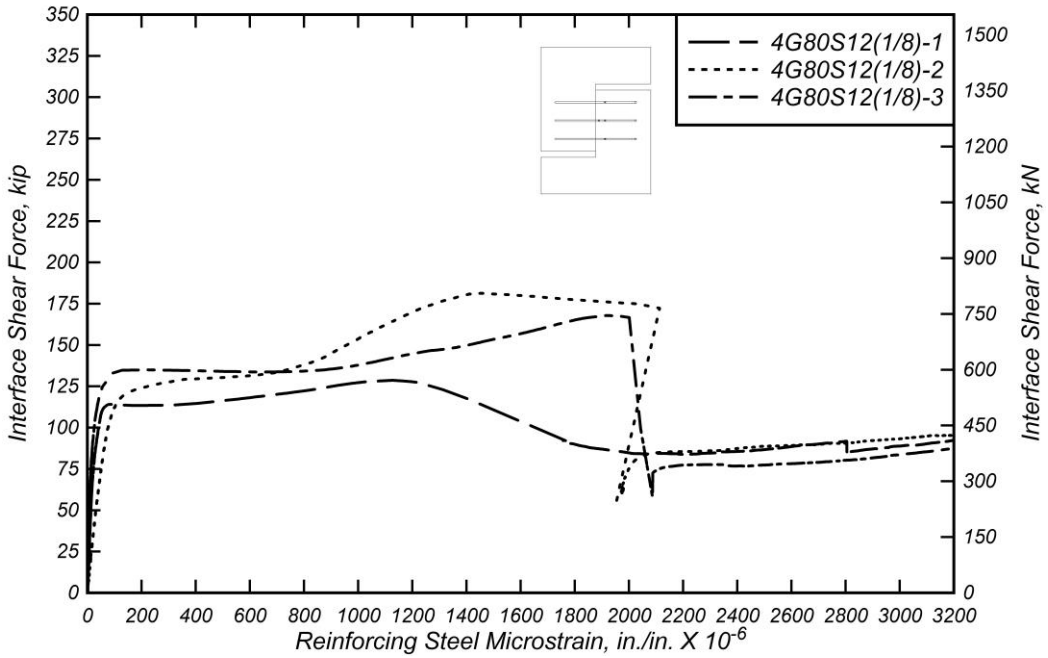

Figure 5.16: Interface shear force versus average reinforcing steel microstrain for 4G80S12(1/8) specimens.

Table 5.19: Specimen 4G80S4(1/8) strain gauge readings at peak interface shear force.

Spec	s_1, in./in. (mm/mm)	s_2, in./in. (mm/mm)	s_3, in./in. (mm/mm)	s_4, in./in. (mm/mm)	s_5, in./in. (mm/mm)	s_6, in./in. (mm/mm)	s_7, in./in. (mm/mm)	s_8, in./in. (mm/mm)	s_9, in./in. (mm/mm)
4G80S4(1/8)-1	0.0024	-	0.0018	0.0011	0.0018	-	0.0016	0.0012	-
4G80S4(1/8)-2	0.0026	-	-	-	-	-	0.0019	-	-
4G80S4(1/8)-3	0.0008	-	0.0010	-	-	-	-	-	0.0007
Mean	0.0019	-	0.0014	0.0011	0.0018	-	0.0017	0.0012	0.0007
Median	0.0024	-	0.0014	0.0011	0.0018	-	0.0017	0.0012	0.0007
STDEV	0.0010	-	0.0006	-	-	-	0.0002	-	-
COV	52%	-	39%	-	-	-	12%	-	-

Table 5.20: Specimen 4G80S12(1/8) strain gauge readings at peak interface shear force.

Spec	s_1, in./in. (mm/mm)	s_2, in./in. (mm/mm)	s_3, in./in. (mm/mm)	s_4, in./in. (mm/mm)	s_5, in./in. (mm/mm)
4G80S12(1/8)-1	0.0011	-	0.0014	0.0012	0.0008
4G80S12(1/8)-2	-	-	0.0013	-	0.0014
4G80S12(1/8)-3	0.0020	-	0.0014	0.0019	-
Mean	0.0015	-	0.0014	0.0016	0.0011
Median	0.0015	-	0.0014	0.0016	0.0011
STDEV	0.0006	-	0.00006	0.0005	0.0004
COV	38%	-	4%	30%	40%

Table 5.21: Summary of average strain readings at peak interface shear force of specimen groups analyzing influence of reinforcing steel bar spacing.

Spec	s_1, in./in. (mm/mm)	s_2, in./in. (mm/mm)	s_3, in./in. (mm/mm)	s_4, in./in. (mm/mm)	s_5, in./in. (mm/mm)	s_6, in./in. (mm/mm)	s_7, in./in. (mm/mm)	s_8, in./in. (mm/mm)	s_9, in./in. (mm/mm)
4G80S4 (1/8)	0.0019	-	0.0014	0.0011	0.0018	-	0.0017	0.0012	0.0007
4G80S6 (1/8)	-	0.0022	0.0019	0.0026	0.0028	0.0021	0.0015	N/A	N/A
4G80S12 (1/8)	0.0015	-	0.0014	0.0016	0.0011	N/A	N/A	N/A	N/A

5.3.3 Interface Shear Force versus Crack Width

The interface shear force versus crack width response for specimen groups 4G80S4(1/8), and 4G80S12(1/8) can be observed in Figure 5.17 and Figure 5.18. Figure 5.10 shows the interface shear force versus crack width response for specimen group 4G80S6(1/8). Each figure shows the force-crack width response for all

specimens in each group. Tabulated values of points of interest such as crack width at peak load and crack width at first bar fracture for each specimen group are presented in Table 5.22 and Table 5.23. A summary for comparison purposes of the three specimen groups is presented in Table 5.24.

The comparison between specimen groups in Table 5.24 displays a clear difference in post-cracked behavior. This different reflects a greater capacity achieved by 4G80S4(1/8) and 4G80S6(1/8) specimens, and it indicates that reducing the spacing between reinforcing steel U-bars increases the capacity of specimens. This can be attributed to aggregate interlock controlling the post-cracking response, and thus a higher clamping force can be developed allowing the specimens to reach a higher peak load in specimens with a larger reinforcing steel ratio. The average peak load, V_{ult}, is 238.56 kip (1061.2 kN) for 4G80S4(1/8) specimens, 238.70 kip (1061.8 kN) for 4G80S6(1/8) specimens, and 160.47 kip (713.78 kN) for 4G80S12(1/8) specimens. An increase in peak load capacity of 48% is observed when reducing the reinforcing steel U-bar spacing from 12 in. (304.8 mm) to 6 in. (152.4 mm) and 4 in. (101.6 mm). This shows a significant increase in peak load capacity can be achieved by increasing the number of reinforcing steel U-bars and reducing the spacing.

The post-peak behavior is controlled by dowel action in the reinforcing steel U-bars. Figure 5.17 and Figure 5.18 show that 4G80S4(1/8) specimens present the highest post-peak average sustained load, while 4G80S12(1/8) specimens present the lowest post-peak average sustained load. This behavior is expected, as 4G80S4(1/8) specimens contain a higher reinforcing steel ratio, which directly affects the force generated to dowel action. It is worth noting that the increase in post-peak average sustained load is proportional to the inverse of the spacing and therefore linearly proportional to the reinforcing steel ratio across the interface.

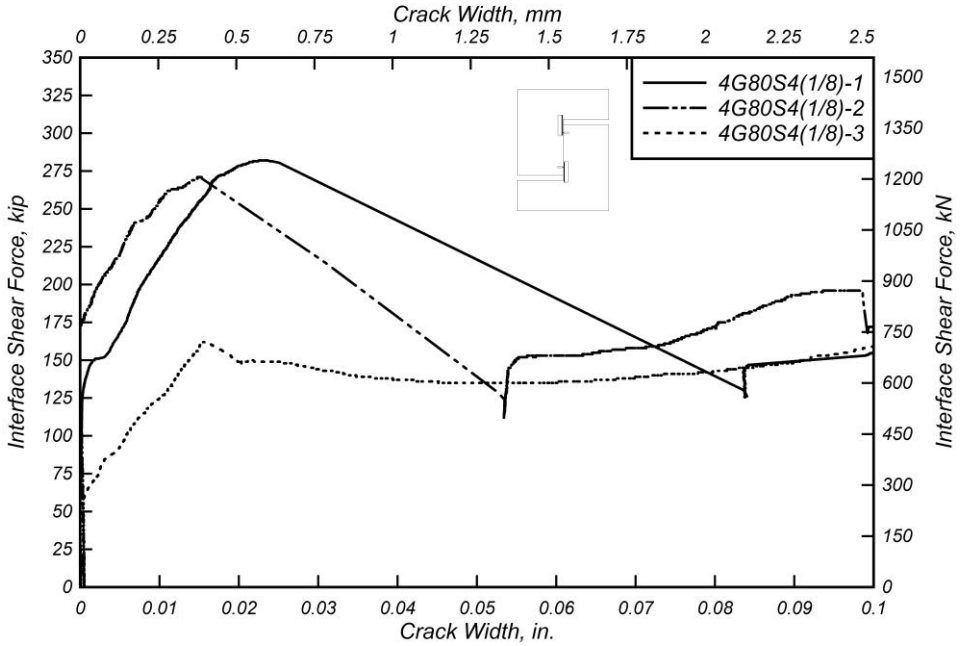

Figure 5.17: Interface shear force versus crack width for 4G80S4(1/8) specimens.

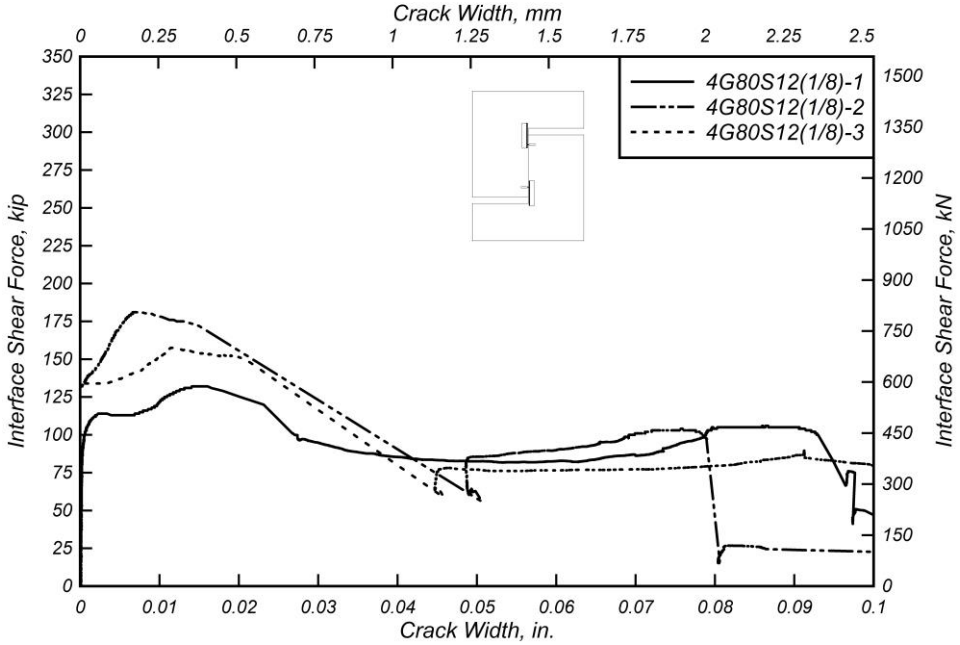

Figure 5.18: Interface shear force versus crack width for 4G80S12(1/8) specimens.

Table 5.22: Specimen 4G80S4(1/8) crack width measurements.

Specimen	w_{ult}, in. (mm)	V_{ult}, kip (kN)	w_b, in. (mm)	V_b, kip (kN)
4G80S4(1/8)-1	0.0234 (0.5937)	282.25 (1255.5)	0.2061 (5.236)	202.22 (899.51)
4G80S4(1/8)-2	0.0149 (0.3794)	271.13 (1206.0)	0.0986 (2.504)	194.67 (865.92)
4G80S4(1/8)-3	0.0156 (0.3962)	162.30 (721.95)	0.1358 (3.449)	193.49 (860.70)
Mean	0.0180 (0.4565)	238.56 (1061.2)	0.1468 (3.730)	196.79 (875.38)
Median	0.0156 (0.3962)	271.13 (1206.0)	0.1358 (3.449)	194.67 (865.92)
STDEV	0.0047 (0.1192)	66.28 (294.81)	0.0546 (1.387)	4.735 (21.06)
COV	26%	28%	37%	2%

Table 5.23: Specimen 4G80S12(1/8) crack width measurements.

Specimen	w_{ult}, in. (mm)	V_{ult}, kip (kN)	w_b, in. (mm)	V_b, kip (kN)
4G80S12(1/8)-1	0.0154 (0.3910)	132.13 (587.74)	0.0928 (2.356)	101.23 (450.28)
4G80S12(1/8)-2	0.0070 (0.1768)	181.29 (806.42)	0.0790 (2.006)	96.99 (431.42)
4G80S12(1/8)-3	0.0160 (0.4062)	167.97 (747.19)	0.1070 (2.719)	99.99 (444.79)
Mean	0.0128 (0.3247)	160.47 (713.78)	0.0929 (2.360)	99.40 (442.16)
Median	0.0154 (0.3910)	167.97 (747.19)	0.0928 (2.356)	99.99 (444.79)
STDEV	0.0051 (0.1283)	25.43 (113.10)	0.0140 (0.356)	2.181 (9.701)
COV	40%	16%	15%	2%

Table 5.24: Summary of crack width readings for specimens analyzing influence of reinforcing steel bar spacing.

Specimen	w_{ult}, in. (mm)	V_{ult}, kip (kN)	w_b, in. (mm)	V_b, kip (kN)
4G80S4(1/8)	0.0180 (0.4565)	238.56 (1061.2)	0.1468 (3.730)	196.79 (875.38)
4G80S6(1/8)	0.0297 (0.7532)	238.70 (1061.8)	0.2039 (5.178)	148.87 (662.20)
4G80S12(1/8)	0.0128 (0.3247)	160.47 (713.78)	0.0929 (2.360)	99.40 (442.16)

5.4 INFLUENCE OF REINFORCING BAR SIZE

This section presents the experimental results and discussion for test specimens reinforced with #4 (#13M) and #5 (#16M) reinforcing steel U-bars. All specimens discussed in this section have three Grade 80 ksi (550 MPa) reinforcing steel U-bars spaced at 6 in. (152.4 mm) and a nominal concrete strength of 5000 psi (35 MPa). The effect of bar size is discussed separately across four interface preparations which are As Cast, 1/8 in, (3.175 mm), 1/4 in. (6.35 mm), and Exposed Aggregate, and later the general observations on the influence of bar size are discussed. Details of the specimens such as bar size, bar spacing, and interface preparation can be found in section (d) of Table 3.1. Detailed drawings showing dimensions of the specimens, as well as location of the reinforcing steel U-bars are presented in Chapter 3.

5.4.1 Interface Shear Force versus Interface Shear Displacement

5.4.1.1 Interface Preparation: As Cast

Figure 5.19 and Figure 5.20 present the interface shear force versus interface shear displacement response curves for specimen groups 4G80S6(AC) and 5G80S6(AC), respectively. All specimens in the specimen groups mentioned are constructed with an As Cast interface preparation. The behavior of all specimens is similar with the exception of specimen 4G80S6(AC)-3, which underperforms considerably compared to the other specimens in the group. The peak load, V_{ult}, and displacement at peak load, Δ_{ult}, are approximately 26% and 33% lower compared to the other specimens in the group. This pattern, however, does not repeat itself when analyzing the interface shear load and displacement when cracking occurs. Therefore, the underperformance of the 4G80S6(AC)-3 specimen in terms of force-displacement response cannot be attributed to a weak concrete-to-concrete bond, but rather to a lower aggregate interlock influence possibly caused by the variability generated during the interface preparation process. Table 5.25 and Table 5.26 present tabulated values of the main points of study for specimen groups 4G80S6(AC) and 5G80S6(AC), respectively.

Table 5.27 presents a summary of the tabulated values of the main points of interest for specimen groups 4G80S6(AC) and 5G80S6(AC). In the initial loading stages,

specimen group 4G80S6(AC) presents a slightly larger average interface shear load at cracking, V_{cr}, with 142.83 kip (635.35 kN) compared to the 5G80S6(AC) specimen group with 127.53 kip (567.30 kN) and a larger average peak load capacity with 262.65 kip (1168.3 kN) compared to the 5G80S6(AC) group with 259.87 kip (1156.0 kN). On the other hand, the specimen group 5G80S6(AC) presents a larger post-peak average sustained load at first bar fracture than the 4G80S6(AC) specimens, with values of 224.37 kip (998.05 kN) and 149.63 kip (665.60 kN) for specimen groups 5G80S6(AC) and 4G80S6(AC), respectively. This indicates a 50% increase in average sustained load capacity when the reinforcing steel bars across the interface increase from #4 (#13M) to #5 (#16M). This increase is directly related to the reinforcing steel ratio across the interface, as the increase in reinforcing steel bar size across the interface results in a 55% increase in the reinforcing steel ratio. The higher sustained load capacity is attributed to the larger reinforcing steel ratio across the interface, which is directly related to the dowel action mechanism controlling the post-peak response.

The average dissipated energy until bar fracture by 5G80S6(AC) specimens, E_b, is 20.26 kip-ft (27.47 kJ) and 11.74 kip-ft (15.92 kJ) for 4G80S6(AC) specimens, which corresponds to a 68% increase in E_b when increasing the reinforcing steel bar size from #4 (#13M) to #5 (#16M). Shear displacement at first bar fracture, Δ_b, was 1.242 in. (31.55 mm) and 0.919 in. (23.35 mm) for 5G80S6(AC) and 4G80S6(AC), respectively, indicating a 35% increase in Δ_b.

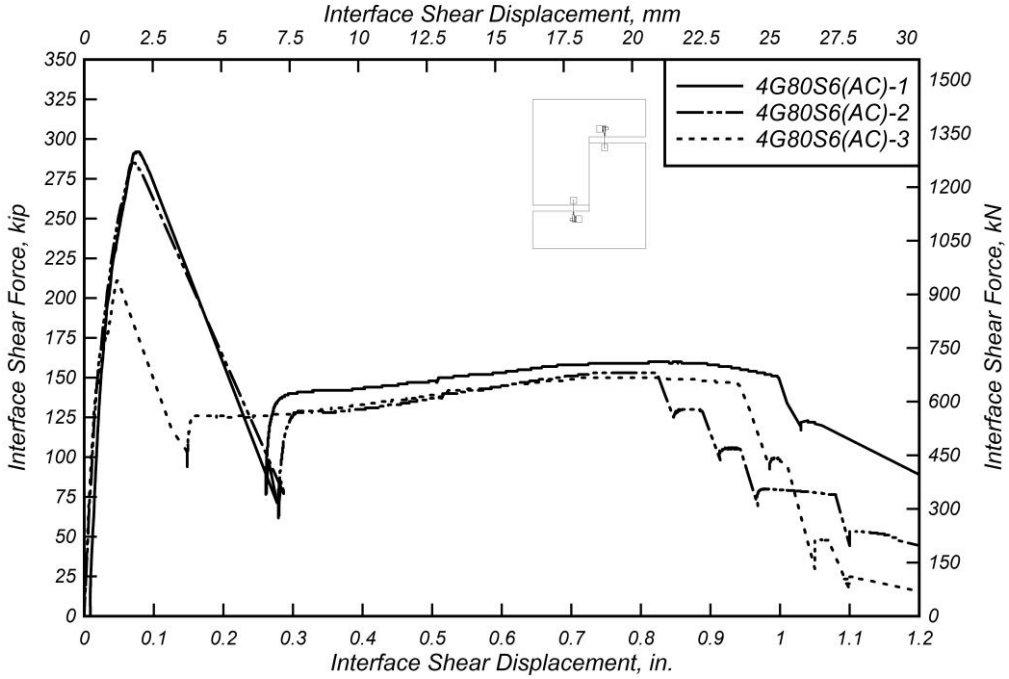

Figure 5.19: Interface shear force versus interface shear displacement for 4G80S6(AC) specimens.

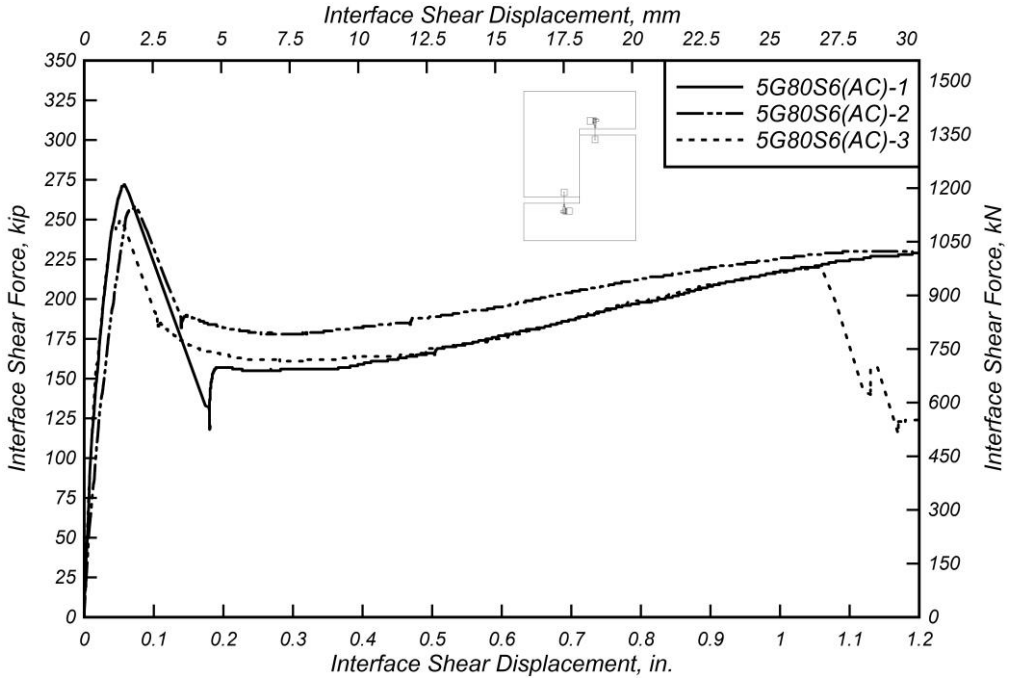

Figure 5.20: Interface shear force versus interface shear displacement for 5G80S6(AC) specimens.

Table 5.25: Specimen 4G80S6(AC) shear test results.

Spec	Δ_{ult}, in. (mm)	V_{ult}, kip (kN)	σ_{ult}, ksi (MPa)	$V_{sus,min}$, kip (kN)	$V_{sus,max}$, kip (kN)	Δ_{cr}, in. (mm)	V_{cr}, kip (kN)	Δ_{b}, in. (mm)	V_b, kip (kN)	E_b, kip-ft (kJ)
4G80S6 (AC)-1	0.077 (1.96)	292.03 (1299)	1.217 (8.39)	140.31 (624.1)	159.75 (710.6)	0.021 (0.54)	132.20 (588.1)	0.995 (25.3)	150.66 (670.2)	13.43 (18.21)
4G80S6 (AC)-2	0.072 (1.83)	284.98 (1268)	1.187 (8.19)	128.36 (571.0)	153.38 (682.3)	0.020 (0.50)	153.40 (682.4)	0.822 (20.9)	152.78 (679.6)	10.73 (14.55)
4G80S6 (AC)-3	0.048 (1.22)	210.93 (938.3)	0.879 (6.06)	125.31 (557.4)	150.42 (669.1)	0.017 (0.43)	142.90 (635.7)	0.941 (23.9)	145.46 (647.0)	11.07 (15.01)
Mean	0.066 (1.67)	262.65 (1168)	1.094 (7.55)	131.33 (584.2)	154.52 (687.3)	0.019 (0.49)	142.83 (635.4)	0.919 (23.4)	149.63 (665.6)	11.74 (15.92)
Median	0.072 (1.83)	284.98 (1268)	1.187 (8.19)	128.36 (571.0)	153.38 (682.3)	0.020 (0.50)	142.90 (635.7)	0.941 (23.9)	150.66 (670.2)	11.07 (15.01)
STDEV	0.016 (0.39)	44.93 (199.8)	0.187 (1.29)	7.928 (35.26)	4.768 (21.21)	0.002 (0.06)	10.60 (47.15)	0.089 (2.25)	3.766 (16.75)	1.470 (1.993)
COV	24%	17%	17%	6%	3%	12%	7%	10%	3%	13%

Table 5.26: Specimen 5G80S6(AC) shear test results.

Spec	Δ_{ult}, in. (mm)	V_{ult}, kip (kN)	σ_{ult}, ksi (MPa)	$V_{sus,min}$, kip (kN)	$V_{sus,max}$, kip (kN)	Δ_{cr}, in. (mm)	V_{cr}, kip (kN)	Δ_{b}, in. (mm)	V_b, kip (kN)	E_b, kip-ft (kJ)
5G80S6 (AC)-1	0.058 (1.47)	271.63 (1208)	1.132 (7.80)	155.04 (689.7)	232.39 (1034)	0.010 (0.26)	108.00 (480.4)	1.456 (37.0)	225.46 (1003)	23.88 (32.38)
5G80S6 (AC)-2	0.071 (1.80)	257.72 (1146)	1.074 (7.40)	177.97 (791.7)	230.47 (1025)	0.020 (0.50)	116.50 (518.2)	1.215 (30.9)	228.09 (1015)	20.59 (27.92)
5G80S6 (AC)-3	0.052 (1.32)	250.26 (1113)	1.043 (7.19)	161.17 (716.9)	219.77 (977.6)	0.017 (0.43)	158.10 (703.3)	1.055 (26.8)	219.56 (976.7)	16.30 (22.10)
Mean	0.060 (1.53)	259.87 (1156)	1.083 (7.47)	164.73 (732.7)	227.54 (1012)	0.016 (0.40)	127.53 (567.3)	1.242 (31.6)	224.37 (998.1)	20.26 (27.47)
Median	0.058 (1.47)	257.72 (1146)	1.074 (7.40)	161.17 (716.9)	230.47 (1025)	0.017 (0.43)	116.50 (518.2)	1.215 (30.9)	225.46 (1003)	20.59 (27.92)
STDEV	0.010 (0.25)	10.85 (48.25)	0.045 (0.31)	11.87 (52.81)	6.800 (30.25)	0.005 (0.13)	26.81 (119.3)	0.202 (5.13)	4.368 (19.43)	3.803 (5.157)
COV	16%	4%	4%	7%	3%	31%	21%	16%	2%	19%

Table 5.27: Summary of averages of 4G80S6(AC) and 5G80S6(AC) specimens with As Cast interface finish.

Spec	Δ_{ult}, in. (mm)	V_{ult}, kip (kN)	σ_{ult}, ksi (MPa)	$V_{sus,min}$, kip (kN)	$V_{sus,max}$, kip (kN)	Δ_{cr}, in. (mm)	V_{cr}, kip (kN)	Δ_{b}, in. (mm)	V_b, kip (kN)	E_b, kip-ft (kJ)
4G80S6 (AC)	0.066 (1.67)	262.65 (1168)	1.094 (7.55)	131.33 (584.2)	154.52 (687.3)	0.019 (0.49)	142.83 (635.4)	0.919 (23.4)	149.63 (665.6)	11.74 (15.92)
5G80S6 (AC)	0.060 (1.53)	259.87 (1156)	1.083 (7.47)	164.73 (732.7)	227.54 (1012)	0.016 (0.40)	127.53 (567.3)	1.242 (31.6)	224.37 (998.1)	20.26 (27.47)

5.4.1.2 Interface Preparation: Roughened with 1/8 in. (3.175 mm)

Figure 5.2 and Figure 5.21 present the interface shear force versus interface shear displacement response curves for specimen groups 4G80S6(1/8) and 5G80S6(1/8), respectively. All specimens in both specimen groups are constructed with a surface intentionally roughened to an amplitude of 1/8 in. (3.175 mm). The behavior in all specimens is similar, although specimen 5G80S6(1/8)-2 reaches a considerably larger average peak-load, V_{ult}, as seen in Figure 5.21. The lower V_{ult} reached by specimens 5G80S6(1/8)-1 and 5G80S6(1/8)-3 may be related to the maximum aggregate size (3/8 in. [9.525 mm]). The shear interface surface is roughened with ridges to an amplitude of 1/8 in. (3.175 mm), therefore the maximum aggregates are larger than the ridges. This may create voids in the shear interface that cause a weaker concrete-to-concrete cohesion bond.

In general, it can be seen that specimen group 5G80S6(1/8) reinforced with #5 (#16M) steel bars crossing the interface exhibited a larger capacity, as can be observed from the tabulated values shown in Table 5.29. Initially, a higher stiffness and a 13% higher peak-load, V_{ult}, can be observed in the 5G80S6(1/8) specimens. The main differences between the performance of the two specimen groups becomes more apparent in the post-cracked stage of the force-displacement response, with the larger capacity and energy dissipated by the 5G80S6(1/8) specimens when compared to the 4G80S6(1/8) specimens. This indicates that for specimens with the surface intentionally roughened to and amplitude of 1/8 in. (3.175 mm), increasing the reinforcing steel bar size from #4 (#13M) to #5 (#16M) results in an increase in capacity and performance.

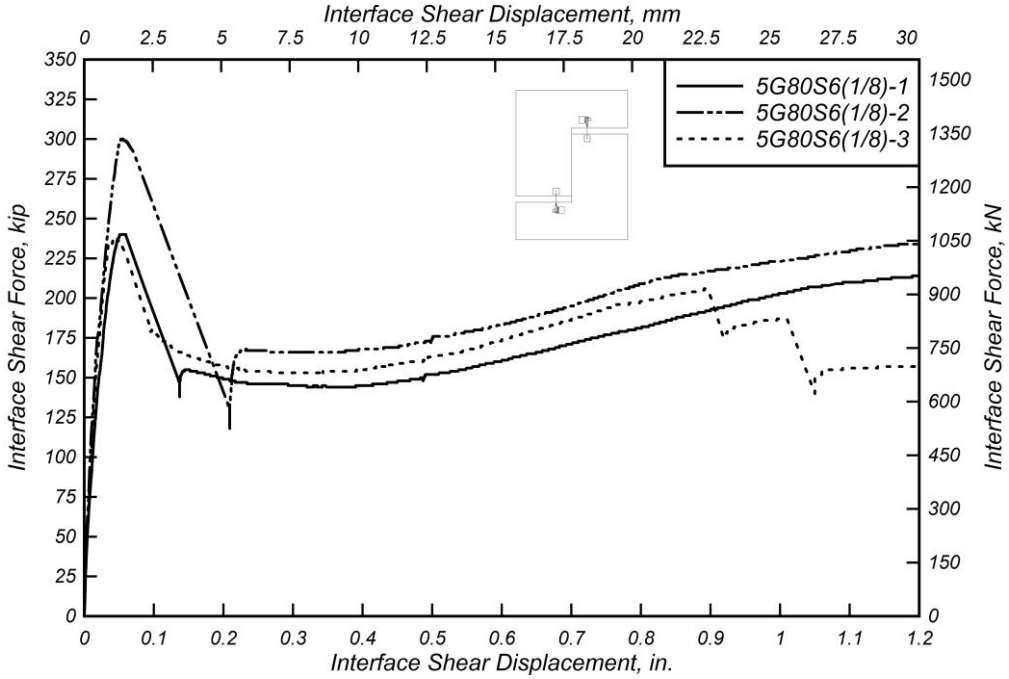

Figure 5.21: Interface shear force versus interface shear displacement for 5G80S6(1/8) specimens.

Table 5.28: Specimen 5G80S6(1/8) shear test results.

Spec	Δ_{ult}, in. (mm)	V_{ult}, kip (kN)	σ_{ult}, ksi (MPa)	$V_{sus,min}$, kip (kN)	$V_{sus,max}$, kip (kN)	Δ_{cr}, in. (mm)	V_{cr}, kip (kN)	Δ_{b}, in. (mm)	V_b, kip (kN)	E_b, kip-ft (kJ)
5G80S6 (1/8)-1	0.053 (1.35)	240.38 (1069)	1.002 (6.91)	144.04 (640.7)	221.13 (983.6)	0.021 (0.54)	151.70 (674.8)	1.385 (35.2)	220.63 (981.4)	20.82 (28.23)
5G80S6 (1/8)-2	0.054 (1.37)	300.13 (1335)	1.251 (8.62)	165.55 (736.4)	234.51 (1043)	0.018 (0.46)	171.60 (763.3)	1.315 (33.4)	225.72 (1004)	22.29 (30.22)
5G80S6 (1/8)-3	0.044 (1.12)	238.06 (1059)	0.992 (6.84)	152.81 (679.7)	205.95 (916.1)	0.017 (0.43)	155.30 (690.8)	0.895 (22.7)	205.82 (915.5)	12.96 (17.57)
Mean	0.050 (1.28)	259.52 (1154)	1.081 (7.46)	154.13 (685.6)	220.53 (981.0)	0.019 (0.48)	159.53 (709.6)	1.198 (30.4)	217.39 (967.0)	18.69 (25.34)
Median	0.053 (1.35)	240.38 (1069)	1.002 (6.91)	152.81 (679.7)	221.13 (983.6)	0.018 (0.46)	155.30 (690.8)	1.315 (33.4)	220.63 (981.4)	20.82 (28.23)
STDEV	0.006 (0.14)	35.19 (156.5)	0.147 (1.01)	10.82 (48.11)	14.29 (63.56)	0.002 (0.06)	10.60 (47.17)	0.265 (6.73)	10.34 (45.99)	5.019 (6.805)
COV	11%	14%	14%	7%	6%	12%	7%	22%	5%	27%

Table 5.29: Summary of averages of 4G80S6(1/8) and 5G80S6(1/8) specimens with 1/8 in. (3.175 mm) interface finish.

Spec	Δ_{ult}, in. (mm)	V_{ult}, kip (kN)	σ_{ult}, ksi (MPa)	$V_{sus,min}$, kip (kN)	$V_{sus,max}$, kip (kN)	Δ_{cr}, in. (mm)	V_{cr}, kip (kN)	Δ_{b}, in. (mm)	V_b, kip (kN)	E_b, kip-ft (kJ)
4G80S6 (1/8)	0.073 (1.86)	238.70 (1062)	0.995 (6.86)	129.01 (573.9)	153.62 (683.4)	0.016 (0.40)	109.44 (486.8)	1.018 (25.9)	148.87 (662.2)	12.61 (17.10)
5G80S6 (1/8)	0.050 (1.28)	259.52 (1154)	1.081 (7.46)	154.13 (685.6)	220.53 (981.0)	0.019 (0.48)	159.53 (709.6)	1.198 (30.4)	217.39 (967.0)	18.69 (25.34)

5.4.1.3 Interface Preparation: Roughened with 1/4 in. (6.35 mm)

Figure 5.22 and Figure 5.23 present the interface shear force versus interface shear displacement response curves for specimen groups 4G80S6(1/4) and 5G80S6(1/4), respectively. All specimens in both specimen groups are constructed with a surface roughened to an amplitude of 1/4 in. (6.35 mm). Significant variability can be observed in the pre-peak force-displacement response of specimen group 4G80S6(1/4), as shown in Figure 5.22, with the value of displacements at peak-load, Δ_{ult}, range from 0.030 in. (0.762 mm) to 0.063 in. (1.60 mm) with a COV of 38% as shown in Table 5.30. Specimens 5G80S6(1/4) present a slightly lower variability with Δ_{ult} ranging from 0.054 in. (1.372 mm) to 0.083 in. (2.108 mm) and a COV of 22%, as shown in Table 5.31.

In general, it can be seen that specimen group 5G80S6(1/4) reinforced with #5 (#16M) steel bars displayed a larger capacity, which can be confirmed quantitatively by comparison of the values presented in Table 5.32. In this case, Δ_{ult} and V_{ult} are 43% and 29% higher, respectively, for specimen group 5G80S6(1/4) compared to the 4G80S6(1/4) specimen group. Additionally, the energy dissipated before first bar fracture, E_b, is 79% higher in specimen group 5G80S6(1/4). The average sustained load at first bar fracture in specimen group 4G80S6(1/4) is 153.56 kip (683.07 kN) and 227.31 kip (1011.1 kN) for specimen group 5G80S6(1/4), indicating a 48% increase in average sustained load capacity. This large increase in capacity is directly related to the 55% increase in reinforcing steel ratio across the interface when the reinforcing steel bar size is increased from #4 (#13M) to #5 (#16M).

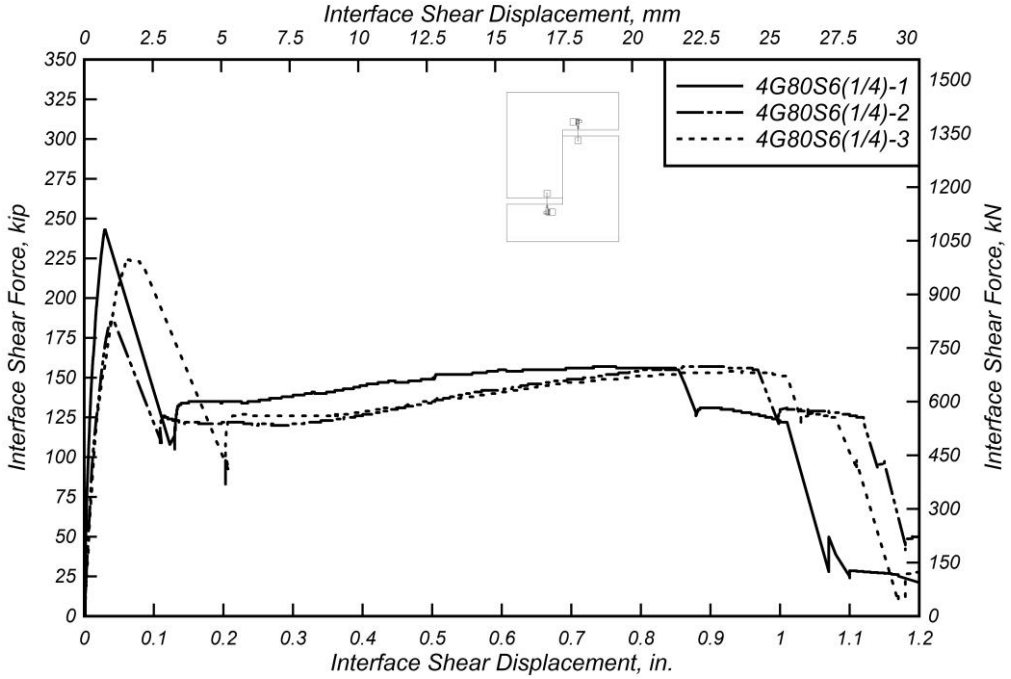

Figure 5.22: Interface shear force versus interface shear displacement for 4G80S6(1/4) specimens.

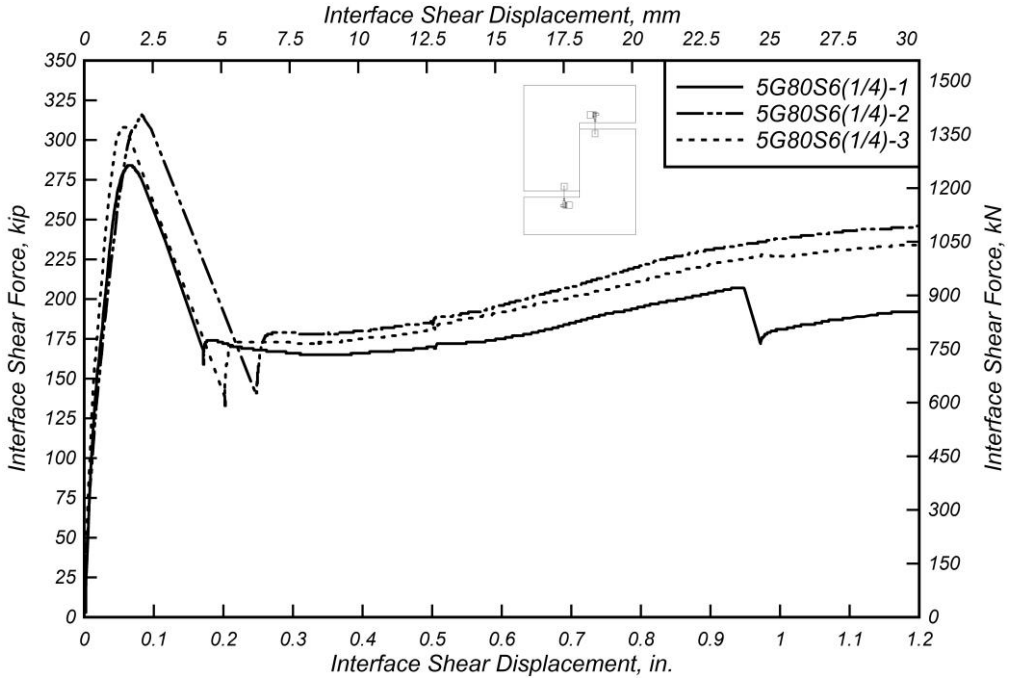

Figure 5.23: Interface shear force versus interface shear displacement for 5G80S6(1/4) specimens.

Table 5.30: Specimen 4G80S6(1/4) shear test results.

Spec	Δ_{ult}, in. (mm)	V_{ult}, kip (kN)	σ_{ult}, ksi (MPa)	$V_{sus,min}$, kip (kN)	$V_{sus,max}$, kip (kN)	Δ_{cr}, in. (mm)	V_{cr}, kip (kN)	Δ_{b}, in. (mm)	V_b, kip (kN)	E_b, kip-ft (kJ)
4G80S6 (1/4)-1	0.030 (0.76)	243.07 (1081)	1.013 (6.98)	134.34 (597.6)	156.75 (697.3)	0.007 (0.17)	105.70 (470.2)	0.854 (21.7)	154.52 (687.3)	10.73 (14.55)
4G80S6 (1/4)-2	0.041 (1.04)	186.03 (827.5)	0.775 (5.34)	119.82 (533.0)	157.04 (698.6)	0.014 (0.35)	109.60 (487.5)	0.968 (24.6)	154.86 (688.9)	11.13 (15.09)
4G80S6 (1/4)-3	0.063 (1.60)	224.61 (999.1)	0.936 (6.45)	125.59 (558.7)	153.71 (683.7)	0.017 (0.43)	118.80 (528.5)	1.006 (25.6)	151.30 (673.0)	12.19 (16.52)
Mean	0.045 (1.14)	217.90 (969.3)	0.908 (6.26)	126.58 (563.1)	155.83 (693.2)	0.013 (0.32)	111.37 (495.4)	0.943 (23.9)	153.56 (683.1)	11.35 (15.39)
Median	0.041 (1.04)	224.61 (999.1)	0.936 (6.45)	125.59 (558.7)	156.75 (697.3)	0.014 (0.35)	109.60 (487.5)	0.968 (24.6)	154.52 (687.3)	11.13 (15.09)
STDEV	0.017 (0.43)	29.11 (129.5)	0.121 (0.84)	7.311 (32.52)	1.845 (8.205)	0.005 (0.13)	6.726 (29.92)	0.079 (2.01)	1.965 (8.739)	0.751 (1.018)
COV	38%	13%	13%	6%	1%	42%	6%	8%	1%	7%

Table 5.31: Specimen 5G80S6(1/4) shear test results.

Spec	Δ_{ult}, in. (mm)	V_{ult}, kip (kN)	σ_{ult}, ksi (MPa)	$V_{sus,min}$, kip (kN)	$V_{sus,max}$, kip (kN)	Δ_{cr}, in. (mm)	V_{cr}, kip (kN)	Δ_{b}, in. (mm)	V_b, kip (kN)	E_b, kip-ft (kJ)
5G80S6 (1/4)-1	0.064 (1.63)	283.85 (1263)	1.183 (8.15)	164.97 (733.8)	207.40 (922.6)	0.018 (0.47)	152.60 (678.8)	0.948 (24.1)	206.76 (919.7)	14.71 (19.94)
5G80S6 (1/4)-2	0.083 (2.11)	315.53 (1404)	1.315 (9.07)	177.92 (791.4)	246.02 (1094)	0.014 (0.35)	112.80 (501.8)	1.289 (32.7)	245.51 (1092)	23.18 (31.43)
5G80S6 (1/4)-3	0.054 (1.37)	308.23 (1371)	1.284 (8.86)	171.56 (763.1)	235.51 (1048)	0.012 (0.31)	138.90 (617.9)	1.359 (34.5)	229.67 (1022)	23.57 (31.95)
Mean	0.067 (1.70)	302.54 (1346)	1.261 (8.69)	171.48 (762.8)	229.64 (1022)	0.015 (0.37)	134.77 (599.5)	1.199 (30.5)	227.31 (1011)	20.48 (27.77)
Median	0.064 (1.63)	308.23 (1371)	1.284 (8.86)	171.56 (763.1)	235.51 (1048)	0.014 (0.35)	138.90 (617.9)	1.289 (32.7)	229.67 (1022)	23.18 (31.43)
STDEV	0.015 (0.37)	16.59 (73.79)	0.069 (0.48)	6.475 (28.80)	19.97 (88.82)	0.003 (0.08)	20.22 (89.94)	0.220 (5.59)	19.48 (86.66)	5.008 (6.790)
COV	22%	5%	5%	4%	9%	22%	15%	18%	9%	24%

Table 5.32: Summary of averages of 4G80S6(1/4) and 5G80S6(1/4) specimens with 1/4 in. (6.35 mm) interface finish.

Spec	Δ_{ult}, in. (mm)	V_{ult}, kip (kN)	σ_{ult}, ksi (MPa)	$V_{sus,min}$, kip (kN)	$V_{sus,max}$, kip (kN)	Δ_{cr}, in. (mm)	V_{cr}, kip (kN)	Δ_{b}, in. (mm)	V_b, kip (kN)	E_b, kip-ft (kJ)
4G80S6 (1/4)	0.045 (1.14)	217.90 (969.3)	0.908 (6.26)	126.58 (563.1)	155.83 (693.2)	0.013 (0.32)	111.37 (495.4)	0.943 (23.9)	153.56 (683.1)	11.35 (15.39)
5G80S6 (1/4)	0.067 (1.70)	302.54 (1346)	1.261 (8.69)	171.48 (762.8)	229.64 (1022)	0.015 (0.37)	134.77 (599.5)	1.199 (30.5)	227.31 (1011)	20.48 (27.77)

5.4.1.4 Interface Preparation: Exposed Aggregate

Figure 5.24 presents the interface shear force versus interface shear displacement response curve for specimen group 4G80S6(EA). In this figure it can be seen that specimen 4G80S6(EA)-1 presents a different force-displacement response characterized by higher values of Δ_{ult} and V_{ult}, but inferior post-peak response. Additionally, specimens 4G80S6(EA)-2 and 4G80S6(EA)-3 present a "double peak" response, where the maximum sustained shear interface load, $V_{sus,max}$, is similar-to/higher-than the peak-load, V_{ult}. These results indicate that in some cases (two out of the three specimens tested), exposing the aggregate of the shear interface may allow the aggregate interlock mechanism to contribute to the force-displacement response during the post-peak stage. It is important to note that bleed water moves upwards to the shear interface during the vibration process during the construction of the test specimens, thus creating a weak layer of concrete on the shear interface during the first cast of the interface in all cases of interface preparation discussed before. The process of exposing the aggregate on the shear interface involves removing the top layer of concrete paste over which the Concrete Retarder Formula S chemical was applied. This essentially removes the weak layer; therefore, it may allow for a stronger aggregate interlock. This may explain the "double peak" behavior exhibited by test specimens 4G80S6(EA)-2 and 4G80S6(EA)-3.

Specimen group 5G80S6(EA) also presents different behavior between specimens, as can be observed in Figure 5.25. Specimen 5G80S6(EA)-1 reached a peak load approximately 20% higher than the other specimens. In the initial stages, the behavior is similar in all specimens. During the post-cracking stage, however, specimen 5G80S6(EA)-1 also presents a larger stiffness. This indicates that the different behavior exhibited by this specimen can also be attributed to the aggregate interlock mechanism having a higher influence on the response, again due to the fact that exposing the aggregate increases the propensity to enhance aggregate interlock. Nonetheless, the limited testing performed indicates that this increased strength and stiffness due to the aggregate interlock may not always develop, and additional testing and surface preparation trials using different aggregates and surface

preparation mechanisms to develop the Exposed Aggregate finishing should be investigated.

Table 5.35 shows a comparison of the main points of study between both specimen groups. A higher post-crack stiffness can be observed when #5 (#16M) bars are used. On the other hand, specimens reinforced with #4 (#13M) bars display a higher post-peak performance which may be explained by the variability of the exposed aggregate shear interface preparation.

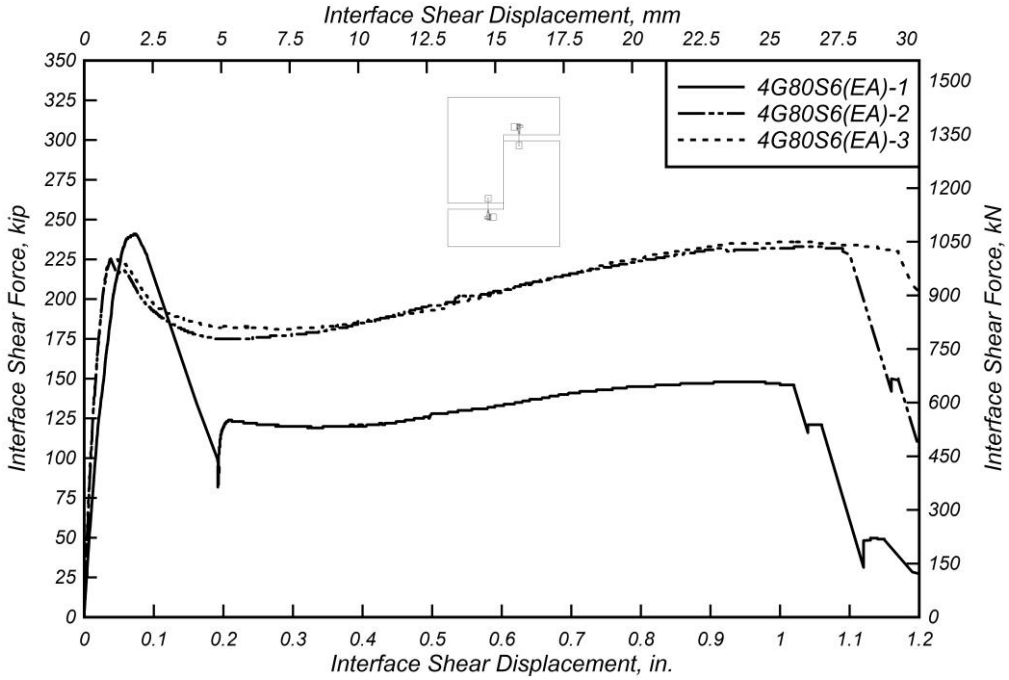

Figure 5.24: Interface shear force versus interface shear displacement for 4G80S6(EA) specimens.

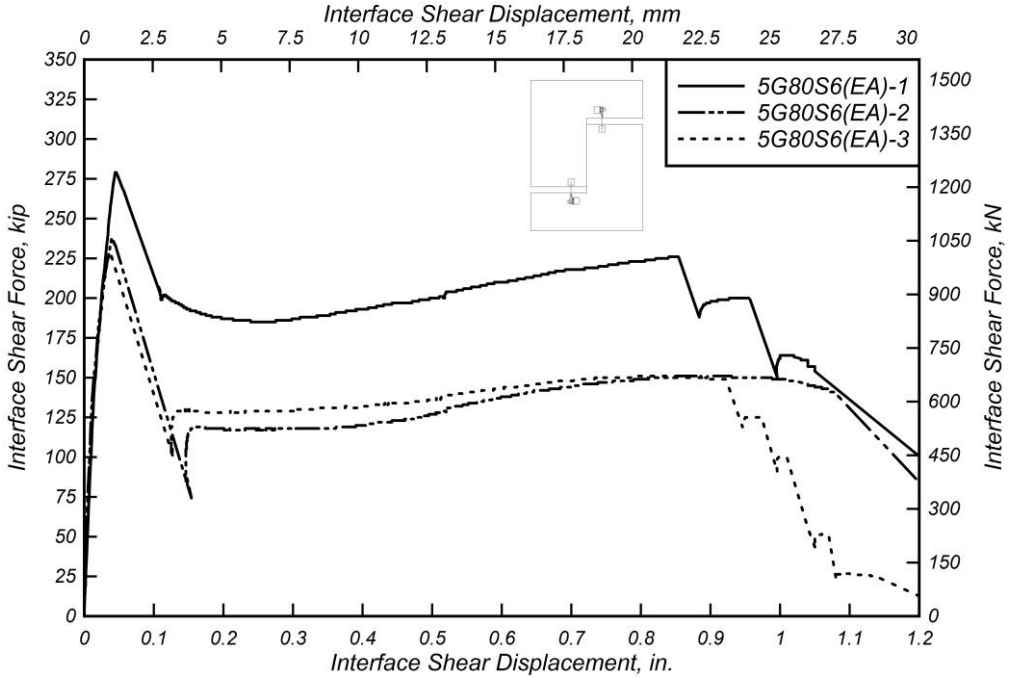

Figure 5.25: Interface shear force versus interface shear displacement for 5G80S6(EA) specimens.

Table 5.33: Specimen 4G80S6(EA) shear test results.

Spec	Δ_{ult}, in. (mm)	V_{ult}, kip (kN)	σ_{ult}, ksi (MPa)	$V_{sus,min}$, kip (kN)	$V_{sus,max}$, kip (kN)	Δ_{cr}, in. (mm)	V_{cr}, kip (kN)	Δ_{b}, in. (mm)	V_b, kip (kN)	E_b, kip-ft (kJ)
4G80S6 (EA)-1	0.073 (1.85)	241.11 (1073)	1.005 (6.93)	119.20 (530.2)	148.28 (659.6)	0.017 (0.44)	107.90 (635.4)	1.023 (26.0)	145.13 (645.6)	11.93 (16.17)
4G80S6 (EA)-2	0.038 (0.97)	225.49 (1003)	0.940 (6.48)	174.99 (778.4)	232.89 (1035)	0.013 (0.33)	129.90 (465.5)	1.094 (27.8)	230.33 (1025)	18.45 (25.01)
4G80S6 (EA)-3	0.040 (1.02)	226.29 (1007)	0.943 (6.50)	180.92 (804.8)	235.67 (1048)	0.008 (0.20)	91.96 (495.4)	1.173 (29.8)	227.54 (1012)	20.21 (27.40)
Mean	0.050 (1.28)	230.96 (1027)	0.962 (6.64)	158.37 (704.5)	205.61 (914.6)	0.013 (0.32)	109.92 (489.0)	1.097 (27.9)	201.00 (894.1)	16.86 (22.86)
Median	0.040 (1.02)	226.29 (1007)	0.943 (6.50)	174.99 (778.4)	232.89 (1036)	0.013 (0.33)	107.90 (635.4)	1.094 (27.8)	227.54 (1012)	18.45 (25.01)
STDEV	0.020 (0.50)	8.796 (39.13)	0.037 (0.25)	34.05 (151.5)	49.67 (221.0)	0.005 (0.12)	19.05 (84.74)	0.075 (1.91)	48.40 (215.3)	4.363 (5.916)
COV	39%	4%	4%	22%	24%	38%	17%	7%	24%	26%

Table 5.34: Specimen 5G80S6(EA) shear test results.

Spec	Δ_{ult}, in. (mm)	V_{ult}, kip (kN)	σ_{ult}, ksi (MPa)	$V_{sus,min}$, kip (kN)	$V_{sus,max}$, kip (kN)	Δ_{cr}, in. (mm)	V_{cr}, kip (kN)	Δ_{b}, in. (mm)	V_b, kip (kN)	E_b, kip-ft (kJ)
5G80S6 (EA)-1	0.045 (1.14)	279.43 (1243)	1.164 (8.03)	185.15 (823.6)	226.21 (1006)	0.012 (0.30)	120.50 (567.3)	0.854 (21.7)	226.26 (1007)	14.52 (19.69)
5G80S6 (EA)-2	0.040 (1.02)	236.33 (1051)	0.985 (6.79)	117.23 (521.5)	150.66 (670.2)	0.013 (0.34)	148.60 (709.6)	1.076 (27.3)	140.96 (627.0)	12.49 (16.93)
5G80S6 (EA)-3	0.037 (0.94)	229.12 (1019)	0.955 (6.58)	128.03 (569.5)	151.17 (672.4)	0.011 (0.27)	126.20 (599.5)	0.923 (23.4)	148.27 (659.5)	10.95 (14.85)
Mean	0.041 (1.03)	248.29 (1105)	1.035 (7.13)	143.47 (638.2)	176.01 (783.0)	0.012 (0.30)	131.77 (625.5)	0.951 (24.2)	171.83 (764.3)	12.65 (17.16)
Median	0.040 (1.02)	236.33 (1051)	0.985 (6.79)	128.03 (569.5)	151.17 (672.4)	0.012 (0.30)	126.20 (599.5)	0.923 (23.4)	148.27 (659.5)	12.49 (16.93)
STDEV	0.004 (0.10)	27.21 (121.0)	0.113 (0.78)	36.50 (162.4)	43.47 (193.4)	0.001 (0.03)	14.85 (74.65)	0.114 (2.89)	47.28 (210.3)	1.790 (2.427)
COV	10%	11%	11%	25%	25%	11%	11%	12%	28%	14%

Table 5.35: Summary of averages of 4G80S6(EA) and 5G80S6(EA) specimens with Exposed Aggregate interface finish.

Spec	Δ_{ult}, in. (mm)	V_{ult}, kip (kN)	σ_{ult}, ksi (MPa)	$V_{sus,min}$, kip (kN)	$V_{sus,max}$, kip (kN)	Δ_{cr}, in. (mm)	V_{cr}, kip (kN)	Δ_{b}, in. (mm)	V_b, kip (kN)	E_b, kip-ft (kJ)
4G80S6 (EA)	0.050 (1.28)	230.96 (1027)	0.962 (6.64)	158.37 (704.5)	205.61 (914.6)	0.013 (0.32)	109.92 (489.0)	1.097 (27.9)	201.00 (894.1)	16.86 (22.86)
5G80S6 (EA)	0.041 (1.03)	248.29 (1105)	1.035 (7.13)	143.47 (638.2)	176.01 (783.0)	0.012 (0.30)	131.77 (625.5)	0.951 (24.2)	171.83 (764.3)	12.65 (17.16)

5.4.2 Interface Shear Force versus Strain

5.4.2.1 Interface Preparation: As Cast

Figure 5.26 and Figure 5.27 present the interface shear force versus reinforcing steel bar strain relationship for specimen groups 4G80S6(AC), and 5G80S6(AC), respectively. The curves shown correspond to the average strain measurements from all strain gauges contained in each test specimen plotted versus the interface shear force. As shown in Figure 5.26, all specimens present similar behavior except specimen 4G80S6(AC)-3, which confirms the discussion provided in the previous section about the variability related to the development of aggregate interlock. The initial behavior is characterized by a linear force-strain response with similar stiffness for all specimens until the cracking shear load is reached. After cracking occurs, the specimens experience a rapid increase in strain on the reinforcing steel U-bars as the load continues to grow until peak load. The force-strain response of specimen 4G80S6(AC)-3 shows that it reaches a significantly lower peak load and shows a

steep drop in shear load in the post-peak response, unlike the other specimens which show a smooth softening curve moving into the sustained load phase of the force-strain response. The behavior of test specimen group 5G80S6(AC) is similar across all specimens, as shown in Figure 5.27.

Table 5.36 and Table 5.37 present values of strain measurements at peak load for all strain gauges in specimen groups 4G80S6(AC) and 5G80S6(AC), respectively. Table 5.38 presents a summary of average strain gauges measurements at peak load for both specimen groups. From these values it can be observed that specimen group 4G80S6(AC) reached higher strains at peak load when compared to specimen group 5G80S6(AC).

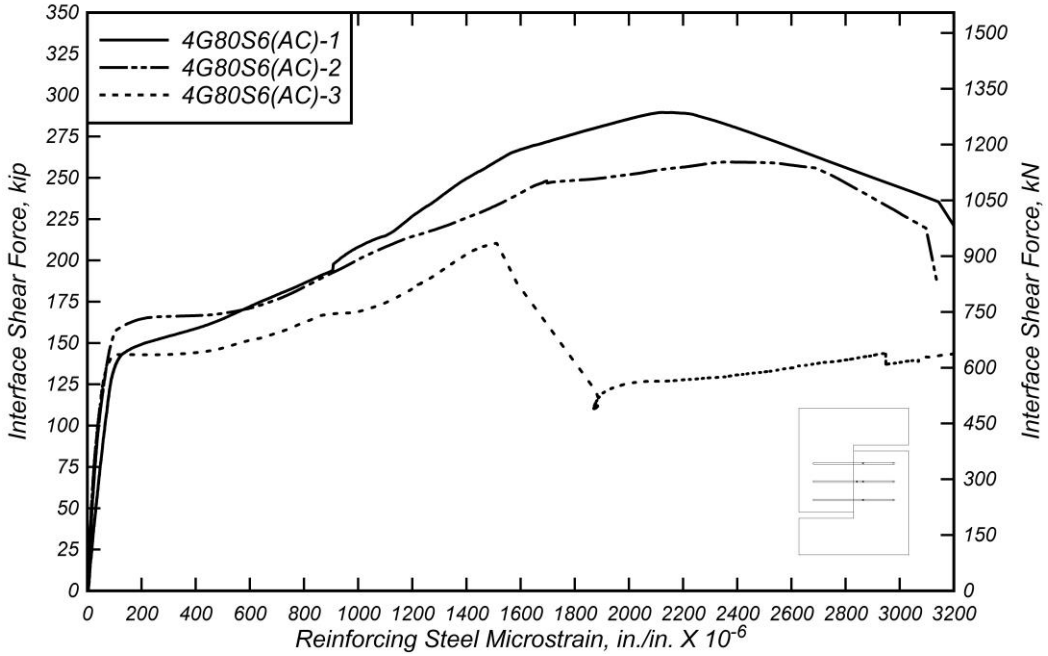

Figure 5.26: Interface shear force versus average reinforcing steel microstrain for 4G80S6(AC) specimens.

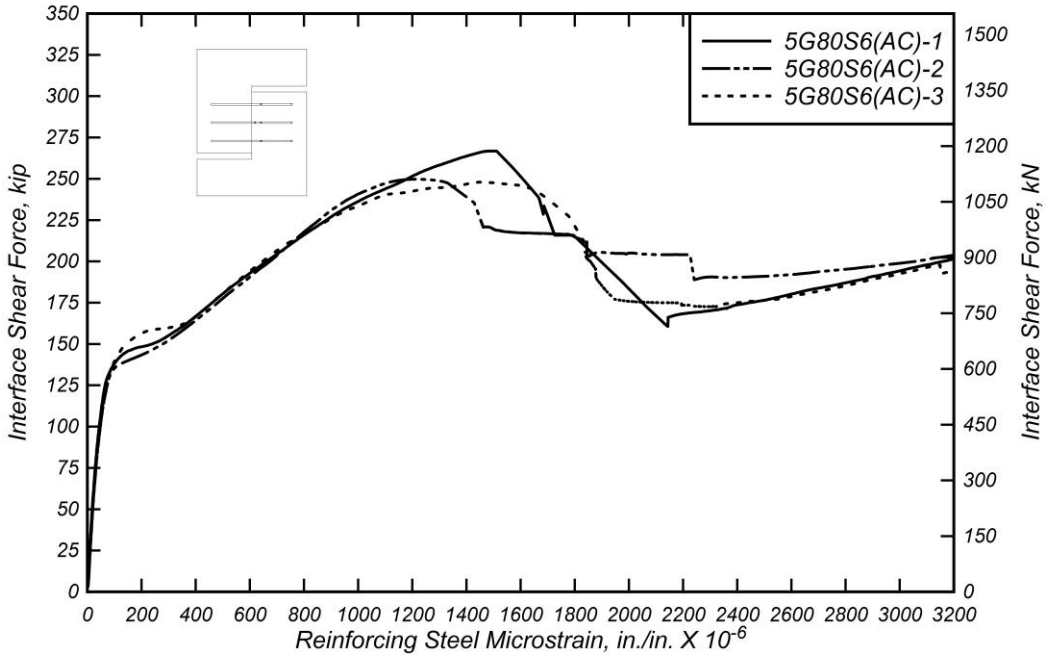

Figure 5.27: Interface shear force versus average reinforcing steel microstrain for 5G80S6(AC) specimens.

Table 5.36: Specimen 4G80S6(AC) strain gauge readings at peak interface shear force.

Spec	s_1, in./in. (mm/mm)	s_2, in./in. (mm/mm)	s_3, in./in. (mm/mm)	s_4, in./in. (mm/mm)	s_5, in./in. (mm/mm)	s_6, in./in. (mm/mm)	s_7, in./in. (mm/mm)
4G80S6 (AC)-1	-	-	-	0.0027	-	0.0023	0.0017
4G80S6 (AC)-2	0.0027	0.0023	-	-	0.0031	-	0.0017
4G80S6 (AC)-3	-	-	0.0018	0.0025	0.0015	-	0.0015
Mean	0.0027	0.0023	0.0018	0.0026	0.0023	0.0023	0.0016
Median	0.0027	0.0023	0.0018	0.0026	0.0023	0.0023	0.0017
STDEV	-	-	-	0.0002	0.0011	-	0.0001
COV	-	-	-	7%	47%	-	9%

Table 5.37: Specimen 5G80S6(AC) strain gauge readings at peak interface shear force.

Spec	s_1, in./in. (mm/mm)	s_2, in./in. (mm/mm)	s_3, in./in. (mm/mm)	s_4, in./in. (mm/mm)	s_5, in./in. (mm/mm)	s_6, in./in. (mm/mm)	s_7, in./in. (mm/mm)
5G80S6 (AC)-1	0.0017	0.0015	-	0.0021	0.0014	0.0016	0.0018
5G80S6 (AC)-2	0.0011	-	0.0018	-	0.0011	0.0014	-
5G80S6 (AC)-3	0.0016	0.0016	-	0.0023	0.0014	0.0014	0.0015
Mean	0.0015	0.0016	0.0018	0.0022	0.0013	0.0015	0.0016
Median	0.0016	0.0016	0.0018	0.0022	0.0014	0.0014	0.0016
STDEV	0.00031	5.12E-05	-	0.00011	0.00021	9.29E-05	0.00020
COV	21%	3%	-	5%	16%	6%	13%

Table 5.38: Summary of strain gauge readings at peak interface shear force for 4G80S6(AC) and 5G80S6(AC) (As Cast) specimens.

Spec	s_1, in./in. (mm/mm)	s_2, in./in. (mm/mm)	s_3, in./in. (mm/mm)	s_4, in./in. (mm/mm)	s_5, in./in. (mm/mm)	s_6, in./in. (mm/mm)	s_7, in./in. (mm/mm)
4G80S6(AC)	0.0027	0.0023	0.0018	0.0026	0.0023	0.0023	0.0016
5G80S6(AC)	0.0015	0.0016	0.0018	0.0022	0.0013	0.0015	0.0016

5.4.2.2 Interface Preparation: Roughened to 1/8 in. (3.175 mm)

The interface shear force versus reinforcing steel U-bar strain response for specimen group 4G80S6(1/8) is shown in Figure 5.6 and for specimen group 5G80S6(1/8) in Figure 5.28. These curves correspond to the average strain measurements from all strain gauges contained in each test specimen plotted versus the interface shear force. The behavior is similar in most specimens. There is an initial linear branch up until the interface shear cracking force is reached. The post-crack force-strain response is characterized by a reduction in stiffness resulting in a more rapid increase in strain until peak load. Post-peak behavior begins with a softening curve, followed by a hardening branch.

In Figure 5.28, it can be seen that specimen 5G80S6(1/8)-2 reaches a significantly higher peak load compared to the other specimens in the group, which has already been discussed in previous sections of this report. Table 5.7 and Table 5.39 present tabulated values of strain measurements at peak load for all strain gauges in specimen groups 4G80S6(1/8) and 5G80S6(1/8), respectively. Section 5.2.2 provides a description of the behavior exhibited by specimen group 4G80S6(1/8). From the

comparison of both specimen groups it can be observed that specimen group 4G80S6(1/8) show larger average strains at lower peak load values.

Table 5.40 shows a summary of strain measurements for both specimen groups for comparison. From this table, the discussion in the previous paragraph can be confirmed to show that specimen group 4G80S6(1/8), which is constructed with #4 (#13M) reinforcing steel bars across the interface, exhibits higher average strains at peak load.

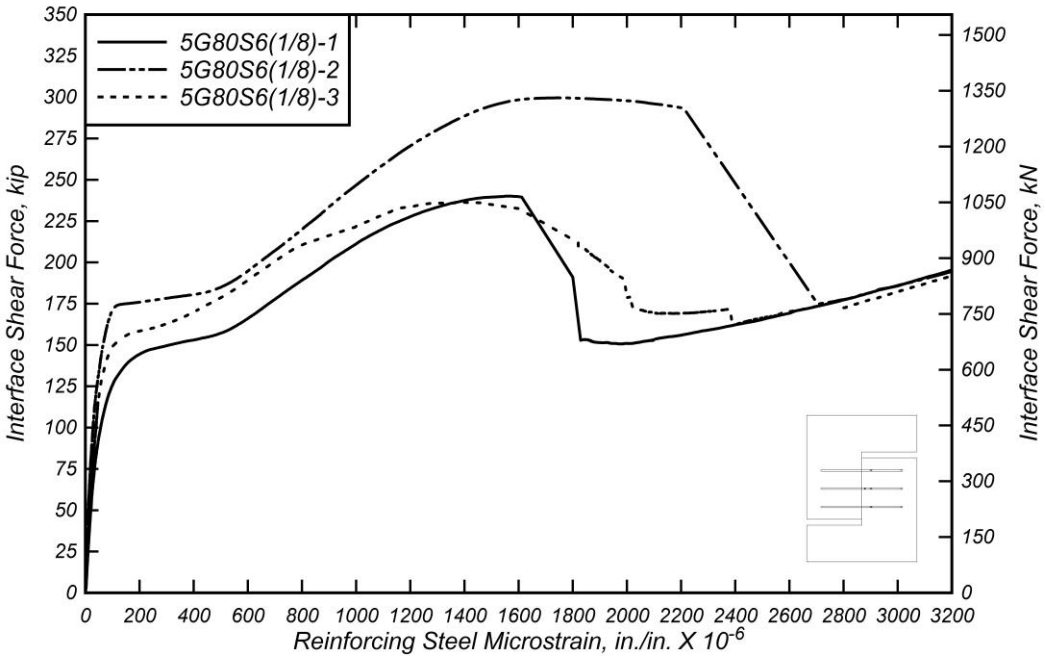

Figure 5.28: Interface shear force versus average reinforcing steel microstrain for 5G80S6(1/8) specimens.

Table 5.39: Specimen 5G80S6(1/8) strain gauge readings at peak interface shear force.

Spec	s_1, in./in. (mm/mm)	s_2, in./in. (mm/mm)	s_3, in./in. (mm/mm)	s_4, in./in. (mm/mm)	s_5, in./in. (mm/mm)	s_6, in./in. (mm/mm)	s_7, in./in. (mm/mm)
5G80S6 (1/8)-1	0.0013	0.0016	0.0015	-	-	0.0015	0.0011
5G80S6 (1/8)-2	0.0012	-	0.0016	-	-	-	0.0018
5G80S6 (1/8)-3	0.0012	0.0013	-	0.0016	-	0.0015	-
Mean	0.0012	0.0015	0.0015	-	-	0.0015	0.0014
Median	0.0012	0.0015	0.0015	-	-	0.0015	0.0014
STDEV	7.7E-05	1.7E-04	7.1E-05	-	-	1.9E-05	4.8E-04
COV	9%	12%	5%	-	-	1%	34%

Table 5.40: Summary of strain gauge readings at peak interface shear force for 4G80S6(1/8) and 5G80S6(1/8) (1/8 in. (3.175 mm)) specimens.

Spec	s_1, in./in. (mm/mm)	s_2, in./in. (mm/mm)	s_3, in./in. (mm/mm)	s_4, in./in. (mm/mm)	s_5, in./in. (mm/mm)	s_6, in./in. (mm/mm)	s_7, in./in. (mm/mm)
4G80S6(1/8)	-	0.0022	0.0019	0.0026	0.0028	0.0021	0.0015
5G80S6(1/8)	0.0012	0.0015	0.0015	-	-	0.0015	0.0014

5.4.2.3 Interface Preparation: Roughened to 1/4 in. (6.35 mm)

The interface shear force versus reinforcing steel U-bar strain response for specimen groups 4G80S6(1/4) and 5G80S6(1/4) are shown in Figure 5.29 and Figure 5.30, respectively. These curves correspond to the average strain measurements from all strain gauges contained in each test specimen plotted versus the interface shear force and general trends of the responses have been discussed previously. Worth of note, it can be seen in Figure 5.29 that specimen 4G80S6(1/4)-2 presents a significantly lower peak load and strain at peak load, although there were no observations or indications in the construction of the specimen or during testing that could suggest this lower performance. Table 5.41 presents values of strain measurements at peak load for all strain gauges in specimen group 4G80S6(1/4) where the underperformance of specimen 4G80S6(1/4)-2 can be confirmed by the significantly lower strain values at peak load.

Table 5.43 shows a summary of strain measurements for specimen groups 4G80S6(1/4) and 5G80S6(1/4). The values in this table show that, in general, specimen group 5G80S6(1/4) presents lower average strain values at peak load, but it also presents significantly larger peak load values.

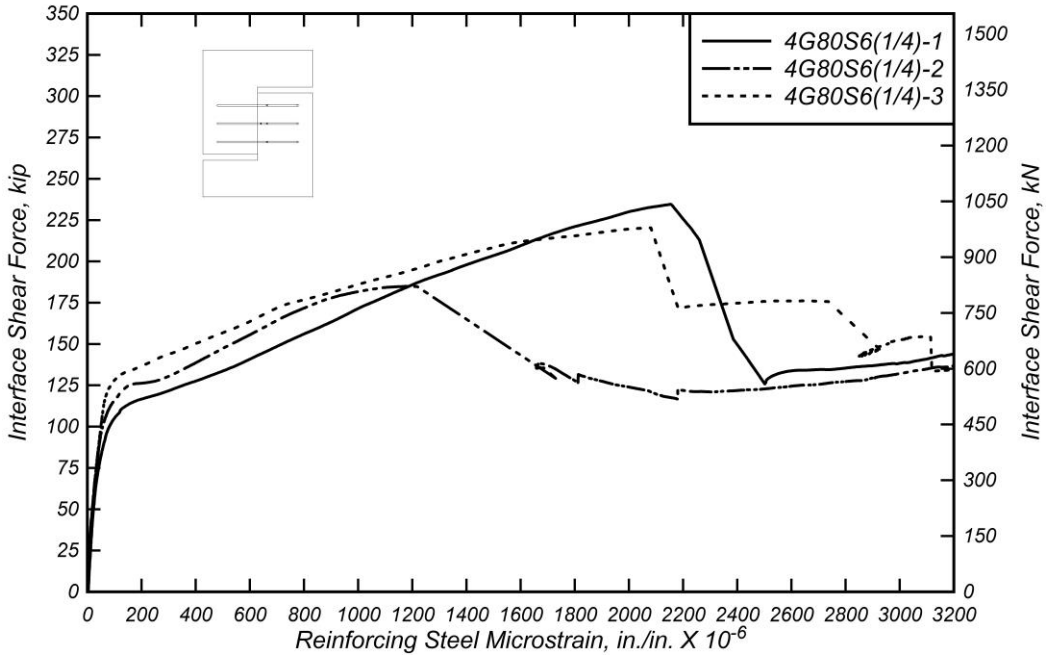

Figure 5.29: Interface shear force versus average reinforcing steel microstrain for 4G80S6(1/4) specimens.

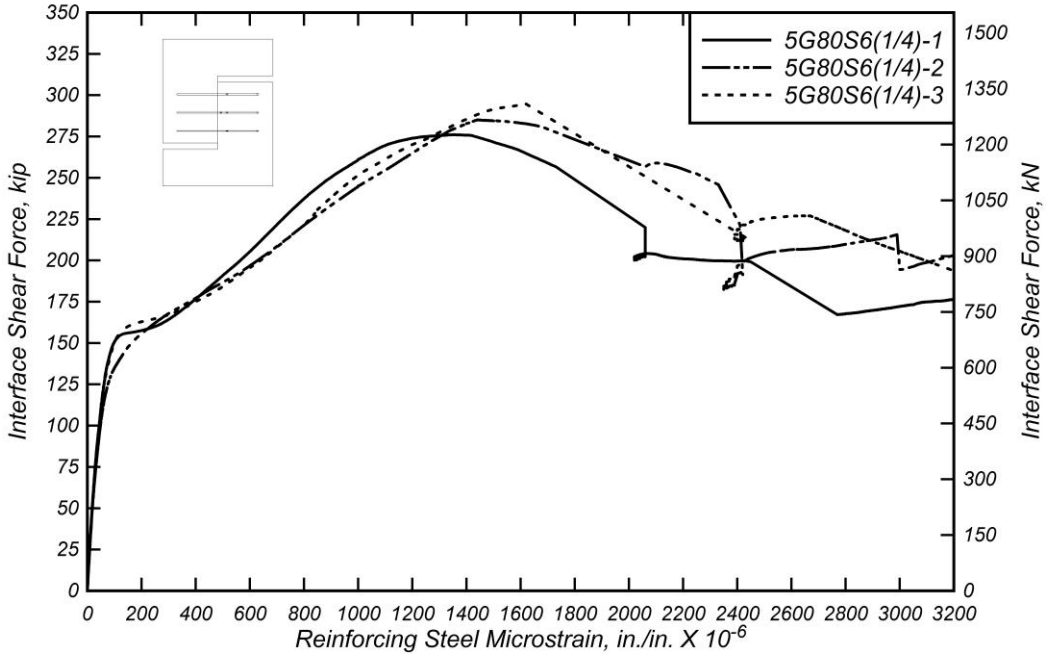

Figure 5.30: Interface shear force versus average reinforcing steel microstrain for 5G80S6(1/4) specimens.

Table 5.41: Specimen 4G80S6(1/4) strain gauge readings at peak interface shear force.

Spec	s_1, in./in. (mm/mm)	s_2, in./in. (mm/mm)	s_3, in./in. (mm/mm)	s_4, in./in. (mm/mm)	s_5, in./in. (mm/mm)	s_6, in./in. (mm/mm)	s_7, in./in. (mm/mm)
4G80S6 (1/4)-1	0.0026	-	-	0.0026	0.0024	0.0021	-
4G80S6 (1/4)-2	0.0011	-	-	-	0.0012	0.0014	-
4G80S6 (1/4)-3	-	0.0021	-	-	0.0025	0.0016	0.0013
Mean	0.0018	0.0021	-	0.0026	0.0020	0.0017	0.0013
Median	0.0018	0.0021	-	0.0026	0.0024	0.0016	0.0013
STDEV	0.0010	-	-	-	0.0007	0.0004	-
COV	55%	-	-	-	36%	21%	-

Table 5.42: Specimen 5G80S6(1/4) strain gauge readings at peak interface shear force.

Spec	s_1, in./in. (mm/mm)	s_2, in./in. (mm/mm)	s_3, in./in. (mm/mm)	s_4, in./in. (mm/mm)	s_5, in./in. (mm/mm)	s_6, in./in. (mm/mm)	s_7, in./in. (mm/mm)
5G80S6 (1/4)-1	0.0014	0.0011	-	0.0018	0.0012	0.0019	-
5G80S6 (1/4)-2	0.0022	0.0024	0.0020	0.0020	0.0013	0.0018	0.002205
5G80S6 (1/4)-3	0.0012	0.0017	-	-	0.0022	-	-
Mean	0.0016	0.0017	0.0020	0.0019	0.0016	0.0018	0.0022
Median	0.0014	0.0017	0.0020	0.0019	0.0013	0.0018	0.0022
STDEV	0.00053	0.00063	-	0.00019	0.00058	5.55E-05	-
COV	33%	36%	-	10%	37%	3%	-

Table 5.43: Summary of strain gauge readings at peak interface shear force for 4G80S6(1/4) and 5G80S6(1/4) (1/4 in. (6.35 mm)) specimens.

Spec	s_1, in./in. (mm/mm)	s_2, in./in. (mm/mm)	s_3, in./in. (mm/mm)	s_4, in./in. (mm/mm)	s_5, in./in. (mm/mm)	s_6, in./in. (mm/mm)	s_7, in./in. (mm/mm)
4G80S6(1/4)	0.0018	0.0021	-	0.0026	0.0020	0.0017	0.0013
5G80S6(1/4)	0.0016	0.0017	0.0020	0.0019	0.0016	0.0018	0.0022

5.4.2.4 Interface Preparation: Exposed Aggregate

The interface shear force versus reinforcing steel U-bar strain response for specimen groups 4G80S6(EA) and 5G80S6(EA) are shown in Figure 5.31 and Figure 5.32, respectively. In Figure 5.31 it can be seen that specimen 4G80S6(EA)-1 reaches its peak load at a higher strain value, which also indicates a larger crack width as explained in the following section. Figure 5.32 shows that specimen 5G80S6(EA)-1 reaches a higher peak load for slightly lower strain values compared to the other

specimens in the group. Both of these highlight the variability of the results observed, especially when the surface is roughened to a nominal amplitude of 1/4 in. (6.35 mm). Table 5.44 and Table 5.45 present strain gauge measurements at peak load for all strain gauges in specimen group 4G80S6(EA) and 5G80S6(EA), respectively. In Table 5.44 it can be observed that the strain gauge measurements at peak load are significantly higher for specimen 4G80S6(EA)-1 when compared to the other specimens within its group, meanwhile Table 5.45 shows that specimen 5G80S6(EA)-1 exhibits lower strain gauge measurements at peak load when compared to the other specimens within its group.

Table 5.46 summarizes the average strain gauge measurements at peak load for specimen groups 4G80S6(EA) and 5G80S6(EA). The strain gauge measurements presented in this table show that specimen group 4G80S6(EA) reached lower average strains at peak load.

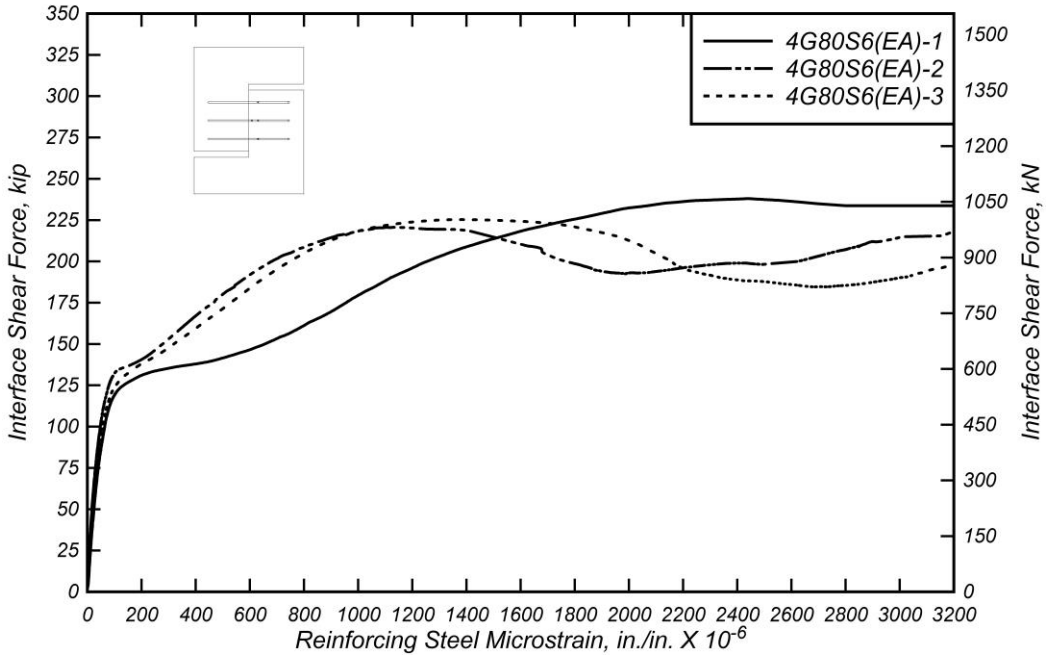

Figure 5.31: Interface shear force versus average reinforcing steel microstrain for 4G80S6(EA) specimens.

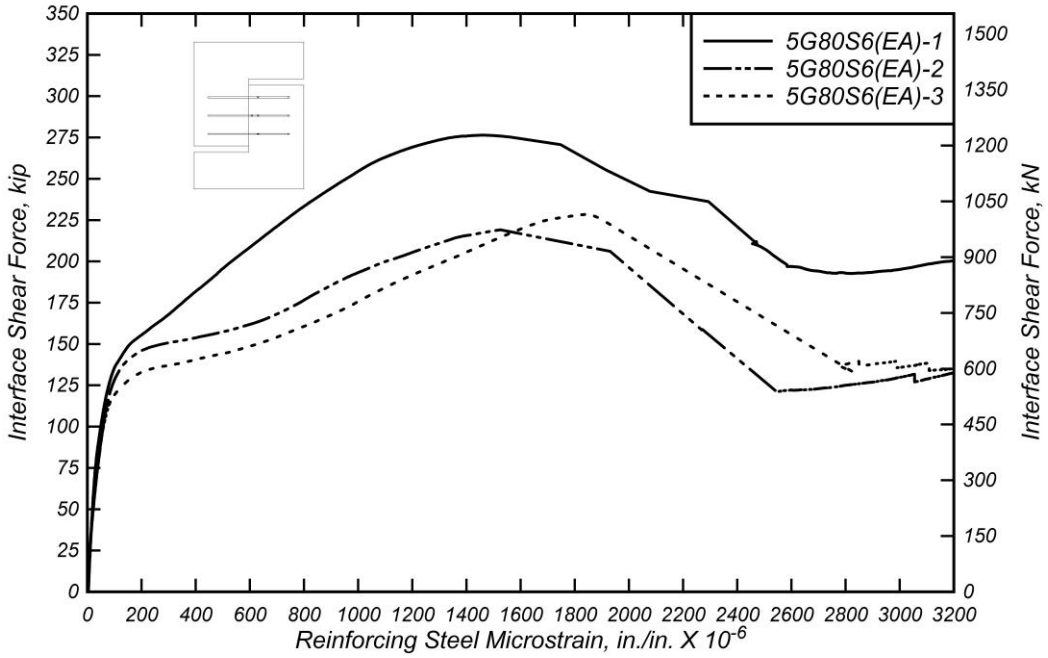

Figure 5.32: Interface shear force versus average reinforcing steel microstrain for 5G80S6(EA) specimens.

Table 5.44: Specimen 4G80S6(EA) strain gauge readings at peak interface shear force.

Spec	s_1, in./in. (mm/mm)	s_2, in./in. (mm/mm)	s_3, in./in. (mm/mm)	s_4, in./in. (mm/mm)	s_5, in./in. (mm/mm)	s_6, in./in. (mm/mm)	s_7, in./in. (mm/mm)
4G80S6 (EA)-1	0.0016	0.0025	0.0024	0.0023	0.0017	0.0024	0.0028
4G80S6 (EA)-2	-	0.0012	0.0011	0.0018	-	0.0015	0.0009
4G80S6 (EA)-3	0.0014	0.0016	0.0013	0.0019	0.0011	0.0013	0.0013
Mean	0.0015	0.0018	0.0016	0.0020	0.0014	0.0017	0.0017
Median	0.0015	0.0016	0.0013	0.0019	0.0014	0.0015	0.0013
STDEV	0.0001	0.0006	0.0007	0.0003	0.0004	0.0006	0.0010
COV	9%	37%	44%	14%	33%	35%	59%

Table 5.45: Specimen 5G80S6(EA) strain gauge readings at peak interface shear force.

Spec	s_1, in./in. (mm/mm)	s_2, in./in. (mm/mm)	s_3, in./in. (mm/mm)	s_4, in./in. (mm/mm)	s_5, in./in. (mm/mm)	s_6, in./in. (mm/mm)	s_7, in./in. (mm/mm)
5G80S6 (EA)-1	0.0014	-	0.0011	0.0018	0.0015	0.0015	-
5G80S6 (EA)-2	0.0017	0.0021	-	0.0025	0.0014	0.0024	0.0021
5G80S6 (EA)-3	0.0013	0.0019	0.0019	0.0026	0.0017	0.0019	0.0018
Mean	0.0015	0.0020	0.0015	0.0023	0.0015	0.0019	0.0020
Median	0.0014	0.0020	0.0015	0.0025	0.0015	0.0019	0.0020
STDEV	0.0002	0.0001	0.0006	0.0005	0.0002	0.0004	0.0002
COV	14%	7%	37%	21%	11%	24%	11%

Table 5.46: Summary of strain gauge readings at peak interface shear force for 4G80S6(EA) and 5G80S6(EA) (Exposed Aggregate) specimens.

Spec	s_1, in./in. (mm/mm)	s_2, in./in. (mm/mm)	s_3, in./in. (mm/mm)	s_4, in./in. (mm/mm)	s_5, in./in. (mm/mm)	s_6, in./in. (mm/mm)	s_7, in./in. (mm/mm)
4G80S6(EA)	0.0015	0.0018	0.0016	0.0020	0.0014	0.0017	0.0017
5G80S6(EA)	0.0015	0.0020	0.0015	0.0023	0.0015	0.0019	0.0020

5.4.3 Interface Shear Force versus Crack Width

5.4.3.1 Interface Preparation: As Cast

Figure 5.33 and Figure 5.34 present the interface shear force versus crack width response for specimen groups 4G80S6(AC) and 5G80S6(AC). All specimens discussed in this section were constructed with an As Cast interface preparation. Each figure shows the force-crack width response for all specimens in each group. Tabulated values of points of interest such as crack width at peak load and crack width at first bar fracture for each specimen group are presented in Table 5.47 and Table 5.48.

In Figure 5.33 it can be observed that most specimens behave similarly with negligible crack width in the initial stages before the cohesion bond is broken. Following cracking, crack width begins to steadily increase until peak load is reached. During this stage, it can be seen that specimen 4G80S6(AC)-3 reaches a significantly lower peak load, V_{ult}, and lower crack width at peak load, w_{ult}, compared to the other specimens within the specimen group. As discussed in Section 5.4.1, this underperformance was attributed to the variability that originates from the process

implemented to obtain the As Cast interface preparation, which may have weakened the aggregate interlock mechanism, thus preventing the test specimen from reaching a larger peak value. Figure 5.34 shows that specimen 5G80S6(AC)-1 displayed larger post-cracked stiffness (slope) and it reached a higher peak load compared to the other specimens in the group. In the post-peak stage, a sudden increase in interface shear load can be observed. This behavior is attributed to a sensor malfunction, as the interface shear force versus interface shear displacement, seen in Figure 5.20, does not show any indication that this specimen is an outlier.

Table 5.49 presents a summary of average crack width points of interest for specimen groups 4G80S6(AC) and 5G80S6(AC). Specimens reinforced with #4 (#13M) bars presented a slightly larger capacity than specimens reinforced with #5 (#16M), which is not expected behavior. This may be explained by the significant variability of the interface preparation process to obtain an As Cast surface preparation. Additionally, specimens reinforced with #5 (#16M) reinforcing steel U-bars displayed a smooth post-peak descending branch compared to the more abrupt behavior shown by the specimens reinforced with #4 (#13M) reinforcing steel U-bars.

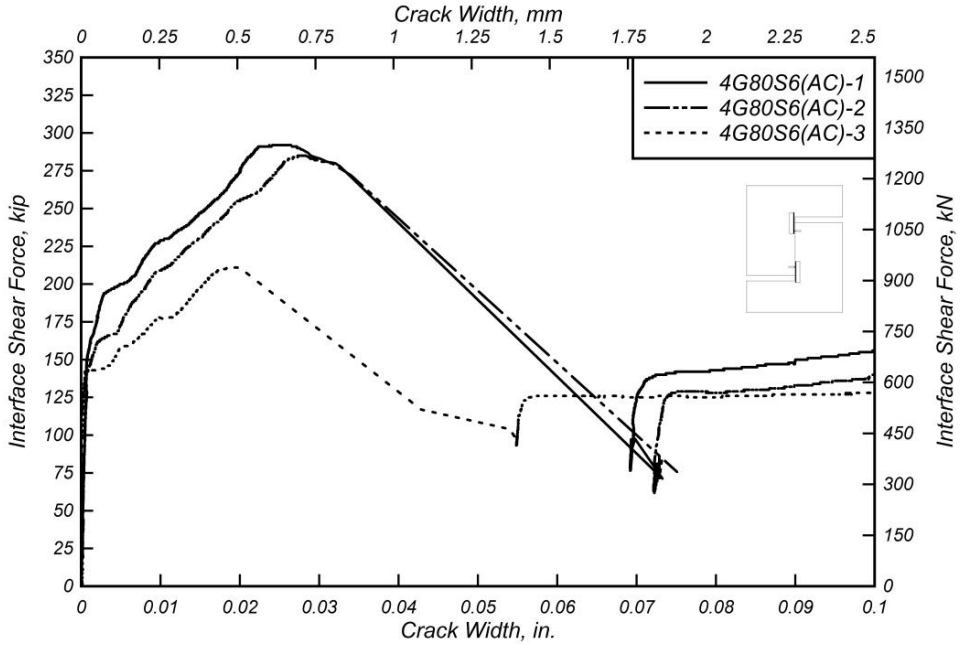

Figure 5.33: Interface shear force versus crack width for 4G80S6(AC) specimens.

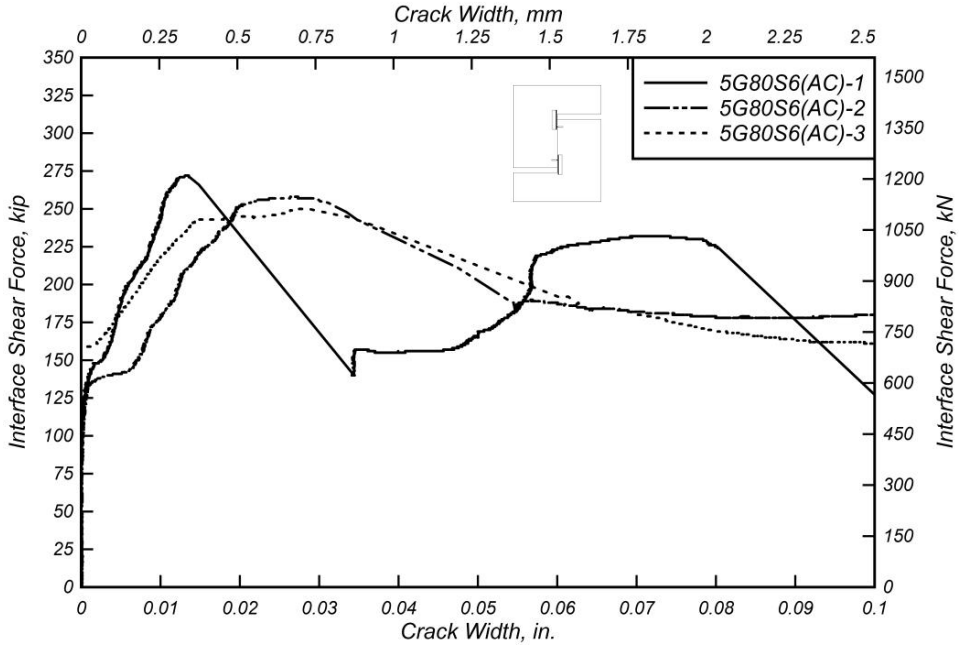

Figure 5.34: Interface shear force versus crack width for 5G80S6(AC) specimens.

Table 5.47: Specimen 4G80S4(AC) crack width measurements.

Specimen	w_{ult}, in. (mm)	V_{ult}, kip (kN)	w_b, in. (mm)	V_b, kip (kN)
4G80S6(AC)-1	0.0260 (0.6603)	292.03 (1299.0)	0.1239 (3.147)	150.66 (670.18)
4G80S6(AC)-2	0.0279 (0.7084)	284.98 (1267.7)	0.1372 (3.485)	152.78 (679.61)
4G80S6(AC)-3	0.0193 (0.4896)	210.93 (938.25)	0.2245 (5.702)	145.46 (647.04)
Mean	0.0244 (0.6194)	262.64 (1168.3)	0.1619 (4.112)	149.64 (665.61)
Median	0.0260 (0.6603)	284.98 (1267.7)	0.1372 (3.485)	150.66 (670.18)
STDEV	0.0045 (0.1150)	44.93 (199.85)	0.0546 (1.388)	3.767 (16.76)
COV	19%	17%	34%	3%

Table 5.48: Specimen 5G80S6(AC) crack width measurements.

Specimen	w_{ult}, in. (mm)	V_{ult}, kip (kN)	w_b, in. (mm)	V_b, kip (kN)
5G80S6(AC)-1	0.0134 (0.3401)	271.63 (1208.3)	0.0800 (2.032)	225.46 (1002.9)
5G80S6(AC)-2	0.0267 (0.6786)	257.72 (1146.4)	0.1728 (4.388)	228.09 (1014.6)
5G80S6(AC)-3	0.0276 (0.7012)	250.26 (1113.2)	0.1615 (4.103)	219.56 (976.65)
Mean	0.0272 (0.6899)	253.99 (1129.8)	0.1671 (4.245)	223.82 (995.62)
Median	0.0272 (0.6899)	253.99 (1129.8)	0.1671 (4.245)	223.82 (995.62)
STDEV	0.0006 (0.0160)	5.274 (23.46)	0.0079 (0.2016)	6.029 (26.82)
COV	2%	2%	5%	3%

Table 5.49: Summary of crack width measurements for 4G80S6(AC) and 5G80S6(AC) (As Cast) specimens.

Specimen	w_{ult}, in. (mm)	V_{ult}, kip (kN)	w_b, in. (mm)	V_b, kip (kN)
4G80S6(AC)	0.0244 (0.6194)	262.64 (1168.3)	0.1619 (4.112)	149.64 (665.61)
5G80S6(AC)	0.0272 (0.6899)	253.99 (1129.8)	0.1671 (4.245)	223.82 (995.62)

5.4.3.2 Interface Preparation: Roughened to 1/8 in. (3.175 mm)

Figure 5.2 presents the interface shear force versus crack width response for specimen group 4G80S6(1/8). Figure 5.35 presents the interface shear force versus crack width response for specimen group 5G80S6(1/8). All specimens discussed in this section were constructed with a surface intentionally roughened to an amplitude of 1/8 in. (3.175 mm). The figure shows the force-crack width response for all specimens in the group. Tabulated values of points of interest such as crack width at peak load and crack width at first bar fracture for specimen group 5G80S6(1/8) are presented in Table 5.50. In the mentioned figure, it can be observed that all specimens present similar behavior showing negligible crack width in the initial stages before the interface shear force at cracking, V_{cr}, is reached. After the shear interface is cracked, the crack width begins to steadily grow until peak load is reached. The post-peak response is characterized by a smooth softening branch, followed by a sustained load phase until first bar fracture. An exception to the behavior is shown by specimen

5G80S6(1/8)-2. As it can be seen in Figure 5.35, specimen 5G80S6(1/8)-2 presents comparable post-cracked stiffness, but it reaches a peak load approximately 25% higher than the other specimens in the group. This behavior originates from the variability of the process used to obtain an interface roughness of 1/8 in. (3.175 mm). A description of the interface shear force versus crack width behavior shown by specimen group 4G80S6(1/8) is presented in Section 5.2.3.

Table 5.51 presents a summary of average crack width points of interest for specimen groups 4G80S6(1/8) and 5G80S6(1/8). Specimens reinforced with #5 (#16M) reinforcing steel U-bars reach a larger average peak load, V_{ult}, and a value of average crack width at peak load, w_{ult}, 50% lower compared to specimens constructed with #4 (#13M) reinforcing steel bars. This behavior is expected due to the reinforcing steel ratio being 50% higher in specimen group 5G80S6(1/8). The clamping force is directly related to the area of reinforcing steel, therefore test specimens with a higher reinforcing steel ratio are expected to show lower values of crack width.

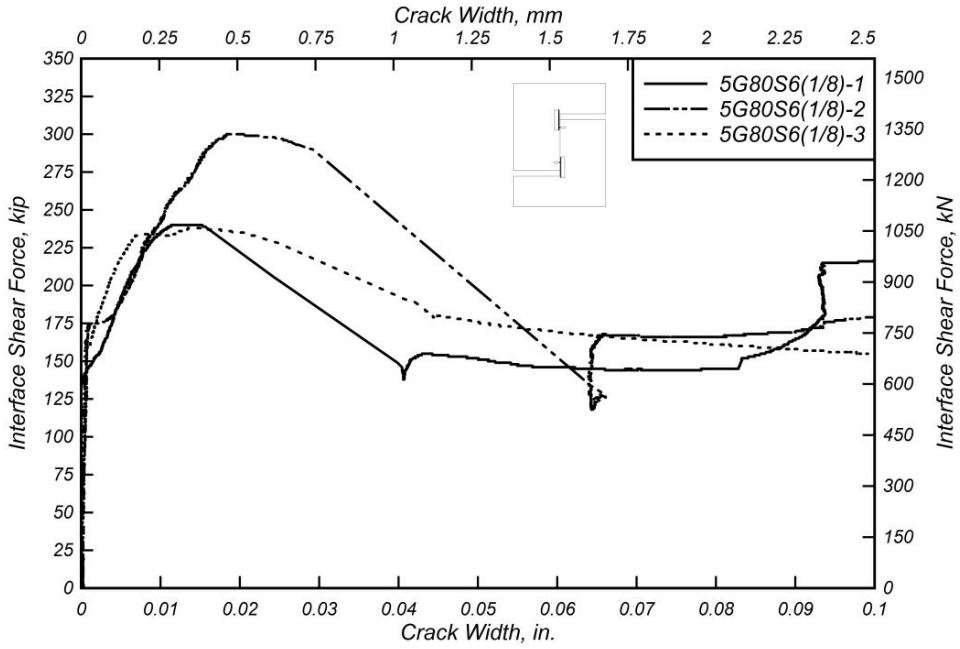

Figure 5.35: Interface shear force versus crack width for 5G80S6(1/8) specimens.

Table 5.50: Specimen 5G80S6(1/8) crack width measurements.

Specimen	w_{ult}, in. (mm)	V_{ult}, kip (kN)	w_b, in. (mm)	V_b, kip (kN)
5G80S6(1/8)-1	0.0123 (0.3117)	240.38 (1069.3)	0.1160 (2.947)	220.63 (981.40)
5G80S6(1/8)-2	0.0186 (0.4720)	300.13 (1335.0)	0.1755 (4.459)	225.72 (1004.1)
5G80S6(1/8)-3	0.0141 (0.3586)	238.06 (1059.0)	0.2171 (5.514)	205.82 (915.52)
Mean	0.0150 (0.3808)	259.52 (1154.4)	0.1696 (4.307)	217.39 (967.00)
Median	0.0141 (0.3586)	240.38 (1069.3)	0.1755 (4.459)	220.63 (981.40)
STDEV	0.0032 (0.0824)	35.18 (156.50)	0.0508 (1.291)	10.34 (46.00)
COV	22%	14%	30%	5%

Table 5.51: Summary of crack width measurements for 4G80S6(1/8) and 5G80S6(1/8) (1/8 in. (3.175 mm)) specimens.

Specimen	w_{ult}, in. (mm)	V_{ult}, kip (kN)	w_b, in. (mm)	V_b, kip (kN)
4G80S6(1/8)	0.0297 (0.7532)	238.70 (1061.8)	0.2039 (5.178)	148.87 (662.20)
5G80S6(1/8)	0.0150 (0.3808)	259.52 (1154.4)	0.1696 (4.307)	217.39 (967.00)

5.4.3.3 Interface Preparation: 1/4 in. (6.35 mm)

Figure 5.36 and Figure 5.37 present the interface shear force versus crack width response for specimen groups 4G80S6(1/4) and 5G80S6(1/4). All specimens discussed in this section were constructed with a surface roughened to an amplitude of 1/4 in. (6.35 mm). Each figure shows the force-crack width response for all specimens in each group. Tabulated values of points of interest such as crack width at peak load and crack width at first bar fracture for each specimen group are presented in Table 5.52 and Table 5.53.

Significant variability in the force-crack width response can be observed in Figure 5.36. Specimens 4G80S6(1/4)-1 and 4G80S6(1/4)-3 reach similar peak load values, but their response curves display significantly different behavior. Specimen 4G80S6(1/4)-1 reaches a larger peak load, V_{ult}, at smaller crack width, w_{ult}. Specimen 4G80S6(1/4)-1 also shows negligible crack width measurements until it reaches a load of approximately 200 kip (890 kN), which is approximately double of that

shown by specimen 4G80S6(1/4)-3. This behavior exhibited by specimen 4G80S6(1/4)-1 may be attributed to a stronger concrete-to-concrete cohesion bond at the shear interface, thus resulting in a response with larger stiffness. This in consistent with results presented in Figure 5.22 where it can be observed that specimen 4G80S6(1/4)-1 displays a significantly larger stiffness in the force-displacement response compared to specimen 4G80S6(1/4)-3. Additionally, specimen 4G80S6(1/4)-2 presents a different force-crack width response reaching a peak load 20% and 30% lower compared to specimens 4G80S6(1/4)-3 and 4G80S6(1/4)-1, respectively. The behavior presented by this specimen is a result of the variability introduced by the process to roughen the surface to an amplitude of 1/4 in. (6.35 mm).

Figure 5.37 presents the interface shear force versus crack width response for specimen group 5G80S6(1/4). Significant variability of crack width values at peak load, w_{ult}, is observed, ranging from 0.010 in. (0.2533 mm) to 0.0275 in. (0.6985 mm) with a COV of 46%. Peak load values, V_{ult}, show less variability, however, ranging from 283.85 kip (1262.6 kN) to 315.53 kip (1403.6 kN) with a COV of 5%. The variability observed in w_{ult} values for specimens 5G80S6(1/4)-1 and 5G80S6(1/4)-2 may be related to the variability created by the intentional roughening of the interface surface. The response of specimen 5G80S6(1/4)-3, however, appears to be related to a stronger concrete-to-concrete cohesion bond formed at the shear interface, as this specimen shows negligible crack width until an interface shear load significantly larger is reached.

Table 5.54 presents a summary of the average points of interest for specimen groups 4G80S6(1/4) and 5G80S6(1/4). From the table it can be observed that specimens reinforced with #5 (#16M) reinforcing steel U-bars show a crack width at peak load 13% lower and peak load 30% larger than in specimens constructed with #4 (#13M) reinforcing steel bars. This larger capacity may be related to the higher reinforcing steel ratio crossing the interface in specimens reinforced with #5 (#16M) bars. A larger reinforcing steel ratio can produce a larger clamping force which is directly related to the aggregate interlock mechanism controlling this phase of the response.

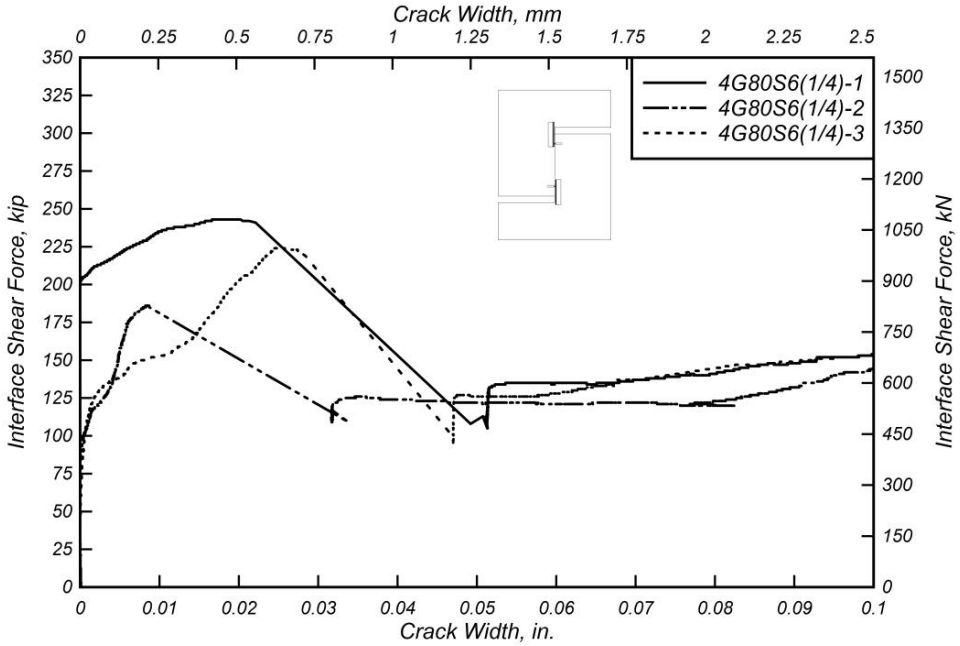

Figure 5.36: Interface shear force versus crack width for 4G80S6(1/4) specimens.

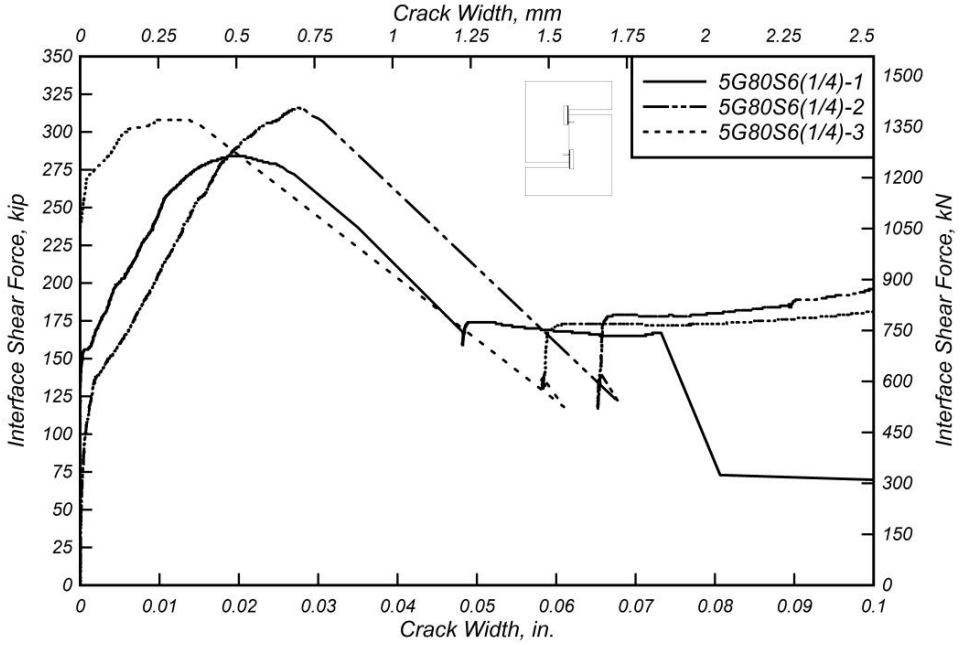

Figure 5.37: Interface shear force versus crack width for 5G80S6(1/4) specimens.

Table 5.52: Specimen 4G80S4(1/4) crack width measurements.

Specimen	w_{ult}, in. (mm)	V_{ult}, kip (kN)	w_b, in. (mm)	V_b, kip (kN)
4G80S6(1/4)-1	0.0188 (0.4767)	243.07 (1081.2)	0.1163 (2.955)	154.52 (687.35)
4G80S6(1/4)-2	0.0084 (0.2146)	186.03 (827.52)	0.1163 (2.953)	154.86 (688.84)
4G80S6(1/4)-3	0.0249 (0.6313)	224.61 (999.11)	0.1131 (2.874)	151.30 (673.03)
Mean	0.0174 (0.4409)	217.90 (969.28)	0.1152 (2.927)	153.56 (683.07)
Median	0.0188 (0.4767)	224.61 (999.11)	0.1163 (2.953)	154.52 (687.35)
STDEV	0.0083 (0.2106)	29.10 (129.45)	0.0018 (0.046)	1.962 (8.728)
COV	48%	13%	2%	1%

Table 5.53: Specimen 5G80S6(1/4) crack width measurements.

Specimen	w_{ult}, in. (mm)	V_{ult}, kip (kN)	w_b, in. (mm)	V_b, kip (kN)
5G80S6(1/4)-1	0.0194 (0.4928)	283.85 (1262.6)	0.0672 (1.707)	206.76 (919.73)
5G80S6(1/4)-2	0.0275 (0.6985)	315.53 (1403.6)	0.1367 (3.472)	245.51 (1092.1)
5G80S6(1/4)-3	0.0100 (0.2533)	308.23 (1371.1)	0.1762 (4.477)	229.67 (1021.6)
Mean	0.0190 (0.4815)	302.54 (1345.7)	0.1267 (3.219)	227.31 (1011.1)
Median	0.0194 (0.4928)	308.23 (1371.1)	0.1367 (3.472)	229.67 (1021.6)
STDEV	0.0088 (0.2228)	16.59 (73.79)	0.0552 (1.402)	19.48 (86.65)
COV	46%	5%	44%	9%

Table 5.54: Summary of crack width measurements for 4G80S6(1/4) and 5G80S6(1/4) (1/4 in. (6.35 mm)) specimens.

Specimen	w_{ult}, in. (mm)	V_{ult}, kip (kN)	w_b, in. (mm)	V_b, kip (kN)
4G80S6(1/4)	0.0174 (0.4409)	217.90 (969.28)	0.1152 (2.927)	153.56 (683.07)
5G80S6(1/4)	0.0190 (0.4815)	302.54 (1345.7)	0.1267 (3.219)	227.31 (1011.1)

5.4.3.4 Interface Preparation: Exposed Aggregate

Figure 5.38 and Figure 5.39 present the interface shear force versus crack width response for specimen groups 4G80S6(EA) and 5G80S6(EA). All specimens discussed in this section were constructed with an Exposed Aggregate interface

preparation. Each figure shows the force-crack width response for all specimens in each group. Tabulated values of points of interest such as crack width at peak load and crack width at first bar fracture for each specimen group are presented in Table 5.55 and Table 5.56.

In Figure 5.38 it can be seen that specimen 4G80S6(EA)-1 shows a significantly lower post-crack stiffness compared to the other specimens in the group. As discussed in Section 5.4.1.4, these results indicate that exposing the aggregate of the interface surface may allow the aggregate interlock mechanism to contribute to the force-crack width response during the post-peak stage as is the case for specimens 4G80S6(EA)-2 and 4G80S6(EA)-3. However, this extended contribution by the aggregate interlock mechanism may not always develop, as it does not appear in the force-crack width response of specimen 4G80S6(EA)-1. During the sustained load phase of the force-crack width response it can be observed that specimens 4G80S6(EA)-2 and 4G80S6(EA)-3 maintain higher sustained loads. This appears to be related to the higher contribution of the aggregate interlock mechanism in these specimens, which may extend its contribution further into the post-peak phase of the response.

Figure 5.39 shows the interface shear force versus crack width response of specimen group 5G80S6(EA). In this figure it can be seen that specimen 5G80S6(EA)-1 presents similar behavior to specimens 4G80S6(EA)-2 and 4G80S6(EA)-3, presenting a high post-cracked stiffness and larger sustained load compared to the other specimens in the group. These results indicate that by using an Exposed Aggregate interface preparation, it may be possible to increase the contribution of the aggregate interlock mechanism not only in peak load capacity, but also in post-peak sustained load capacity. Additional testing and surface preparation trials using different aggregates and surface preparation mechanisms to develop the Exposed Aggregate surface finishing should be investigated.

Table 5.57 presents a summary of average crack width points of interest for specimen groups 4G80S6(EA) and 5G80S6(EA). In this table it can be seen that specimens reinforced with #5 (#16M) reinforcing steel U-bars reach a higher peak load, V_{ult}, at

lower crack width, w_{ult}. However, based on results from specimens 4G80S6(EA)-2, 4G80S6(EA)-3, and 5G80S6(EA)-1, it is important to perform further research into the use of an Exposed Aggregate shear interface.

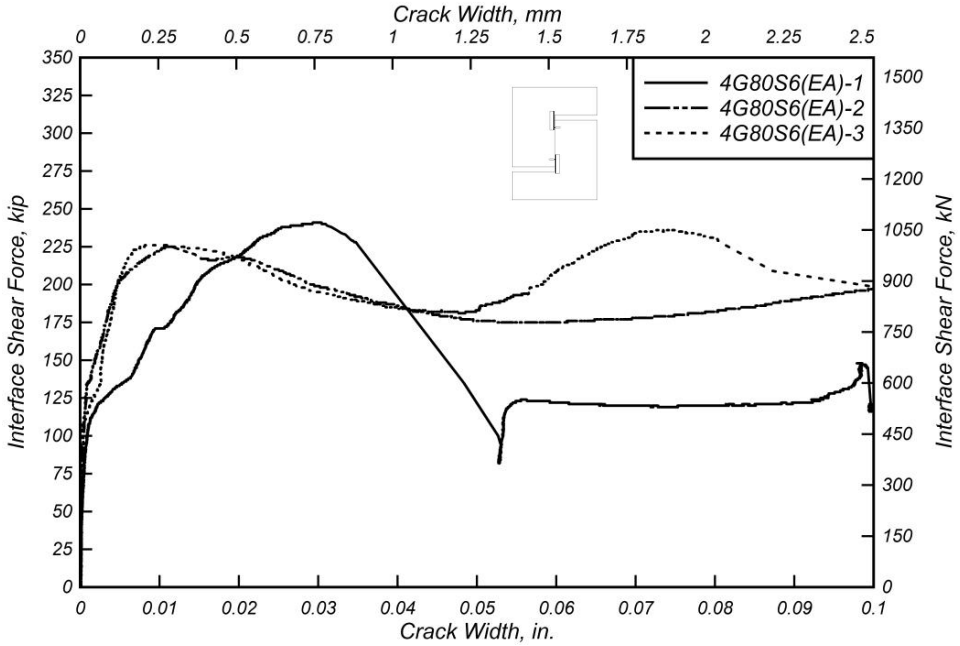

Figure 5.38: Interface shear force versus crack width for 4G80S6(EA) specimens.

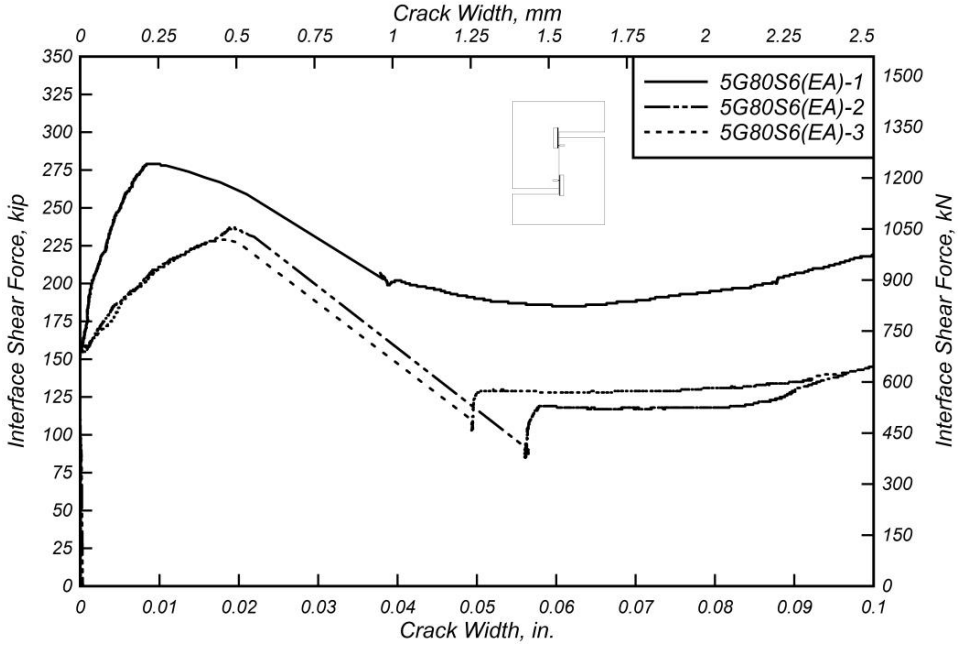

Figure 5.39: Interface shear force versus crack width for 5G80S6(EA) specimens.

Table 5.55: Specimen 4G80S6(EA) crack width measurements.

Specimen	w_{ult}, in. (mm)	V_{ult}, kip (kN)	w_b, in. (mm)	V_b, kip (kN)
4G80S6(EA)-1	0.0300 (0.7625)	241.11 (1072.5)	0.0993 (2.522)	145.13 (645.55)
4G80S6(EA)-2	0.0114 (0.2905)	225.49 (1003.0)	0.1432 (3.686)	230.33 (1024.6)
4G80S6(EA)-3	0.0093 (0.2371)	226.29 (1006.6)	0.0806 (2.048)	227.54 (1012.1)
Mean	0.0169 (0.4300)	230.96 (1027.4)	0.1077 (2.736)	201.00 (894.08)
Median	0.0114 (0.2905)	226.29 (1006.6)	0.0993 (2.522)	227.54 (1012.1)
STDEV	0.0114 (0.2829)	8.798 (39.13)	0.0321 (0.8158)	48.41 (215.32)
COV	67%	4%	30%	24%

Table 5.56: Specimen 5G80S6(EA) crack width measurements.

Specimen	w_{ult}, in. (mm)	V_{ult}, kip (kN)	w_b, in. (mm)	V_b, kip (kN)
5G80S6(EA)-1	0.0090 (0.2290)	279.43 (1243.0)	0.1053 (2.675)	226.26 (1006.4)
5G80S6(EA)-2	0.0193 (0.4897)	236.63 (1052.6)	0.1200 (3.047)	140.96 (627.03)
5G80S6(EA)-3	0.0180 (0.4584)	229.12 (1019.2)	0.1259 (3.197)	148.27 (659.53)
Mean	0.0154 (0.3924)	248.39 (1104.9)	0.1170 (2.973)	171.83 (764.33)
Median	0.0180 (0.4584)	236.63 (1052.6)	0.1200 (3.047)	148.27 (659.53)
STDEV	0.0056 (0.1423)	27.14 (120.71)	0.0106 (0.2688)	47.28 (210.30)
COV	36%	11%	9%	28%

Table 5.57: Summary of crack width measurements for 4G80S6(EA) and 5G80S6(EA) (Exposed Aggregate) specimens.

Specimen	w_{ult}, in. (mm)	V_{ult}, kip (kN)	w_b, in. (mm)	V_b, kip (kN)
4G80S6(EA)	0.0169 (0.4300)	230.96 (1027.4)	0.1077 (2.736)	201.00 (894.08)
5G80S6(EA)	0.0154 (0.3924)	248.39 (1104.9)	0.1170 (2.973)	171.83 (764.33)

5.5 SUMMARY AND MAIN FINDINGS

This section provides a summary of experimental findings and a discussion on main findings regarding: (i) influence of reinforcing steel grade, (ii) influence of reinforcing steel bar spacing, and (iii) influence of reinforcing steel bar size. A comparison between experimentally measured capacity and calculated capacities per AASHTO and ACI 318-14 code provisions is also presented.

Figure 5.40 shows the peak shear stress normalized by concrete strength versus the reinforcing steel ratio normalized by the concrete strength and the elastic modulus of the reinforcing steel. The effect analyzed in this figure is the influence of reinforcing steel grade, including data corresponding to test specimen groups 4G60S6(1/8), 4G80S6(1/8), 4G100S6(1/8), and 4G120S6(1/8) reinforced with Grade 60 (420 MPa), Grade 80 (550 MPa), Grade 100 (690 MPa), and Grade 120 (830 MPa), respectively. Note that all data points presented in this figure correspond to specimens with a shear interface roughened to an amplitude of 1/8 in. (3.175 mm). The figure also shows a thick line representing the AASHTO (2015) shear friction design equation (Equation 2-1), and a thin line representing the AASHTO (2015) shear friction design equation considering f_y = 80 ksi (550 MPa) nominal yield strength, thus exceeding the currently allowed limit of f_y = 60 ksi (420 MPa) nominal yield strength. As observed in the figure, the data points are all above the curve, which indicates that increasing the nominal yield strength limit to 80 ksi (550 MPa) will maintain the conservative nature of the design equation. In the figure, it can be observed that one 4G80S6(1/8) specimen and one 4G120S6(1/8) specimen over-performed compared to the rest of the specimens in the figure. However, the data points do not display an overall trend to show increased capacity as reinforcing steel grade increases.

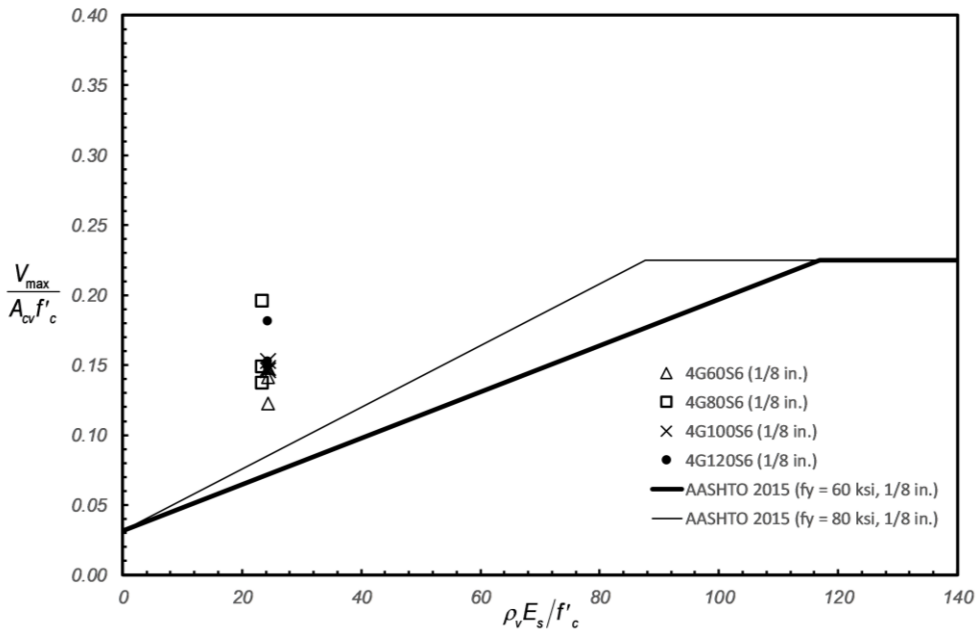

Figure 5.40: Experimental normalized peak shear stress versus normalized reinforcement stiffness across the interface – influence of reinforcing steel grade.

Figure 5.41 shows the peak shear stress normalized by concrete strength versus the reinforcing steel ratio normalized by the concrete strength and the elastic modulus of the reinforcing steel. The effect analyzed in this figure is the influence of reinforcing steel bar spacing. The figure presents data corresponding to test specimens 4G80S4(1/8), 4G80S6(1/8), and 4G80S12(1/8) built with reinforcing steel bars spaced at 4 in. (101.6 mm), 6 in. (152.4 mm), and 12 in. (304.8 mm), respectively. Additionally, this figure shows two lines. The first line corresponds to AASHTO (2015) shear friction design equation for a surface roughened to an amplitude of 1/8 in. (3.175 mm). The second line corresponds to the same design equation with a nominal yield strength limit of f_y = 80 ksi (550 MPa). The figure shows that all data points are above the curve, which is an indication that the design equation remains conservative when the nominal yield strength limit is increased to 80 ksi (550 MPa). Additionally, it can be observed that there is a trend of reaching larger peak loads as the reinforcing steel ratio increases. This indicates that steel reinforcement ratio significantly impacts the shear capacity, as it is directly related to the clamping force generated by the reinforcing steel bars crossing the interface.

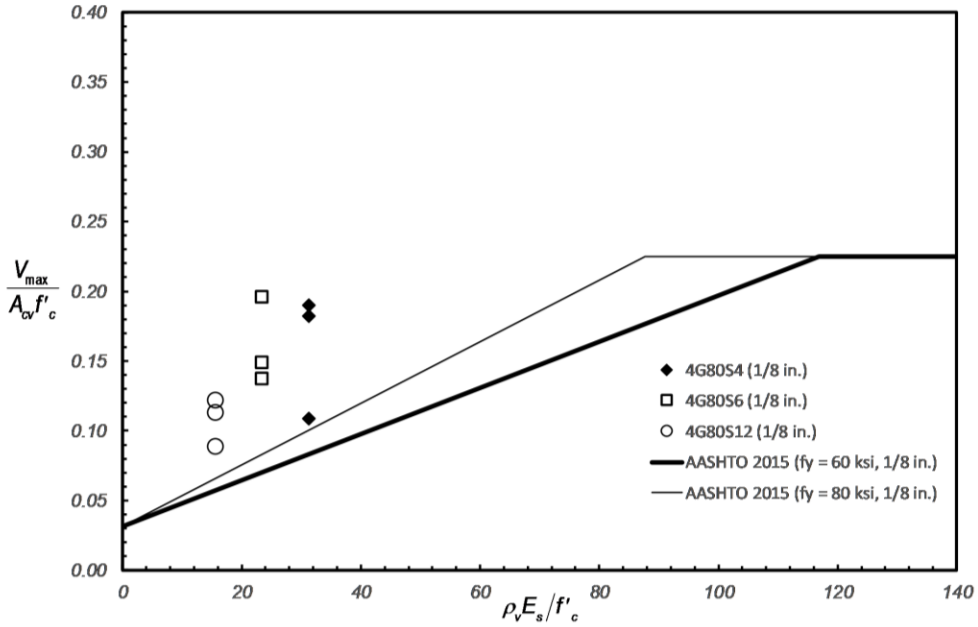

Figure 5.41: Experimental normalized peak shear stress versus normalized reinforcement stiffness across the interface – influence of reinforcing steel bar spacing.

Figure 5.42 shows the peak shear stress normalized by concrete strength versus the reinforcing steel ratio normalized by the concrete strength and the elastic modulus of the reinforcing steel. The effect analyzed in this figure is the influence of reinforcing steel bar size. The figure shows test data corresponding to test specimens constructed with reinforcing steel bars size #4 (#13M) and #5 (#16M). This figure includes AASHTO (2015) shear friction design equations curves corresponding to surface roughened to an amplitude of 1/4 in. (6.35 mm), surface not intentionally roughened (As Cast), and an Exposed Aggregate surface. AASHTO (2015) does not include provisions for Exposed Aggregate, therefore it was taken as an interpolation between the 1/8 in. (3.175 mm) curve and the As Cast curve. Additionally, the figure includes the AASHTO (2015) mentioned considering a nominal yield strength of 80 ksi (550 MPa). It can be observed in the figure that all data points are above the lines corresponding to each surface preparation. This indicates that the design equation will remain conservative if the nominal yield strength is increased to 80 ksi (550 MPa). The figure also shows a distinct pattern of increased interface shear capacity as the reinforcing steel bar size increases from #4 (#13M) to #5 (#16M).

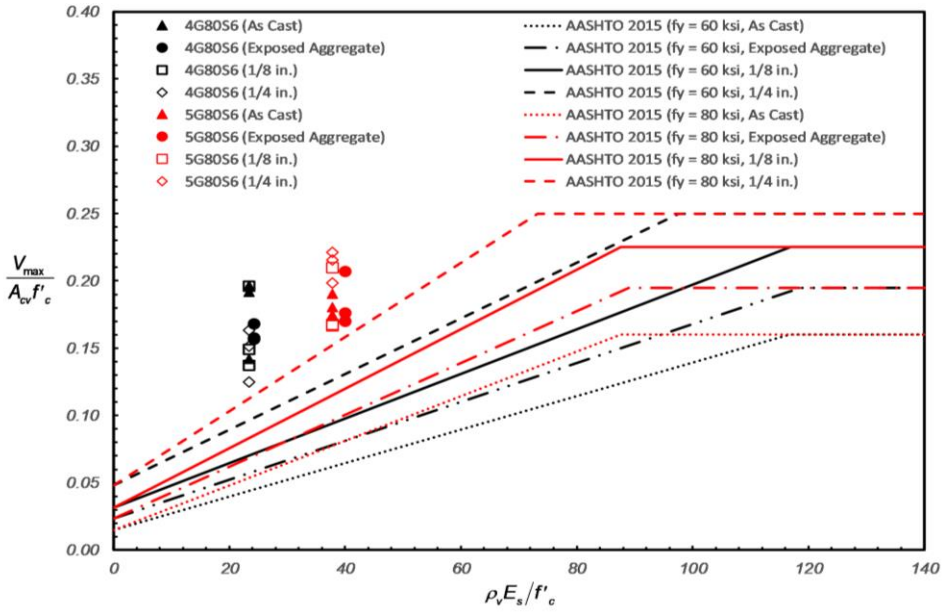

Figure 5.42: Experimental normalized peak shear stress versus normalized reinforcement stiffness across the interface – influence of reinforcing steel bar size.

Figure 5.43 and Figure 5.44 present the ratio of the experimentally measured peak loads, V_{max}, to the shear capacity per AASHTO (2015) and ACI 318-14 code provisions, respectively. In these figures, each data set consists of two columns. The first column corresponds to the ratio considering the nominal yield strength of f_y = 80 ksi (550 MPa), or f_y = 100 ksi (690 MPa) and f_y = 120 ksi (830 MPa), for specimen groups 4G100S6(1/8) and 4G120S6(1/8), respectively. The second column corresponds to using the ratio considering the nominal yield strength limit of f_y = 60 ksi (420 MPa). Table 5.58 shows a summary of the ratio of experimentally measured shear resistance to nominal interface shear resistance per AASHTO (2015) and ACI 318-14, V_{max}/V_{ni}. As seen in the table, increasing the nominal yield strength to 80 ksi (550 MPa) reduces the V_{max}/V_{ni} ratio in all cases for both code provisions. These results indicate that an increase in the nominal yield strength limit to 80 ksi (550 MPa) will provide a more efficient design while still remaining conservative for both AASHTO (2015) and ACI 318-14 code provisions. It is important to note that when considering f_y = 80 ksi (550 MPa) all specimen groups indicate V_{max}/V_{ni} ratios greater than 1.5, with the exception of specimen groups 4G120S6(1/8), 4G80S6(1/4), and 5G80S6(1/4), per AASHTO (2015) code provisions. All specimen groups indicate

V_{max}/V_{ni} ratios greater that 1.5 when considering f_y = 80 ksi (550 MPa), per ACI 318-14 code provisions.

From the presented data it can be seen that ACI 318-14 provisions result in higher V_{max}/V_{ni} ratios when compared to the AASHTO (2015) provisions, therefore, increasing the nominal yield strength limit to f_y = 80 ksi (550 MPa) would increase the efficiency while maintaining a conservative approach. It is important to note that test specimens constructed with #4 (#13M) reinforcing steel bars and an As Cast surface preparation displayed the highest V_{max}/V_{ni} ratios. These results indicate that the interface shear capacity of this type of surface preparation may be underestimated which results in an overly conservative design.

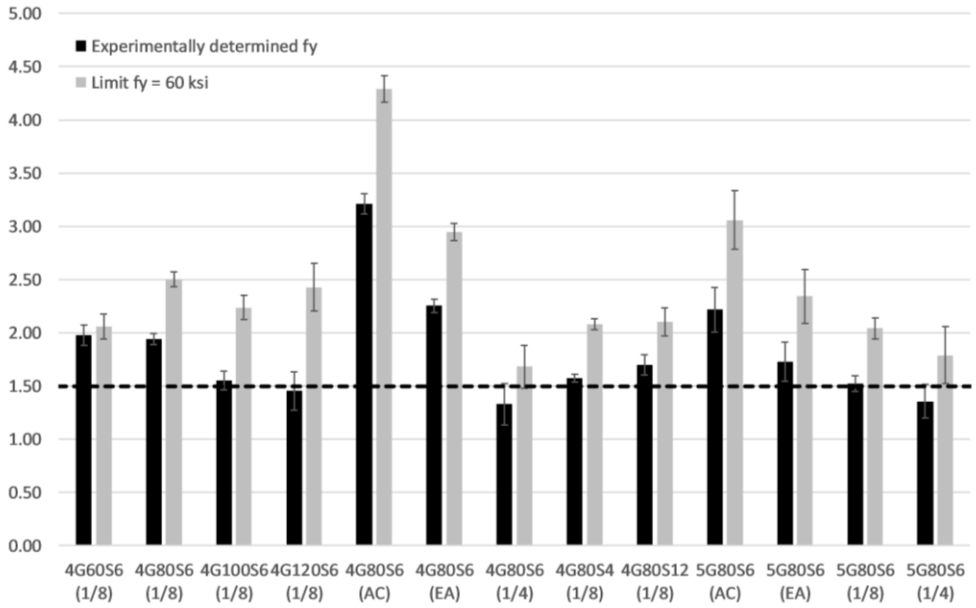

Figure 5.43: Comparison of experimentally measured strength with AASHTO (2015) calculated strength.

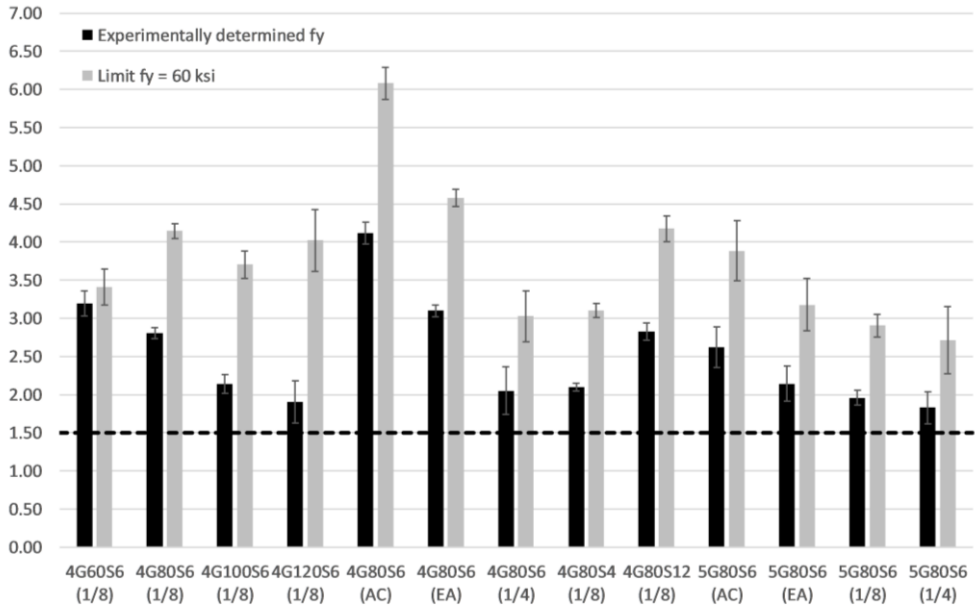

Figure 5.44: Comparison of experimentally measured strength with ACI 318-14 calculated strength.

Table 5.58: Ratio of measured strength, V_{max}, to nominal strength, V_{ni}

Specimen label	V_{max}, kip (kN)	AASHTO (2015) Section 5.8.4				ACI 318-14 Section 22.9			
		Experimental f_y		Limit f_y = 60 ksi (420 MPa)		Experimental f_y		Limit f_y = 60 ksi (420 MPa)	
		V_{ni}, kip (kN)	V_{max}/V_{ni}	V_{ni}, kip (kN)	V_{max}/V_{ni}	V_{nh}, kip (kN)	V_{max}/V_{nh}	V_{nh}, kip (kN)	V_{max}/V_{nh}
4G60S6 (1/8)	196.33 (873.33)	99.28 (441.6)	1.98	95.40 (424.4)	2.06	61.48 (273.5)	3.19	57.60 (256.2)	3.41
4G80S6 (1/8)	238.67 (1061.6)	122.88 (546.6)	1.94	95.40 (424.4)	2.50	85.08 (378.5)	2.81	57.60 (256.2)	4.14
4G100S6 (1/8)	213.33 (948.95)	137.56 (611.9)	1.55	95.40 (424.4)	2.24	99.76 (443.8)	2.14	57.60 (256.2)	3.70
4G120S6 (1/8)	231.67 (1030.5)	159.36 (708.9)	1.45	95.40 (424.4)	2.43	121.56 (540.8)	1.91	57.60 (256.2)	4.02
4G80S6 (AC)	262.67 (1168.4)	81.81 (363.9)	3.21	61.20 (272.2)	4.29	63.81 (283.9)	4.12	43.20 (192.2)	6.08
4G80S6 (EA)	230.67 (1026.1)	102.35 (455.3)	2.25	78.30 (348.3)	2.95	74.45 (331.2)	3.10	50.40 (224.2)	4.58
4G80S6 (1/4)	218.00 (969.71)	163.96 (729.3)	1.33	129.60 (576.5)	1.68	106.36 (473.1)	2.05	72.00 (320.3)	3.03
4G80S4 (1/8)	238.33 (1060.2)	151.25 (672.8)	1.58	114.60 (509.8)	2.08	113.45 (504.6)	2.10	76.80 (341.6)	3.10
4G80S12 (1/8)	160.33 (713.20)	94.52 (420.5)	1.70	76.20 (339.0)	2.10	56.72 (252.3)	2.83	38.40 (170.8)	4.18
5G80S6 (AC)	260.00 (1156.5)	117.26 (521.6)	2.22	84.96 (377.9)	3.06	99.26 (441.5)	2.62	66.96 (297.9)	3.88
5G80S6 (EA)	248.33 (1104.6)	143.70 (639.2)	1.73	106.02 (471.6)	2.34	115.80 (515.1)	2.14	78.12 (347.5)	3.18
5G80S6 (1/8)	259.33 (1153.6)	170.14 (756.8)	1.52	127.08 (565.3)	2.04	132.34 (588.7)	1.96	89.28 (397.1)	2.90
5G80S6 (1/4)	302.67 (1346.3)	223.03 (992.1)	1.36	169.20 (752.6)	1.79	165.43 (735.9)	1.83	111.60 (496.4)	2.71

6.0 EFFECT OF SURFACE PREPARATION AND CONCRETE STRENGTH ON SHEAR FRICTION

6.1 INTRODUCTION

This chapter presents test results from push-off test specimens with a focus on establishing the effect of surface preparation and nominal concrete strength on shear friction. The effects analyzed in this section are: (1) influence of interface preparation, and (2) influence of nominal concrete strength. The details of each push-off test specimen discussed in this chapter can be found in the test matrix presented in Table 3.1, section (b), and (e). The discussion in this chapter focuses on results for interface shear force versus interface shear displacement, interface shear force versus strain, and interface shear force versus crack width. The methods implemented for data collection and the instrumentation utilized are presented in Section 3.5.

6.2 INFLUENCE OF SURFACE PREPARATION

This section focusses on the influence of interface preparation. All specimens discussed in this section are reinforced with three (3) #4 (#13M) or #5 (#16M) Grade 80 ksi (550 MPa) reinforcing steel U-bars spaced at 6 in. (152.4 mm) with a nominal concrete strength of 5000 psi (35 MPa). Since the variable of interest in this discussion is interface preparation, the test specimens discussed in this section are constructed with As Cast, 1/8 in. (3.175 mm), 1/4 in. (6.35 mm), and Exposed Aggregate interface preparations. Details of the specimens such as bar size, bar spacing, and interface preparation can be found in section (b) of Table 3.1; drawings showing dimensions of the specimens, as well as location of the reinforcing steel U-bars are presented in Chapter 3. Properties of the reinforcing steel used, and the concrete used are presented in Section 4.1 and Section 4.2, respectively.

6.2.1 Interface Shear Force versus Interface Shear Displacement

6.2.1.1 Reinforcing Steel U-bar Size: #4 (#13M)

Figure 6.1 to Figure 6.4 present the interface shear force versus interface shear displacement response curves for specimen groups 4G80S6(AC), 4G80S6(1/8), 4G80S6(1/4), and 4G80S6(EA), respectively. Table 6.1 to Table 6.4 present tabulated values for the main characteristic points of the test results for the specimen. Discussions regarding Figure 6.1 to Figure 6.4 and Table 6.1 to Table 6.4 are presented in Section 5.4.1.

Table 6.5 presents average values of the main points of interest of the interface shear force versus interface shear displacement response for specimen groups 4G80S6(AC), 4G80S6(1/8), 4G80S6(1/4), and 4G80S6(EA). From this table it can be observed that the average peak load, V_{ult}, is larger for specimen group 4G80S6(AC) with a V_{ult} value of 262.65 kip (1168.3 kN). The other specimen groups present average peak load values ranging from 217.90 kip (969.28 kN) to 238.70 kip (1061.8 kN). A similar trend is observed when comparing V_{cr}, where the average interface shear load at cracking is similar for specimen groups 4G80S6(1/8), 4G80S6(EA), and 4G80S6(1/4), with V_{cr} values 109.44 kip (486.80 kN), 109.92 kip (488.95 kN), and 111.37 kip (495.38 kN), respectively, while specimen group 4G80S6(AC) reaches a larger V_{cr} value of 142.83 kip (635.35 kN). These results indicate that specimens with an As Cast interface preparation not only formed a stronger concrete-to-concrete cohesion bond, thus reaching a larger V_{cr}, but also had a larger aggregate interlock contribution to the force-displacement response.

Specimen groups constructed with an interface preparation of 1/8 in. (3.175 mm) and 1/4 in. (6.35 mm) reached lower peak load values when compared to specimens constructed with an As Cast surface preparation, as mentioned in the previous paragraph. These results may be explained by comparing the maximum aggregate size and the size of the ridges present on the shear interface. The maximum aggregate size is 3/8 in. (9.525 mm), whereas the ridges on the shear interface have a depth of 1/8 in. (3.175 mm) and 1/4 in. (6.35 mm). The larger size of the maximum aggregates

may cause voids to form, as they will not fit inside the ridges, thus weakening the concrete-to-concrete cohesion bond between the top and bottom layer of concrete.

From Table 6.5 it can be inferred that during post-peak stage of the force-displacement response, specimen groups 4G80S6(EA) outperforms all other specimen groups in terms of average sustained load at first bar fracture, V_b, and energy dissipated by the specimen until first bar fracture, E_b. Specimen group 4G80S6(EA) reaches a V_b value of 201.00 kip (894.09 kN), which is 31% larger than the second highest V_b value. Additionally, specimen group 4G80S6(EA) reaches an E_b value of 16.86 kip-ft (22.86 kJ), which is 34% larger than the second highest E_b value. This significant increase in post-peak capacity appears to be related to the Exposed Aggregate interface preparation, as it may cause the aggregate interlock mechanism to extend its contribution to the post-peak shear capacity into the sustained load stage of the force-displacement response, as previously discussed in Section 5.4.1.4.

It is worth noting that, per current AASHTO and ACI design provisions, test specimens with an As Cast interface preparation are expected to perform at lower levels than test specimens with an interface intentionally roughened. The results discussed in this section may indicate that the shear interface capacity of specimens constructed with an As Cast interface preparation is underestimated and, therefore, is unnecessarily conservative. Additional testing and surface preparation trials using different methods to obtain an As Cast surface preparation should be investigated.

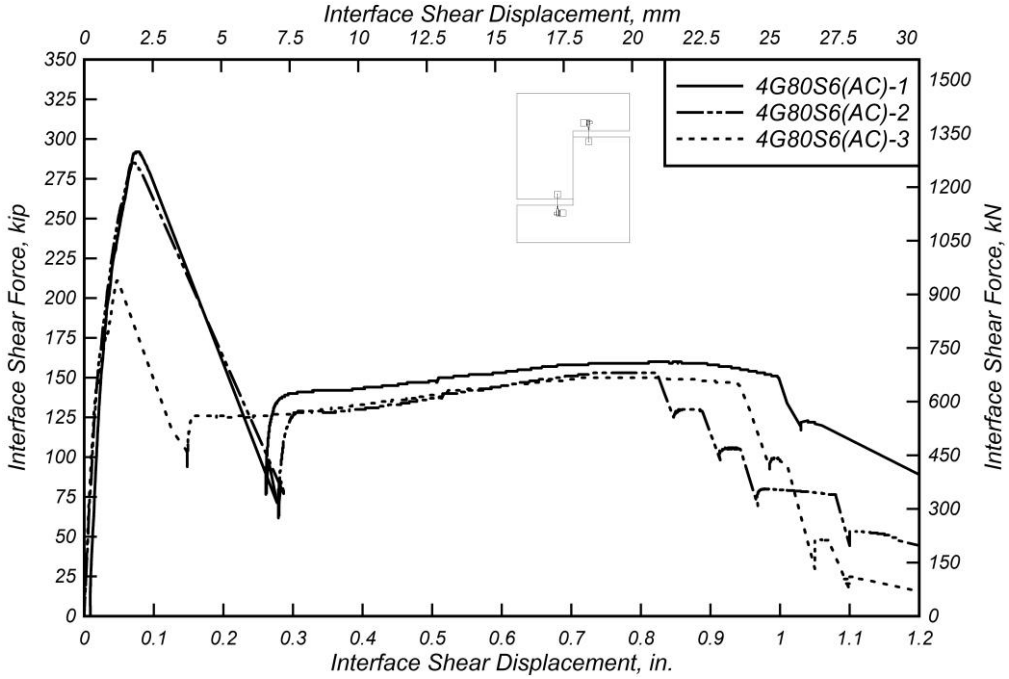

Figure 6.1: Interface shear force versus interface shear displacement for 4G80S6(AC) specimens (As Cast).

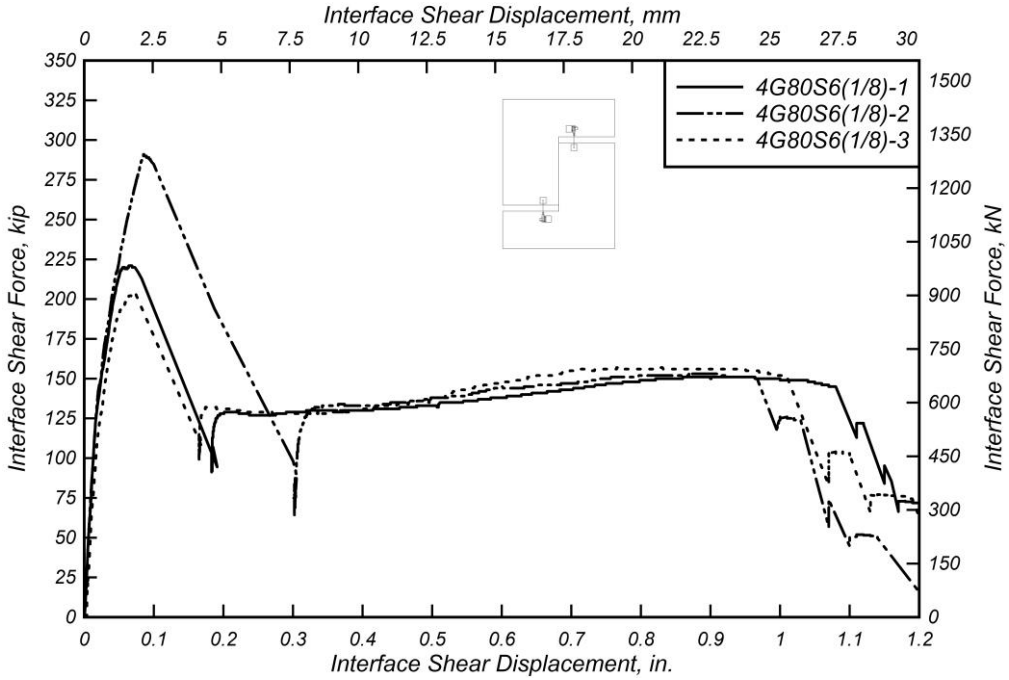

Figure 6.2: Interface shear force versus interface shear displacement the 4G80S6(1/8) specimens (1/8 in. (3.175 mm)).

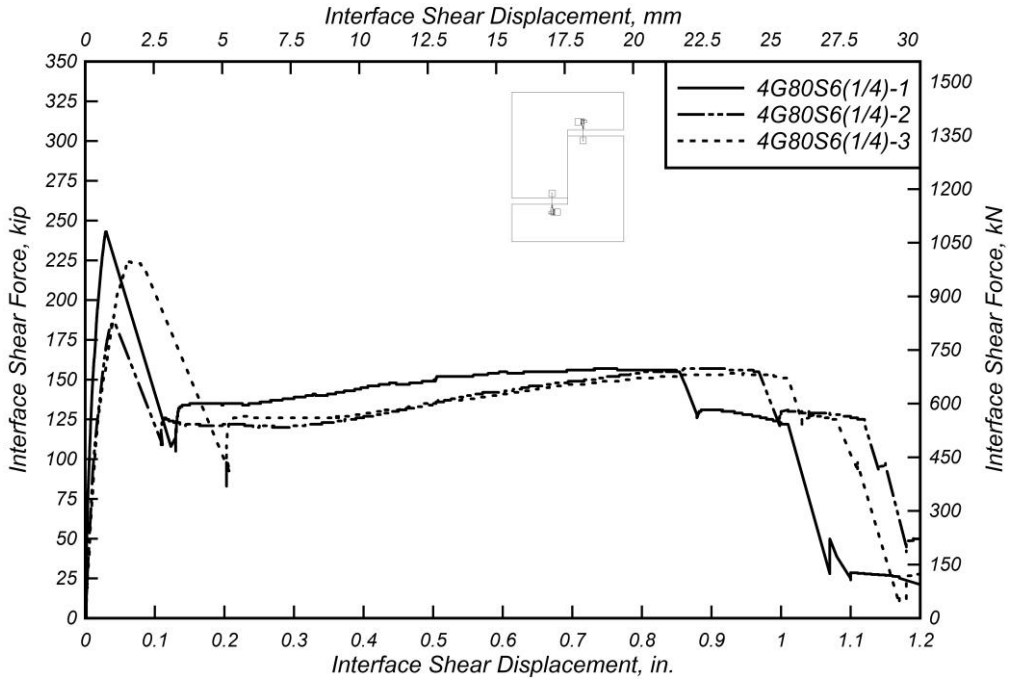

Figure 6.3: Interface shear force versus interface shear displacement for 4G80S6(1/4) specimens (1/4 in. (6.35 mm)).

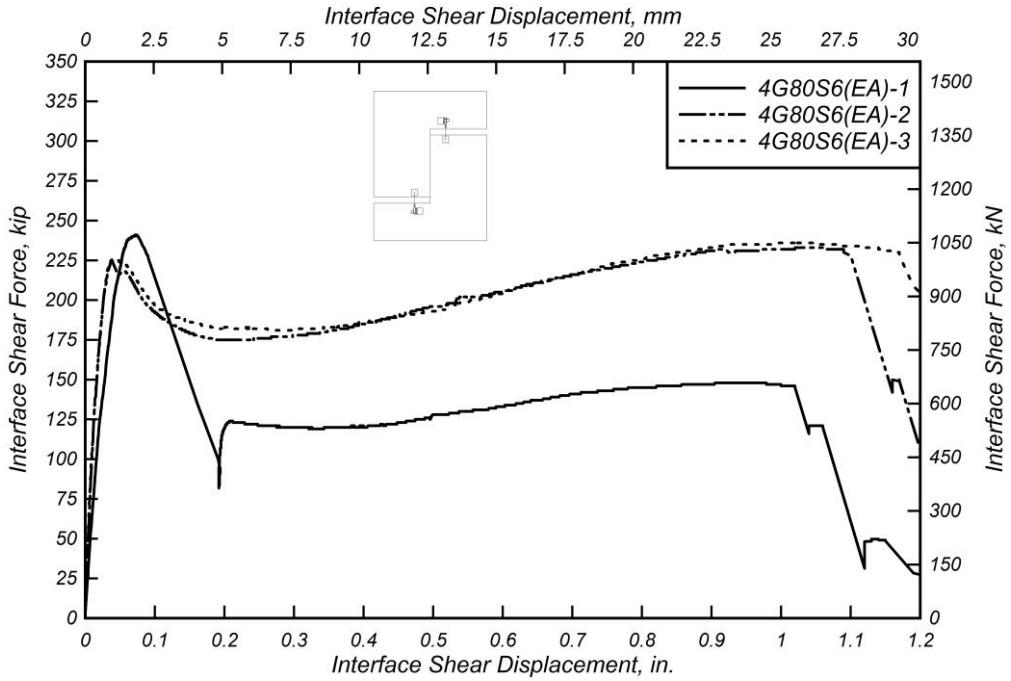

Figure 6.4: Interface shear force versus interface shear displacement for 4G80S6(EA) specimens (Exposed Aggregate).

Table 6.1: Specimen 4G80S6(AC) shear test results.

Spec	Δ_{ult}, in. (mm)	V_{ult}, kip (kN)	σ_{ult}, ksi (MPa)	$V_{sus,min}$, kip (kN)	$V_{sus,max}$, kip (kN)	Δ_{cr}, in. (mm)	V_{cr}, kip (kN)	Δ_{b}, in. (mm)	V_b, kip (kN)	E_b, kip-ft (kJ)
4G80S6 (AC)-1	0.077 (1.96)	292.03 (1299)	1.217 (8.39)	140.31 (624.1)	159.75 (710.6)	0.021 (0.54)	132.20 (588.1)	0.995 (25.3)	150.66 (670.2)	13.43 (18.21)
4G80S6 (AC)-2	0.072 (1.83)	284.98 (1268)	1.187 (8.19)	128.36 (571.0)	153.38 (682.3)	0.020 (0.50)	153.40 (682.4)	0.822 (20.9)	152.78 (679.6)	10.73 (14.55)
4G80S6 (AC)-3	0.048 (1.22)	210.93 (938.3)	0.879 (6.06)	125.31 (557.4)	150.42 (669.1)	0.017 (0.43)	142.90 (635.7)	0.941 (23.9)	145.46 (647.0)	11.07 (15.01)
Mean	0.066 (1.67)	262.65 (1168)	1.094 (7.55)	131.33 (584.2)	154.52 (687.3)	0.019 (0.49)	142.83 (635.4)	0.919 (23.4)	149.63 (665.6)	11.74 (15.92)
Median	0.072 (1.83)	284.98 (1268)	1.187 (8.19)	128.36 (571.0)	153.38 (682.3)	0.020 (0.50)	142.90 (635.7)	0.941 (23.9)	150.66 (670.2)	11.07 (15.01)
STDEV	0.016 (0.39)	44.93 (199.8)	0.187 (1.29)	7.928 (35.26)	4.768 (21.21)	0.002 (0.06)	10.60 (47.15)	0.089 (2.25)	3.766 (16.75)	1.470 (1.993)
COV	24%	17%	17%	6%	3%	12%	7%	10%	3%	13%

Table 6.2: Specimen 4G80S6(1/8) shear test results.

Spec	Δ_{ult}, in. (mm)	V_{ult}, kip (kN)	σ_{ult}, ksi (MPa)	$V_{sus,min}$, kip (kN)	$V_{sus,max}$, kip (kN)	Δ_{cr}, in. (mm)	V_{cr}, kip (kN)	Δ_{b}, in. (mm)	V_b, kip (kN)	E_b, kip-ft (kJ)
4G80S6 (1/8)-1	0.065 (1.65)	221.21 (984.0)	0.922 (6.36)	126.72 (563.7)	151.44 (673.6)	0.015 (0.37)	112.5 (500.4)	1.079 (27.4)	145.00 (645.0)	12.92 (17.52)
4G80S6 (1/8)-2	0.085 (2.16)	290.99 (1294)	1.212 (8.36)	132.37 (588.8)	152.83 (679.8)	0.016 (0.40)	119.00 (529.3)	0.962 (24.4)	150.57 (669.8)	12.73 (17.26)
4G80S6 (1/8)-3	0.070 (1.78)	203.91 (907.0)	0.850 (5.86)	127.94 (569.1)	156.60 (696.6)	0.016 (0.41)	96.81 (430.6)	1.012 (25.7)	151.03 (671.8)	12.19 (16.53)
Mean	0.073 (1.86)	238.70 (1062)	0.995 (6.86)	129.01 (573.9)	153.62 (683.4)	0.016 (0.40)	109.44 (486.8)	1.018 (25.9)	148.87 (662.2)	12.61 (17.10)
Median	0.070 (1.78)	221.21 (984.0)	0.922 (6.36)	127.94 (569.1)	152.83 (679.8)	0.016 (0.40)	112.50 (500.4)	1.012 (25.7)	150.57 (669.8)	12.73 (17.26)
STDEV	0.010 (0.26)	46.10 (205.1)	0.192 (1.32)	2.973 (13.22)	2.670 (11.88)	0.001 (0.02)	11.41 (50.74)	0.059 (1.49)	3.357 (14.93)	0.377 (0.512)
COV	14%	19%	19%	2%	2%	5%	10%	6%	2%	3%

Table 6.3: Specimen 4G80S6(1/4) shear test results.

Spec	Δ_{ult}, in. (mm)	V_{ult}, kip (kN)	σ_{ult}, ksi (MPa)	$V_{sus,min}$, kip (kN)	$V_{sus,max}$, kip (kN)	Δ_{cr}, in. (mm)	V_{cr}, kip (kN)	Δ_{b}, in. (mm)	V_b, kip (kN)	E_b, kip-ft (kJ)
4G80S6 (1/4)-1	0.030 (0.76)	243.07 (1081)	1.013 (6.98)	134.34 (597.6)	156.75 (697.3)	0.007 (0.17)	105.70 (470.2)	0.854 (21.7)	154.52 (687.3)	10.73 (14.55)
4G80S6 (1/4)-2	0.041 (1.04)	186.03 (827.5)	0.775 (5.34)	119.82 (533.0)	157.04 (698.6)	0.014 (0.35)	109.60 (487.5)	0.968 (24.6)	154.86 (688.9)	11.13 (15.09)
4G80S6 (1/4)-3	0.063 (1.60)	224.61 (999.1)	0.936 (6.45)	125.59 (558.7)	153.71 (683.7)	0.017 (0.43)	118.80 (528.5)	1.006 (25.6)	151.30 (673.0)	12.19 (16.52)
Mean	0.045 (1.14)	217.90 (969.3)	0.908 (6.26)	126.58 (563.1)	155.83 (693.2)	0.013 (0.32)	111.37 (495.4)	0.943 (23.9)	153.56 (683.1)	11.35 (15.39)
Median	0.041 (1.04)	224.61 (999.1)	0.936 (6.45)	125.59 (558.7)	156.75 (697.3)	0.014 (0.35)	109.60 (487.5)	0.968 (24.6)	154.52 (687.3)	11.13 (15.09)
STDEV	0.017 (0.43)	29.11 (129.5)	0.121 (0.84)	7.311 (32.52)	1.845 (8.205)	0.005 (0.13)	6.726 (29.92)	0.079 (2.01)	1.965 (8.739)	0.751 (1.018)
COV	38%	13%	13%	6%	1%	42%	6%	8%	1%	7%

Table 6.4: Specimen 4G80S6(EA) shear test results.

Spec	Δ_{ult}, in. (mm)	V_{ult}, kip (kN)	σ_{ult}, ksi (MPa)	$V_{sus,min}$, kip (kN)	$V_{sus,max}$, kip (kN)	Δ_{cr}, in. (mm)	V_{cr}, kip (kN)	Δ_{b}, in. (mm)	V_b, kip (kN)	E_b, kip-ft (kJ)
4G80S6 (EA)-1	0.073 (1.85)	241.11 (1073)	1.005 (6.93)	119.20 (530.2)	148.28 (659.6)	0.017 (0.44)	107.90 (635.4)	1.023 (26.0)	145.13 (645.6)	11.93 (16.17)
4G80S6 (EA)-2	0.038 (0.97)	225.49 (1003)	0.940 (6.48)	174.99 (778.4)	232.89 (1036)	0.013 (0.33)	129.90 (465.5)	1.094 (27.8)	230.33 (1025)	18.45 (25.01)
4G80S6 (EA)-3	0.040 (1.02)	226.29 (1007)	0.943 (6.50)	180.92 (804.8)	235.67 (1048)	0.008 (0.20)	91.96 (495.4)	1.173 (29.8)	227.54 (1012)	20.21 (27.40)
Mean	0.050 (1.28)	230.96 (1027)	0.962 (6.64)	158.37 (704.5)	205.61 (914.6)	0.013 (0.32)	109.92 (489.0)	1.097 (27.9)	201.00 (894.1)	16.86 (22.86)
Median	0.040 (1.02)	226.29 (1007)	0.943 (6.50)	174.99 (778.4)	232.89 (1036)	0.013 (0.33)	107.90 (635.4)	1.094 (27.8)	227.54 (1012)	18.45 (25.01)
STDEV	0.020 (0.50)	8.796 (39.13)	0.037 (0.25)	34.05 (151.5)	49.67 (221.0)	0.005 (0.12)	19.05 (84.74)	0.075 (1.91)	48.40 (215.3)	4.363 (5.916)
COV	39%	4%	4%	22%	24%	38%	17%	7%	24%	26%

Table 6.5: Summary of averages of each specimen group analyzing influence of interface preparation.

Spec	Δ_{ult}, in. (mm)	V_{ult}, kip (kN)	σ_{ult}, ksi (MPa)	$V_{sus,min}$, kip (kN)	$V_{sus,max}$, kip (kN)	Δ_{cr}, in. (mm)	V_{cr}, kip (kN)	Δ_{b}, in. (mm)	V_b, kip (kN)	E_b, kip-ft (kJ)
4G80S6 (AC)	0.066 (1.67)	262.65 (1168)	1.094 (7.55)	131.33 (584.2)	154.52 (687.3)	0.019 (0.49)	142.83 (635.4)	0.919 (23.4)	149.63 (665.6)	11.74 (15.92)
4G80S6 (1/8)	0.073 (1.86)	238.70 (1062)	0.995 (6.86)	129.01 (573.9)	153.62 (683.4)	0.016 (0.40)	109.44 (486.8)	1.018 (25.9)	148.87 (662.2)	12.61 (17.10)
4G80S6 (1/4)	0.045 (1.14)	217.90 (969.3)	0.908 (6.26)	126.58 (563.1)	155.83 (693.2)	0.013 (0.32)	111.37 (495.4)	0.943 (23.9)	153.56 (683.1)	11.35 (15.39)
4G80S6 (EA)	0.050 (1.28)	230.96 (1027)	0.962 (6.64)	158.37 (704.5)	205.61 (914.6)	0.013 (0.32)	109.92 (489.0)	1.097 (27.9)	201.00 (894.1)	16.86 (22.86)

6.2.1.2 Reinforcing Steel U-bar size: #5 (#16M)

Figure 6.5 to Figure 6.6 present the interface shear force versus interface shear displacement response curves for specimen groups 5G80S6(AC), 5G80S6(1/8), 5G80S6(1/4), and 5G80S6(EA), respectively. Table 6.6 to Table 6.9 present tabulated values for the main points of interest regarding the mentioned specimen groups. Discussions regarding Figure 6.5 to Figure 6.8 and Table 6.6 to Table 6.9 are presented in Section 5.4.1.

Table 6.10 compares values of the main points of interest for specimen groups 5G80S6(AC), 5G80S6(1/8), 5G80S6(1/4), and 5G80S6(EA). As it can be inferred from the table, specimen group 5G80S6(1/4) reaches a significantly larger peak load, V_{ult}, at 302.54 kip (1345.7 kN). Values of V_{ult} for specimen groups 5G80S6(AC),

5G80S6(1/8), and 5G80S6(EA) are 259.87 kip (1156.0 kN), 259.52 kip (1154.4 kN), and 248.29 kip (11 kN), respectively. These results suggest that an interface roughness of 1/4 in. (6.35 mm) significantly increased the interface shear capacity compared to the other three types of interface preparation. It is worth noting that in test specimens constructed with #4 (#13M) reinforcing steel bars, specimens with an interface roughness of 1/4 in. (6.35 mm) reached the lowest peak load compared to the specimens with the three other surface preparations. In test specimens constructed with #5 (#16M) reinforcing steel bars, specimens with an interface roughness of 1/4 in. (6.35 mm) reached the largest peak load when compared to the specimens with the three other surface preparations. This indicates that the process of roughening the interface causes significant variability in test results. It is also worth noting that increasing reinforcing steel U-bar size from #4 (#13M) to #5 (#16M) increased V_{ult} in all cases of interface preparation, with the exception of As Cast interface preparation.

During the post-peak stage of the force-displacement response, specimen groups 5G80S6(AC), 5G80S6(1/8), and 5G80S6(1/4) present similar average sustained loads at first bar fracture, V_b, ranging from 217.39 kip (967.00 kN) to 227.31 kip (1011.1 kN). Specimen group 5G80S6(EA) presented significantly lower V_b with 171.83 kip (764.34 kN).

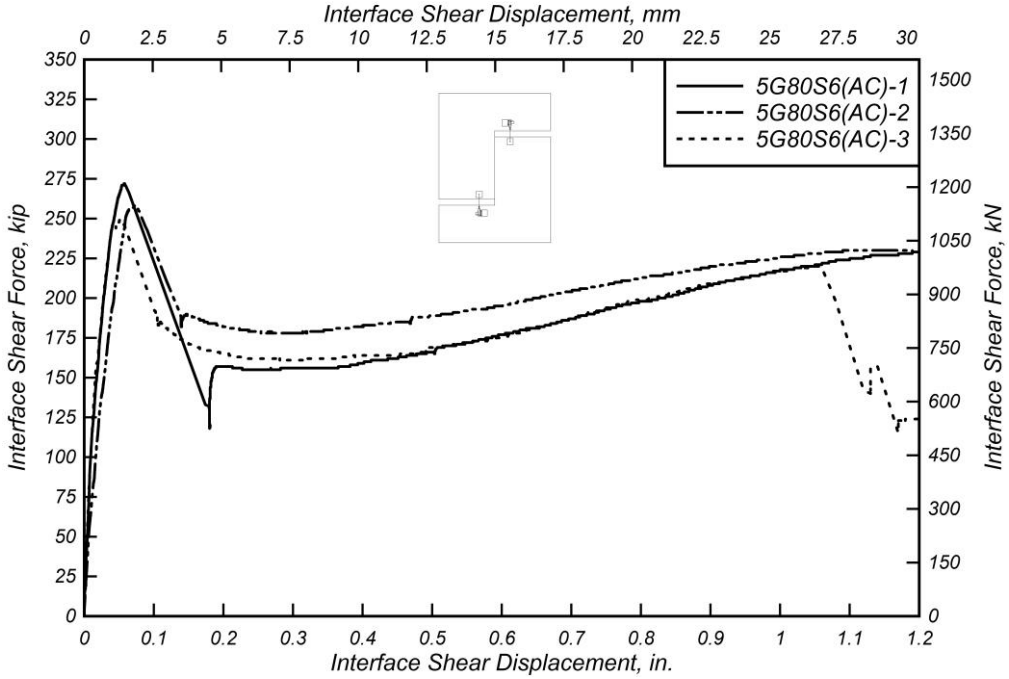

Figure 6.5: Interface shear force versus interface shear displacement for 5G80S6(AC) specimens (As Cast).

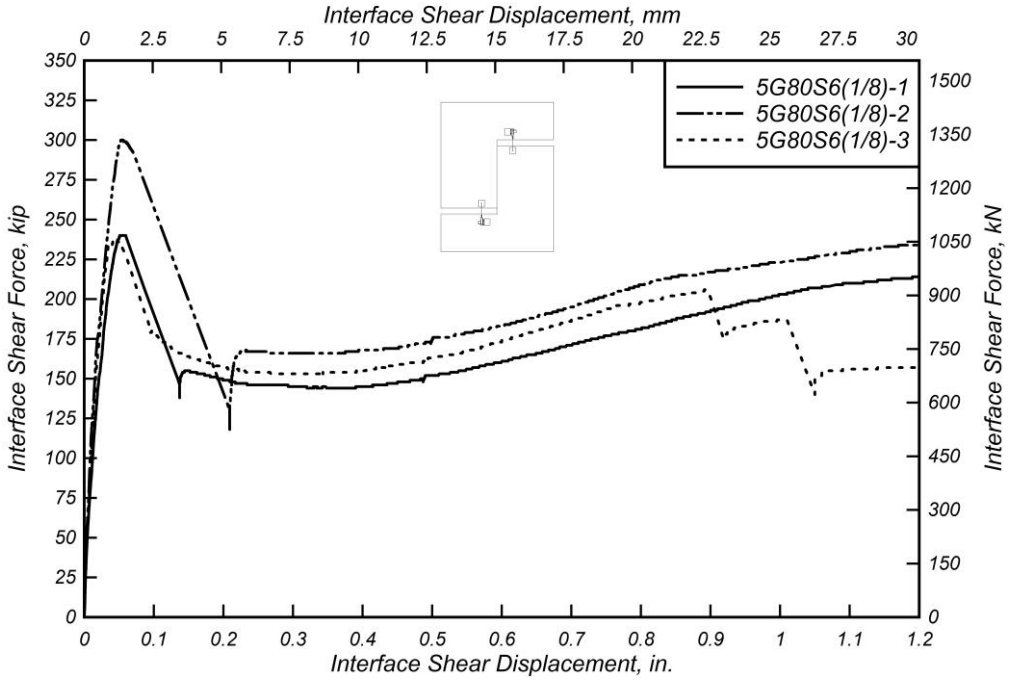

Figure 6.6: Interface shear force versus interface shear displacement the 5G80S6(1/8) specimens (1/8 in. (3.175 mm)).

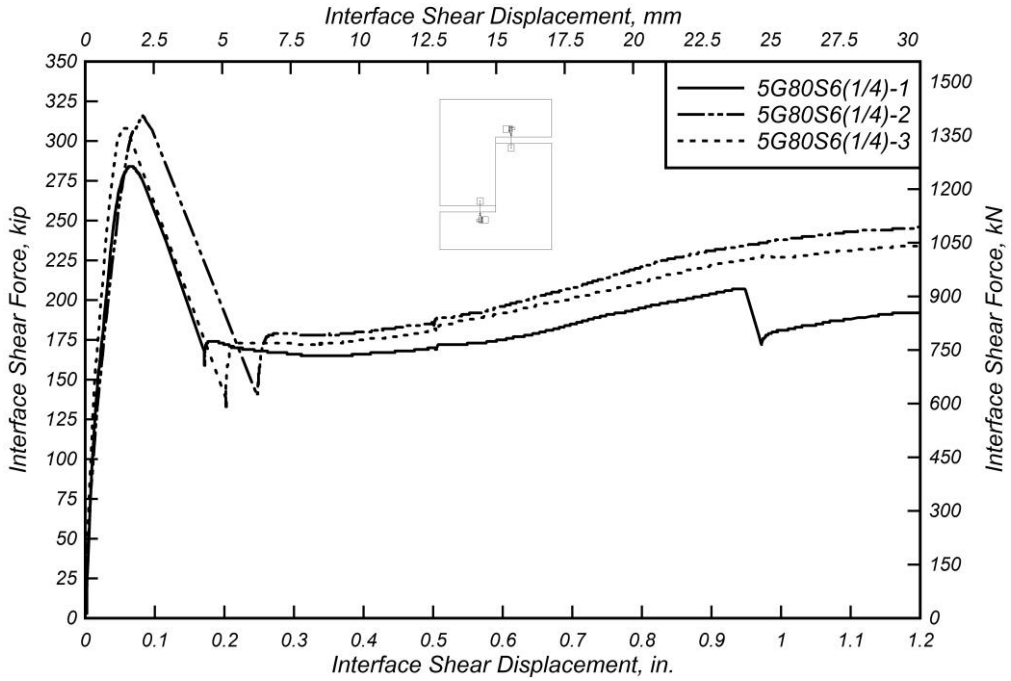

Figure 6.7: Interface shear force versus interface shear displacement for 5G80S6(1/4) specimens (1/4 in. (6.35 mm)).

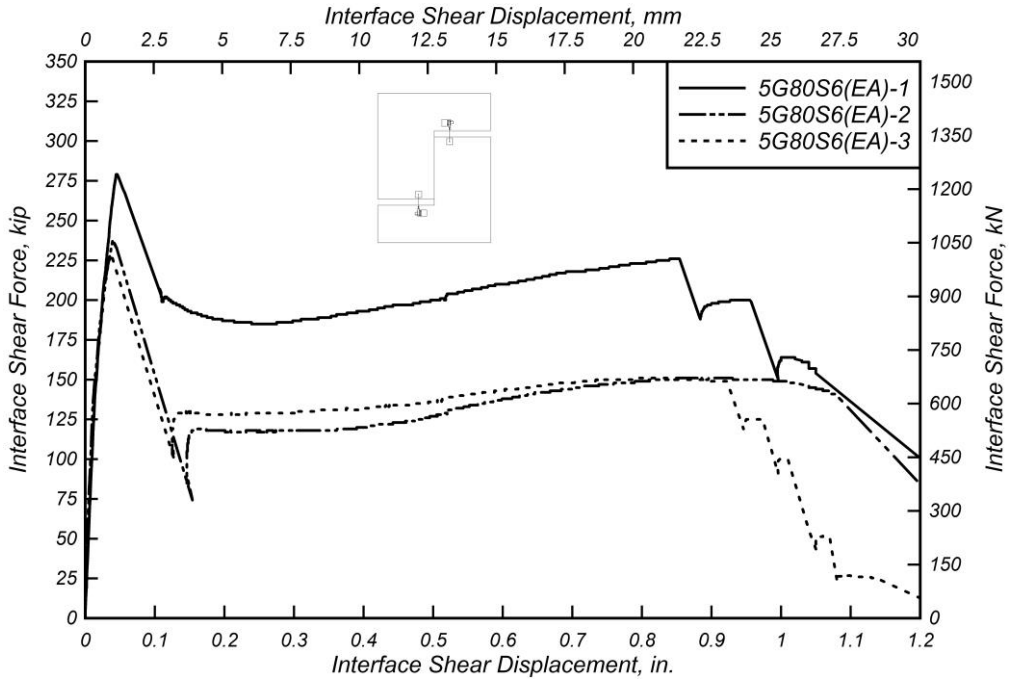

Figure 6.8: Interface shear force versus interface shear displacement for 5G80S6(EA) specimens (Exposed Aggregate).

Table 6.6: Specimen 5G80S6(AC) shear test results.

Spec	Δ_{ult}, in. (mm)	V_{ult}, kip (kN)	σ_{ult}, ksi (MPa)	$V_{sus,min}$, kip (kN)	$V_{sus,max}$, kip (kN)	Δ_{cr}, in. (mm)	V_{cr}, kip (kN)	Δ_{b}, in. (mm)	V_b, kip (kN)	E_b, kip-ft (kJ)
5G80S6 (AC)-1	0.058 (1.47)	271.63 (1208)	1.132 (7.80)	155.04 (689.7)	232.39 (1034)	0.010 (0.26)	108.00 (480.4)	1.456 (37.0)	225.46 (1003)	23.88 (32.38)
5G80S6 (AC)-2	0.071 (1.80)	257.72 (1146)	1.074 (7.40)	177.97 (791.7)	230.47 (1025)	0.020 (0.50)	116.50 (518.2)	1.215 (30.9)	228.09 (1015)	20.59 (27.92)
5G80S6 (AC)-3	0.052 (1.32)	250.26 (1113)	1.043 (7.19)	161.17 (716.9)	219.77 (977.6)	0.017 (0.43)	158.10 (703.3)	1.055 (26.8)	219.56 (976.7)	16.30 (22.10)
Mean	0.060 (1.53)	259.87 (1156)	1.083 (7.47)	164.73 (732.7)	227.54 (1012)	0.016 (0.40)	127.53 (567.3)	1.242 (31.6)	224.37 (998.1)	20.26 (27.47)
Median	0.058 (1.47)	257.72 (1146)	1.074 (7.40)	161.17 (716.9)	230.47 (1025)	0.017 (0.43)	116.50 (518.2)	1.215 (30.9)	225.46 (1003)	20.59 (27.92)
STDEV	0.010 (0.25)	10.85 (48.25)	0.045 (0.31)	11.87 (52.81)	6.800 (30.25)	0.005 (0.13)	26.81 (119.3)	0.202 (5.13)	4.368 (19.43)	3.803 (5.157)
COV	16%	4%	4%	7%	3%	31%	21%	16%	2%	19%

Table 6.7: Specimen 5G80S6(1/8) shear test results.

Spec	Δ_{ult}, in. (mm)	V_{ult}, kip (kN)	σ_{ult}, ksi (MPa)	$V_{sus,min}$, kip (kN)	$V_{sus,max}$, kip (kN)	Δ_{cr}, in. (mm)	V_{cr}, kip (kN)	Δ_{b}, in. (mm)	V_b, kip (kN)	E_b, kip-ft (kJ)
5G80S6 (1/8)-1	0.053 (1.35)	240.38 (1069)	1.002 (6.91)	144.04 (640.7)	221.13 (983.6)	0.021 (0.54)	151.70 (674.8)	1.385 (35.2)	220.63 (981.4)	20.82 (28.23)
5G80S6 (1/8)-2	0.054 (1.37)	300.13 (1335)	1.251 (8.62)	165.55 (736.4)	234.51 (1043)	0.018 (0.46)	171.60 (763.3)	1.315 (33.4)	225.72 (1004)	22.29 (30.22)
5G80S6 (1/8)-3	0.044 (1.12)	238.06 (1059)	0.992 (6.84)	152.81 (679.7)	205.95 (916.1)	0.017 (0.43)	155.30 (690.8)	0.895 (22.7)	205.82 (915.5)	12.96 (17.57)
Mean	0.050 (1.28)	259.52 (1154)	1.081 (7.46)	154.13 (685.6)	220.53 (981.0)	0.019 (0.48)	159.53 (709.6)	1.198 (30.4)	217.39 (967.0)	18.69 (25.34)
Median	0.053 (1.35)	240.38 (1069)	1.002 (6.91)	152.81 (679.7)	221.13 (983.6)	0.018 (0.46)	155.30 (690.8)	1.315 (33.4)	220.63 (981.4)	20.82 (28.23)
STDEV	0.006 (0.14)	35.19 (156.5)	0.147 (1.01)	10.82 (48.11)	14.29 (63.56)	0.002 (0.06)	10.60 (47.17)	0.265 (6.73)	10.34 (45.99)	5.019 (6.805)
COV	11%	14%	14%	7%	6%	12%	7%	22%	5%	27%

Table 6.8: Specimen 5G80S6(1/4) shear test results.

Spec	Δ_{ult}, in. (mm)	V_{ult}, kip (kN)	σ_{ult}, ksi (MPa)	$V_{sus,min}$, kip (kN)	$V_{sus,max}$, kip (kN)	Δ_{cr}, in. (mm)	V_{cr}, kip (kN)	Δ_{b}, in. (mm)	V_b, kip (kN)	E_b, kip-ft (kJ)
5G80S6 (1/4)-1	0.064 (1.63)	283.85 (1263)	1.183 (8.15)	164.97 (733.8)	207.40 (922.6)	0.018 (0.47)	152.60 (678.8)	0.948 (24.1)	206.76 (919.7)	14.71 (19.94)
5G80S6 (1/4)-2	0.083 (2.11)	315.53 (1404)	1.315 (9.07)	177.92 (791.4)	246.02 (1094)	0.014 (0.35)	112.80 (501.8)	1.289 (32.7)	245.51 (1092)	23.18 (31.43)
5G80S6 (1/4)-3	0.054 (1.37)	308.23 (1371)	1.284 (8.86)	171.56 (763.1)	235.51 (1048)	0.012 (0.31)	138.90 (617.9)	1.359 (34.5)	229.67 (1022)	23.57 (31.95)
Mean	0.067 (1.70)	302.54 (1346)	1.261 (8.69)	171.48 (762.8)	229.64 (1022)	0.015 (0.37)	134.77 (599.5)	1.199 (30.5)	227.31 (1011)	20.48 (27.77)
Median	0.064 (1.63)	308.23 (1371)	1.284 (8.86)	171.56 (763.1)	235.51 (1048)	0.014 (0.35)	138.90 (617.9)	1.289 (32.7)	229.67 (1022)	23.18 (31.43)
STDEV	0.015 (0.37)	16.59 (73.79)	0.069 (0.48)	6.475 (28.80)	19.97 (88.82)	0.003 (0.08)	20.22 (89.94)	0.220 (5.59)	19.48 (86.66)	5.008 (6.790)
COV	22%	5%	5%	4%	9%	22%	15%	18%	9%	24%

Table 6.9: Specimen 5G80S6(EA) shear test results.

Spec	Δ_{ult}, in. (mm)	V_{ult}, kip (kN)	σ_{ult}, ksi (MPa)	$V_{sus,min}$, kip (kN)	$V_{sus,max}$, kip (kN)	Δ_{cr}, in. (mm)	V_{cr}, kip (kN)	Δ_{b}, in. (mm)	V_b, kip (kN)	E_b, kip-ft (kJ)
5G80S6 (EA)-1	0.045 (1.14)	279.43 (1243)	1.164 (8.03)	185.15 (823.6)	226.21 (1006)	0.012 (0.30)	120.50 (567.3)	0.854 (21.7)	226.26 (1007)	14.52 (19.69)
5G80S6 (EA)-2	0.040 (1.02)	236.33 (1051)	0.985 (6.79)	117.23 (521.5)	150.66 (670.2)	0.013 (0.34)	148.60 (709.6)	1.076 (27.3)	140.96 (627.0)	12.49 (16.93)
5G80S6 (EA)-3	0.037 (0.94)	229.12 (1019)	0.955 (6.58)	128.03 (569.5)	151.17 (672.4)	0.011 (0.27)	126.20 (599.5)	0.923 (23.4)	148.27 (659.5)	10.95 (14.85)
Mean	0.041 (1.03)	248.29 (1105)	1.035 (7.13)	143.47 (638.2)	176.01 (783.0)	0.012 (0.30)	131.77 (625.5)	0.951 (24.2)	171.83 (764.3)	12.65 (17.16)
Median	0.040 (1.02)	236.33 (1051)	0.985 (6.79)	128.03 (569.5)	151.17 (672.4)	0.012 (0.30)	126.20 (599.5)	0.923 (23.4)	148.27 (659.5)	12.49 (16.93)
STDEV	0.004 (0.10)	27.21 (121.0)	0.113 (0.78)	36.50 (162.4)	43.47 (193.4)	0.001 (0.03)	14.85 (74.65)	0.114 (2.89)	47.28 (210.3)	1.790 (2.427)
COV	10%	11%	11%	25%	25%	11%	11%	12%	28%	14%

Table 6.10: Summary of averages of specimen groups analyzing influence of interface preparation.

Spec	Δ_{ult}, in. (mm)	V_{ult}, kip (kN)	σ_{ult}, ksi (MPa)	$V_{sus,min}$, kip (kN)	$V_{sus,max}$, kip (kN)	Δ_{cr}, in. (mm)	V_{cr}, kip (kN)	Δ_{b}, in. (mm)	V_b, kip (kN)	E_b, kip-ft (kJ)
5G80S6 (AC)	0.060 (1.53)	259.87 (1156)	1.083 (7.47)	164.73 (732.7)	227.54 (1012)	0.016 (0.40)	127.53 (567.3)	1.242 (31.6)	224.37 (998.1)	20.26 (27.47)
5G80S6 (1/8)	0.050 (1.28)	259.52 (1154)	1.081 (7.46)	154.13 (685.6)	220.53 (981.0)	0.019 (0.48)	159.53 (709.6)	1.198 (30.4)	217.39 (967.0)	18.69 (25.34)
5G80S6 (1/4)	0.067 (1.70)	302.54 (1346)	1.261 (8.69)	171.48 (762.8)	229.64 (1022)	0.015 (0.37)	134.77 (599.5)	1.199 (30.5)	227.31 (1011)	20.48 (27.77)
5G80S6 (EA)	0.041 (1.03)	248.29 (1105)	1.035 (7.13)	143.47 (638.2)	176.01 (783.0)	0.012 (0.30)	131.77 (625.5)	0.951 (24.2)	171.83 (764.3)	12.65 (17.16)

6.2.2 Interface Shear Force versus Strain

6.2.2.1 Reinforcing Steel U-bar Size: #4 (#13M)

Figure 6.9 to Figure 6.12 present the interface shear force versus reinforcing steel U-bar strain relationship for specimen groups 4G80S6(AC), 4G80S6(1/8), 4G80S6(1/4), and 4G80S6(EA), respectively. The curves shown correspond to the average strain measurements from all strain gauges contained in each test specimen plotted versus the interface shear force. Table 6.11 to Table 6.14 present tabulated values for the main points of interest regarding the mentioned specimen groups. As it can be observed in these tables, several strain gauges were damaged before the peak load was reached, thus limiting the analysis that can be carried out with the strain gauges data. Additionally, significant variability was observed in the strain gauge

measurements with COV values ranging from 7% to 59%. Discussions regarding Figure 6.9 to Figure 6.12 and Table 6.11 to Table 6.14 are presented in Section 5.4.2.

Table 6.15 shows a comparison of the average interface shear strain for specimen groups 4G80S6(AC), 4G80S6(1/8), 4G80S6(1/4), and 4G80S6(EA). It can be inferred from this table that specimen group 4G80S6(EA) reaches its peak load at a significantly lower strain value compared to the other specimen groups. This behavior is consistent with results discussed in Section 6.2.1 and Section 6.2.3, as the Exposed Aggregate interface preparation appears to reduce the interface shear displacement and crack width at peak load. Note that for specimens discussed in this section, the reinforcing steel strain only surpasses the nominal yield strain of 2760 microstrain after the peak interface shear load is reached.

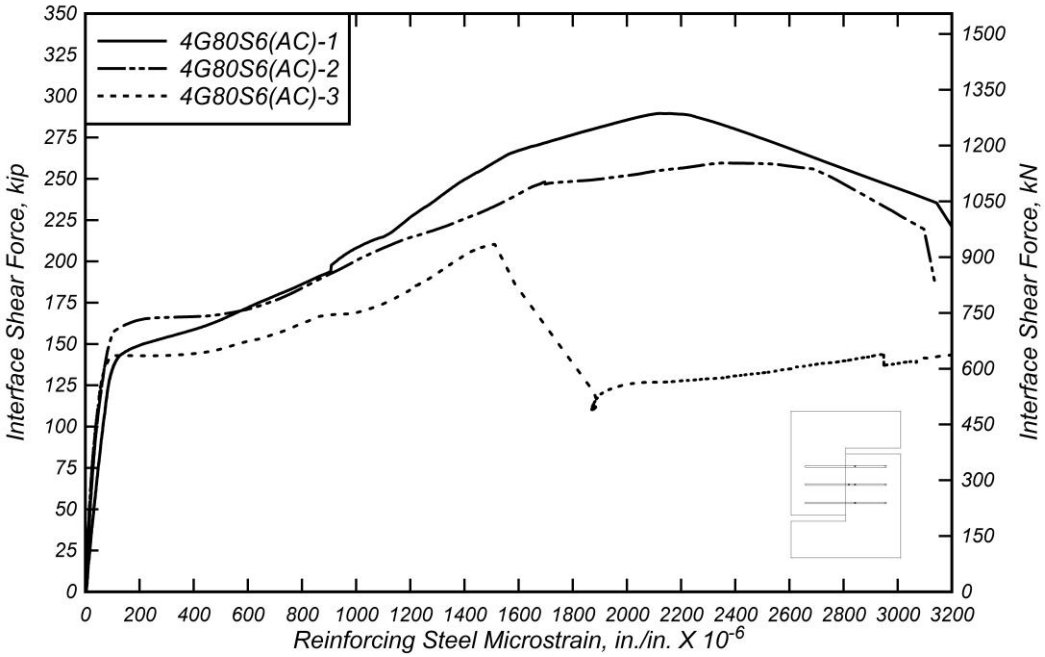

Figure 6.9: Interface shear force versus average reinforcing steel microstrain for 4G80S6(AC) specimens (As Cast).

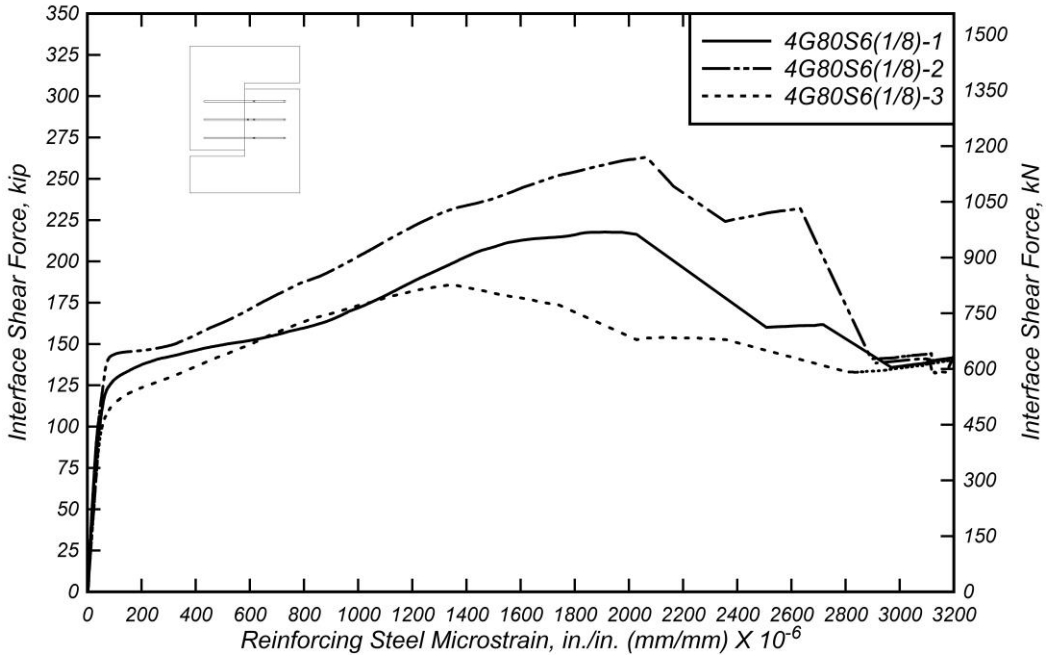

Figure 6.10: Interface shear force versus average reinforcing steel microstrain for 4G80S6(1/8) specimens (1/8 in. (3.175 mm)).

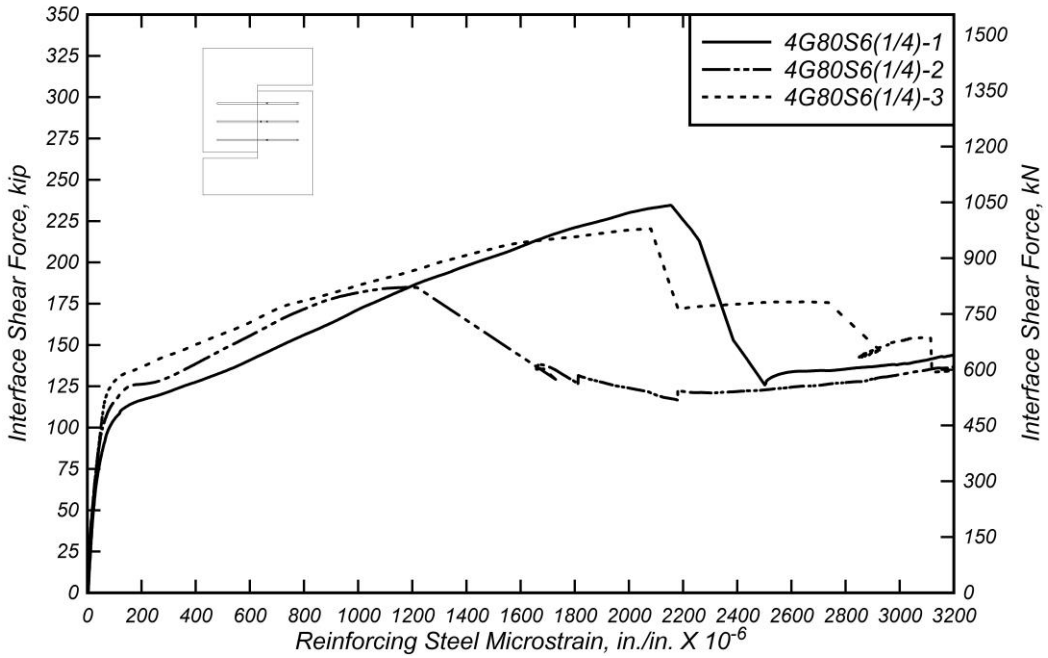

Figure 6.11: Interface shear force versus average reinforcing steel microstrain for 4G80S6(1/4) specimens (1/4 in. (6.35 mm)).

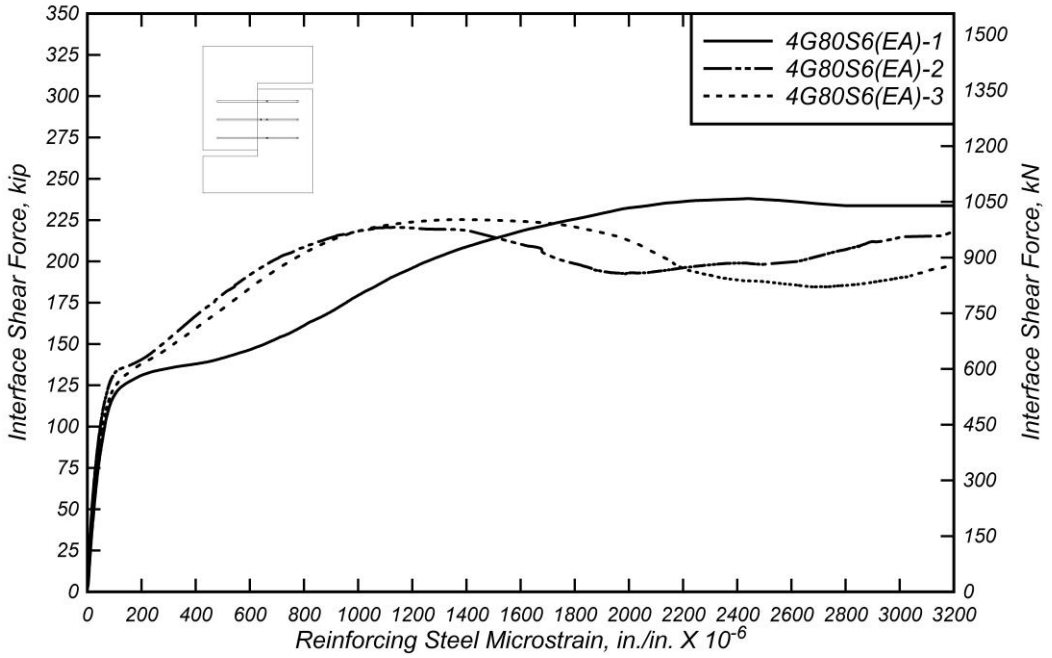

Figure 6.12: Interface shear force versus average reinforcing steel microstrain for 4G80S6(EA) specimens (Exposed Aggregate).

Table 6.11: Specimen 4G80S6(AC) strain gauge readings at peak interface shear force.

Specimen	s_1, in./in. (mm/mm)	s_2, in./in. (mm/mm)	s_3, in./in. (mm/mm)	s_4, in./in. (mm/mm)	s_5, in./in. (mm/mm)	s_6, in./in. (mm/mm)	s_7, in./in. (mm/mm)
4G80S6(AC)-1	-	-	-	0.0027	-	0.0023	0.0017
4G80S6(AC)-2	0.0027	0.0023	-	-	0.0031	-	0.0017
4G80S6(AC)-3	-	-	0.0018	0.0025	0.0015	-	0.0015
Mean	0.0027	0.0023	0.0018	0.0026	0.0023	0.0023	0.0016
Median	0.0027	0.0023	0.0018	0.0026	0.0023	0.0023	0.0017
STDEV	-	-	-	0.0002	0.0011	-	0.0001
COV	-	-	-	7%	47%	-	9%

Table 6.12: Specimen 4G80S6(1/8) strain gauge readings at peak interface shear force.

Specimen	s_1, in./in. (mm/mm)	s_2, in./in. (mm/mm)	s_3, in./in. (mm/mm)	s_4, in./in. (mm/mm)	s_5, in./in. (mm/mm)	s_6, in./in. (mm/mm)	s_7, in./in. (mm/mm)
4G80S6(1/8)-1	-	-	0.0019	-	0.0025	0.0018	-
4G80S6(1/8)-2	-	-	-	-	0.0030	0.0025	0.0017
4G80S6(1/8)-3	-	0.0022	-	0.0026	-	0.0018	0.0012
Mean	-	0.0022	0.0019	0.0026	0.0028	0.0021	0.0015
Median	-	0.0022	0.0019	0.0026	0.0028	0.0018	0.0015
STDEV	-	-	-	-	0.0004	0.0004	0.0004
COV	-	-	-	-	13%	19%	26%

Table 6.13: Specimen 4G80S6(1/4) strain gauge readings at peak interface shear force.

Specimen	s_1, in./in. (mm/mm)	s_2, in./in. (mm/mm)	s_3, in./in. (mm/mm)	s_4, in./in. (mm/mm)	s_5, in./in. (mm/mm)	s_6, in./in. (mm/mm)	s_7, in./in. (mm/mm)
4G80S6(1/4)-1	0.0026	-	-	0.0026	0.0024	0.0021	-
4G80S6(1/4)-2	0.0011	-	-	-	0.0012	0.0014	-
4G80S6(1/4)-3	-	0.0021	-	-	0.0025	0.0016	0.0013
Mean	0.0018	0.0021	-	0.0026	0.0020	0.0017	0.0013
Median	0.0018	0.0021	-	0.0026	0.0024	0.0016	0.0013
STDEV	0.0010	-	-	-	0.0007	0.0004	-
COV	55%	-	-	-	36%	21%	-

Table 6.14: Specimen 4G80S6(EA) strain gauge readings at peak interface shear force.

Specimen	s_1, in./in. (mm/mm)	s_2, in./in. (mm/mm)	s_3, in./in. (mm/mm)	s_4, in./in. (mm/mm)	s_5, in./in. (mm/mm)	s_6, in./in. (mm/mm)	s_7, in./in. (mm/mm)
4G80S6(EA)-1	0.0016	0.0025	0.0024	0.0023	0.0017	0.0024	0.0028
4G80S6(EA)-2	-	0.0012	0.0011	0.0018	-	0.0015	0.0009
4G80S6(EA)-3	0.0014	0.0016	0.0013	0.0019	0.0011	0.0013	0.0013
Mean	0.0015	0.0018	0.0016	0.0020	0.0014	0.0017	0.0017
Median	0.0015	0.0016	0.0013	0.0019	0.0014	0.0015	0.0013
STDEV	0.0001	0.0006	0.0007	0.0003	0.0004	0.0006	0.0010
COV	9%	37%	44%	14%	33%	35%	59%

Table 6.15: Summary of average strain gauge readings of each specimen group analyzing influence of interface preparation.

Specimen	s_1, in./in. (mm/mm)	s_2, in./in. (mm/mm)	s_3, in./in. (mm/mm)	s_4, in./in. (mm/mm)	s_5, in./in. (mm/mm)	s_6, in./in. (mm/mm)	s_7, in./in. (mm/mm)
4G80S6(AC)	0.0027	0.0023	0.0018	0.0026	0.0023	0.0023	0.0016
4G80S6(1/8)	-	0.0022	0.0019	0.0026	0.0028	0.0021	0.0015
4G80S6(1/4)	0.0018	0.0021	-	0.0026	0.0020	0.0017	0.0013
4G80S6(EA)	0.0015	0.0018	0.0016	0.0020	0.0014	0.0017	0.0017

6.2.2.2 Reinforcing Steel U-bar Size: #5 (#16M)

Figure 6.13 to Figure 6.16 present the interface shear force versus reinforcing steel U-bar strain relationship for specimen groups 5G80S6(AC), 5G80S6(1/8), 5G80S6(1/4), and 5G80S6(EA), respectively. The curves shown correspond to the average strain measurements from all strain gauges contained in each test specimen plotted versus the interface shear force. Table 6.16 to Table 6.19 present tabulated values for the

main points of interest regarding the mentioned specimen groups. As it can be observed in these tables, several strain gauges were damaged before the peak load was reached, thus limiting the analysis that can be carried out with the strain gauges data. Additionally, significant variability was observed in the strain gauge measurements with COV values ranging from 3% to 37%. Discussions regarding Figure 6.13 to Figure 6.16 and Table 6.16 to Table 6.19 are presented in Section 5.4.2.

Table 6.20 shows a comparison of strain gauge measurements at peak load for specimen groups 5G80S6(AC), 5G80S6(1/8), 5G80S6(1/4), and 5G80S6(EA). From this table it can be observed that all specimen groups displayed similar average strain values at peak load Note that for specimens discussed in this section, the reinforcing steel strain only surpasses the nominal yield strain of 2760 microstrain after the peak interface shear load is reached.

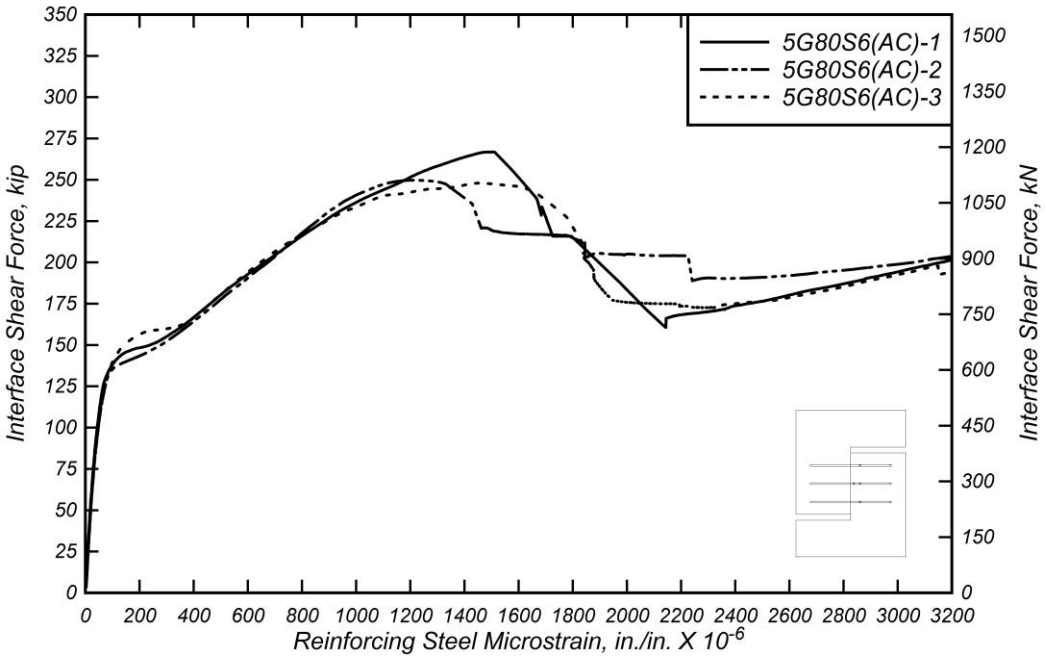

Figure 6.13: Interface shear force versus average reinforcing steel microstrain for 5G80S6(AC) specimens (As Cast).

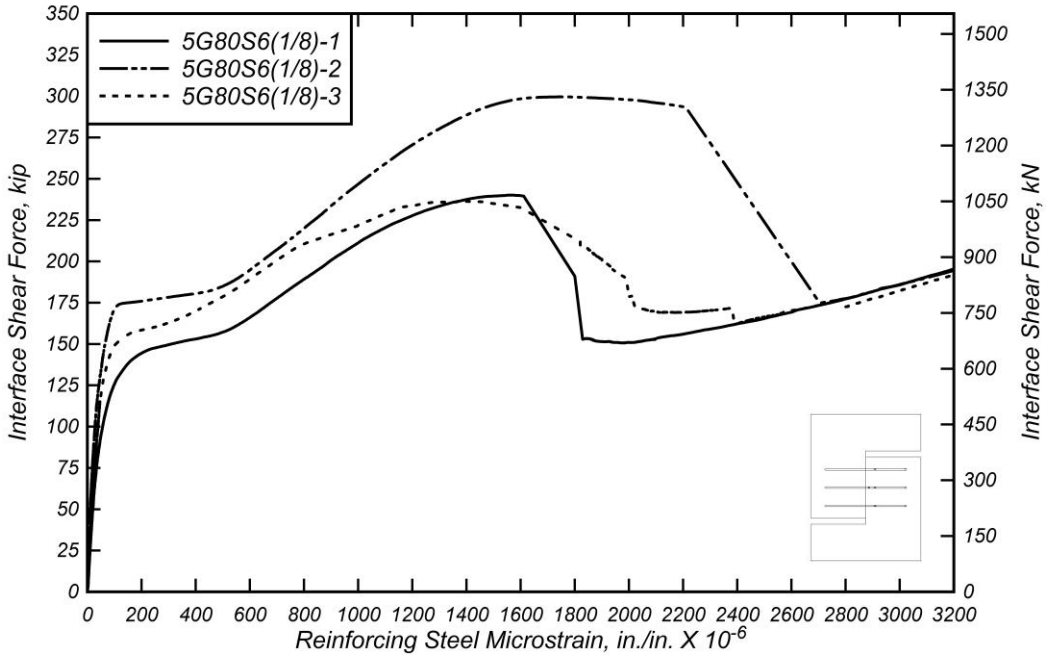

Figure 6.14: Interface shear force versus average reinforcing steel microstrain for 5G80S6(1/8) specimens (1/8 in. (3.175 mm)).

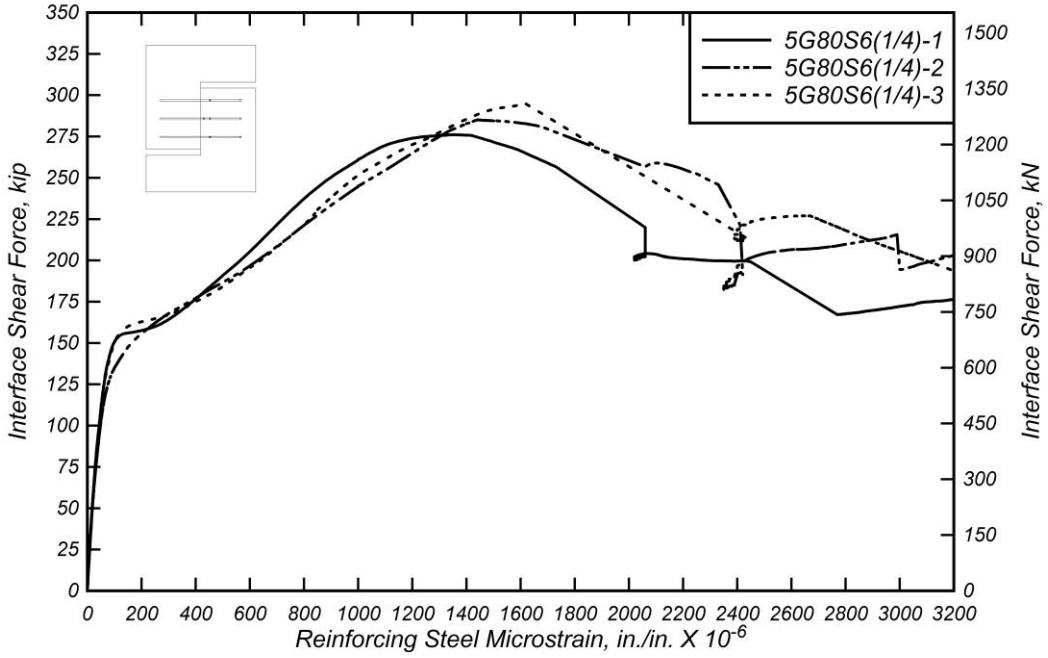

Figure 6.15: Interface shear force versus average reinforcing steel microstrain for 5G80S6(1/4) specimens (1/4 in. (6.35 mm)).

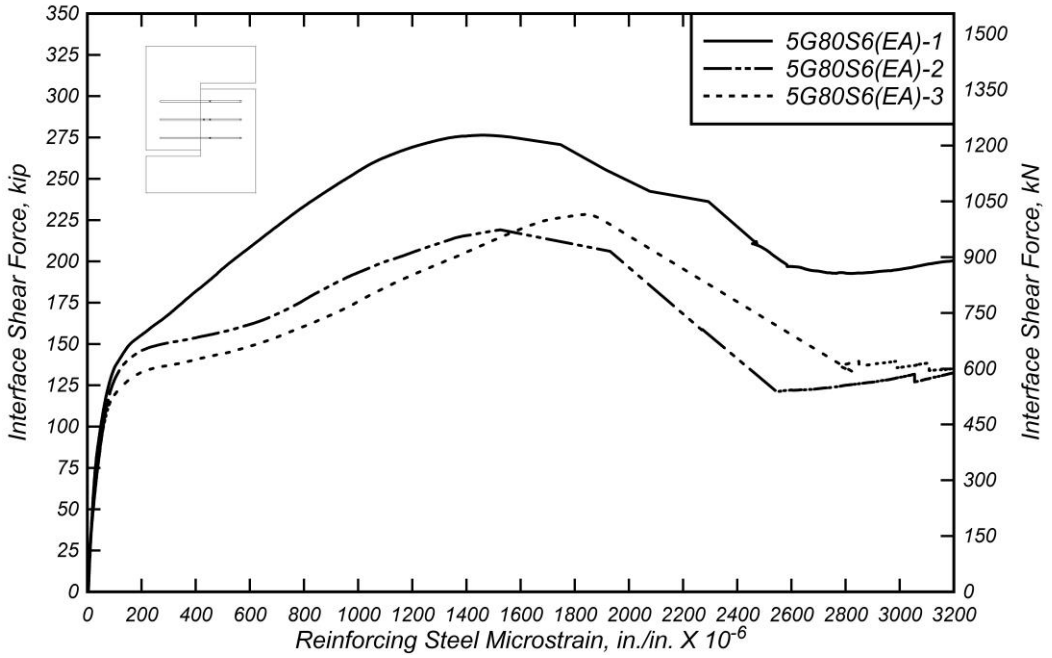

Figure 6.16: Interface shear force versus average reinforcing steel microstrain for 5G80S6(EA) specimens (Exposed Aggregate).

Table 6.16: Specimen 5G80S6(AC) strain gauge readings at peak interface shear force.

Specimen	s_1, in./in. (mm/mm)	s_2, in./in. (mm/mm)	s_3, in./in. (mm/mm)	s_4, in./in. (mm/mm)	s_5, in./in. (mm/mm)	s_6, in./in. (mm/mm)	s_7, in./in. (mm/mm)
5G80S6(AC)-1	0.0017	0.0015	-	0.0021	0.0014	0.0016	0.0018
5G80S6(AC)-2	0.0011	-	0.0018	-	0.0011	0.0014	-
5G80S6(AC)-3	0.0016	0.0016	-	0.0023	0.0014	0.0014	0.0015
Mean	0.0015	0.0016	0.0018	0.0022	0.0013	0.0015	0.0016
Median	0.0016	0.0016	0.0018	0.0022	0.0014	0.0014	0.0016
STDEV	0.00031	5.12E-05	-	0.00011	0.00021	9.29E-05	0.00020
COV	21%	3%	-	5%	16%	6%	13%

Table 6.17: Specimen 5G80S6(1/8) strain gauge readings at peak interface shear force.

Specimen	s_1, in./in. (mm/mm)	s_2, in./in. (mm/mm)	s_3, in./in. (mm/mm)	s_4, in./in. (mm/mm)	s_5, in./in. (mm/mm)	s_6, in./in. (mm/mm)	s_7, in./in. (mm/mm)
5G80S6(1/8)-1	0.0013	0.0016	0.0015	-	-	0.0015	0.0011
5G80S6(1/8)-2	0.0012	-	0.0016	-	-	-	0.0018
5G80S6(1/8)-3	0.0012	0.0013	-	0.0016	-	0.0015	-
Mean	0.0012	0.0015	0.0015	-	-	0.0015	0.0014
Median	0.0012	0.0015	0.0015	-	-	0.0015	0.0014
STDEV	7.7E-05	1.7E-04	7.1E-05	-	-	1.9E-05	4.8E-04
COV	9%	12%	5%	-	-	1%	34%

Table 6.18: Specimen 5G80S6(1/4) strain gauge readings at peak interface shear force.

Specimen	s_1, in./in. (mm/mm)	s_2, in./in. (mm/mm)	s_3, in./in. (mm/mm)	s_4, in./in. (mm/mm)	s_5, in./in. (mm/mm)	s_6, in./in. (mm/mm)	s_7, in./in. (mm/mm)
5G80S6(1/4)-1	0.0014	0.0011	-	0.0018	0.0012	0.0019	-
5G80S6(1/4)-2	0.0022	0.0024	0.0020	0.0020	0.0013	0.0018	0.0022
5G80S6(1/4)-3	0.0012	0.0017	-	-	0.0022	-	-
Mean	0.0016	0.0017	0.0020	0.0019	0.0016	0.0018	0.0022
Median	0.0014	0.0017	0.0020	0.0019	0.0013	0.0018	0.0022
STDEV	0.00053	0.00063	-	0.00019	0.00058	5.55E-05	-
COV	33%	36%	-	10%	37%	3%	-

Table 6.19: Specimen 5G80S6(EA) strain gauge readings at peak interface shear force.

Specimen	s_1, in./in. (mm/mm)	s_2, in./in. (mm/mm)	s_3, in./in. (mm/mm)	s_4, in./in. (mm/mm)	s_5, in./in. (mm/mm)	s_6, in./in. (mm/mm)	s_7, in./in. (mm/mm)
5G80S6(EA)-1	0.0014	-	0.0011	0.0018	0.0015	0.0015	-
5G80S6(EA)-2	0.0017	0.0021	-	0.0025	0.0014	0.0024	0.0021
5G80S6(EA)-3	0.0013	0.0019	0.0019	0.0026	0.0017	0.0019	0.0018
Mean	0.0015	0.0020	0.0015	0.0023	0.0015	0.0019	0.0020
Median	0.0014	0.0020	0.0015	0.0025	0.0015	0.0019	0.0020
STDEV	0.0002	0.0001	0.0006	0.0005	0.0002	0.0004	0.0002
COV	14%	7%	37%	21%	11%	24%	11%

Table 6.20: Summary of average strain gauge readings of each specimen group analyzing influence of interface preparation.

Specimen	s_1, in./in. (mm/mm)	s_2, in./in. (mm/mm)	s_3, in./in. (mm/mm)	s_4, in./in. (mm/mm)	s_5, in./in. (mm/mm)	s_6, in./in. (mm/mm)	s_7, in./in. (mm/mm)
5G80S6(AC)	0.0015	0.0016	0.0018	0.0022	0.0013	0.0015	0.0016
5G80S6(1/8)	0.0012	0.0015	0.0015	-	-	0.0015	0.0014
5G80S6(1/4)	0.0016	0.0017	0.0020	0.0019	0.0016	0.0018	0.0022
5G80S6(EA)	0.0015	0.0020	0.0015	0.0023	0.0015	0.0019	0.0020

6.2.3 Interface Shear Force versus Crack Width

6.2.3.1 Reinforcing Steel U-bar Size: #4 (#13M)

Figure 6.17 to Figure 6.20 present the interface shear force versus crack width response for specimen groups 4G80S6(AC), 4G80S6(1/8), 4G80S6(1/4), and 4G80S6(EA). Each figure shows the force-crack width response for all specimens in each group. Tabulated values of points of interest are presented in Table 6.21 to Table

6.24. Discussion regarding Figure 6.17 to Figure 6.20, and Table 6.21 to Table 6.24 are presented in Section 5.4.3.

Table 6.25 presents a comparison of the average crack width values for specimen groups 4G80S6(AC), 4G80S6(1/8), 4G80S6(1/4), and 4G80S6(EA). From the table it can be inferred that specimen groups 4G80S6(AC) and 4G80S6(1/8) reach similar average crack width at peak load, although, specimens with an As Cast interface preparation reached peak loads slightly larger than specimens with 1/8 in. (3.175 mm) interface preparation. Specimen group 4G80S6(1/4) shows smaller average crack width at peak load, but for significantly lower peak load values. Specimens with an Exposed Aggregate interface preparation show the lowest average crack width at peak load compared to the other specimen groups. These results are consistent with the discussion presented in Section 6.2.2.1 where it was observed that specimen group 4G80S6(EA) showed lower strain values compared to the other specimen groups. The smaller crack width at peak load reached by specimen group 4G80S6(EA) is beneficial and therefore additional testing to get further insight into the behavior of an Exposed Aggregate interface preparation is recommended.

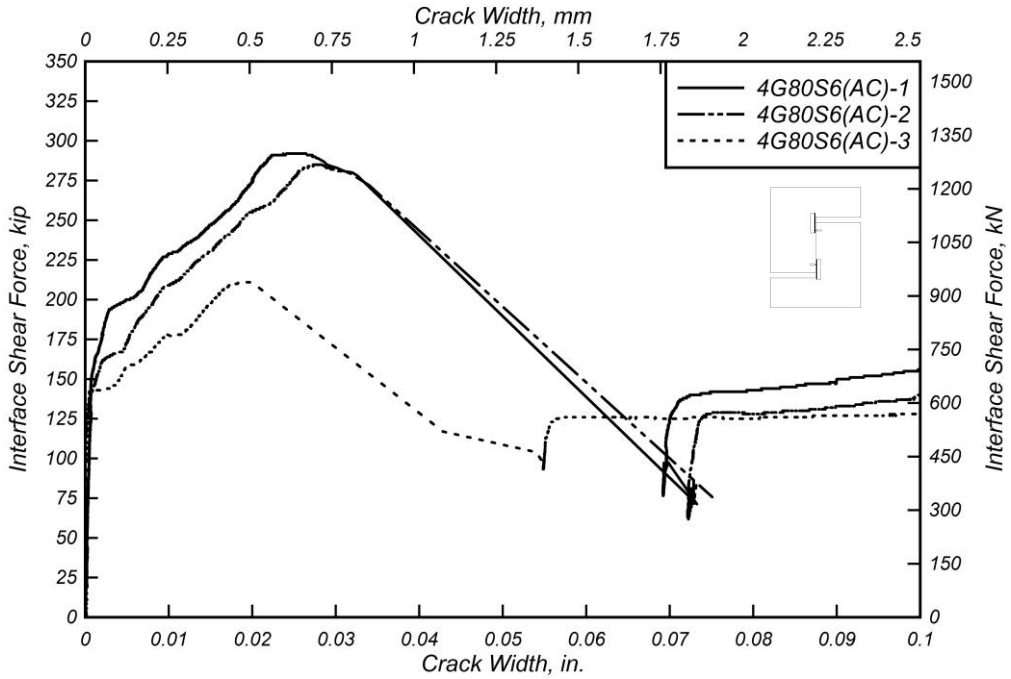

Figure 6.17: Interface shear force versus crack width for 4G80S6(AC) specimens (As Cast).

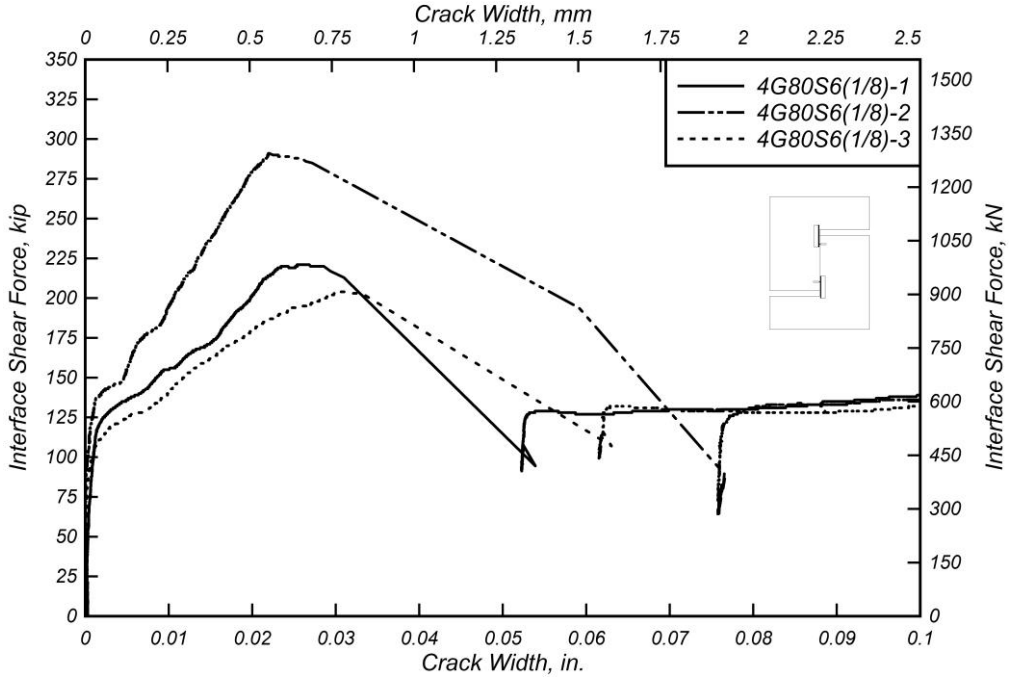

Figure 6.18: Interface shear force versus crack width for 4G80S6(1/8) specimens (1/8 in. (3.175 mm)).

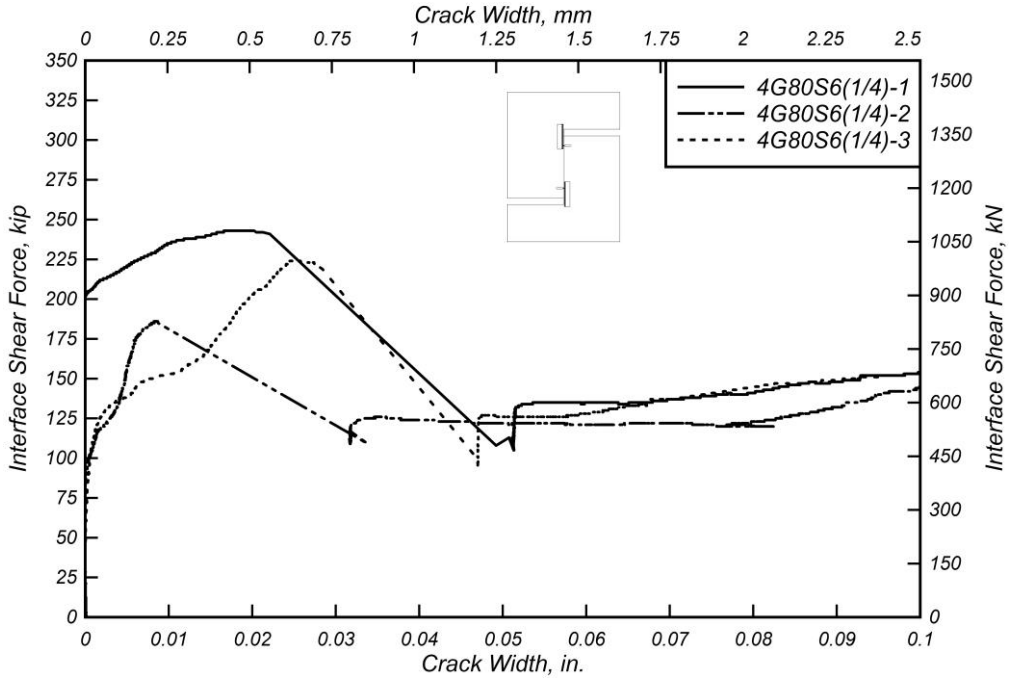

Figure 6.19: Interface shear force versus crack width for 4G80S6(1/4) specimens (1/4 in. (6.35 mm)).

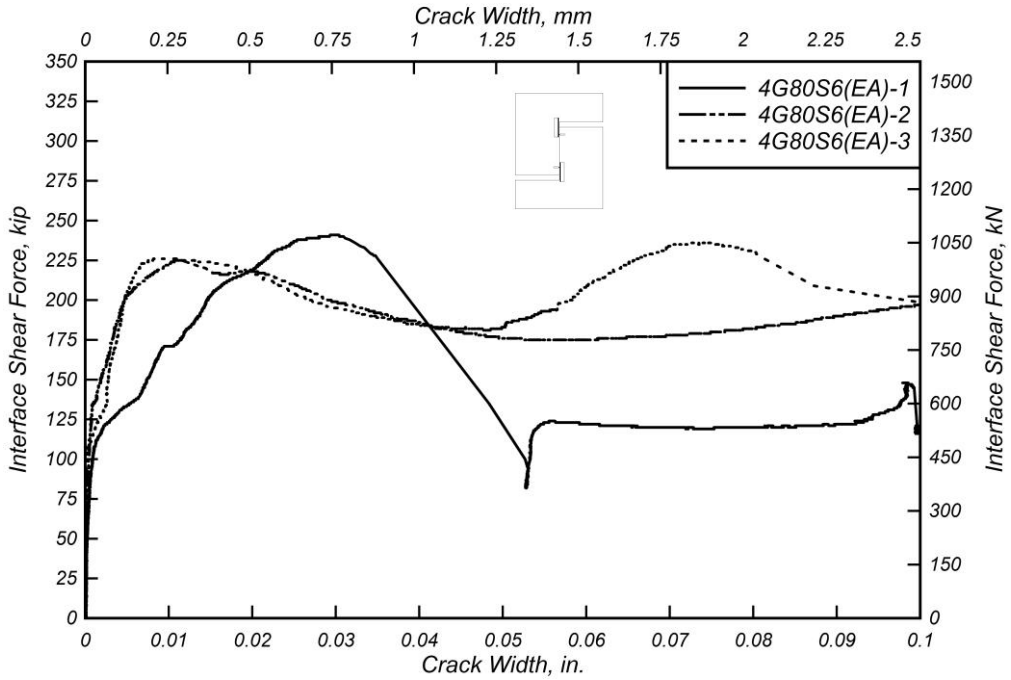

Figure 6.20: Interface shear force versus crack width for 4G80S6(EA) specimens (Exposed Aggregate).

Table 6.21: Specimen 4G80S6(AC) crack width measurements.

Specimen	w_{ult}, in. (mm)	V_{ult}, kip (kN)	w_b, in. (mm)	V_b, kip (kN)
4G80S6(AC)-1	0.0260 (0.6603)	292.03 (1299.0)	0.1239 (3.147)	150.66 (670.18)
4G80S6(AC)-2	0.0279 (0.7084)	284.98 (1267.7)	0.1372 (3.485)	152.78 (679.61)
4G80S6(AC)-3	0.0193 (0.4896)	210.93 (938.25)	0.2245 (5.702)	145.46 (647.04)
Mean	0.0244 (0.6194)	262.64 (1168.3)	0.1619 (4.112)	149.64 (665.61)
Median	0.0260 (0.6603)	284.98 (1267.7)	0.1372 (3.485)	150.66 (670.18)
STDEV	0.0045 (0.1150)	44.93 (199.85)	0.0546 (1.388)	3.767 (16.76)
COV	19%	17%	34%	3%

Table 6.22: Specimen 4G80S6(1/8) crack width measurements.

Specimen	w_{ult}, in. (mm)	V_{ult}, kip (kN)	w_b, in. (mm)	V_b, kip (kN)
4G80S6(1/8)-1	0.0256 (0.6510)	221.21 (983.98)	0.1732 (4.398)	145.00 (645.01)
4G80S6(1/8)-2	0.0327 (0.8314)	290.99 (1294.4)	0.2602 (6.610)	150.57 (669.77)
4G80S6(1/8)-3	0.0306 (0.7771)	203.91 (907.04)	0.1782 (4.526)	151.03 (671.81)
Mean	0.0297 (0.7532)	238.70 (1061.8)	0.2039 (5.178)	148.87 (662.20)
Median	0.0306 (0.7771)	221.21 (983.98)	0.1782 (4.526)	150.57 (669.77)
STDEV	0.0036 (0.0926)	46.10 (205.07)	0.0489 (1.242)	3.354 (14.92)
COV	12%	19%	24%	2%

Table 6.23: Specimen 4G80S6(1/4) crack width measurements.

Specimen	w_{ult}, in. (mm)	V_{ult}, kip (kN)	w_b, in. (mm)	V_b, kip (kN)
4G80S6(1/4)-1	0.0188 (0.4767)	243.07 (1081.2)	0.1163 (2.955)	154.52 (687.35)
4G80S6(1/4)-2	0.0084 (0.2146)	186.03 (827.52)	0.1163 (2.953)	154.86 (688.84)
4G80S6(1/4)-3	0.0249 (0.6313)	224.61 (999.11)	0.1131 (2.874)	151.30 (673.03)
Mean	0.0174 (0.4409)	217.90 (969.28)	0.1152 (2.927)	153.56 (683.07)
Median	0.0188 (0.4767)	224.61 (999.11)	0.1163 (2.953)	154.52 (687.35)
STDEV	0.0083 (0.2106)	29.10 (129.45)	0.0018 (0.046)	1.962 (8.728)
COV	48%	13%	2%	1%

Table 6.24: Specimen 4G80S6(EA) crack width measurements.

Specimen	w_{ult}, in. (mm)	V_{ult}, kip (kN)	w_b, in. (mm)	V_b, kip (kN)
4G80S6(EA)-1	0.0300 (0.7625)	241.11 (1072.5)	0.0993 (2.522)	145.13 (645.55)
4G80S6(EA)-2	0.0114 (0.2905)	225.49 (1003.0)	0.1432 (3.637)	230.33 (1024.6)
4G80S6(EA)-3	0.0093 (0.2371)	226.29 (1006.6)	0.0806 (2.048)	227.54 (1012.1)
Mean	0.0169 (0.4300)	230.96 (1027.4)	0.1077 (2.736)	201.00 (894.08)
Median	0.0114 (0.2905)	226.29 (1006.6)	0.0993 (2.522)	227.54 (1012.1)
STDEV	0.0114 (0.2829)	8.798 (39.13)	0.0321 (0.8158)	48.41 (215.30)
COV	67%	4%	30%	24%

Table 6.25: Summary of crack width measurements for As Cast, 1/8 in. (3.175 mm), 1/4 in. (6.35 mm), and Exposed Aggregate specimens.

Specimen	w_{ult}, in. (mm)	V_{ult}, kip (kN)	w_b, in. (mm)	V_b, kip (kN)
4G80S6(AC)	0.0244 (0.6194)	262.64 (1168.3)	0.1619 (4.112)	149.64 (665.61)
4G80S6(1/8)	0.0297 (0.7532)	238.70 (1061.8)	0.2039 (5.178)	148.87 (662.20)
4G80S6(1/4)	0.0174 (0.4409)	217.90 (969.28)	0.1152 (2.927)	153.56 (683.07)
4G80S6(EA)	0.0169 (0.4300)	230.96 (1027.4)	0.1077 (2.736)	201.00 (894.08)

6.2.3.2 Reinforcing Steel U-bar Size: #5 (#16M)

Figure 6.21 to Figure 6.24 present the interface shear force versus crack width response for specimen groups 5G80S6(AC), 5G80S6(1/8), 5G80S6(1/4), and 5G80S6(EA). Each figure shows the force-crack width response for all specimens in each group. Tabulated values of points of interest such as crack width at peak load and crack width at first bar fracture for each specimen group are presented in Table 6.26 to Table 6.29. Discussion regarding Figure 6.21 to Figure 6.24, and Table 6.26 to Table 6.29 are presented in Section 5.4.3.

Table 6.30 presents a comparison of the average crack width values for specimen groups 5G80S6(AC), 5G80S6(1/8), 5G80S6(1/4), and 5G80S6(EA). From the table it can be inferred that specimen group 5G80S6(1/8) reached the lowest average crack width, w_{ult}, at 0.0150 in. (0.3808 mm) with a corresponding peak load of 259.52 kip (1154.4 kN). Specimen groups 5G80S6(EA) reached a similar value of w_{ult} with 0.0154 in. (0.3924 mm) with a corresponding peak load of 248.39 kip (1104.9 kN), therefore showing similar post-crack stiffness as specimen group 5G80S6(1/8). Additionally, specimen group 5G80S6(1/4) reached larger w_{ult} with a corresponding larger average peak load, thus displaying similar stiffness as specimen groups 5G80S6(1/8) and 5G80S6(EA).

It is important to note that for specimens with an interface preparation of 1/8 in. (3.175 mm) and Exposed Aggregate, the average crack width at peak load decreased when increasing the size of reinforcing steel bars crossing the interface from #4 (#13M) to #5 (#16M). Specimens with an As Cast and 1/4 in. (6.35 mm) interface

preparation increased average crack width when increasing reinforcing steel bar size from #4 (#13M) to #5 (#16M).

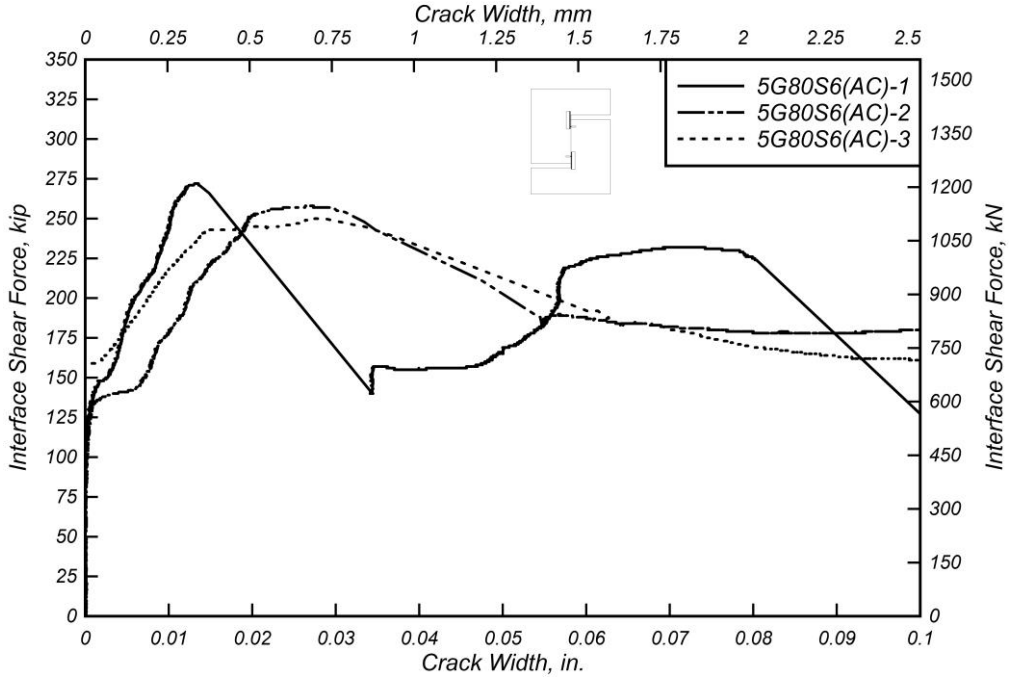

Figure 6.21: Interface shear force versus crack width for 5G80S6(AC) specimens (As Cast).

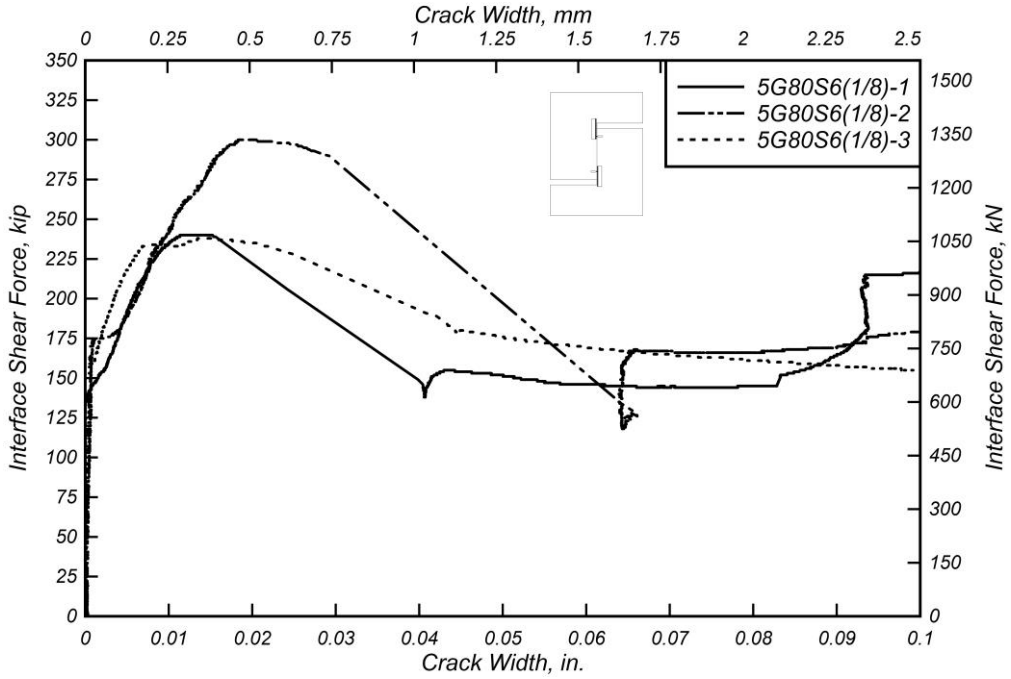

Figure 6.22: Interface shear force versus crack width for 5G80S6(1/8) specimens (1/8 in. (3.175 mm)).

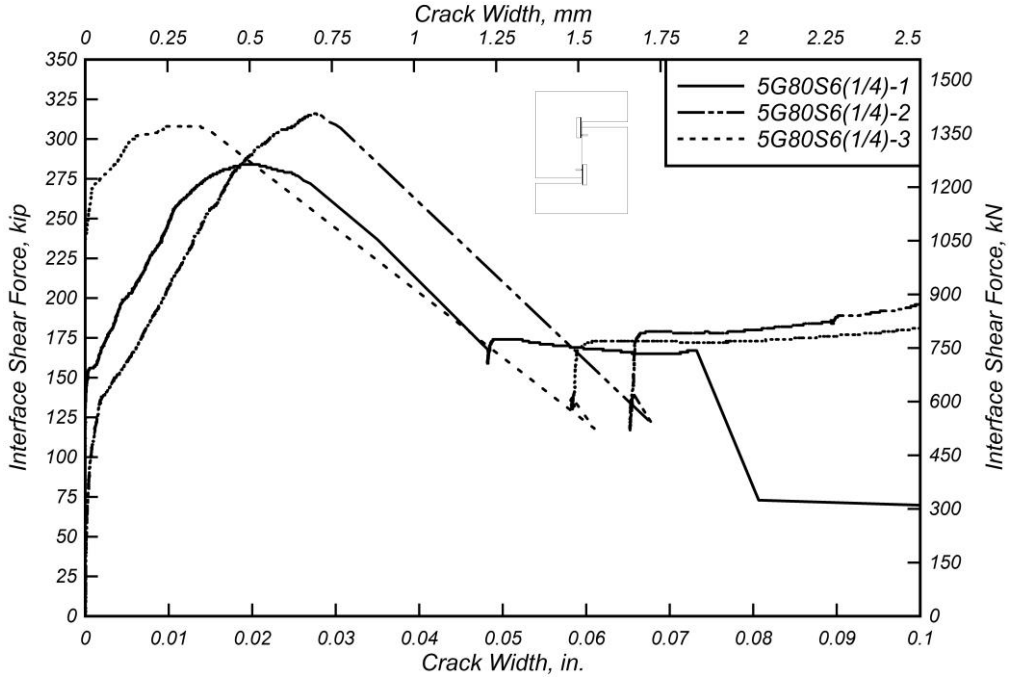

Figure 6.23: Interface shear force versus crack width for 5G80S6(1/4) specimens (1/4 in. (6.35 mm)).

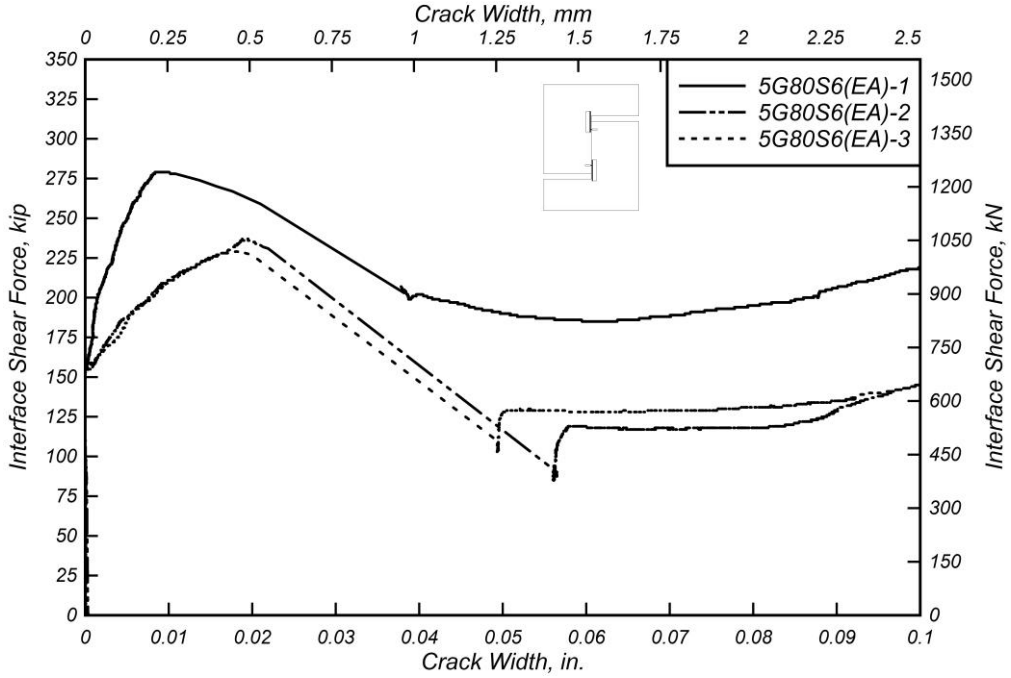

Figure 6.24: Interface shear force versus crack width for 5G80S6(EA) specimens (Exposed Aggregate).

Table 6.26: Specimen 5G80S6(AC) crack width measurements.

Specimen	w_{ult}, in. (mm)	V_{ult}, kip (kN)	w_b, in. (mm)	V_b, kip (kN)
5G80S6(AC)-1	0.0134 (0.3401)	271.63 (1208.3)	0.0800 (2.032)	225.46 (1002.9)
5G80S6(AC)-2	0.0267 (0.6786)	257.72 (1146.4)	0.1728 (4.388)	228.09 (1014.6)
5G80S6(AC)-3	0.0276 (0.7012)	250.26 (1113.2)	0.1615 (4.103)	219.56 (976.65)
Mean	0.0272 (0.6899)	253.99 (1129.8)	0.1671 (4.245)	223.82 (995.62)
Median	0.0272 (0.6899)	253.99 (1129.8)	0.1671 (4.245)	223.82 (995.62)
STDEV	0.0006 (0.0160)	5.274 (23.46)	0.0079 (0.2016)	6.029 (26.82)
COV	2%	2%	5%	3%

Table 6.27: Specimen 5G80S6(1/8) crack width measurements.

Specimen	w_{ult}, in. (mm)	V_{ult}, kip (kN)	w_b, in. (mm)	V_b, kip (kN)
5G80S6(1/8)-1	0.0123 (0.3117)	240.38 (1069.3)	0.1160 (2.947)	220.63 (981.40)
5G80S6(1/8)-2	0.0186 (0.4720)	300.13 (1335.0)	0.1755 (4.459)	225.72 (1004.1)
5G80S6(1/8)-3	0.0141 (0.3586)	238.06 (1059.0)	0.2171 (5.514)	205.82 (915.52)
Mean	0.0150 (0.3808)	259.52 (1154.4)	0.1696 (4.307)	217.39 (967.00)
Median	0.0141 (0.3586)	240.38 (1069.3)	0.1755 (4.459)	220.63 (981.40)
STDEV	0.0032 (0.0824)	35.18 (156.50)	0.0508 (1.291)	10.34 (46.00)
COV	22%	14%	30%	5%

Table 6.28: Specimen 5G80S6(1/4) crack width measurements.

Specimen	w_{ult}, in. (mm)	V_{ult}, kip (kN)	w_b, in. (mm)	V_b, kip (kN)
5G80S6(1/4)-1	0.0194 (0.4928)	283.85 (1262.6)	0.0672 (1.707)	206.76 (919.73)
5G80S6(1/4)-2	0.0275 (0.6985)	315.53 (1403.6)	0.1367 (3.472)	245.51 (1092.1)
5G80S6(1/4)-3	0.0100 (0.2533)	308.23 (1371.1)	0.1762 (4.477)	229.67 (1021.6)
Mean	0.0190 (0.4815)	302.54 (1345.7)	0.1267 (3.219)	227.31 (1011.1)
Median	0.0194 (0.4928)	308.23 (1371.1)	0.1367 (3.472)	229.67 (1021.6)
STDEV	0.0088 (0.2228)	16.59 (73.79)	0.0552 (1.402)	19.48 (86.65)
COV	46%	5%	44%	9%

Table 6.29: Specimen 5G80S6(EA) crack width measurements.

Specimen	w_{ult}, in. (mm)	V_{ult}, kip (kN)	w_b, in. (mm)	V_b, kip (kN)
5G80S6(EA)-1	0.0090 (0.2290)	279.43 (1243.0)	0.1053 (2.675)	226.26 (1006.4)
5G80S6(EA)-2	0.0193 (0.4897)	236.63 (1052.6)	0.1200 (3.047)	140.96 (627.03)
5G80S6(EA)-3	0.0180 (0.4584)	229.12 (1019.2)	0.1259 (3.197)	148.27 (659.53)
Mean	0.0154 (0.3924)	248.39 (1104.9)	0.1170 (2.973)	171.83 (764.33)
Median	0.0180 (0.4584)	236.63 (1052.6)	0.1200 (3.047)	148.27 (659.53)
STDEV	0.0056 (0.1423)	27.14 (120.71)	0.0106 (0.2688)	47.28 (210.30)
COV	36%	11%	9%	28%

Table 6.30: Summary of crack width measurements for As Cast, 1/8 in. (3.175 mm), 1/4 in. (6.35 mm), and Exposed Aggregate specimens.

Specimen	w_{ult}, in. (mm)	V_{ult}, kip (kN)	w_b, in. (mm)	V_b, kip (kN)
5G80S6(AC)	0.0272 (0.6899)	253.99 (1129.8)	0.1671 (4.245)	223.82 (995.62)
5G80S6(1/8)	0.0150 (0.3808)	259.52 (1154.4)	0.1696 (4.307)	217.39 (967.00)
5G80S6(1/4)	0.0190 (0.4815)	302.54 (1345.7)	0.1267 (3.219)	227.31 (1011.1)
5G80S6(EA)	0.0154 (0.3924)	248.39 (1104.9)	0.1170 (2.973)	171.83 (764.33)

6.3 INFLUENCE OF NOMINAL CONCRETE STRENGTH

This section presents the experimental results and discussion for test specimens built with nominal concrete strength of 3000 psi (20 MPa), 5000 psi (35 MPa), and 6000 psi (40 MPa). All specimens discussed in this section are reinforced with three (3) #4 (#13M) Grade 80 ksi (550 MPa) reinforcing steel U-bars spaced at 6 in. (152.4 mm) with an interface preparation of 1/8 in. (3.175 mm) interface roughness. Details of the specimens such as bar size, bar spacing, and interface preparation can be found in section (e) of Table 3.1, while drawings showing specimen dimensions, as well as location of the reinforcing steel U-bars are presented in Chapter 3.

6.3.1 Interface Shear Force versus Interface Shear Displacement

The interface shear force versus interface shear displacement response for specimen groups 4G80S6F3(1/8), 4G80S6(1/8), and 4G80S6F6(1/8) are presented in Figure 6.25 to Figure 6.27, respectively. Discussions regarding Figure 6.26 and Table 6.32 can be found in Section 5.2.1. The tabulated values of the main points of study are presented in Table 6.31 to Table 6.33. In Figure 6.25 it can be observed that all specimens present similar behavior with the exception of specimen 4G80S6F3(1/8)-1 where the displacement at first bar fracture, Δ_b, was lower compared to the other two specimens in the group. Additionally, specimen group 4G80S6F3(1/8) presented variability in displacement at peak load, Δ_{ult} with values ranging from 0.075 in. (1.905 mm) to 0.125 in. (3.175 mm) with a COV of 25%. The peak loads, V_{ult}, for specimen group 4G80S6F3(1/8) showed small variations ranging from 223.26 kip (993.11 kN) to 229.31 kip (1020.0 kN) with a COV of 1%. Figure 6.27 shows the interface shear force versus interface shear displacement response of specimen group 4G80S6F6(1/8). In this figure it can be observed that all specimens present similar behavior, with the exception of specimen 4G80S6F6(1/8)-1, which reached a slightly lower peak load. Additionally, the first bar fracture in specimen 4G80S6F6(1/8)-2 occurred at a significantly lower displacement value compared to the other two specimens in the group.

Table 6.34 shows the average tabulated values of the main points of interest for specimen groups 4G80S6F3(1/8), 4G80S6(1/8), and 4G80S6F6(1/8). From the table it can be observed that a trend relating peak load and nominal concrete strength appears, as the results show that average peak load is directly proportional nominal concrete strength with V_{ult} values of 226.86 kip (1009.1 kN), 238.70 kip (1061.8 kN), and 260.28 kip (1157.8 kN) for specimen groups 4G80S6F3(1/8), 4G80S6(1/8), and 4G80S6F6(1/8), respectively. The same trend appears regarding interface shear load at the moment when cracking occurs where V_{cr} values are 98.53 kip (438.30 kN), 109.44 kip (486.80 kN), and 133.20 kip (592.50 kN), for specimen groups 4G80S6F3(1/8), 4G80S6(1/8), and 4G80S6F6(1/8), respectively. These results indicate that increasing concrete nominal strength may increase the strength of the concrete-to-concrete cohesion bond created at the shear interface.

Additionally, Table 6.34 also shows a trend regarding average displacement at peak load, where it can be observed that average displacement at peak load is inversely proportional to nominal concrete strength, that is as nominal concrete strength increases, average displacement at peak load decreases.

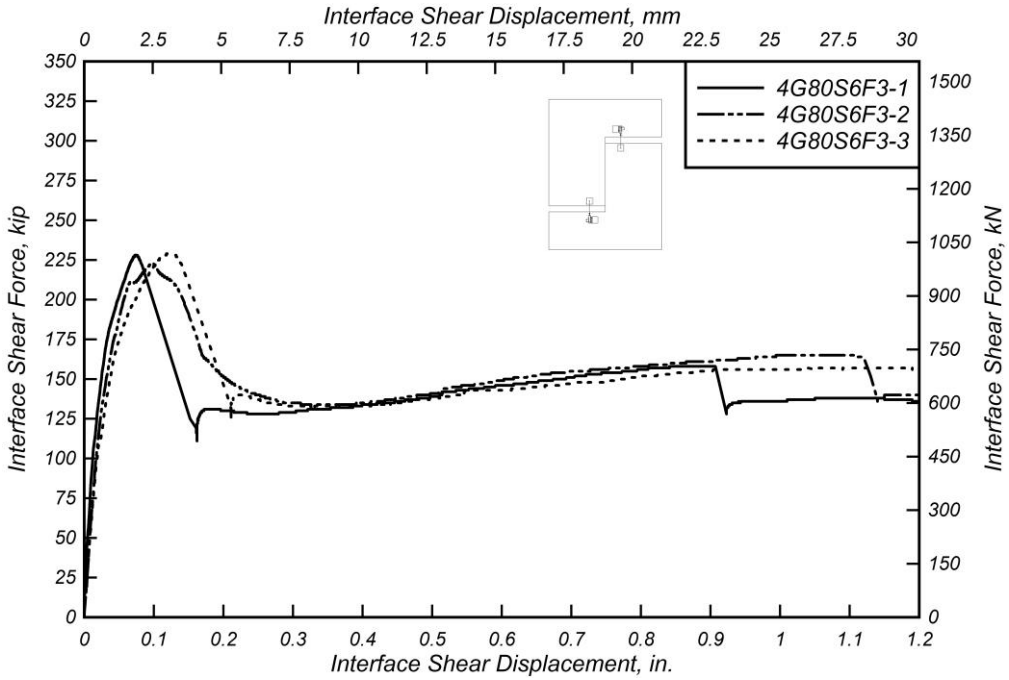

Figure 6.25: Interface shear force versus interface shear displacement for 4G80S6F3(1/8) specimens.

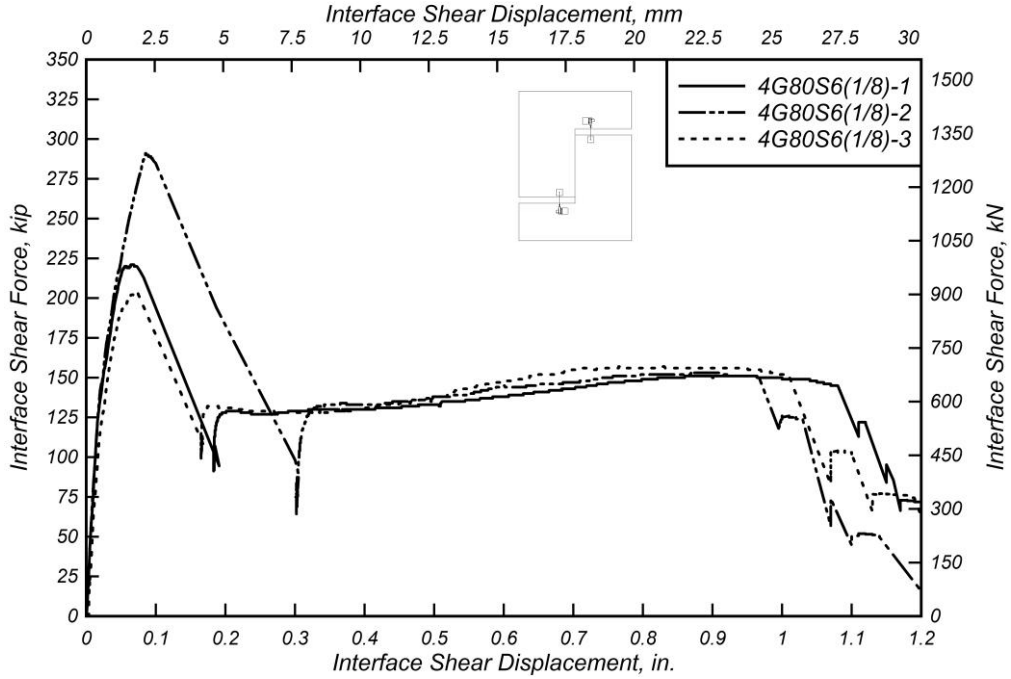

Figure 6.26: Interface shear force versus interface shear displacement the 4G80S6(1/8) specimens.

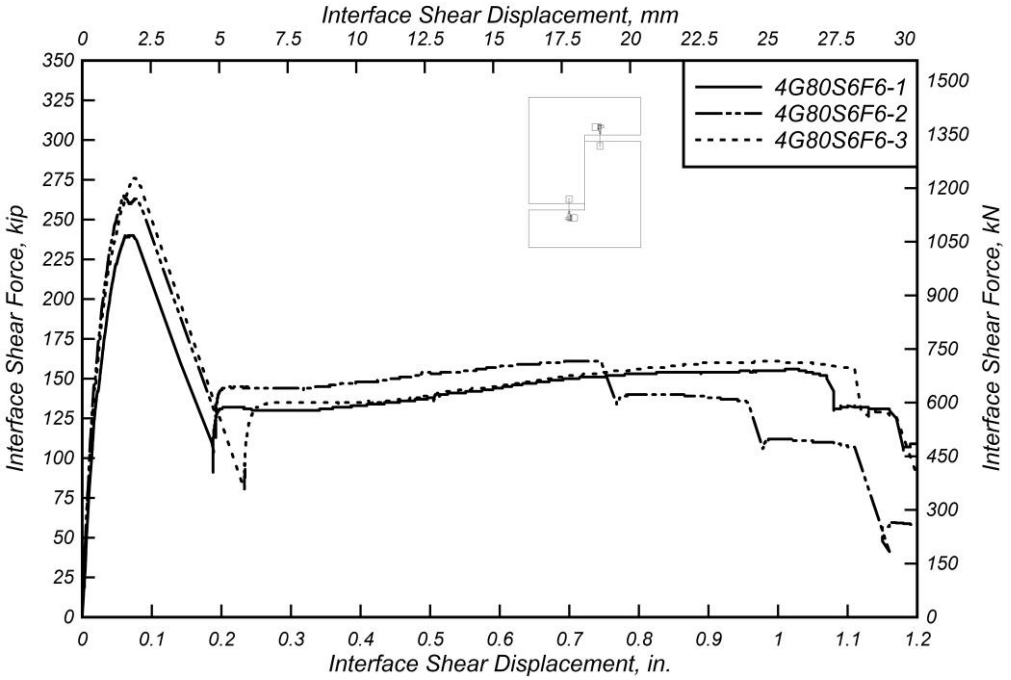

Figure 6.27: Interface shear force versus interface shear displacement for 4G80S6F6(1/8) specimens.

Table 6.31: Specimen 4G80S6F3(1/8) shear test results.

Spec	Δ_{ult}, in. (mm)	V_{ult}, kip (kN)	σ_{ult}, ksi (MPa)	$V_{sus,min}$, kip (kN)	$V_{sus,max}$, kip (kN)	Δ_{cr}, in. (mm)	V_{cr}, kip (kN)	Δ_{b}, in. (mm)	V_b, kip (kN)	E_b, kip-ft (kJ)
4G80S6F3(1/8)-1	0.075 (1.91)	228.01 (1014)	0.950 (6.55)	128.19 (570.2)	158.35 (704.4)	0.013 (0.32)	102.40 (455.5)	0.907 (23.0)	158.03 (703.0)	11.10 (15.05)
4G80S6F3(1/8)-2	0.099 (2.52)	223.26 (993.1)	0.930 (6.41)	133.76 (595.0)	165.34 (735.5)	0.015 (0.37)	87.50 (389.2)	1.115 (28.3)	164.01 (729.6)	14.50 (19.66)
4G80S6F3(1/8)-3	0.125 (3.18)	229.31 (1020)	0.955 (6.59)	132.39 (588.9)	157.25 (699.5)	0.020 (0.50)	105.70 (470.2)	1.301 (33.1)	154.46 (687.1)	16.46 (22.31)
Mean	0.100 (2.53)	226.86 (1009)	0.945 (6.52)	131.45 (584.7)	160.31 (713.1)	0.016 (0.40)	98.53 (438.3)	1.108 (28.1)	158.83 (706.5)	14.02 (19.01)
Median	0.099 (2.52)	228.01 (1014)	0.950 (6.55)	132.39 (588.9)	158.35 (704.4)	0.015 (0.37)	102.40 (455.5)	1.115 (28.3)	158.03 (703.0)	14.50 (19.66)
STDEV	0.025 (0.64)	3.185 (14.17)	0.013 (0.09)	2.902 (12.91)	4.388 (19.52)	0.004 (0.10)	9.697 (43.13)	0.197 (5.01)	4.825 (21.46)	2.710 (3.675)
COV	25%	1%	1%	2%	3%	24%	10%	18%	3%	19%

Table 6.32: Specimen 4G80S6(1/8) shear test results.

Spec	Δ_{ult}, in. (mm)	V_{ult}, kip (kN)	σ_{ult}, ksi (MPa)	$V_{sus,min}$, kip (kN)	$V_{sus,max}$, kip (kN)	Δ_{cr}, in. (mm)	V_{cr}, kip (kN)	Δ_{b}, in. (mm)	V_b, kip (kN)	E_b, kip-ft (kJ)
4G80S6(1/8)-1	0.065 (1.65)	221.21 (984.0)	0.922 (6.36)	126.72 (563.7)	151.44 (673.6)	0.015 (0.37)	112.5 (500.4)	1.079 (27.4)	145.00 (645.0)	12.92 (17.52)
4G80S6(1/8)-2	0.085 (2.16)	290.99 (1294)	1.212 (8.36)	132.37 (588.8)	152.83 (679.8)	0.016 (0.40)	119.00 (529.3)	0.962 (24.4)	150.57 (669.8)	12.73 (17.26)
4G80S6(1/8)-3	0.070 (1.78)	203.91 (907.0)	0.850 (5.86)	127.94 (569.1)	156.60 (696.6)	0.016 (0.41)	96.81 (430.6)	1.012 (25.7)	151.03 (671.8)	12.19 (16.53)
Mean	0.073 (1.86)	238.70 (1062)	0.995 (6.86)	129.01 (573.9)	153.62 (683.4)	0.016 (0.40)	109.44 (486.8)	1.018 (25.9)	148.87 (662.2)	12.61 (17.10)
Median	0.070 (1.78)	221.21 (984.0)	0.922 (6.36)	127.94 (569.1)	152.83 (679.8)	0.016 (0.40)	112.50 (500.4)	1.012 (25.7)	150.57 (669.8)	12.73 (17.26)
STDEV	0.010 (0.26)	46.10 (205.1)	0.192 (1.32)	2.973 (13.22)	2.670 (11.88)	0.001 (0.02)	11.41 (50.74)	0.059 (1.49)	3.357 (14.93)	0.377 (0.512)
COV	14%	19%	19%	2%	2%	5%	10%	6%	2%	3%

Table 6.33: Specimen 4G80S6F6(1/8) shear test results.

Spec	Δ_{ult}, in. (mm)	V_{ult}, kip (kN)	σ_{ult}, ksi (MPa)	$V_{sus,min}$, kip (kN)	$V_{sus,max}$, kip (kN)	Δ_{cr}, in. (mm)	V_{cr}, kip (kN)	Δ_{b}, in. (mm)	V_b, kip (kN)	E_b, kip-ft (kJ)
4G80S6F6(1/8)-1	0.070 (1.78)	240.20 (1069)	1.001 (6.90)	129.89 (577.8)	155.80 (693.0)	0.015 (0.38)	111.70 (496.9)	1.065 (27.1)	151.96 (676.0)	13.28 (18.00)
4G80S6F6(1/8)-2	0.060 (1.52)	264.66 (1177)	1.103 (7.60)	143.46 (638.1)	161.17 (716.9)	0.016 (0.41)	143.20 (637.0)	0.746 (19.0)	160.53 (714.1)	10.17 (13.79)
4G80S6F6(1/8)-3	0.075 (1.91)	275.97 (1228)	1.150 (7.93)	134.46 (598.1)	160.87 (715.6)	0.019 (0.47)	144.70 (643.7)	1.105 (28.1)	155.85 (693.3)	14.41 (19.53)
Mean	0.068 (1.74)	260.28 (1158)	1.084 (7.48)	135.94 (604.7)	159.28 (708.5)	0.017 (0.42)	133.20 (592.5)	0.972 (24.7)	156.11 (694.4)	12.62 (17.11)
Median	0.070 (1.78)	264.66 (1177)	1.103 (7.60)	134.46 (598.1)	160.87 (715.6)	0.016 (0.41)	143.20 (637.0)	1.065 (27.1)	155.85 (693.3)	13.28 (18.00)
STDEV	0.008 (0.19)	18.28 (81.33)	0.076 (0.53)	6.904 (30.71)	3.017 (13.42)	0.002 (0.05)	18.63 (82.89)	0.197 (5.00)	4.291 (19.09)	2.195 (2.976)
COV	11%	7%	7%	5%	2%	11%	14%	20%	3%	17%

Table 6.34: Summary of averages of each specimen group analyzing influence of nominal concrete strength.

Spec	Δ_{ult}, in. (mm)	V_{ult}, kip (kN)	σ_{ult}, ksi (MPa)	$V_{sus,min}$, kip (kN)	$V_{sus,max}$, kip (kN)	Δ_{cr}, in. (mm)	V_{cr}, kip (kN)	Δ_{b}, in. (mm)	V_b, kip (kN)	E_b, kip-ft (kJ)
4G80S6F3(1/8)	0.100 (2.53)	226.86 (1009)	0.945 (6.52)	131.45 (584.7)	160.31 (713.1)	0.016 (0.40)	98.53 (438.3)	1.108 (28.1)	158.83 (706.5)	14.02 (19.01)
4G80S6(1/8)	0.073 (1.86)	238.70 (1062)	0.995 (6.86)	129.01 (573.9)	153.62 (683.4)	0.016 (0.40)	109.44 (486.8)	1.018 (25.9)	148.87 (662.2)	12.61 (17.10)
4G80S6F6(1/8)	0.068 (1.74)	260.28 (1158)	1.084 (7.48)	135.94 (604.7)	159.28 (708.5)	0.017 (0.42)	133.20 (592.5)	0.972 (24.7)	156.11 (694.4)	12.62 (17.11)

6.3.2 Interface Shear Force versus Strain

The interface shear force versus reinforcing steel U-bar strain relationships are presented in Figure 6.28 to Figure 6.30 for specimen groups 4G80S6F3(1/8), 4G80S6(1/8), and 4G80S6F6(1/8), respectively. The curves shown correspond to the average strain measurements from all strain gauges contained in each test specimen plotted versus the interface shear force. From these figures, it can be observed that all specimens present similar force-strain responses. Discussion pertaining Figure 6.29 is presented in Section 5.2.2. Table 6.35 to Table 6.37 show strain readings from strain gauges in each specimen at peak load. Significant variability of strain gauge readings is observed with COV reaching 38%. It is important to note that a number of strain gauges were damaged before the peak load was reached.

Table 6.38 shows a comparison of the average interface shear strain relationship of the three specimen groups being discussed. From the table it can be seen that, in general, specimen group 4G80S6(1/8) shows the lowest strain values at peak load compared to specimen group 4G80S6F3(1/8) and 4G80S6F6(1/8). This may be attributed to the reinforcing steel U-bars crushing the concrete around them, thus reducing the strain.

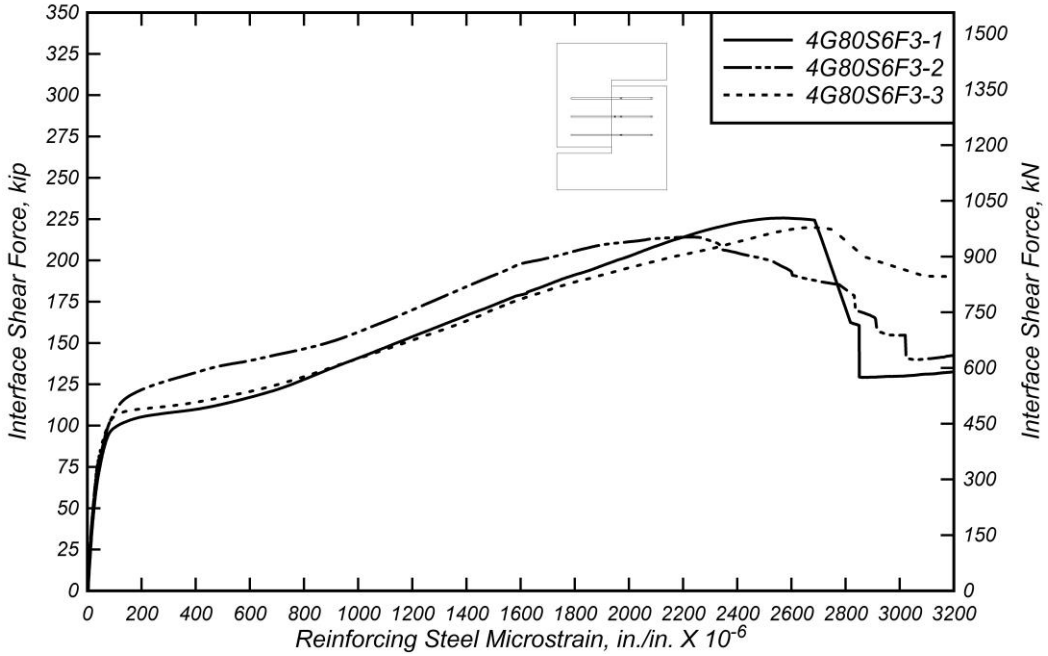

Figure 6.28: Interface shear force versus average reinforcing steel microstrain for 4G80S6F3(1/8) specimens.

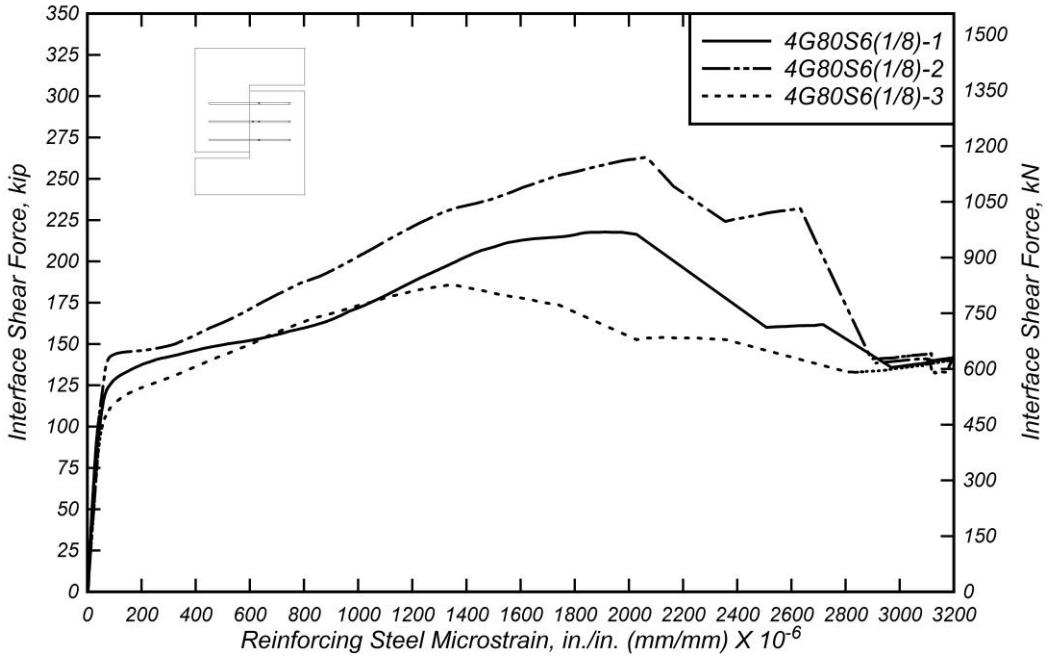

Figure 6.29: Interface shear force versus average reinforcing steel microstrain for 4G80S6(1/8) specimens.

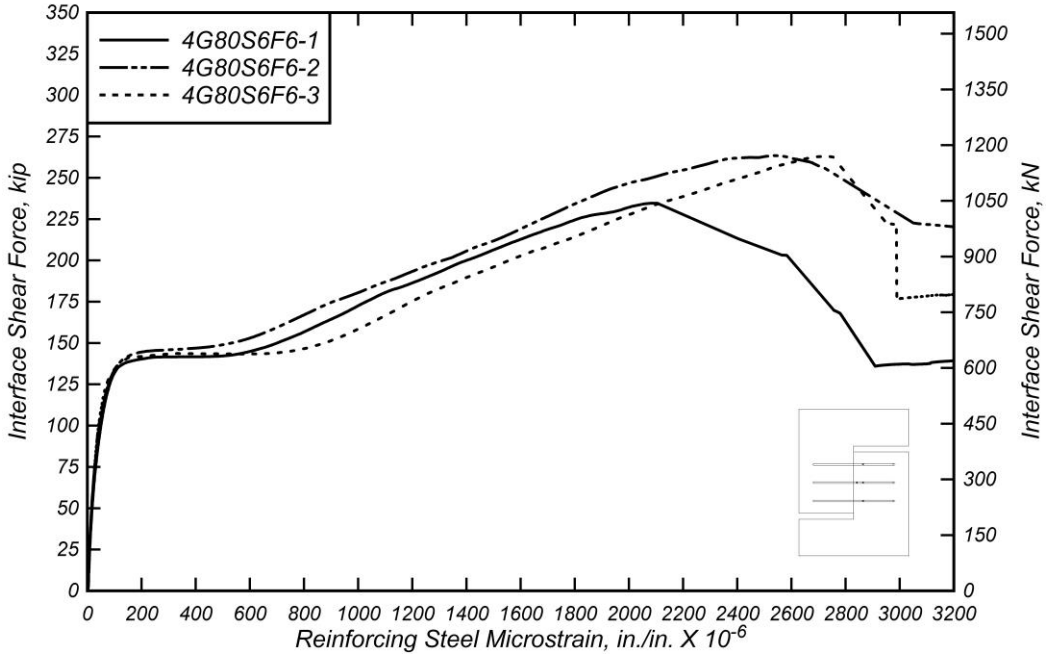

Figure 6.30: Interface shear force versus average reinforcing steel microstrain for 4G80S6F6(1/8) specimens.

Table 6.35: Specimen 4G80S6F3(1/8) strain gauge readings at peak interface shear force.

Specimen	s_1, in./in. (mm/mm)	s_2, in./in. (mm/mm)	s_3, in./in. (mm/mm)	s_4, in./in. (mm/mm)	s_5, in./in. (mm/mm)	s_6, in./in. (mm/mm)	s_7, in./in. (mm/mm)
4G80S6F3(1/8)-1	0.0012	0.0025	0.0027	0.0026	0.0015	0.0024	0.0025
4G80S6F3(1/8)-2	0.0025	0.0019	0.0019	0.0025	0.0024	0.0029	0.0023
4G80S6F3(1/8)-3	0.0028	0.0035	0.0026	0.0035	0.0025	0.0039	0.0027
Mean	0.0022	0.0026	0.0024	0.0029	0.0021	0.0030	0.0025
Median	0.0025	0.0025	0.0026	0.0026	0.0024	0.0029	0.0025
STDEV	0.000826	0.000779	0.000452	0.000555	0.000584	0.000761	0.000205
COV	38%	30%	19%	19%	28%	25%	8%

Table 6.36: Specimen 4G80S6(1/8) strain gauge readings at peak interface shear force.

Specimen	s_1, in./in. (mm/mm)	s_2, in./in. (mm/mm)	s_3, in./in. (mm/mm)	s_4, in./in. (mm/mm)	s_5, in./in. (mm/mm)	s_6, in./in. (mm/mm)	s_7, in./in. (mm/mm)
4G80S6(1/8)-1	-	-	0.0019	-	0.0025	0.0018	-
4G80S6(1/8)-2	-	-	-	-	0.0030	0.0025	0.0017
4G80S6(1/8)-3	-	0.0022	-	0.0026	-	0.0018	0.0012
Mean	-	0.0022	0.0019	0.0026	0.0028	0.0021	0.0015
Median	-	0.0022	0.0019	0.0026	0.0028	0.0018	0.0015
STDEV	-	-	-	-	0.0004	0.0004	0.0004
COV	-	-	-	-	13%	19%	26%

Table 6.37: Specimen 4G80S6F6(1/8) strain gauge readings at peak interface shear force.

Specimen	s_1, in./in. (mm/mm)	s_2, in./in. (mm/mm)	s_3, in./in. (mm/mm)	s_4, in./in. (mm/mm)	s_5, in./in. (mm/mm)	s_6, in./in. (mm/mm)	s_7, in./in. (mm/mm)
4G80S6F6(1/8)-1	0.0019	-	-	0.0028	0.0014	0.0024	0.0026
4G80S6F6(1/8)-2	0.0015	0.0024	0.0026	0.0025	-	0.0025	0.0024
4G80S6F6(1/8)-3	0.0014	-	0.0027	0.0033	0.0016	0.0035	0.0029
Mean	0.0016	0.0024	0.0026	0.0029	0.0015	0.0028	0.0026
Median	0.0015	0.0024	0.0026	0.0028	0.0015	0.0025	0.0026
Stdv	0.000284	-	5.43E-05	0.000394	0.000185	0.000643	0.000292
COV	18%	-	2%	14%	12%	23%	11%

Table 6.38: Summary of average strain gauge readings at peak interforce shear load.

Specimen	s_1, in./in. (mm/mm)	s_2, in./in. (mm/mm)	s_3, in./in. (mm/mm)	s_4, in./in. (mm/mm)	s_5, in./in. (mm/mm)	s_6, in./in. (mm/mm)	s_7, in./in. (mm/mm)
4G80S6F3(1/8)	0.0022	0.0026	0.0024	0.0029	0.0021	0.0030	0.0025
4G80S6(1/8)	-	0.0022	0.0019	0.0026	0.0028	0.0021	0.0015
4G80S6F6(1/8)	0.0016	0.0024	0.0026	0.0029	0.0015	0.0028	0.0026

6.3.3 Interface Shear Force versus Crack Width

Figure 6.31 to Figure 6.33 show the interface shear force versus crack width relationship for specimen groups 4G80S6F3(1/8), 4G80S6(1/8), and 4G80S6F6(1/8). Table 6.39 to Table 6.41 show tabulated values for the main points of study for specimen groups 4G80S6F3(1/8), 4G80S6(1/8), and 4G80S6F6(1/8). All specimens present the same behavior in the initial stages characterized by negligible crack width due to the uncracked concrete-to-concrete bond. After the cohesion bond is lost, the force-crack width response is characterized by a hardening branch until peak load is reached. Table 6.39 to Table 6.41 show that significant variability of crack widths at peak load, w_{ult}, are observed, with COV ranging from 12% to 30%.

Table 6.42 shows a comparison between the average crack width values for specimen groups 4G80S6F3(1/8), 4G80S6(1/8), and 4G80S6F6(1/8). From the table it can be inferred that the average crack widths at peak load, w_{ult}, tend to be reduced as nominal concrete strength increases. Average crack widths at peak load are 0.0436 in. (1.107 mm), 0.0297 in. (0.753 mm), and 0.0299 in. (0.758 mm), for specimen groups 4G80S6F3(1/8), 4G80S6(1/8), and 4G80S6F6(1/8) respectively. These results indicate that larger crack widths at peak load, w_{ult}, may be expected when concrete with nominal strength is lower.

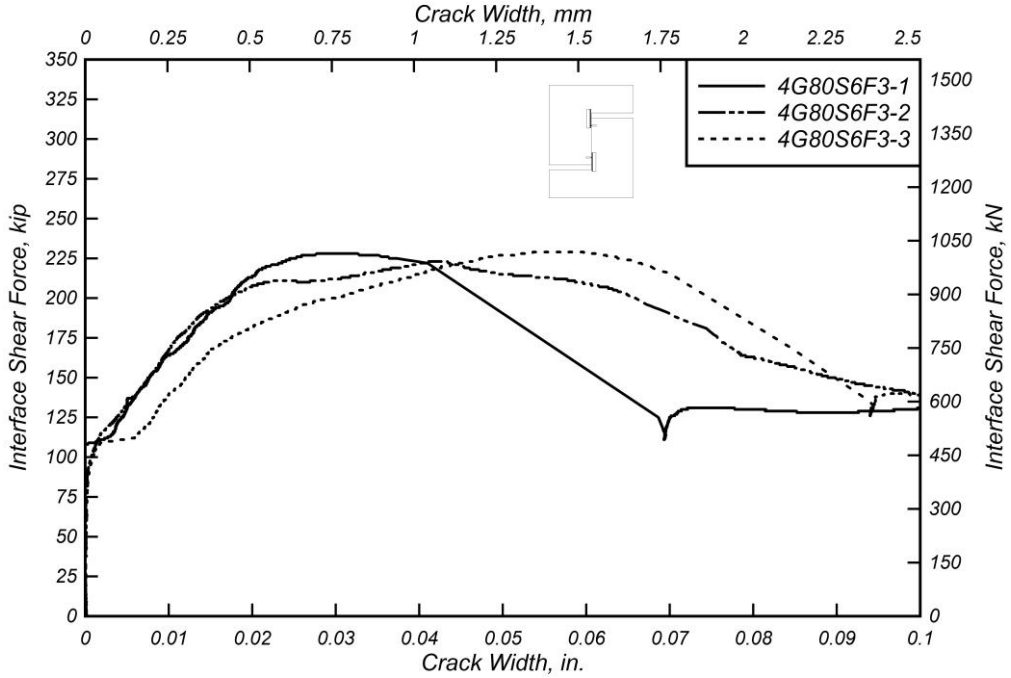

Figure 6.31: Interface shear force versus crack width for 4G80S6F3(1/8) specimens.

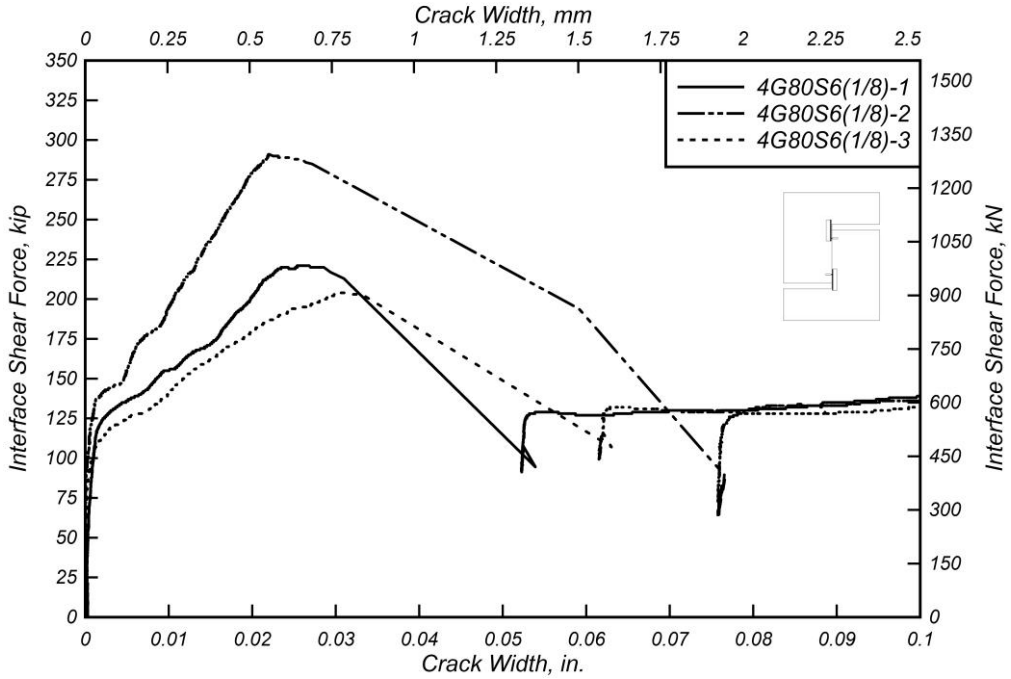

Figure 6.32: Interface shear force versus crack width for 4G80S6(1/8) specimens.

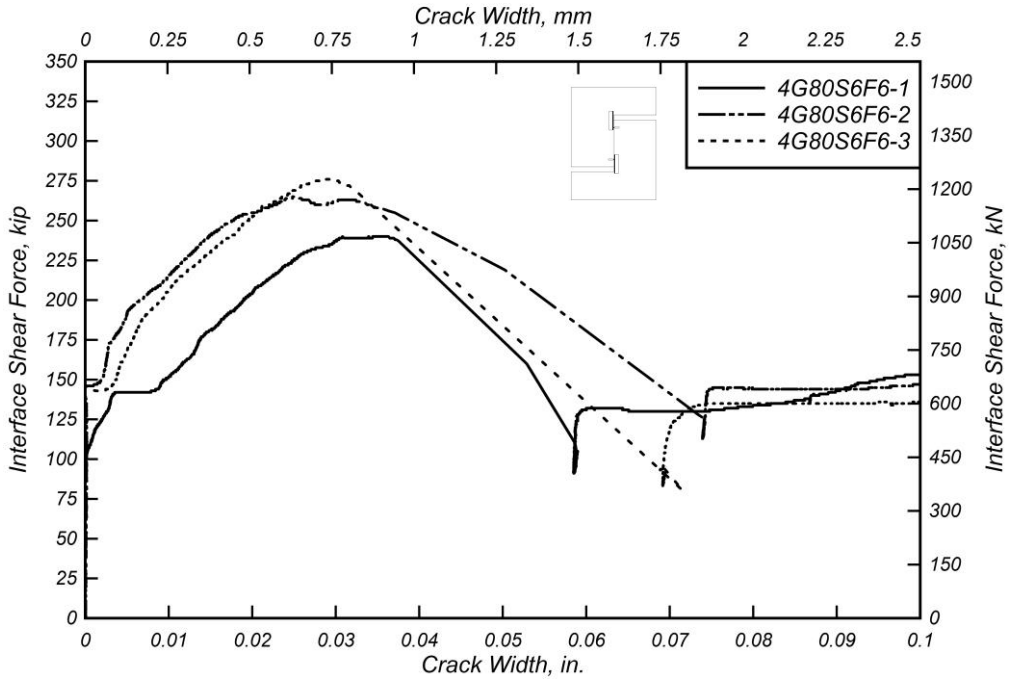

Figure 6.33: Interface shear force versus crack width for 4G80S6F6(1/8) specimens.

Table 6.39: Specimen 4G80S6F3(1/8) crack width measurements.

Specimen	w_{ult}, in. (mm)	V_{ult}, kip (kN)	w_b, in. (mm)	V_b, kip (kN)
4G80S6F3(1/8)-1	0.0312 (0.7926)	228.01 (1014.2)	0.1652 (4.196)	158.03 (702.95)
4G80S6F3(1/8)-2	0.0426 (1.081)	223.16 (992.66)	0.1956 (4.969)	164.01 (729.55)
4G80S6F3(1/8)-3	0.0570 (1.447)	229.31 (1020.0)	0.2243 (5.698)	154.46 (687.07)
Mean	0.0436 (1.107)	226.83 (1009.0)	0.1951 (4.954)	158.83 (706.52)
Median	0.0426 (1.081)	228.01 (1014.2)	0.1956 (4.969)	158.03 (702.95)
STDEV	0.0129 (0.3278)	3.240 (14.41)	0.0296 (0.7515)	4.825 (21.46)
COV	30%	1%	15%	3%

Table 6.40: Specimen 4G80S6(1/8) crack width measurements.

Specimen	w_{ult}, in. (mm)	V_{ult}, kip (kN)	w_b, in. (mm)	V_b, kip (kN)
4G80S6(1/8)-1	0.0256 (0.6510)	221.21 (983.98)	0.1732 (4.398)	145.00 (645.01)
4G80S6(1/8)-2	0.0327 (0.8314)	290.99 (1294.4)	0.2602 (6.610)	150.57 (669.77)
4G80S6(1/8)-3	0.0306 (0.7771)	203.91 (907.04)	0.1782 (4.526)	151.03 (671.81)
Mean	0.0297 (0.7532)	238.70 (1061.8)	0.2039 (5.178)	148.87 (662.20)
Median	0.0306 (0.7771)	221.21 (983.98)	0.1782 (4.526)	150.57 (669.77)
STDEV	0.0036 (0.0926)	46.10 (205.07)	0.0489 (1.242)	3.354 (14.92)
COV	12%	19%	24%	2%

Table 6.41: Specimen 4G80S6F6(1/8) crack width measurements.

Specimen	w_{ult}, in. (mm)	V_{ult}, kip (kN)	w_b, in. (mm)	V_b, kip (kN)
4G80S6F6(1/8)-1	0.0356 (0.9042)	240.20 (1068.5)	0.1142 (2.900)	151.96 (675.95)
4G80S6F6(1/8)-2	0.0251 (0.6366)	264.66 (1177.3)	0.1449 (3.680)	160.53 (714.08)
4G80S6F6(1/8)-3	0.0289 (0.7341)	275.97 (1227.6)	0.1753 (4.452)	155.85 (693.25)
Mean	0.0299 (0.7583)	260.28 (1157.8)	0.1448 (3.678)	156.11 (694.42)
Median	0.0289 (0.7341)	264.66 (1177.3)	0.1449 (3.680)	155.85 (693.25)
STDEV	0.0053 (0.1354)	18.28 (81.33)	0.0305 (0.776)	4.292 (19.09)
COV	18%	7%	21%	3%

Table 6.42: Summary of crack width measurements for 4G80S6F3(1/8), 4G80S6(1/8), and 4G80S6F6(1/8) specimens.

Specimen	w_{ult}, in. (mm)	V_{ult}, kip (kN)	w_b, in. (mm)	V_b, kip (kN)
4G80S6F3(1/8)	0.0436 (1.107)	226.83 (1009.0)	0.1951 (4.954)	158.83 (706.52)
4G80S6(1/8)	0.0297 (0.7532)	238.70 (1061.8)	0.2039 (5.178)	148.87 (662.20)
4G80S6F6(1/8)	0.0299 (0.7583)	260.28 (1157.8)	0.1448 (3.678)	156.11 (694.42)

6.4 SUMMARY AND MAIN FINDINGS

This section provides a summary of experimental findings and a discussion on main findings regarding: (i) influence of shear interface preparation, and (ii) influence of nominal concrete strength. A comparison between experimentally measured capacity and calculated capacities per AASHTO and ACI 318-14 code provisions is presented.

Figure 6.34 presents the peak shear stress normalized by concrete strength versus the reinforcing steel ratio normalized by the concrete strength and the elastic modulus of the reinforcing steel. The data points presented in this figure are experimentally determined peak loads for specimen groups compared to analyze the influence of shear interface preparation on shear friction for specimens constructed with #4 (#13M) reinforcing steel bars. Data points corresponding to test specimens 4G80S6(AC), 4G80S6(EA), 4G80S6(1/8), and 4G80S6(1/4) constructed with a shear interface surface preparation As Cast, Exposed Aggregate, 1/8 in. (3.175 mm) roughness, and 1/4 in. (6.35 mm) roughness, respectively, are shown in this figure. Additionally, there are curves shown corresponding to AASHTO (2015) shear friction design equation (Equation 2-1) for a surface not intentionally roughened (As Cast), an Exposed Aggregate surface, a surface roughness of 1/4 in. (6.35 mm), a surface roughness of 1/8 in. (3.175 mm), in addition to the mentioned four curves considering a nominal yield strength limit of f_y = 80 ksi. As it can be observed in the figure, all data points are above their respective curves, which indicates that by allowing the nominal yield strength limit to be raised to 80 ksi (550 MPa), the shear capacity design will remain conservative.

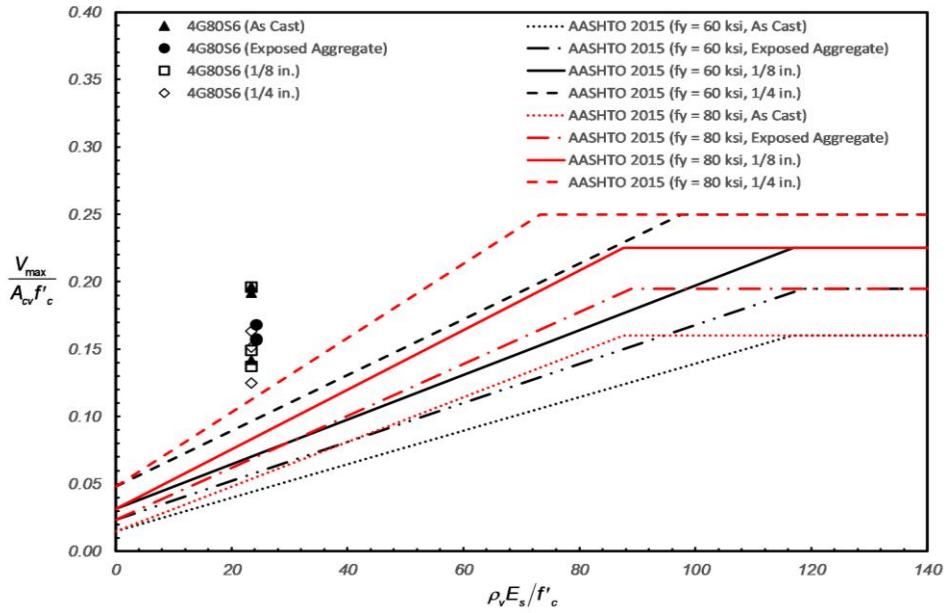

Figure 6.34: Experimental normalized peak shear stress versus normalized reinforcement stiffness across the interface – influence of interface preparation #4 (#13M) reinforcing steel bars.

Figure 6.35 presents the peak shear stress normalized by concrete strength versus the reinforcing steel ratio normalized by the concrete strength and the elastic modulus of the reinforcing steel. The data points presented in this figure are experimentally determined peak loads for specimen groups compared to analyze the influence of shear interface preparation on shear friction for specimens constructed with #5 (#16M) reinforcing steel bars. Data points corresponding to test specimens 5G80S6(AC), 5G80S6(EA), 5G80S6(1/8), and 5G80S6(1/4) constructed with a shear interface surface preparation As Cast, Exposed Aggregate, 1/8 in. (3.175 mm) roughness, and 1/4 in. (6.35 mm) roughness, respectively, are shown in this figure. As discussed in the previous paragraph, the figure also shows four AASHTO design equation curves corresponding to each surface preparation, in addition to four more curves corresponding to the AASHTO design equations considering a nominal yield strength of 80 ksi (550 MPa). All data points are above their respective AASHTO design equation curve which is an indication that allowing the nominal yield strength limit to be raised to 80 ksi (550 MPa) maintains a conservative design.

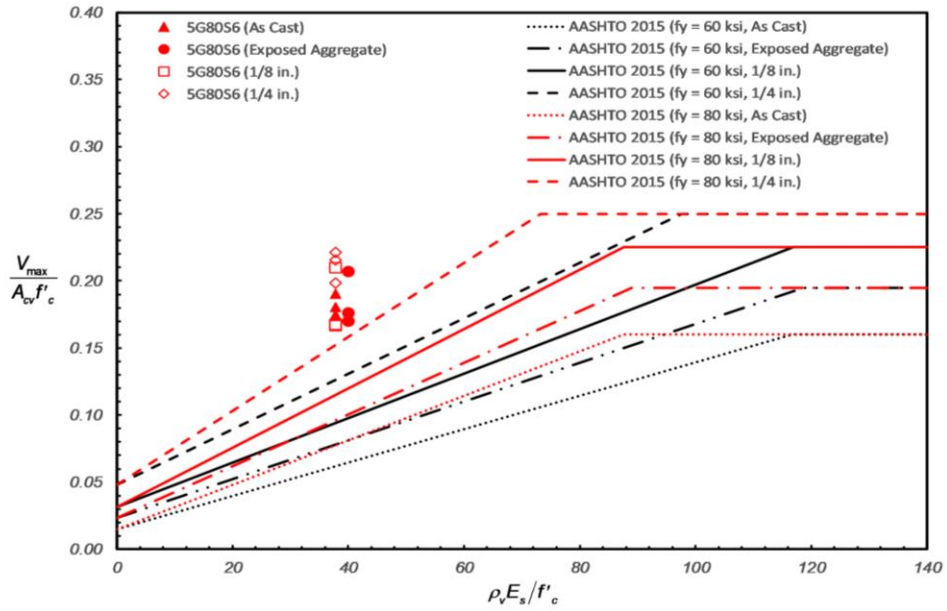

Figure 6.35: Experimental normalized peak shear stress versus normalized reinforcement stiffness across the interface – influence of interface preparation #5 (#16M) reinforcing steel bars.

Figure 6.36 presents the peak shear stress normalized by concrete strength versus the reinforcing steel ratio normalized by the concrete strength and the elastic modulus of the reinforcing steel. The data points presented in this figure are experimentally determined peak loads for specimen groups compared to analyze the influence or nominal concrete strength. Data points corresponding to test results from specimens 4G80S6F3(1/8), 4G80S6(1/8), and 4G80S6F6(1/8) are presented in the figure.

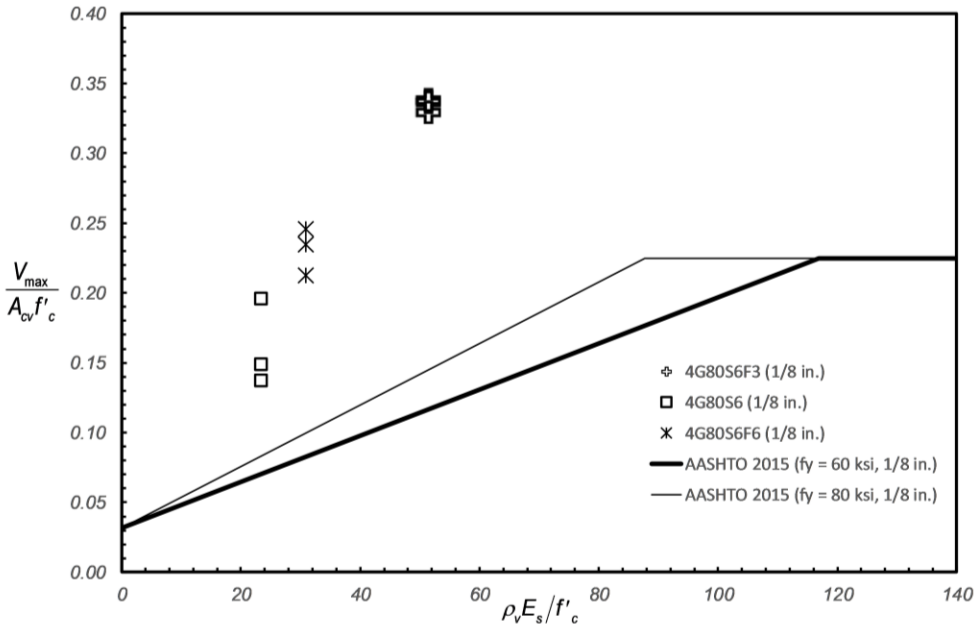

Figure 6.36: Experimental normalized peak shear stress versus normalized reinforcement stiffness across the interface – influence of nominal concrete strength.

Figure 6.37 and Figure 6.38 present the ratio of the experimentally measured peak loads, V_{max}, to the shear capacity per AASHTO (2015) and ACI 318-14 code provisions, respectively. In these figures, each data set consists of two columns. The first column corresponds to the ratio considering the nominal yield strength of f_y = 80 ksi (550 MPa). The second column corresponds to the ratio considering the nominal yield strength limit of f_y = 60 ksi (420 MPa). Table 6.43 shows a summary of the ratio of experimentally measured shear resistance to nominal interface shear resistance per AASHTO (2015) and ACI 318-14, V_{max}/V_{ni}. As seen in the table, increasing the nominal yield strength to 80 ksi (550 MPa) reduces the V_{max}/V_{ni} ratio in all cases for both code provisions. These results indicate that an increase in the nominal yield strength limit to 80 ksi (550 MPa) will provide a more efficient design while still remaining conservative for both AASHTO (2015) and ACI 318-14 code provisions. It is important to note that when considering f_y = 80 ksi (550 MPa) all specimen groups indicate V_{max}/V_{ni} ratios greater than 1.5, with the exception of specimen groups 4G80S6(1/4) and 5G80S6(1/4). Additionally, the results show that ratios are larger when calculated per ACI 318-14 provisions, which indicates a higher level of conservatism.

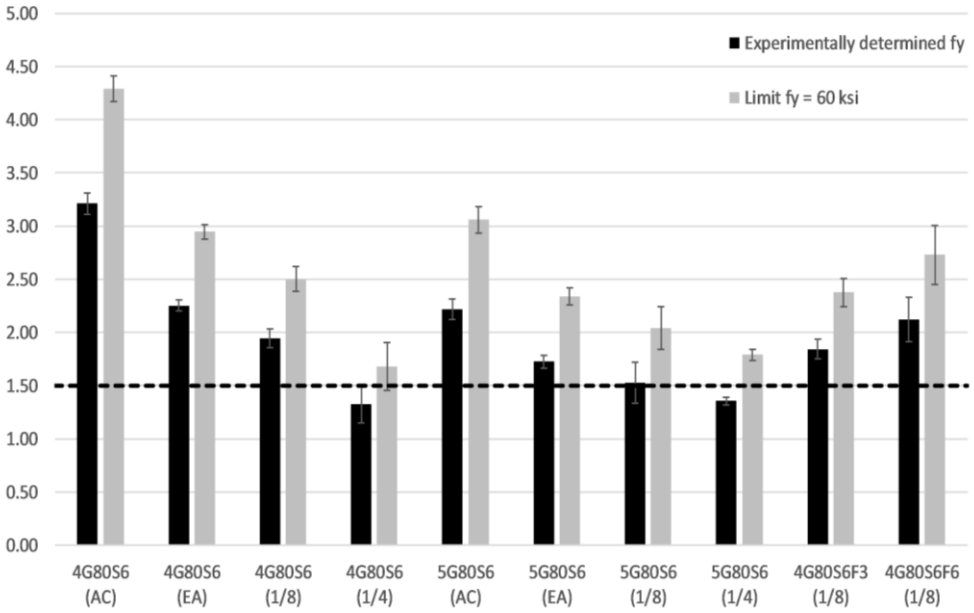

Figure 6.37: Comparison of experimentally measured strength with AASHTO (2015) calculated strength.

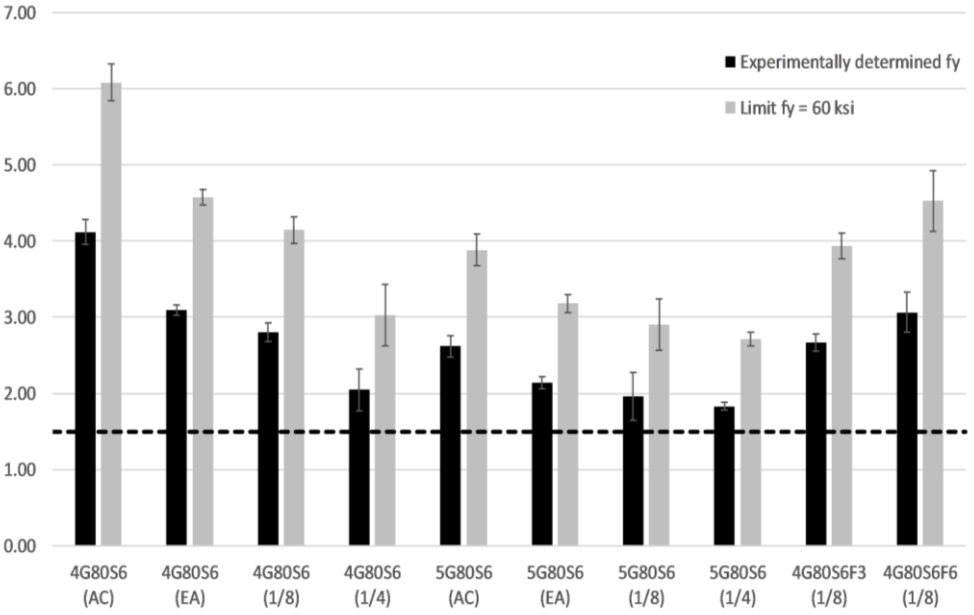

Figure 6.38: Comparison of experimentally measured strength with ACI 318-14 calculated strength.

Table 6.43: Ratio of measured strength, V_{max}, to nominal strength, V_{ni}.

Specimen label	V_{max}, kip (kN)	AASHTO (2015) Section 5.8.4				ACI 318-14 Section 22.9			
		Experimental f_y		Limit f_y = 60 ksi (420 MPa)		Experimental f_y		Limit f_y = 60 ksi (420 MPa)	
		V_{ni}, kip (kN)	V_{max}/V_{ni}	V_{ni}, kip (kN)	V_{max}/V_{ni}	V_{nh}, kip (kN)	V_{max}/V_{nh}	V_{nh}, kip (kN)	V_{max}/V_{nh}
4G80S6 (AC)	262.67 (1168)	81.81 (363.9)	3.21	61.20 (272.2)	4.29	63.81 (283.9)	4.12	43.20 (192.2)	6.08
4G80S6 (EA)	230.67 (1026)	102.35 (455.3)	2.25	78.30 (348.3)	2.95	74.45 (331.2)	3.10	50.40 (224.2)	4.58
4G80S6 (1/8)	238.67 (1062)	122.88 (546.6)	1.94	95.40 (424.4)	2.50	85.08 (378.5)	2.81	57.60 (256.2)	4.14
4G80S6 (1/4)	218.00 (969.7)	163.96 (729.3)	1.33	129.60 (576.5)	1.68	106.36 (473.1)	2.05	72.00 (320.3)	3.03
4G80S4 (1/8)	238.33 (1060)	151.25 (672.8)	1.58	114.60 (509.8)	2.08	113.45 (504.6)	2.10	76.80 (341.6)	3.10
4G80S12 (1/8)	160.33 (713.2)	94.52 (420.5)	1.70	76.20 (339.0)	2.10	56.72 (252.3)	2.83	38.40 (170.8)	4.18
5G80S6 (AC)	260.00 (1157)	117.26 (521.6)	2.22	84.96 (377.9)	3.06	99.26 (441.5)	2.62	66.96 (297.9)	3.88
5G80S6 (EA)	248.33 (1105)	143.70 (639.2)	1.73	106.02 (471.6)	2.34	115.80 (515.1)	2.14	78.12 (347.5)	3.18
5G80S6 (1/8)	259.33 (1154)	170.14 (756.8)	1.52	127.08 (565.3)	2.04	132.34 (588.7)	1.96	89.28 (397.1)	2.90
5G80S6 (1/4)	302.67 (1346)	223.03 (992.1)	1.36	169.20 (752.6)	1.79	165.43 (735.9)	1.83	111.60 (496.4)	2.71
4G80S6 F3(1/8)	226.67 (1008)	122.88 (546.6)	1.84	95.40 (424.4)	2.38	85.08 (378.5)	2.66	57.60 (256.2)	3.94
4G80S6 F6(1/8)	260.67 (1159.5)	122.88 (546.6)	2.12	95.40 (424.4)	2.73	85.08 (378.5)	3.06	57.60 (256.2)	4.53

7.0 CONCLUSION

The objective of this research report was to evaluate and define the performance of high strength steel (HSS) reinforcing steel bars in shear friction applications. This was accomplished by implementing an experimental program that consisted in testing forty five push-off test specimens focusing on the influence of reinforcing steel grade, interface preparation, reinforcing steel bar spacing, reinforcing steel bar size, and nominal concrete strength. Results for test specimens with four reinforcing steel types (ASTM A706 Grade 60 (420 MPa), ASTM A708 Grade 80 (550 MPa), ASTM A615 Grade 100 (690 MPa), and ASTM A1035 Grade 120 (830 MPa)), four interface preparations (As Cast, Exposed Aggregate, 1/8 in. (3.175 mm), and 1/4 in. (6.35 mm)), three reinforcing steel bar spacings (4 in. (101.6 mm), 6 in. (152.4 mm), and 12 in. (304.8 mm)), two reinforcing steel bar sizes (#4 (#13M) and #5 (#16M)), and three nominal concrete strengths (3 ksi (20.7 MPa), 5 ksi (34.5 MPa), and 6 ksi (41.4 MPa)) are presented.

The following conclusions can be drawn from the test results presented in this research report:

1. The use of HHS reinforcing bars as interface shear reinforcement did not have a significant impact on peak shear force or shear force at cracking. These slight increases, however, were accompanied by significant increases in crack width and interface shear displacement. Additionally, specimens reinforced with HSS bars showed significantly larger sustained interface shear forces. Specimens with Grade 80 and Grade 100 reinforcing steel bars across the interface presented similar sustained interface shear forces, although specimens with Grade 120 reinforcing steel bars across the interface presented the largest increase in sustained interface shear force. These results demonstrate that using higher strength steel reinforcement leads to the development of greater loads due to dowel action.

2. Significantly higher peak shear forces were observed in specimens with reduced spacing between reinforcing steel bars crossing the shear interface. Specimens with three reinforcing steel bars spaced at 6 in. (152.4 mm) and four reinforcing steel bars spaced at 4 in. (101.6 mm) exhibited similar peak shear forces when compared to specimens with two reinforcing steel bars spaced at 12 in. (304.8 mm). In addition, specimens with 4 in. (101.6 mm) spacing between reinforcing steel bars presented significantly lower interface shear displacement and crack width at peak shear force compared to specimens with 6 in. (152.4 mm) spacing between reinforcing steel bars. This is due to a higher reinforcement ratio in specimens with lower spacing between reinforcing steel bars, as it is directly related to the clamping force.

3. An increase in peak shear load was observed in specimens reinforced with #5 (#16M) steel bars when compared to specimens reinforced with #4 (#13M) bars, with the exception of specimens constructed with an As Cast shear interface surface preparation, which presented no change in peak shear load when reinforcing steel bar size is increased. Additionally, specimens with #5 (#16M) reinforcing steel bars presented smaller interface shear displacements at peak shear load when compared to specimens with #4 (#13M) reinforcing steel bars, with the exception of specimens constructed with a shear interface surface roughened to an amplitude of 1/4 in. (6.35 mm), which presented a significant increase when reinforcing steel bar size was increased.

4. Surface preparation has a significant impact on shear friction performance. However, substantial variability was observed when comparing results from test specimens constructed with different surface preparations.

5. In some cases, implementing an Exposed Aggregate surface preparation on the shear interface enhanced the aggregate interlock and allowed it to contribute to the post-peak shear capacity. Nonetheless, the limited testing performed indicates that this aggregate interlock enhancement does not always develop. Additional testing and surface preparation trails are

recommended in order to gain further insight into the Exposed Aggregate surface preparation behavior.

6. An underestimation of shear friction capacity was observed in specimens constructed with an As Cast surface preparation. Additional testing is recommended in order to gain further insight into the behavior of the As Cast surface preparation.

8.0 REFERENCES

AASHTO (2014*). AASHTO Load Resistance Factor Design Bridge Design Specifications, Customary U.S. Units.* American Association of State Highway and Transportation Officials, Washington, DC.

AASHTO (2012*). AASHTO Load Resistance Factor Design Bridge Design Specifications, Customary U.S. Units.* American Association of State Highway and Transportation Officials, Washington, DC.

AASHTO (2007*). AASHTO Load Resistance Factor Design Bridge Design Specifications, Customary U.S. Units.* American Association of State Highway and Transportation Officials, Washington, DC.

AASHTO (2004*). AASHTO Load Resistance Factor Design Bridge Design Specifications, Customary U.S. Units.* American Association of State Highway and Transportation Officials, Washington, DC.

AASHTO (1998*). AASHTO Load Resistance Factor Design Bridge Design Specifications, Customary U.S. Units.* American Association of State Highway and Transportation Officials, Washington, DC.

ACI (2014). Building Code Requirements for Structural Concrete (ACI 318-14) and Commentary. American Concrete Institute, Farmington Hills, MI.

ACI (2011). Building Code Requirements for Structural Concrete (ACI 318-11) and Commentary. American Concrete Institute, Farmington Hills, MI.

ACI (2002). Building Code Requirements for Structural Concrete (ACI 318-02) and Commentary. American Concrete Institute, Farmington Hills, MI.

ASTM Standard A615/A615M, 2014, "Standard Specification for Deformed and Plain Carbon-Steel Bars for Concrete Reinforcement," ASTM International, West Conshocken, PA, 2016, DOI: 10.1520/A0615_A0615M, www.astm.org

ASTM Standard A706/A706M, 2014, "Standard Specification for Low-Alloy Steel Deformed and Plain Bars for Concrete Reinforcement," ASTM International, West Conshocken, PA, 2016, DOI: 10.1520/A0706_A0706M, www.astm.org

ASTM Standard A1035/A1035M-16b, 2014, "Standard Specification for Deformed and Plain, Low-Carbon, Chromium, Steel Bars for Concrete Reinforcement," ASTM International, West Conshocken, PA, 2016, DOI: 10.1520/A1035_A1035M-16B, www.astm.org

ASTM Standard C31/31M, 2012, “Standard Practice for Making and Curing Concrete Test Specimens in the Field,” ASTM International, West Conshocken, PA, 2012, DOI: 10.1520/C0031_C0031M-12, www.astm.org

ASTM Standard C39, 2012a, “Standard Test Method for Compressive Strength of Cylindrical Concrete Specimens,” ASTM International, West Conshocken, PA, 2012, DOI: 10.1520/C0039_C0039M-12A, www.astm.org

ASTM Standard C138, 2013, “Standard Test Method for Density (Unit Weight), Yield, and Air Content (Gravimetric) of Concrete,” ASTM International, West Conshocken, PA, 2013, DOI: 10.1520/C0138_C0138M, www.astm.org

ASTM Standard C143, 2012, “Standard Test Method for slump of Hydraulic-Cement Concrete,” ASTM International, West Conshocken, PA, 2012, DOI: 10.1520/C0143_C0143M-12,www.astm.org

ASTM Standard C231, 2014, “Standard Test Method for Air Content of Freshly Mixed Concrete by the Pressure Method,” ASTM International, West Conshocken, PA, 2010, DOI: 10.1520/C0231_C0231M-14, www.astm.org

ASTM Standard E8/E8M-16a, 2016, “Standard Test Methods for Tension Testing of Metallic Materials,” ASTM International, West Conshocken, PA, 2016, DOI: 10.1520/E0008_E0008M-16a, www.astm.org

ASTM Standard E83, 2010a, “Standard Practice for Verification and Classification of Extensometer Systems,” ASTM International, West Conshocken, PA, 2010, DOI: 10.1520/E0083-10A, www.astm.org

Barbosa, A. R., Trejo, D., and Nielson, D. (2017). “High strength reinforcing steel bars: Concrete shear friction interface.” SPR 762-Part A, Report no. FHWA-OR-RD-17-08, Oregon DOT, Salem, OR.

Barbosa, A. R., Trejo, D., and Nielson, D. (2017). “Effect of high-strength reinforcement steel on shear friction behavior.” Journal of Structural Engineering, 22(8), 04017038

Birkeland, P. W., and Birkeland, H. W. (1966). "Connections in precast concrete construction." ACI Journal Proceedings, 63(3), 345-368.

Fang, Z., Jiang, H., Liu, A., Feng, J., and Chen, Y. (2018). “Horizontal Shear Behaviors of Normal Weight and Lightweight Concrete Composite T-Beams”. International Journal of Concrete Structures and Materials, 12(1), 55.

Harries, K. A., Zeno, G. A., and Shahrooz, B. (2012). "Toward an improved understanding of shear-friction behavior." ACI Structural Journal, 109(6), 835-844.

Hofbeck, J. A., Ibrahim, I. O., and Mattock, A. H. (1969). "Shear transfer in reinforced concrete." ACI Journal Proceedings, 66(2), 119-128.

Hwang, S.-J., Yu, H.-W., and Lee, H.-J. (2000). "Theory of interface shear capacity of reinforced concrete." Journal of Structural Engineering, 126(6), 700-707.

Julio, E. N.B.S., Branco, F. A.B., and Silva, V. D. (2004). "Concrete-to-concrete bond strength. Influence of the roughness of the substrate surface." Construction and Building Materials, 18(9), 675-681.

Kahn, L. F., and Mitchell, A. D. (2002). "Shear friction tests with high-strength concrete." ACI Structural Journal 99(1), 98-103.

Kahn, L. F., and Slapkus, A. (2004). "Interface shear in high strength composite T-beams." PCI Journal 49(4), 102-110.

Kim, Y. H., Huste, M. B. D., Trejo, D., and Cline, D. B. H. (2010). "Shear characteristics and design for high-strength self-consolidating concrete." Journal of Structural Engineering, 136(8), 989-1000.

Kovach, J. D. (2008). "Horizontal shear capacity of composite concrete beams without interface ties." (Master's thesis). Lehigh University.

Li, C., Lequesne, R. D., and Matamoros, A. (2017) "Composite action in prestressed NU I-girder bridge deck systems constructed with bond breakers to facilitate deck removal." Report No. K-Tran: KU-15-1. 2017.

Loov, R. E., and Patnaik, A. K. (1994). "Horizontal shear strength of composite concrete beams with a rough interface." PCI Journal, 39(1), 48-69.

Mattock, A. H., Li, W. K., and Wang, T. C. (1976). "Shear transfer in lightweight reinforced concrete." PCI Journal, 21(1), 20-39.

Mansur, M. A., Vinayagam, T., and Tan, K.-H. (2008). "Shear transfer across a crack in reinforced high-strength concrete." Journal of Materials in Civil Engineering, 20(4), 294-302.

Menzel, C. A. (1939). "Some factors influencing results of pull-out bond tests." ACI Journal Proceedings, 35(6), 517-542.

Mirza, S. A., MacGregor, J. G., & Hatzinikolas, M. (1979). Statistical descriptions of strength of concrete. Journal of the Structural Division, 105(6), 1021-1037.

Mirza, S. A., & MacGregor, J. G. (1979). Variability of mechanical properties of reinforcing bars. Journal of the Structural Division, 105(5), 921-937.

ODOT (2014). *Bridge Design and Drafting Manual*. Oregon Department of Transportation, Salem, OR.

ODOT (2015). *Standard Specifications*. Oregon Department of Transportation, Salem, OR.

Park, P., and Paulay, T. (1975). Reinforced Concrete Structures, John Wiley & Sons, New York.

Patnaik, A. K. (2001). "Behavior of composite concrete beams with smooth interface." Journal of Structural Engineering, 127(4), 359-366.

Santos, P. M. D., and Júlio, E. N. B. S. (2012). "A state-of-the-art review on shear-friction." Engineering Structures, 45, 435-448.

Santos, P. M. D., and Julio, E. N. B. S. (2014). "Interface shear transfer on composite concrete members." ACI Structural Journal, 111(1), 113-122.

Saemann, J. C., and Washa, G. W. (1964). "Horizontal Shear Connections Between Precast Beams and Cast-in-Place." ACI Journal Proceedings, 61(11), 1383-1408.

Scholz, D. P., Wallenfelsz, J. A., Lijeron, C., and Roberts-Wollmann, C. L. (2007). "Recommendations for the connection between full-depth precast bridge deck panel systems and precast I-beams." Virginia Tech, VTechWorks.

Scott, J. (2010). "Interface shear strength in lightweight concrete bridge girders." (Master's thesis). Virginia Polytechnic Institute and State University.

Shaw, D. M., and Sneed, L. H. (2014). Interface Shear Transfer of Lightweight-Aggregate Concretes Cast At Different Times. PCI Journal, 59(3), 130-144.

Sneed, L. H., Krc, K., Wermanger, S., and Meinheit, D. (2016). "Examination of the Effective Coefficient of Friction for Shear Friction Design". PCI Journal, 61(2), 38-55.

Soltani, M., and Ross, B.E. (2017). "Database Evaluation of Interface Shear Transfer in Reinforced Concrete Members." ACI Structural Journal, 114(2), 383-394.

Trejo, D., Barbosa, A. R., and Link, T. (2014). Seismic Performance of Circular Reinforced Concrete Bridge Columns Constructed with Grade 80 Reinforcement (No. FHWA-OR-RD-15-02).

Trejo, D., and Kim, Y. H. (2011). "Development of Precast Bridge Deck Overhang System: Technical Report." Texas Transportation Institute, Texas A&M University System.

Wallenfelsz, J. A. (2006). "Horizontal shear transfer for full-depth precast concrete bridge deck panels." (Master's thesis). Virginia Polytechnic Institute and State University.

Walraven, J. C., and Reinhardt, H. W. (1981). "Theory and experiments on the mechanical behaviour of cracks in plain and reinforced concrete subjected to shear loading." HERON, 26(1A), 1-68.

Waweru, R., Palacios, G., and Chao. S.-H. (2014). “Horizontal Shear Strength of Full-Scale Composite Box And Slab Bridge Beams Having Horizontal Shear Reinforcement with Limited Development Length,” 2014 PCI Convention and National Bridge Conference, September 6-9, 2014, Washington, D. C.

Zeno, G. A. (2009). "Use of High-Strength Steel Reinforcement in Shear Friction Applications.” (Master’s thesis). University of Pittsburgh.

APPENDICES

APPENDIX A

INTERFACE SHEAR FRICTION RESISTANCE DESIGN

4G60S6(1/8) Specimens

Calculated Input Manual check

From AASHTO (2015) section 5.8.4-Interface Shear Transfer-Shear Friction

AASHTO (2015) Section 5.8.4.3: Values interpolated between a cast-in-place concrete slab on clean concrete girder surfaces, free of laitance with surface roughened to an amplitude of 0.25 in. and concrete placed against a clean concrete surface, free of laitance, but not intentionally roughened.

Fraction of concrete strength available to resist the interface shear

$K_1 := 0.225$

Limiting interface shear resistance

$K_2 := 1.15ksi$ (1.8 ksi for normalweight)

Cohesion factor

$c_c := 0.1575ksi$

Coefficient of friction

$\mu := 0.8$

Specimen properties

Yield strength of the shear reinforcement

$f_y := 60\frac{kip}{in^2}$

Strength of concrete

$f_c := 5ksi$

Length of contact area

$L_s := 20in$

Width of contact area

$b := 12in$

Interface area of the concrete engaged in shear transfer

$A_{cv} := L_s \cdot b$ $A_{cv} = 240 \cdot in^2$

Size No. of rebar

$R_{no} := 4$

Number of U-bars

$N_r := 3$

Number of bar crossings through shear interface

$N_c := N_r \cdot 2$

Cross section of the shear reinforcement

$A_{vf} := \left(\frac{R_{no}\,in}{8 \cdot 2}\right)^2 \cdot \pi \cdot N_c$ $A_{vf} = 1.178 \cdot in^2$

Specimen shear strength determination

AASHTO (2012) 5.8.4.4
Minimum area of interface shear reinforcement

$Asmin := 0.05 \cdot \frac{A_{cv}}{\frac{f_y}{ksi}}$ $Asmin = 0.2 \cdot in^2$

Minimum area check

$A_{vf} > Asmin = 1$ If 1, then O.K.

AASHTO (2015) 5.5.4.2.1
LRFD shear factor

$\phi := 0.90$

Pressure normal to interface

$p_i := 0 \frac{lbf}{in^2}$

Required force normal to interface

$P_c := p_i \cdot A_{cv}$ $P_c = 0 \cdot kip$

AASHTO (2015) 5.8.4.1-3
Nominal shear strength

$V_n := c_c \cdot A_{cv} + \mu \cdot (A_{vf} \cdot f_y + P_c)$

$V_n = 94.349 \cdot kip$

Factored nominal shear strength

$\phi \cdot V_n = 84.914 \cdot kip$

V_n shall not be greater than the lesser of:

AASHTO (2015) 5.8.4.1-4

$V_{ni1} := K_1 \cdot f_c \cdot A_{cv}$ $V_{ni1} = 270 \cdot kip$ $V_n < V_{ni1} = 1$ If 1, then O.K.

AASHTO (2015) 5.8.4.1-5

$V_{ni2} := K_2 \cdot A_{cv}$ $V_{ni2} = 276 \cdot kip$ $V_n < V_{ni2} = 1$ If 1, then O.K.

4G80S6(1/8) Specimens

Calculated Input Manual check

From AASHTO (2015) section 5.8.4-Interface Shear Transfer-Shear Friction

AASHTO (2015) Section 5.8.4.3: Values interpolated between a cast-in-place concrete slab on clean concrete girder surfaces, free of laitance with surface roughened to an amplitude of 0.25 in. and concrete placed against a clean concrete surface, free of laitance, but not intentionally roughened.

Fraction of concrete strength available to resist the interface shear

$K_1 := 0.225$

Limiting interface shear resistance

$K_2 := 1.15ksi$ (1.8 ksi for normalweight)

Cohesion factor

$c_c := 0.1575ksi$

Coefficient of friction

$\mu := 0.8$

Specimen properties

Yield strength of the shear reinforcement

$f_y := 80\frac{kip}{in^2}$

Strength of concrete

$f_c := 5ksi$

Length of contact area

$L_s := 20in$

Width of contact area

$b := 12in$

Interface area of the concrete engaged in shear transfer

$A_{cv} := L_s \cdot b$ $A_{cv} = 240 \cdot in^2$

Size No. of rebar

$R_{no} := 4$

Number of U-bars

$N_r := 3$

Number of bar crossings through shear interface

$N_c := N_r \cdot 2$

Cross section of the shear reinforcement

$A_{vf} := \left(\frac{R_{no}\,in}{8 \cdot 2}\right)^2 \cdot \pi \cdot N_c$ $A_{vf} = 1.178 \cdot in^2$

Specimen shear strength determination

AASHTO (2012) 5.8.4.4
Minimum area of interface shear reinforcement

$Asmin := 0.05 \cdot \frac{A_{cv}}{\frac{f_y}{ksi}}$ $Asmin = 0.15 \cdot in^2$

Minimum area check

$A_{vf} > Asmin = 1$ If 1, then O.K.

AASHTO (2015) 5.5.4.2.1
LRFD shear factor

$\phi := 0.90$

Pressure normal to interface

$p_i := 0 \frac{lbf}{in^2}$

Required force normal to interface

$P_c := p_i \cdot A_{cv}$ $P_c = 0 \cdot kip$

AASHTO (2015) 5.8.4.1-3
Nominal shear strength

$V_n := c_c \cdot A_{cv} + \mu \cdot (A_{vf} \cdot f_y + P_c)$

$V_n = 113.198 \cdot kip$

Factored nominal shear strength

$\phi \cdot V_n = 101.878 \cdot kip$

V_n shall not be greater than the lesser of:

AASHTO (2015) 5.8.4.1-4

$V_{ni1} := K_1 \cdot f_c \cdot A_{cv}$ $V_{ni1} = 270 \cdot kip$ $V_n < V_{ni1} = 1$ If 1, then O.K.

AASHTO (2015) 5.8.4.1-5

$V_{ni2} := K_2 \cdot A_{cv}$ $V_{ni2} = 276 \cdot kip$ $V_n < V_{ni2} = 1$ If 1, then O.K.

4G100S6(1/8) Specimens

Calculated Input Manual check

From AASHTO (2015) section 5.8.4-Interface Shear Transfer-Shear Friction

AASHTO (2015) Section 5.8.4.3: Values interpolated between a cast-in-place concrete slab on clean concrete girder surfaces, free of laitance with surface roughened to an amplitude of 0.25 in. and concrete placed against a clean concrete surface, free of laitance, but not intentionally roughened.

Fraction of concrete strength available to resist the interface shear

$K_1 := 0.225$

Limiting interface shear resistance

$K_2 := 1.15ksi$ (1.8 ksi for normalweight)

Cohesion factor

$c_c := 0.1575ksi$

Coefficient of friction

$\mu := 0.8$

Specimen properties

Yield strength of the shear reinforcement

$f_y := 100\frac{kip}{in^2}$

Strength of concrete

$f_c := 5ksi$

Length of contact area

$L_s := 20in$

Width of contact area

$b := 12in$

Interface area of the concrete engaged in shear transfer

$A_{cv} := L_s \cdot b$ $A_{cv} = 240 \cdot in^2$

Size No. of rebar

$R_{no} := 4$

Number of U-bars

$N_r := 3$

Number of bar crossings through shear interface

$N_c := N_r \cdot 2$

Cross section of the shear reinforcement

$A_{vf} := \left(\frac{R_{no}\,in}{8 \cdot 2}\right)^2 \cdot \pi \cdot N_c$ $A_{vf} = 1.178 \cdot in^2$

Specimen shear strength determination

AASHTO (2012) 5.8.4.4
Minimum area of interface shear reinforcement

$Asmin := 0.05 \cdot \frac{A_{cv}}{\frac{f_y}{ksi}}$ $Asmin = 0.12 \cdot in^2$

Minimum area check

$A_{vf} > Asmin = 1$ If 1, then O.K.

AASHTO (2015) 5.5.4.2.1
LRFD shear factor

$\phi := 0.90$

Pressure normal to interface

$p_i := 0 \frac{lbf}{in^2}$

Required force normal to interface

$P_c := p_i \cdot A_{cv}$ $P_c = 0 \cdot kip$

AASHTO (2015) 5.8.4.1-3
Nominal shear strength

$V_n := c_c \cdot A_{cv} + \mu \cdot (A_{vf} \cdot f_y + P_c)$

$V_n = 132.048 \cdot kip$

Factored nominal shear strength

$\phi \cdot V_n = 118.843 \cdot kip$

V_n shall not be greater than the lesser of:

AASHTO (2015) 5.8.4.1-4

$V_{ni1} := K_1 \cdot f_c \cdot A_{cv}$ $V_{ni1} = 270 \cdot kip$

$V_n < V_{ni1} = 1$ If 1, then O.K.

AASHTO (2015) 5.8.4.1-5

$V_{ni2} := K_2 \cdot A_{cv}$ $V_{ni2} = 276 \cdot kip$

$V_n < V_{ni2} = 1$ If 1, then O.K.

4G120S6(1/8) Specimens

Calculated Input Manual check

From AASHTO (2015) section 5.8.4-Interface Shear Transfer-Shear Friction

AASHTO (2015) Section 5.8.4.3: Values interpolated between a cast-in-place concrete slab on clean concrete girder surfaces, free of laitance with surface roughened to an amplitude of 0.25 in. and concrete placed against a clean concrete surface, free of laitance, but not intentionally roughened.

Fraction of concrete strength available to resist the interface shear

$K_1 := 0.225$

Limiting interface shear resistance

$K_2 := 1.15ksi$ (1.8 ksi for normalweight)

Cohesion factor

$c_c := 0.1575ksi$

Coefficient of friction

$\mu := 0.8$

Specimen properties

Yield strength of the shear reinforcement

$f_y := 120\frac{kip}{in^2}$

Strength of concrete

$f_c := 5ksi$

Length of contact area

$L_s := 20in$

Width of contact area

$b := 12in$

Interface area of the concrete engaged in shear transfer

$A_{cv} := L_s \cdot b$ $A_{cv} = 240 \cdot in^2$

Size No. of rebar

$R_{no} := 4$

Number of U-bars

$N_r := 3$

Number of bar crossings through shear interface

$N_c := N_r \cdot 2$

Cross section of the shear reinforcement

$A_{vf} := \left(\frac{R_{no}\,in}{8 \cdot 2}\right)^2 \cdot \pi \cdot N_c$ $A_{vf} = 1.178 \cdot in^2$

Specimen shear strength determination

AASHTO (2012) 5.8.4.4
Minimum area of interface shear reinforcement

$Asmin := 0.05 \cdot \frac{A_{cv}}{\frac{f_y}{ksi}}$ $Asmin = 0.1 \cdot in^2$

Minimum area check

$A_{vf} > Asmin = 1$ If 1, then O.K.

AASHTO (2015) 5.5.4.2.1
LRFD shear factor

$\phi := 0.90$

Pressure normal to interface

$p_i := 0 \frac{lbf}{in^2}$

Required force normal to interface

$P_c := p_i \cdot A_{cv}$ $P_c = 0 \cdot kip$

AASHTO (2015) 5.8.4.1-3
Nominal shear strength

$V_n := c_c \cdot A_{cv} + \mu \cdot (A_{vf} \cdot f_y + P_c)$

$V_n = 150.897 \cdot kip$

Factored nominal shear strength

$\phi \cdot V_n = 135.808 \cdot kip$

V_n shall not be greater than the lesser of:

AASHTO (2015) 5.8.4.1-4

$V_{ni1} := K_1 \cdot f_c \cdot A_{cv}$ $V_{ni1} = 270 \cdot kip$

$V_n < V_{ni1} = 1$ If 1, then O.K.

AASHTO (2015) 5.8.4.1-5

$V_{ni2} := K_2 \cdot A_{cv}$ $V_{ni2} = 276 \cdot kip$

$V_n < V_{ni2} = 1$ If 1, then O.K.

4G80S6(AC) Specimens

Calculated Input Manual check

From AASHTO (2015) section 5.8.4-Interface Shear Transfer-Shear Friction

AASHTO (2015) Section 5.8.4.3: Values for concrete placed against a clean concrete surface, free of laitance, but not intentionally roughened.

Fraction of concrete strength available to resist the interface shear	$K_1 := 0.200$	
Limiting interface shear resistance	$K_2 := 0.80ksi$	(1.8 ksi for normalweight)
Cohesion factor	$c_c := 0.075ksi$	
Coefficient of friction	$\mu := 0.6$	

Specimen properties

Yield strength of the shear reinforcement	$f_y := 80\frac{kip}{in^2}$	
Strength of concrete	$f_c := 5ksi$	
Length of contact area	$L_s := 20in$	
Width of contact area	$b := 12in$	
Interface area of the concrete engaged in shear transfer	$A_{cv} := L_s \cdot b$	$A_{cv} = 240 \cdot in^2$
Size No. of rebar	$R_{no} := 4$	
Number of U-bars	$N_r := 3$	
Number of bar crossings through shear interface	$N_c := N_r \cdot 2$	
Cross section of the shear reinforcement	$A_{vf} := \left(\frac{R_{no}\,in}{8 \cdot 2}\right)^2 \cdot \pi \cdot N_c$	$A_{vf} = 1.178 \cdot in^2$

Specimen shear strength determination

AASHTO (2012) 5.8.4.4 Minimum area of interface shear reinforcement	$Asmin := 0.05 \cdot \frac{A_{cv}}{\frac{f_y}{ksi}}$	$Asmin = 0.15 \cdot in^2$

Minimum area check

$A_{vf} > Asmin = 1$ If 1, then O.K.

AASHTO (2015) 5.5.4.2.1
LRFD shear factor

$\phi := 0.90$

Pressure normal to interface

$p_i := 0 \frac{lbf}{in^2}$

Required force normal to interface

$P_c := p_i \cdot A_{cv}$ $P_c = 0 \cdot kip$

AASHTO (2015) 5.8.4.1-3
Nominal shear strength

$V_n := c_c \cdot A_{cv} + \mu \cdot (A_{vf} \cdot f_y + P_c)$

$V_n = 74.549 \cdot kip$

Factored nominal shear strength

$\phi \cdot V_n = 67.094 \cdot kip$

V_n shall not be greater than the lesser of:

AASHTO (2015) 5.8.4.1-4

$V_{ni1} := K_1 \cdot f_c \cdot A_{cv}$ $V_{ni1} = 240 \cdot kip$ $V_n < V_{ni1} = 1$ If 1, then O.K.

AASHTO (2015) 5.8.4.1-5

$V_{ni2} := K_2 \cdot A_{cv}$ $V_{ni2} = 192 \cdot kip$ $V_n < V_{ni2} = 1$ If 1, then O.K.

4G80S6(1/4) Specimens

Calculated Input Manual check

From AASHTO (2015) section 5.8.4-Interface Shear Transfer-Shear Friction

AASHTO (2015) Section 5.8.4.3: Values for cast-in-place concrete slab on clean concrete girder surfaces, free of laitance with surface roughened to an amplitude of 0.25 in.

Fraction of concrete strength available to resist the interface shear

$K_1 := 0.250$

Limiting interface shear resistance

$K_2 := 1.50ksi$ (1.8 ksi for normalweight)

Cohesion factor

$c_c := 0.24ksi$

Coefficient of friction

$\mu := 1.0$

Specimen properties

Yield strength of the shear reinforcement

$f_y := 80\frac{kip}{in^2}$

Strength of concrete

$f_c := 5ksi$

Length of contact area

$L_s := 20in$

Width of contact area

$b := 12in$

Interface area of the concrete engaged in shear transfer

$A_{cv} := L_s \cdot b$ $A_{cv} = 240 \cdot in^2$

Size No. of rebar

$R_{no} := 4$

Number of U-bars

$N_r := 3$

Number of bar crossings through shear interface

$N_c := N_r \cdot 2$

Cross section of the shear reinforcement

$A_{vf} := \left(\frac{R_{no}\,in}{8 \cdot 2}\right)^2 \cdot \pi \cdot N_c$ $A_{vf} = 1.178 \cdot in^2$

Specimen shear strength determination

AASHTO (2012) 5.8.4.4
Minimum area of interface shear reinforcement

$Asmin := 0.05 \cdot \frac{A_{cv}}{\frac{f_y}{ksi}}$ $Asmin = 0.15 \cdot in^2$

Minimum area check

$A_{vf} > Asmin = 1$ If 1, then O.K.

AASHTO (2015) 5.5.4.2.1
LRFD shear factor

$\phi := 0.90$

Pressure normal to interface

$p_i := 0 \frac{lbf}{in^2}$

Required force normal to interface

$P_c := p_i \cdot A_{cv}$ $P_c = 0 \cdot kip$

AASHTO (2015) 5.8.4.1-3
Nominal shear strength

$V_n := c_c \cdot A_{cv} + \mu \cdot (A_{vf} \cdot f_y + P_c)$

$V_n = 151.848 \cdot kip$

Factored nominal shear strength

$\phi \cdot V_n = 136.663 \cdot kip$

V_n shall not be greater than the lesser of:

AASHTO (2015) 5.8.4.1-4

$V_{ni1} := K_1 \cdot f_c \cdot A_{cv}$ $V_{ni1} = 300 \cdot kip$

$V_n < V_{ni1} = 1$ If 1, then O.K.

AASHTO (2015) 5.8.4.1-5

$V_{ni2} := K_2 \cdot A_{cv}$ $V_{ni2} = 360 \cdot kip$

$V_n < V_{ni2} = 1$ If 1, then O.K.

4G80S6(EA) Specimens

Calculated Input Manual check

From AASHTO (2015) section 5.8.4-Interface Shear Transfer-Shear Friction

AASHTO (2015) Section 5.8.4.3: Values interpolated between a cast-in-place concrete slab on clean concrete girder surfaces, free of laitance with surface roughened to an amplitude of 0.125 in. and concrete placed against a clean concrete surface, free of laitance, but not intentionally roughened.

Fraction of concrete strength available to resist the interface shear

$K_1 := 0.213$

Limiting interface shear resistance

$K_2 := 0.975ksi$ (1.8 ksi for normalweight)

Cohesion factor

$c_c := 0.1163ksi$

Coefficient of friction

$\mu := 0.7$

Specimen properties

Yield strength of the shear reinforcement

$f_y := 80\frac{kip}{in^2}$

Strength of concrete

$f_c := 5ksi$

Length of contact area

$L_s := 20in$

Width of contact area

$b := 12in$

Interface area of the concrete engaged in shear transfer

$A_{cv} := L_s \cdot b$ $A_{cv} = 240 \cdot in^2$

Size No. of rebar

$R_{no} := 4$

Number of U-bars

$N_r := 3$

Number of bar crossings through shear interface

$N_c := N_r \cdot 2$

Cross section of the shear reinforcement

$A_{vf} := \left(\frac{R_{no}\,in}{8 \cdot 2}\right)^2 \cdot \pi \cdot N_c$ $A_{vf} = 1.178 \cdot in^2$

Specimen shear strength determination

AASHTO (2012) 5.8.4.4
Minimum area of interface shear reinforcement

$Asmin := 0.05 \cdot \frac{A_{cv}}{\frac{f_y}{ksi}}$ $Asmin = 0.15 \cdot in^2$

Minimum area check

$A_{vf} > Asmin = 1$ If 1, then O.K.

AASHTO (2015) 5.5.4.2.1
LRFD shear factor

$\phi := 0.90$

Pressure normal to interface

$p_i := 0 \frac{lbf}{in^2}$

Required force normal to interface

$P_c := p_i \cdot A_{cv}$ $P_c = 0 \cdot kip$

AASHTO (2015) 5.8.4.1-3
Nominal shear strength

$V_n := c_c \cdot A_{cv} + \mu \cdot (A_{vf} \cdot f_y + P_c)$

$V_n = 93.885 \cdot kip$

Factored nominal shear strength

$\phi \cdot V_n = 84.497 \cdot kip$

V_n shall not be greater than the lesser of:

AASHTO (2015) 5.8.4.1-4

$V_{ni1} := K_1 \cdot f_c \cdot A_{cv}$ $V_{ni1} = 255.6 \cdot kip$ $V_n < V_{ni1} = 1$ If 1, then O.K.

AASHTO (2015) 5.8.4.1-5

$V_{ni2} := K_2 \cdot A_{cv}$ $V_{ni2} = 234 \cdot kip$ $V_n < V_{ni2} = 1$ If 1, then O.K.

4G80S4(1/8) Specimens

Calculated Input Manual check

From AASHTO (2015) section 5.8.4-Interface Shear Transfer-Shear Friction

AASHTO (2015) Section 5.8.4.3: Values interpolated between a cast-in-place concrete slab on clean concrete girder surfaces, free of laitance with surface roughened to an amplitude of 0.25 in. and concrete placed against a clean concrete surface, free of laitance, but not intentionally roughened.

Fraction of concrete strength available to resist the interface shear

$K_1 := 0.225$

Limiting interface shear resistance

$K_2 := 1.15\text{ksi}$ (1.8 ksi for normalweight)

Cohesion factor

$c_c := 0.1575\text{ksi}$

Coefficient of friction

$\mu := 0.8$

Specimen properties

Yield strength of the shear reinforcement

$f_y := 80\frac{\text{kip}}{\text{in}^2}$

Strength of concrete

$f_c := 5\text{ksi}$

Length of contact area

$L_s := 20\text{in}$

Width of contact area

$b := 12\text{in}$

Interface area of the concrete engaged in shear transfer

$A_{cv} := L_s \cdot b$ $A_{cv} = 240\cdot\text{in}^2$

Size No. of rebar

$R_{no} := 4$

Number of U-bars

$N_r := 4$

Number of bar crossings through shear interface

$N_c := N_r \cdot 2$

Cross section of the shear reinforcement

$A_{vf} := \left(\frac{R_{no}\,\text{in}}{8\cdot 2}\right)^2 \cdot \pi \cdot N_c$ $A_{vf} = 1.571\cdot\text{in}^2$

Specimen shear strength determination

AASHTO (2012) 5.8.4.4
Minimum area of interface shear reinforcement

$Asmin := 0.05\cdot\frac{A_{cv}}{\frac{f_y}{\text{ksi}}}$ $Asmin = 0.15\cdot\text{in}^2$

Minimum area check

$A_{vf} > Asmin = 1$ If 1, then O.K.

AASHTO (2015) 5.5.4.2.1
LRFD shear factor

$\phi := 0.90$

Pressure normal to interface

$p_i := 0 \frac{lbf}{in^2}$

Required force normal to interface

$P_c := p_i \cdot A_{cv}$ $P_c = 0 \cdot kip$

AASHTO (2015) 5.8.4.1-3
Nominal shear strength

$V_n := c_c \cdot A_{cv} + \mu \cdot (A_{vf} \cdot f_y + P_c)$

$V_n = 138.331 \cdot kip$

Factored nominal shear strength

$\phi \cdot V_n = 124.498 \cdot kip$

V_n shall not be greater than the lesser of:

AASHTO (2015) 5.8.4.1-4

$V_{ni1} := K_1 \cdot f_c \cdot A_{cv}$ $V_{ni1} = 270 \cdot kip$ $V_n < V_{ni1} = 1$ If 1, then O.K.

AASHTO (2015) 5.8.4.1-5

$V_{ni2} := K_2 \cdot A_{cv}$ $V_{ni2} = 276 \cdot kip$ $V_n < V_{ni2} = 1$ If 1, then O.K.

4G80S12(1/8) Specimens

Calculated Input Manual check

From AASHTO (2015) section 5.8.4-Interface Shear Transfer-Shear Friction

AASHTO (2015) Section 5.8.4.3: Values interpolated between a cast-in-place concrete slab on clean concrete girder surfaces, free of laitance with surface roughened to an amplitude of 0.25 in. and concrete placed against a clean concrete surface, free of laitance, but not intentionally roughened.

Fraction of concrete strength available to resist the interface shear

$K_1 := 0.225$

Limiting interface shear resistance

$K_2 := 1.15ksi$ (1.8 ksi for normalweight)

Cohesion factor

$c_c := 0.1575ksi$

Coefficient of friction

$\mu := 0.8$

Specimen properties

Yield strength of the shear reinforcement

$f_y := 80\frac{kip}{in^2}$

Strength of concrete

$f_c := 5ksi$

Length of contact area

$L_s := 20in$

Width of contact area

$b := 12in$

Interface area of the concrete engaged in shear transfer

$A_{cv} := L_s \cdot b$ $A_{cv} = 240 \cdot in^2$

Size No. of rebar

$R_{no} := 4$

Number of U-bars

$N_r := 2$

Number of bar crossings through shear interface

$N_c := N_r \cdot 2$

Cross section of the shear reinforcement

$A_{vf} := \left(\frac{R_{no}\,in}{8 \cdot 2}\right)^2 \cdot \pi \cdot N_c$ $A_{vf} = 0.785 \cdot in^2$

Specimen shear strength determination

AASHTO (2012) 5.8.4.4
Minimum area of interface shear reinforcement

$Asmin := 0.05 \cdot \frac{A_{cv}}{\frac{f_y}{ksi}}$ $Asmin = 0.15 \cdot in^2$

Minimum area check

$A_{vf} > Asmin = 1$ If 1, then O.K.

AASHTO (2015) 5.5.4.2.1
LRFD shear factor

$\phi := 0.90$

Pressure normal to interface

$p_i := 0 \frac{lbf}{in^2}$

Required force normal to interface

$P_c := p_i \cdot A_{cv}$ $P_c = 0 \cdot kip$

AASHTO (2015) 5.8.4.1-3
Nominal shear strength

$V_n := c_c \cdot A_{cv} + \mu \cdot (A_{vf} \cdot f_y + P_c)$

$V_n = 88.065 \cdot kip$

Factored nominal shear strength

$\phi \cdot V_n = 79.259 \cdot kip$

V_n shall not be greater than the lesser of:

AASHTO (2015) 5.8.4.1-4

$V_{ni1} := K_1 \cdot f_c \cdot A_{cv}$ $V_{ni1} = 270 \cdot kip$

$V_n < V_{ni1} = 1$ If 1, then O.K.

AASHTO (2015) 5.8.4.1-5

$V_{ni2} := K_2 \cdot A_{cv}$ $V_{ni2} = 276 \cdot kip$

$V_n < V_{ni2} = 1$ If 1, then O.K.

5G80S6(AC) Specimens

Calculated Input Manual check

From AASHTO (2015) section 5.8.4-Interface Shear Transfer-Shear Friction

AASHTO (2015) Section 5.8.4.3: Values for concrete placed against a clean concrete surface, free of laitance, but not intentionally roughened.

Fraction of concrete strength available to resist the interface shear	$K_1 := 0.200$	
Limiting interface shear resistance	$K_2 := 0.80\text{ksi}$	(1.8 ksi for normalweight)
Cohesion factor	$c_c := 0.075\text{ksi}$	
Coefficient of friction	$\mu := 0.6$	

Specimen properties

Yield strength of the shear reinforcement	$f_y := 80\frac{\text{kip}}{\text{in}^2}$	
Strength of concrete	$f_c := 5\text{ksi}$	
Length of contact area	$L_s := 20\text{in}$	
Width of contact area	$b := 12\text{in}$	
Interface area of the concrete engaged in shear transfer	$A_{cv} := L_s \cdot b$	$A_{cv} = 240\cdot\text{in}^2$
Size No. of rebar	$R_{no} := 5$	
Number of U-bars	$N_r := 3$	
Number of bar crossings through shear interface	$N_c := N_r \cdot 2$	
Cross section of the shear reinforcement	$A_{vf} := \left(\frac{R_{no}\,\text{in}}{8\cdot 2}\right)^2 \cdot \pi \cdot N_c$	$A_{vf} = 1.841\cdot\text{in}^2$

Specimen shear strength determination

AASHTO (2012) 5.8.4.4 Minimum area of interface shear reinforcement	$Asmin := 0.05\cdot\frac{A_{cv}}{\frac{f_y}{\text{ksi}}}$	$Asmin = 0.15\cdot\text{in}^2$

Minimum area check

$A_{vf} > Asmin = 1$ If 1, then O.K.

AASHTO (2015) 5.5.4.2.1
LRFD shear factor

$\phi := 0.90$

Pressure normal to interface

$p_i := 0 \frac{lbf}{in^2}$

Required force normal to interface

$P_c := p_i \cdot A_{cv}$ $P_c = 0 \cdot kip$

AASHTO (2015) 5.8.4.1-3
Nominal shear strength

$V_n := c_c \cdot A_{cv} + \mu \cdot (A_{vf} \cdot f_y + P_c)$

$V_n = 106.357 \cdot kip$

Factored nominal shear strength

$\phi \cdot V_n = 95.722 \cdot kip$

V_n shall not be greater than the lesser of:

AASHTO (2015) 5.8.4.1-4

$V_{ni1} := K_1 \cdot f_c \cdot A_{cv}$ $V_{ni1} = 240 \cdot kip$ $V_n < V_{ni1} = 1$ If 1, then O.K.

AASHTO (2015) 5.8.4.1-5

$V_{ni2} := K_2 \cdot A_{cv}$ $V_{ni2} = 192 \cdot kip$ $V_n < V_{ni2} = 1$ If 1, then O.K.

5G80S6(1/8) Specimens

Calculated Input Manual check

From AASHTO (2015) section 5.8.4-Interface Shear Transfer-Shear Friction

AASHTO (2015) Section 5.8.4.3: Values interpolated between a cast-in-place concrete slab on clean concrete girder surfaces, free of laitance with surface roughened to an amplitude of 0.25 in. and concrete placed against a clean concrete surface, free of laitance, but not intentionally roughened.

Fraction of concrete strength available to resist the interface shear

$K_1 := 0.225$

Limiting interface shear resistance

$K_2 := 1.15ksi$ (1.8 ksi for normalweight)

Cohesion factor

$c_c := 0.1575ksi$

Coefficient of friction

$\mu := 0.8$

Specimen properties

Yield strength of the shear reinforcement

$f_y := 80\frac{kip}{in^2}$

Strength of concrete

$f_c := 5ksi$

Length of contact area

$L_s := 20in$

Width of contact area

$b := 12in$

Interface area of the concrete engaged in shear transfer

$A_{cv} := L_s \cdot b$ $A_{cv} = 240 \cdot in^2$

Size No. of rebar

$R_{no} := 5$

Number of U-bars

$N_r := 3$

Number of bar crossings through shear interface

$N_c := N_r \cdot 2$

Cross section of the shear reinforcement

$A_{vf} := \left(\frac{R_{no}\,in}{8 \cdot 2}\right)^2 \cdot \pi \cdot N_c$ $A_{vf} = 1.841 \cdot in^2$

Specimen shear strength determination

AASHTO (2012) 5.8.4.4
Minimum area of interface shear reinforcement

$Asmin := 0.05 \cdot \frac{A_{cv}}{\frac{f_y}{ksi}}$ $Asmin = 0.15 \cdot in^2$

Minimum area check

$A_{vf} > Asmin = 1$ If 1, then O.K.

AASHTO (2015) 5.5.4.2.1
LRFD shear factor

$\phi := 0.90$

Pressure normal to interface

$p_i := 0 \frac{lbf}{in^2}$

Required force normal to interface

$P_c := p_i \cdot A_{cv}$ $P_c = 0 \cdot kip$

AASHTO (2015) 5.8.4.1-3
Nominal shear strength

$V_n := c_c \cdot A_{cv} + \mu \cdot (A_{vf} \cdot f_y + P_c)$

$V_n = 155.61 \cdot kip$

Factored nominal shear strength

$\phi \cdot V_n = 140.049 \cdot kip$

V_n shall not be greater than the lesser of:

AASHTO (2015) 5.8.4.1-4

$V_{ni1} := K_1 \cdot f_c \cdot A_{cv}$ $V_{ni1} = 270 \cdot kip$ $V_n < V_{ni1} = 1$ If 1, then O.K.

AASHTO (2015) 5.8.4.1-5

$V_{ni2} := K_2 \cdot A_{cv}$ $V_{ni2} = 276 \cdot kip$ $V_n < V_{ni2} = 1$ If 1, then O.K.

5G80S6(1/4) Specimens

Calculated Input Manual check

From AASHTO (2015) section 5.8.4-Interface Shear Transfer-Shear Friction

AASHTO (2015) Section 5.8.4.3: Values for cast-in-place concrete slab on clean concrete girder surfaces, free of laitance with surface roughened to an amplitude of 0.25 in.

Fraction of concrete strength available to resist the interface shear

$K_1 := 0.250$

Limiting interface shear resistance

$K_2 := 1.50ksi$ (1.8 ksi for normalweight)

Cohesion factor

$c_c := 0.24ksi$

Coefficient of friction

$\mu := 1.0$

Specimen properties

Yield strength of the shear reinforcement

$f_y := 80\frac{kip}{in^2}$

Strength of concrete

$f_c := 5ksi$

Length of contact area

$L_s := 20in$

Width of contact area

$b := 12in$

Interface area of the concrete engaged in shear transfer

$A_{cv} := L_s \cdot b$ $A_{cv} = 240 \cdot in^2$

Size No. of rebar

$R_{no} := 5$

Number of U-bars

$N_r := 3$

Number of bar crossings through shear interface

$N_c := N_r \cdot 2$

Cross section of the shear reinforcement

$A_{vf} := \left(\frac{R_{no}\,in}{8 \cdot 2}\right)^2 \cdot \pi \cdot N_c$ $A_{vf} = 1.841 \cdot in^2$

Specimen shear strength determination

AASHTO (2012) 5.8.4.4
Minimum area of interface shear reinforcement

$Asmin := 0.05 \cdot \frac{A_{cv}}{\frac{f_y}{ksi}}$ $Asmin = 0.15 \cdot in^2$

Minimum area check

$A_{vf} > Asmin = 1$ If 1, then O.K.

AASHTO (2015) 5.5.4.2.1
LRFD shear factor

$\phi := 0.90$

Pressure normal to interface

$p_i := 0 \frac{lbf}{in^2}$

Required force normal to interface

$P_c := p_i \cdot A_{cv}$ $P_c = 0 \cdot kip$

AASHTO (2015) 5.8.4.1-3
Nominal shear strength

$V_n := c_c \cdot A_{cv} + \mu \cdot (A_{vf} \cdot f_y + P_c)$

$V_n = 204.862 \cdot kip$

Factored nominal shear strength

$\phi \cdot V_n = 184.376 \cdot kip$

V_n shall not be greater than the lesser of:

AASHTO (2015) 5.8.4.1-4

$V_{ni1} := K_1 \cdot f_c \cdot A_{cv}$ $V_{ni1} = 300 \cdot kip$ $V_n < V_{ni1} = 1$ If 1, then O.K.

AASHTO (2015) 5.8.4.1-5

$V_{ni2} := K_2 \cdot A_{cv}$ $V_{ni2} = 360 \cdot kip$ $V_n < V_{ni2} = 1$ If 1, then O.K.

5G80S6(EA) Specimens

Calculated Input Manual check

From AASHTO (2015) section 5.8.4-Interface Shear Transfer-Shear Friction

AASHTO (2015) Section 5.8.4.3: Values interpolated between a cast-in-place concrete slab on clean concrete girder surfaces, free of laitance with surface roughened to an amplitude of 0.125 in. and concrete placed against a clean concrete surface, free of laitance, but not intentionally roughened.

Fraction of concrete strength available to resist the interface shear

$K_1 := 0.213$

Limiting interface shear resistance

$K_2 := 0.975\text{ksi}$ (1.8 ksi for normalweight)

Cohesion factor

$c_c := 0.1163\text{ksi}$

Coefficient of friction

$\mu := 0.7$

Specimen properties

Yield strength of the shear reinforcement

$f_y := 80\frac{\text{kip}}{\text{in}^2}$

Strength of concrete

$f_c := 5\text{ksi}$

Length of contact area

$L_s := 20\text{in}$

Width of contact area

$b := 12\text{in}$

Interface area of the concrete engaged in shear transfer

$A_{cv} := L_s \cdot b$ $A_{cv} = 240 \cdot \text{in}^2$

Size No. of rebar

$R_{no} := 5$

Number of U-bars

$N_r := 3$

Number of bar crossings through shear interface

$N_c := N_r \cdot 2$

Cross section of the shear reinforcement

$A_{vf} := \left(\frac{R_{no}\,\text{in}}{8 \cdot 2}\right)^2 \cdot \pi \cdot N_c$ $A_{vf} = 1.841 \cdot \text{in}^2$

Specimen shear strength determination

AASHTO (2012) 5.8.4.4
Minimum area of interface shear reinforcement

$Asmin := 0.05 \cdot \frac{A_{cv}}{\frac{f_y}{\text{ksi}}}$ $Asmin = 0.15 \cdot \text{in}^2$

Minimum area check

$A_{vf} > Asmin = 1$ If 1, then O.K.

AASHTO (2015) 5.5.4.2.1
LRFD shear factor

$\phi := 0.90$

Pressure normal to interface

$p_i := 0 \frac{lbf}{in^2}$

Required force normal to interface

$P_c := p_i \cdot A_{cv}$ $P_c = 0 \cdot kip$

AASHTO (2015) 5.8.4.1-3
Nominal shear strength

$V_n := c_c \cdot A_{cv} + \mu \cdot (A_{vf} \cdot f_y + P_c)$

$V_n = 130.996 \cdot kip$

Factored nominal shear strength

$\phi \cdot V_n = 117.896 \cdot kip$

V_n shall not be greater than the lesser of:

AASHTO (2015) 5.8.4.1-4

$V_{ni1} := K_1 \cdot f_c \cdot A_{cv}$ $V_{ni1} = 255.6 \cdot kip$ $V_n < V_{ni1} = 1$ If 1, then O.K.

AASHTO (2015) 5.8.4.1-5

$V_{ni2} := K_2 \cdot A_{cv}$ $V_{ni2} = 234 \cdot kip$ $V_n < V_{ni2} = 1$ If 1, then O.K.

4G80S6F3(1/8) Specimens

Calculated Input Manual check

From AASHTO (2015) section 5.8.4-Interface Shear Transfer-Shear Friction

AASHTO (2015) Section 5.8.4.3: Values interpolated between a cast-in-place concrete slab on clean concrete girder surfaces, free of laitance with surface roughened to an amplitude of 0.25 in. and concrete placed against a clean concrete surface, free of laitance, but not intentionally roughened.

Fraction of concrete strength available to resist the interface shear

$K_1 := 0.225$

Limiting interface shear resistance

$K_2 := 1.15ksi$ (1.8 ksi for normalweight)

Cohesion factor

$c_c := 0.1575ksi$

Coefficient of friction

$\mu := 0.8$

Specimen properties

Yield strength of the shear reinforcement

$f_y := 80\frac{kip}{in^2}$

Strength of concrete

$f_c := 3ksi$

Length of contact area

$L_s := 20in$

Width of contact area

$b := 12in$

Interface area of the concrete engaged in shear transfer

$A_{cv} := L_s \cdot b$ $A_{cv} = 240 \cdot in^2$

Size No. of rebar

$R_{no} := 4$

Number of U-bars

$N_r := 3$

Number of bar crossings through shear interface

$N_c := N_r \cdot 2$

Cross section of the shear reinforcement

$A_{vf} := \left(\frac{R_{no}\,in}{8 \cdot 2}\right)^2 \cdot \pi \cdot N_c$ $A_{vf} = 1.178 \cdot in^2$

Specimen shear strength determination

AASHTO (2012) 5.8.4.4
Minimum area of interface shear reinforcement

$Asmin := 0.05 \cdot \frac{A_{cv}}{\frac{f_y}{ksi}}$ $Asmin = 0.15 \cdot in^2$

Minimum area check

$A_{vf} > Asmin = 1$ If 1, then O.K.

AASHTO (2015) 5.5.4.2.1
LRFD shear factor

$\phi := 0.90$

Pressure normal to interface

$p_i := 0 \frac{lbf}{in^2}$

Required force normal to interface

$P_c := p_i \cdot A_{cv}$ $P_c = 0 \cdot kip$

AASHTO (2015) 5.8.4.1-3
Nominal shear strength

$V_n := c_c \cdot A_{cv} + \mu \cdot (A_{vf} \cdot f_y + P_c)$

$V_n = 113.198 \cdot kip$

Factored nominal shear strength

$\phi \cdot V_n = 101.878 \cdot kip$

V_n shall not be greater than the lesser of:

AASHTO (2015) 5.8.4.1-4

$V_{ni1} := K_1 \cdot f_c \cdot A_{cv}$ $V_{ni1} = 162 \cdot kip$ $V_n < V_{ni1} = 1$ If 1, then O.K.

AASHTO (2015) 5.8.4.1-5

$V_{ni2} := K_2 \cdot A_{cv}$ $V_{ni2} = 276 \cdot kip$ $V_n < V_{ni2} = 1$ If 1, then O.K.

4G80S6F6(1/8) Specimens

Calculated Input Manual check

From AASHTO (2015) section 5.8.4-Interface Shear Transfer-Shear Friction

AASHTO (2015) Section 5.8.4.3: Values interpolated between a cast-in-place concrete slab on clean concrete girder surfaces, free of laitance with surface roughened to an amplitude of 0.25 in. and concrete placed against a clean concrete surface, free of laitance, but not intentionally roughened.

Fraction of concrete strength available to resist the interface shear

$K_1 := 0.225$

Limiting interface shear resistance

$K_2 := 1.15ksi$ (1.8 ksi for normalweight)

Cohesion factor

$c_c := 0.1575ksi$

Coefficient of friction

$\mu := 0.8$

Specimen properties

Yield strength of the shear reinforcement

$f_y := 80\frac{kip}{in^2}$

Strength of concrete

$f_c := 6ksi$

Length of contact area

$L_s := 20in$

Width of contact area

$b := 12in$

Interface area of the concrete engaged in shear transfer

$A_{cv} := L_s \cdot b$ $A_{cv} = 240 \cdot in^2$

Size No. of rebar

$R_{no} := 4$

Number of U-bars

$N_r := 3$

Number of bar crossings through shear interface

$N_c := N_r \cdot 2$

Cross section of the shear reinforcement

$A_{vf} := \left(\frac{R_{no}\,in}{8 \cdot 2}\right)^2 \cdot \pi \cdot N_c$ $A_{vf} = 1.178 \cdot in^2$

Specimen shear strength determination

AASHTO (2012) 5.8.4.4
Minimum area of interface shear reinforcement

$Asmin := 0.05 \cdot \frac{A_{cv}}{\frac{f_y}{ksi}}$ $Asmin = 0.15 \cdot in^2$

Minimum area check

$A_{vf} > Asmin = 1$ If 1, then O.K.

AASHTO (2015) 5.5.4.2.1
LRFD shear factor

$\phi := 0.90$

Pressure normal to interface

$p_i := 0 \frac{lbf}{in^2}$

Required force normal to interface

$P_c := p_i \cdot A_{cv}$ $P_c = 0 \cdot kip$

AASHTO (2015) 5.8.4.1-3
Nominal shear strength

$V_n := c_c \cdot A_{cv} + \mu \cdot (A_{vf} \cdot f_y + P_c)$

$V_n = 113.198 \cdot kip$

Factored nominal shear strength

$\phi \cdot V_n = 101.878 \cdot kip$

V_n shall not be greater than the lesser of:

AASHTO (2015) 5.8.4.1-4

$V_{ni1} := K_1 \cdot f_c \cdot A_{cv}$ $V_{ni1} = 324 \cdot kip$ $V_n < V_{ni1} = 1$ If 1, then O.K.

AASHTO (2015) 5.8.4.1-5

$V_{ni2} := K_2 \cdot A_{cv}$ $V_{ni2} = 276 \cdot kip$ $V_n < V_{ni2} = 1$ If 1, then O.K.

APPENDIX B

PUSH-OFF TEST SPECIMEN STRUT-AND-TIE MODEL

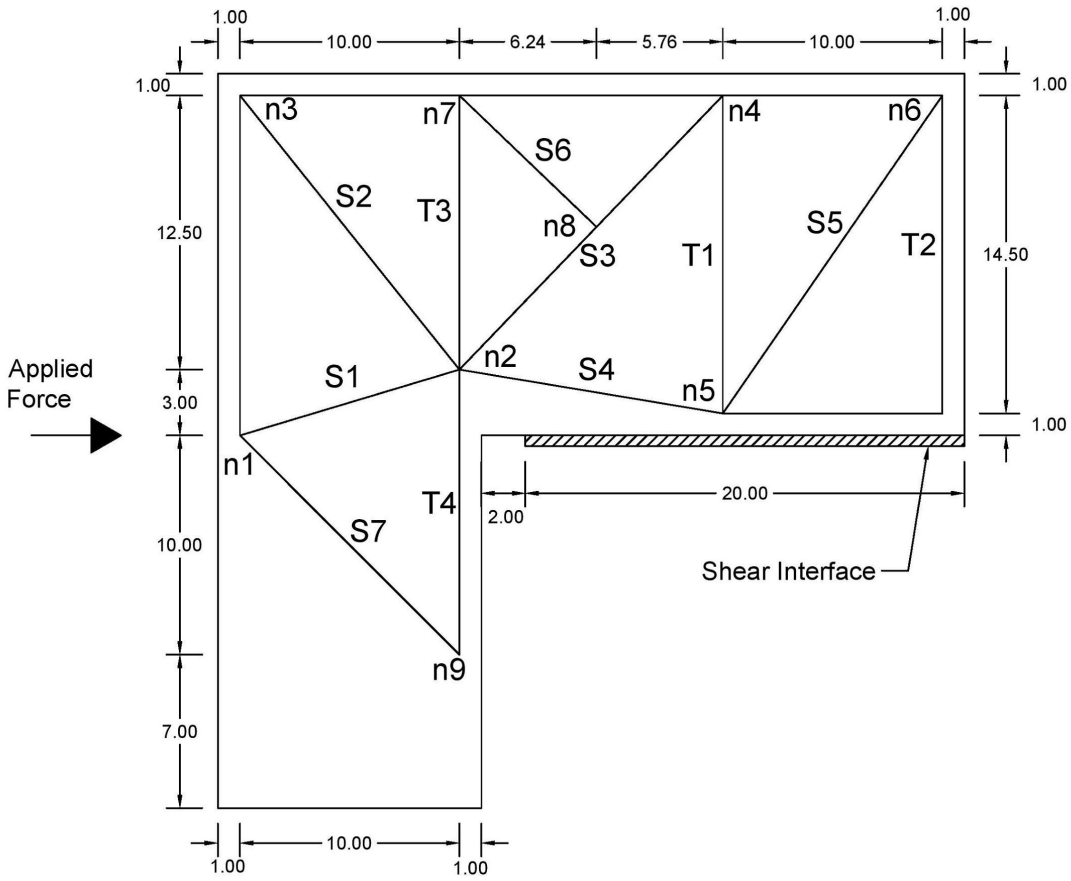

Strut and tie method for test specimen design

Step 1.) Adjust input values according to specimen properties

Need to check value according to instructions highlighted

Input Values

Design load $P := 500kip$

Reinforced concrete specific weight. $\gamma_c := 150 \frac{lbf}{ft^3}$

Nominal compressive strength of concrete. $f'_c := 5500psi$

Nominal yield stress of reinforcing steel. $f_y := 60ksi$

L shape width $b := 16in$

Phi factor for tension in steel in anchorage zones $\phi_n := 0.9$

Phi factor for compression in strut and tie model, Sec. 5.5.4.2. $\phi_{stm} := 0.7$

Step 2.) Compute and check strut s1 according to AASHTO (2014) Sec. 5.6.3.3

Vertical Distance Between Node 1 and 2 $L_{p12} := 3.0in$

Horizontal Distance between Node 1 and 2 $L_{w12} := 10.0in$

$\varepsilon_{s1} := 0.002$ Tensile strain in the concrete in the direction of the tension tie (in./in.)

$L_{s1} := \left(L_{w12}^{\ 2} + L_{p12}^{\ 2}\right)^{\frac{1}{2}} = 10.44 \cdot in$ Length of compression strut s1.

$a_1 := \operatorname{atan}\left(\frac{L_{p12}}{L_{w12}}\right) \cdot rad \quad a_1 = 16.699 \cdot deg$ Angle of strut one measured to the horizontal

AASHTO (2014) Figure 5.6.3.3.2-1

$l_{b1} := 7.118in$ Height of effective bearing plate

$h_{a1} := 6 \cdot \left(\frac{6}{8}\right) in + \left(\frac{6}{8}\ \frac{in}{2}\right) \quad h_{a1} = 4.875 \cdot in$

$l_{a1s} := l_{b1} \cdot \sin(a_1) + h_{a1} \cdot \cos(a_1) \quad l_{a1s} = 6.715 \cdot in$ Width of strut 1 on n1 side

$l_{a1t} := 4.84in \cdot 2 \quad l_{a1t} = 9.68 \cdot in$ Width of strut 1 on node 2 side

$A_{cs1} := \min\left(1.35 l_{a1s} \cdot b, l_{a1t} \cdot b\right) \quad A_{cs1} = 145.039 \cdot in^2$ Approximation of the effective area of strut s1. An overstrength of 1.35 is considered for the testing.

$\varepsilon_{1s1} := \varepsilon_{s1} + \left(\varepsilon_{s1} + 0.002\right) \cdot \cot\left(90deg - a_1\right)^2$ Eq. 5.6.3.3.3-2

$f_{cus1} := \left[\frac{f'_c}{\left(0.8 + 170 \cdot \varepsilon_{1s1}\right)}\right] \quad f_{cus1} = 4.579 \cdot ksi$ Eq. 5.6.3.3.3-1

$0.85 f'_c = 4.675 \cdot ksi$ Maximum value for fcu. Eq. 5.6.3.3.3-1

$f_{cus1} < 0.85 f'_c$ OK

$P_{ns1} := A_{cs1} \cdot \min\left(0.85 f'_c, f_{cus1}\right) \quad P_{ns1} = 664.096 \cdot kip$ Eq. 5.6.3.3.4-1

Note that longitudinal bar 1 passes through node 1.

$P_{r1} := \phi_{stm} \cdot P_{ns1}$ $P_{r1} = 464.867 \cdot kip$ Eq. 5.6.3.2-1

$F_{strut7} := 90kip$ Force directed through strut 7.

$F_{s1} := \frac{P - F_{strut7} \cdot \cos(45deg)}{\cos(a_1)}$ $F_{s1} = 455.574 \cdot kip$ Compressive force in strut s1.

$0.85 \cdot \phi_{stm} \cdot f'_c \cdot A_{cs1} - F_{s1} = 19.065 \cdot kip$ If positive, then node is O.K.

$check\_s1 := P_{r1} - F_{s1}$ $check\_s1 = 9.293 \cdot kip$ $check\_s1 > 0 = 1$

If the above value is less than zero then the compressive force in strut is higher than the capacity of the strut and the design needs to be adjusted

Step 3.) Compute and check strut s2 according to AASHTO (2014) Sec. 5.6.3.3

Vertical Distance Between Node 2 and 3 $L_{p23} := 12.5in$

Horizontal Distance between Node 2 and 3 $L_{w23} := 10.0in$

$\varepsilon_{s2} := 0.002$ Tensile strain in the concrete in the direction of the tension tie (in./in.)

$L_{s2} := \left(L_{w23}^2 + L_{p23}^2\right)^{\frac{1}{2}} = 16.008 \cdot in$ Length of compression strut s2.

$a_2 := \operatorname{atan}\left(\frac{L_{p23}}{L_{w23}}\right) \cdot rad$ $a_2 = 51.34 \cdot deg$ Angle of strut one measured to the horizontal.

$h_{a2} := 2 \cdot 6 \cdot \left(\frac{6}{8}\right) in$ AASHTO (2014) Figure 5.6.3.3.2-1a with s=0 (only 1 bar present).

$l_{a2s} := h_{a2} \cdot \sin(a_2)$ $l_{a2s} = 7.028 \cdot in$ Width of strut 2 on node 3 side

$l_{a2t} := 4.32in \cdot 2$ $l_{a2t} = 8.64 \cdot in$ Width of strut 2 on node 2 side

$A_{cs2} := \min(l_{a2s} \cdot b, l_{a2t} \cdot b)$ $A_{cs2} = 112.445 \cdot in^2$ Approximation of the effective area of strut s1.

$\varepsilon_{1s2} := \varepsilon_{s2} + (\varepsilon_{s2} + 0.002) \cdot \cot(a_2)^2$ Eq. 5.6.3.3.3-2

$f_{cus2} := \left| \frac{f'_c}{(0.8 + 170 \cdot \varepsilon_{1s2})} \right|$ $f_{cus2} = 3.492 \cdot ksi$ Eq. 5.6.3.3.3-1

$0.85 f'_c = 4.675 \cdot ksi$ Maximum value for fcu. Eq. 5.6.3.3.3-1

$f_{cus2} < 0.85f'_c$ OK

$P_{ns2} := A_{cs2} \cdot \min\left(0.85f'_c, f_{cus2}\right)$ $P_{ns2} = 392.616 \cdot kip$ Eq. 5.6.3.3.4-1

Note that longitudinal bar 1 passes through node 3.

$P_{r2} := \phi_{stm} \cdot P_{ns2}$ $P_{r2} = 274.831 \cdot kip$ Eq. 5.6.3.2-1

$F_{s2} := 86.143kip$ Compressive force in strut s2.

$0.65 \cdot \phi_{stm} \cdot f'_c \cdot A_{cs2} - F_{s2} = 195.251 \cdot kip$ If positive, then node is O.K.

$check\_s2 := P_{r2} - F_{s2}$ $check\_s2 = 188.688 \cdot kip$ $check\_s2 > 0 = 1$

If the above value is less than zero then the compressive force in strut is higher than the capacity of the strut and the design needs to be adjusted

Step 4.) Compute the required amount of reinforcing steel for longitudinal bar 1 at n3 to AASHTO (2014) Sec. 5.6.3.4

From node 3 to 1:

$F_{ll1.31} := F_{s1} \cdot \sin\left(a_1\right) - F_{strut7} \cdot \cos(45deg)$ $F_{ll1.31} = 67.269 \cdot kip$ Tension force in longitudinal bar 1.

$A_{ll1.31} := \dfrac{F_{ll1.31}}{\phi_n \cdot f_y}$ $A_{ll1.31} = 1.246 \cdot in^2$ Required area of reinforcement for longitudinal bar 1

$n_{ll1.31} := \dfrac{A_{ll1.31}}{0.44in^2}$ $n_{ll1.31} = 2.831$ Required number of #6 bars for longitudinal bar 1.

3 #6 bars are req. for longitudinal bar 1 - CONTROLS

From node 3 to 4:

$F_{ll1.34} := F_{ll1.31} \cdot \dfrac{\cos\left(a_2\right)}{\sin\left(a_2\right)}$ $F_{ll1.34} = 53.815 \cdot kip$ Tension force in longitudinal bar 1.

$A_{ll1.34} := \dfrac{F_{ll1.34}}{\phi_n \cdot f_y}$ $A_{ll1.34} = 0.997 \cdot in^2$ Required area of reinforcement for longitudinal bar 1

$n_{ll1.34} := \dfrac{A_{ll1.34}}{0.44in^2}$ $n_{ll1.34} = 2.265$ Required number of #6 bars for longitudinal bar 1.

3 #6 bars are req. for longitudinal bar 1

Step 5.) Compute and check strut s3 according to AASHTO (2014) Sec. 5.6.3.3

Vertical Distance Between Node 2 and 4 $L_{p24} := 12.5in$

Horizontal Distance between Node 2 and 4 $L_{w24} := 12.0in$

$\varepsilon_{s3} := 0.002$ Tensile strain in the concrete in the direction of the tension tie (in./in.)

$L_{s3} := \left(L_{w24}^{2} + L_{p24}^{2}\right)^{\frac{1}{2}} = 17.328 \cdot in$ Length of compression strut s3.

$a_3 := \operatorname{atan}\left(\frac{L_{p24}}{L_{w24}}\right) \cdot rad$ $a_3 = 46.169 \cdot deg$ Angle of strut three measured to the horizontal.

AASHTO (2014) Figure 5.6.3.3.2-1

$l_{a3t} := 16.03in$ Width of strut 3 on Node 2 side (compression node)

$l_{a4t} := (0.625in \cdot 2 \cdot 6 + 4.25in)$ $l_{a4t} = 11.75 \cdot in$ Width of strut 3 on Node 4 side

$A_{cs3} := \min\left(l_{a3t} \cdot b \cdot \sin\left(a_3\right), l_{a4t} \cdot b \cdot \sin\left(a_3\right)\right)$ Approximation of the effective area of strut s3

$A_{cs3} = 135.621 \cdot in^{2}$

$\varepsilon_{1s3} := \varepsilon_{s3} + \left(\varepsilon_{s3} + 0.002\right) \cdot \cot\left(a_3\right)^{2}$ Eq. 5.6.3.3.3-2

$f_{cus3} := \left[\frac{f'_c}{\left(0.8 + 170 \cdot \varepsilon_{1s3}\right)}\right]$ $f_{cus3} = 3.113 \cdot ksi$ Eq. 5.6.3.3.3-1

$0.85 f'_c = 4.675 \cdot ksi$ Maximum value for fcu. Eq. 5.6.3.3.3-1

$P_{ns3} := A_{cs3} \cdot \min\left(0.85 f'_c, f_{cus3}\right)$ $P_{ns3} = 422.211 \cdot kip$ Eq. 5.6.3.3.4-1

Note that longitudinal bar 2 passes through node 3, 5, & subsequent bottom nodes.

$P_{r3} := \phi_{stm} \cdot P_{ns3}$ $P_{r3} = 295.547 \cdot kip$ Eq. 5.6.3.2-1

$F_{s3} := 257.327kip$ Compressive force in strut s3

$0.75 \cdot \phi_{stm} \cdot f'_c \cdot A_{cs3} - F_{s3} = 134.278 \cdot kip$ If positive, then node is O.K.

$check\_s3 := P_{r3} - F_{s3}$ $check\_s3 = 38.22 \cdot kip$ $check\_s3 > 0 = 1$

If the above value is less than zero then the compressive force in strut is higher than the capacity of the strut and the design needs to be adjusted

Step 6.) Compute and check strut s4 according to AASHTO (2014) Sec. 5.6.3.3

Vertical Distance Between Node 2 and 5. $L_{p25} := 2.0in$

Horizontal Distance between Node 2 and 5. $L_{w25} := 12.0in$

$\varepsilon_{s4} := 0.002$ Tensile strain in the concrete in the direction of the tension tie (in./in.)

$L_{s4} := \left(L_{w25}^{2} + L_{p25}^{2}\right)^{\frac{1}{2}} = 12.166 \cdot in$ Length of compression strut s4.

$a_4 := \operatorname{atan}\left(\frac{L_{p25}}{L_{w25}}\right) \cdot rad$ $a_4 = 9.462 \cdot deg$ Angle of strut four measured to the horizontal.

AASHTO (2014) Figure 5.6.3.3.2-1

$l_{a5t} := 4.57in \cdot 2$ $l_{a5t} = 9.14 \cdot in$ Width of strut 4 on Node 2 side (compression node)

$l_{a6t} := 3.31in \cdot 2$ $l_{a6t} = 6.62 \cdot in$ Width of strut 2 on Node 5 side (2.0in cover)

$A_{cs4} := \min\left(l_{a5t} \cdot b, l_{a6t} \cdot b\right)$ Approximation of the effective area of strut s4.

$A_{cs4} = 105.92 \cdot in^2$

$\varepsilon_{1s4} := \varepsilon_{s4} + \left(\varepsilon_{s4} + 0.002\right) \cdot \cot\left(90deg - a_4\right)^2$ Eq. 5.6.3.3.3-2

$f_{cus4} := \left[\frac{f'_c}{\left(0.8 + 170 \cdot \varepsilon_{1s4}\right)}\right]$ $f_{cus4} = 4.746 \cdot ksi$ Eq. 5.6.3.3.3-1

$0.85f'_c = 4.675 \cdot ksi$ Maximum value for fcu. Eq. 5.6.3.3.3-1

$P_{ns4} := A_{cs4} \cdot \min\left(0.85f'_c, f_{cus4}\right)$ $P_{ns4} = 495.176 \cdot kip$ Eq. 5.6.3.3.4-1

Note that longitudinal bar 2 passes through node 3, and 5.

$P_{r4} := \phi_{stm} \cdot P_{ns4}$ $P_{r4} = 346.623 \cdot kip$ Eq. 5.6.3.2-1

$F_{s4} := 316.269kip$ Compressive force in strut s4.

$0.85 \cdot \phi_{stm} \cdot f'_c \cdot A_{cs4} - F_{s4} = 30.354 \cdot kip$ If positive, then node is O.K.

$check\_s4 := P_{r4} - F_{s4}$ $check\_s4 = 30.354 \cdot kip$ $check\_s4 > 0 = 1$

If the above value is less than zero then the compressive force in strut is higher than the capacity of the strut and the design needs to be adjusted

Step 7.) Compute and check strut s5 according to AASHTO (2014) Sec. 5.6.3.3

Vertical Distance Between Node 5 and 6 $L_{p56} := 14.5in$

Horizontal Distance between Node 5 and 6 struts $L_{w56} := 10in$

$\varepsilon_{s5} := 0.002$ Tensile strain in the concrete in the direction of the tension tie (in./in.)

$L_{s5} := \left(L_{w56}^{2} + L_{p56}^{2}\right)^{\frac{1}{2}} = 17.614 \cdot in$ Length of compression strut s5.

$a_5 := \operatorname{atan}\left(\frac{L_{p56}}{L_{w56}}\right) \cdot rad \qquad a_5 = 55.408 \cdot deg$ Angle of strut five measured to the horizontal.

AASHTO (2014) Figure 5.6.3.3.2-1

$l_{a7t} := (0.625in \cdot 2 \cdot 6) + \frac{0.625in}{2} \qquad l_{a7t} = 7.813 \cdot in$ Width of strut 5 on Node 5 side

$l_{a8t} := (0.625in \cdot 2 \cdot 6) + 0.625\frac{in}{2} \qquad l_{a8t} = 7.813 \cdot in$ Width of strut 5 on Node 6 side

$A_{cs5} := \min\left(l_{a7t} \cdot b \cdot \sin\left(a_5\right), l_{a8t} \cdot b \cdot \sin\left(a_5\right)\right) \cdot 1.35$ Approximation of the effective area of strut s5.

$A_{cs5} = 138.917 \cdot in^2$

$\varepsilon_{1s5} := \varepsilon_{s5} + \left(\varepsilon_{s5} + 0.002\right) \cdot \cot\left(90deg - a_5\right)^2$ Eq. 5.6.3.3.3-2

$f_{cus5} := \left[\frac{f'_c}{\left(0.8 + 170 \cdot \varepsilon_{1s5}\right)}\right] \qquad f_{cus5} = 2.14 \cdot ksi$ Eq. 5.6.3.3.3-1

$0.85f'_c = 4.675 \cdot ksi$ Maximum value for fcu. Eq. 5.6.3.3.3-1

$P_{ns5} := A_{cs5} \cdot \min\left(0.85f'_c, f_{cus5}\right) \qquad P_{ns5} = 297.328 \cdot kip$ Eq. 5.6.3.3.4-1

Note that longitudinal bar 2 passes through node 3, and 5.

$P_{r5} := \phi_{stm} \cdot P_{ns5} \qquad P_{r5} = 208.13 \cdot kip$ Eq. 5.6.3.2-1

$F_{s5} := 201.269kip$ Compressive force in strut s5.

$0.75 \cdot \phi_{stm} \cdot f'_c \cdot A_{cs5} - F_{s5} = 199.854 \cdot kip$ If positive, then node is O.K.

$check\_s5 := P_{r5} - F_{s5} \qquad check\_s5 = 6.861 \cdot kip \qquad check\_s5 > 0 = 1$

If the above value is less than zero then the compressive force in strut is higher than the capacity of the strut and the design needs to be adjusted

Step 8.) Compute the required amount of reinforcing steel for tie 1 to AASHTO (2014) Sec. 5.6.3.4

$F_{t1} := 96.78kip$ Tension force in tie 1

$A_{t1} := \frac{F_{t1}}{\phi_n \cdot f_y}$ $A_{t1} = 1.792 \cdot in^2$ Required area of reinforcement for tie 1

$n_{t1} := \frac{A_{t1}}{2 \cdot 0.20in^2}$ $n_{t1} = 4.481$ Required number of #4 stirrups for tie 1.

5 #4 stirrups will be used for tie 1

Step 9.) Compute the required amount of reinforcing steel for tie 2 to AASHTO (2014) Sec. 5.6.3.4

$F_{t2} := 165.688kip$ Tension force in tie 2

$A_{t2} := \frac{F_{t2}}{\phi_n \cdot f_y} = 3.068 \cdot in^2$ Required area of reinforcement for tie 2

$n_{t2} := \frac{A_{t2}}{2 \cdot 0.20in^2}$ $n_{t2} = 7.671$ Required number of #4 stirrups for tie 2.

8 #4 stirrups will be used for tie 1

Step 10.) Compute and check strut s6 according to AASHTO (2014) Sec. 5.6.3.3

Vertical Distance Between Node 7 and 8 $L_{p78} := 6.0in$

Horizontal Distance between Node 7 and 8 struts $L_{w78} := 5.24in$

$\varepsilon_{s6} := 0.002$ Tensile strain in the concrete in the direction of the tension tie (in./in.)

$L_{s6} := \left(L_{w78}^2 + L_{p78}^2\right)^{\frac{1}{2}} = 7.966 \cdot in$ Length of compression strut s6.

$a_6 := \operatorname{atan}\left(\frac{L_{p78}}{L_{w78}}\right) \cdot rad$ $a_6 = 48.868 \cdot deg$ Angle of strut six measured to the horizontal.

AASHTO (2014) Figure 5.6.3.3.2-1

$l_{a9t} := (0.625in \cdot 2 \cdot 6)$ $l_{a9t} = 7.5 \cdot in$ Width of strut 6 on Node 7 side

$l_{a10t} := (0.625in \cdot 2 \cdot 6)$ $l_{a10t} = 7.5 \cdot in$ Width of strut 6 on Node 8 side

$A_{cs6} := \min\left(l_{a9t} \cdot b \cdot \sin\left(a_6\right), l_{a10t} \cdot b \cdot \sin\left(a_6\right)\right)$ Approximation of the effective area of strut s6.

$A_{cs6} = 90.384 \cdot in^2$

$\varepsilon_{1s6} := \varepsilon_{s6} + \left(\varepsilon_{s6} + 0.002\right) \cdot \cot\left(90deg - a_6\right)^2$ Eq. 5.6.3.3.3-2

$f_{cus6} := \left[\frac{f'_c}{\left(0.8 + 170 \cdot \varepsilon_{1s6}\right)}\right]$ $f_{cus6} = 2.707 \cdot ksi$ Eq. 5.6.3.3.3-1

$0.85f'_c = 4.675 \cdot ksi$ Maximum value for fcu. Eq. 5.6.3.3.3-1

$P_{ns6} := A_{cs6} \cdot \min\left(0.85f'_c, f_{cus6}\right)$ $P_{ns6} = 244.695 \cdot kip$ Eq. 5.6.3.3.4-1

$P_{r6} := \phi_{stm} \cdot P_{ns6}$ $P_{r6} = 171.286 \cdot kip$ Eq. 5.6.3.2-1

$F_{s6} := 76.6kip$ Compressive force in strut s6.

$0.75 \cdot \phi_{stm} \cdot f'_c \cdot A_{cs6} - F_{s6} = 184.383 \cdot kip$ If positive, then node is O.K.

$check\_s6 := P_{r6} - F_{s6}$ $check\_s6 = 94.686 \cdot kip$ $check\_s6 > 0 = 1$

If the above value is less than zero then the compressive force in strut is higher than the capacity of the strut and the design needs to be adjusted

Step 11.) Compute and check strut s7 according to AASHTO (2014) Sec. 5.6.3.3

Vertical Distance Between Node 1 and 9 $L_{p19} := 10.0in$

Horizontal Distance between Node 1 and 9 $L_{w19} := 10.0in$

$\varepsilon_{s7} := 0.002$ Tensile strain in the concrete in the direction of the tension tie (in./in.)

$L_{s7} := \left(L_{w19}^2 + L_{p19}^2\right)^{\frac{1}{2}} = 14.142 \cdot in$ Length of compression strut s7.

$a_7 := \operatorname{atan}\left(\frac{L_{p19}}{L_{w19}}\right) \cdot rad$ $a_7 = 45 \cdot deg$ Angle of strut seven measured to the horizontal.

AASHTO (2014) Figure 5.6.3.3.2-1

$l_{a11t} := l_{b1}\cdot\sin(a_7) + h_{a1}\cdot\cos(a_7)$ $l_{a11t} = 8.48\cdot in$ Width of strut 7 on Node 1 side

$l_{a12t} := (0.625in\cdot 2\cdot 6)$ $l_{a12t} = 7.5\cdot in$ Width of strut 7 on Node 9 side

$A_{cs7} := \min(l_{a11t}\cdot b\cdot\sin(a_7), l_{a12t}\cdot b\cdot\sin(a_7))$ Approximation of the effective area of strut s7.

$A_{cs7} = 84.853\cdot in^2$

$\varepsilon_{1s7} := \varepsilon_{s7} + (\varepsilon_{s7} + 0.002)\cdot\cot(90deg - a_7)^2$ Eq. 5.6.3.3.3-2

$f_{cus7} := \left[\frac{f'_c}{(0.8 + 170\cdot\varepsilon_{1s7})}\right]$ $f_{cus7} = 3.022\cdot ksi$ Eq. 5.6.3.3.3-1

$0.85f'_c = 4.675\cdot ksi$ Maximum value for fcu. Eq. 5.6.3.3.3-1

$P_{ns7} := A_{cs7}\cdot\min(0.85f'_c, f_{cus7})$ $P_{ns7} = 256.423\cdot kip$ Eq. 5.6.3.3.4-1

$P_{r7} := \phi_{stm}\cdot P_{ns7}$ $P_{r7} = 179.496\cdot kip$ Eq. 5.6.3.2-1

$F_{s7} := 90kip$ Compressive force in strut s5.

$0.75\cdot\phi_{stm}\cdot f'_c\cdot A_{cs7} - F_{s7} = 155.012\cdot kip$ If positive, then node is O.K.

$check\_s7 := P_{r7} - F_{s7}$ $check\_s7 = 89.496\cdot kip$ $check\_s7 > 0 = 1$

If the above value is less than zero then the compressive force in strut is higher than the capacity of the strut and the design needs to be adjusted

APPENDIX C

TEST SETUP OVERALL VIEWS

Test Setup – Facing North East

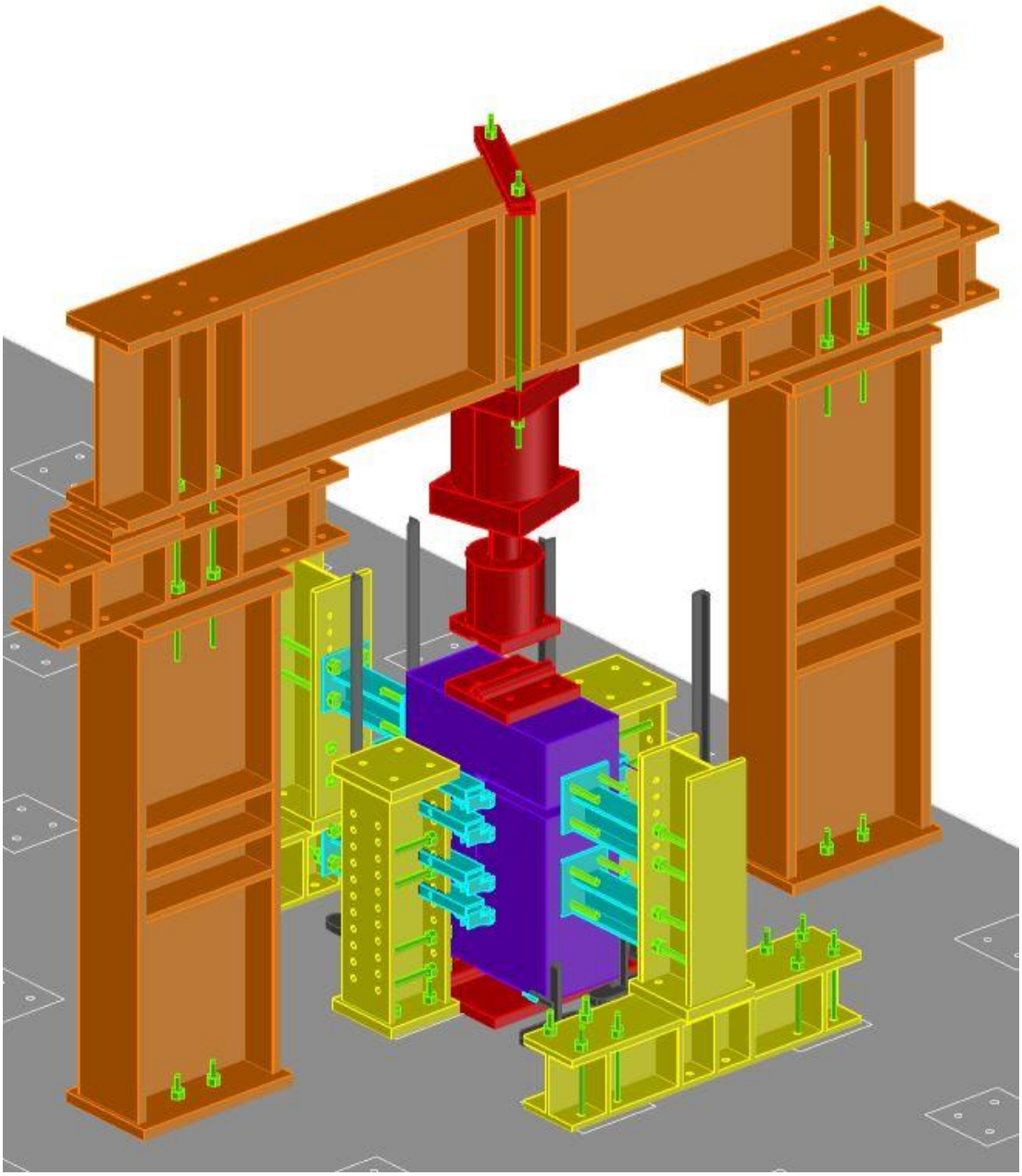

Test Setup – Facing North West

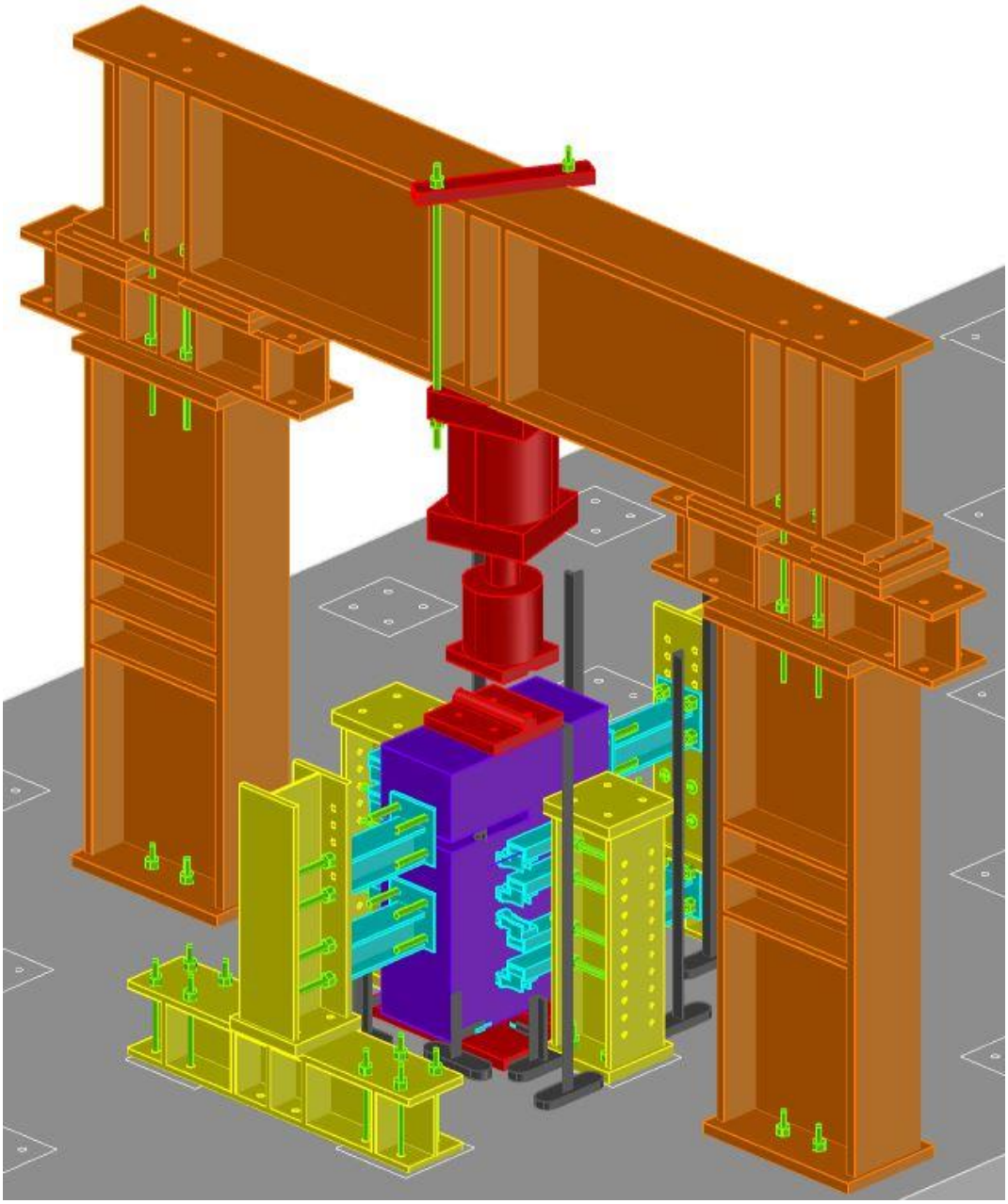

Test Setup – Facing South East

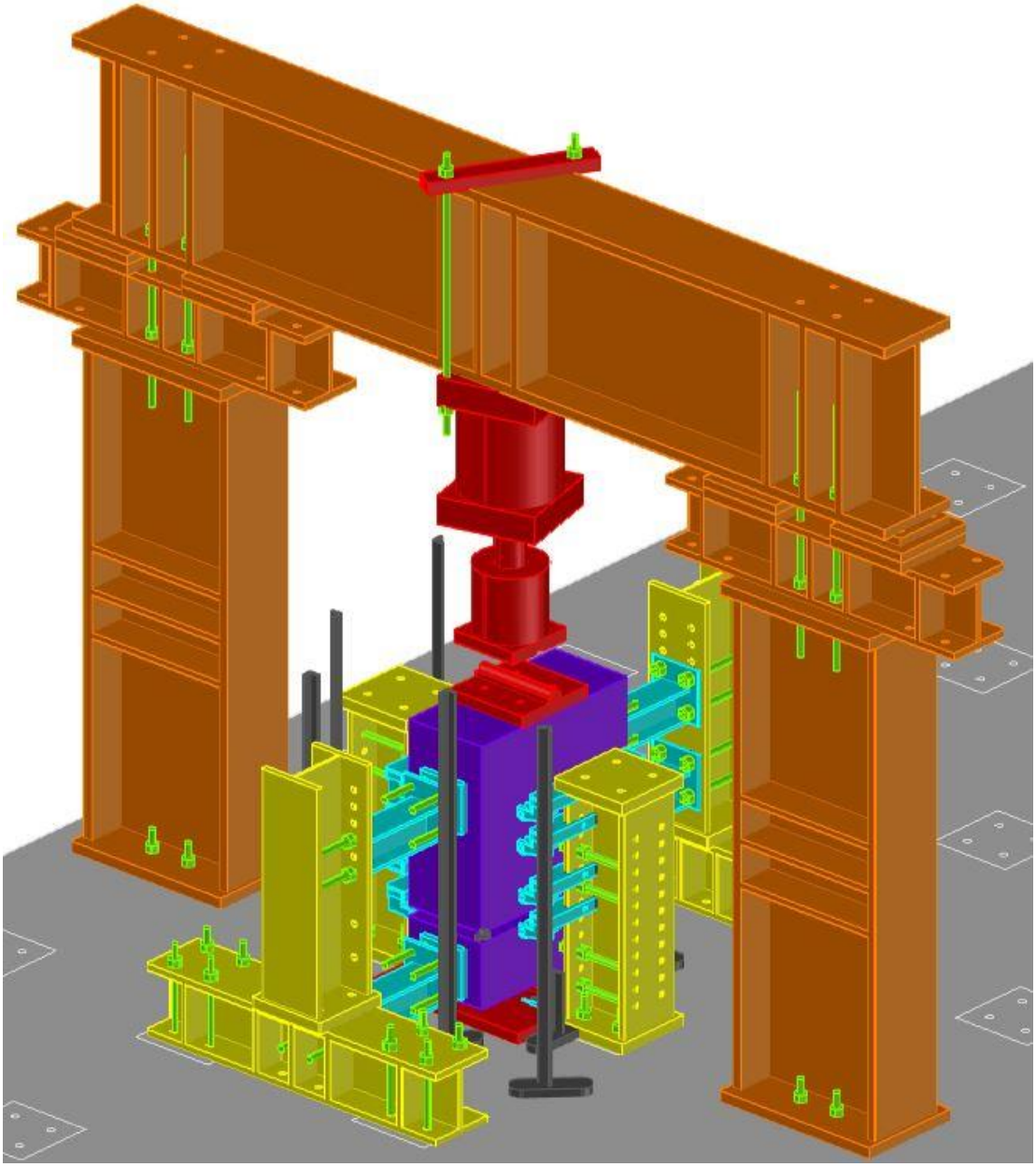

Test Setup – Facing South West

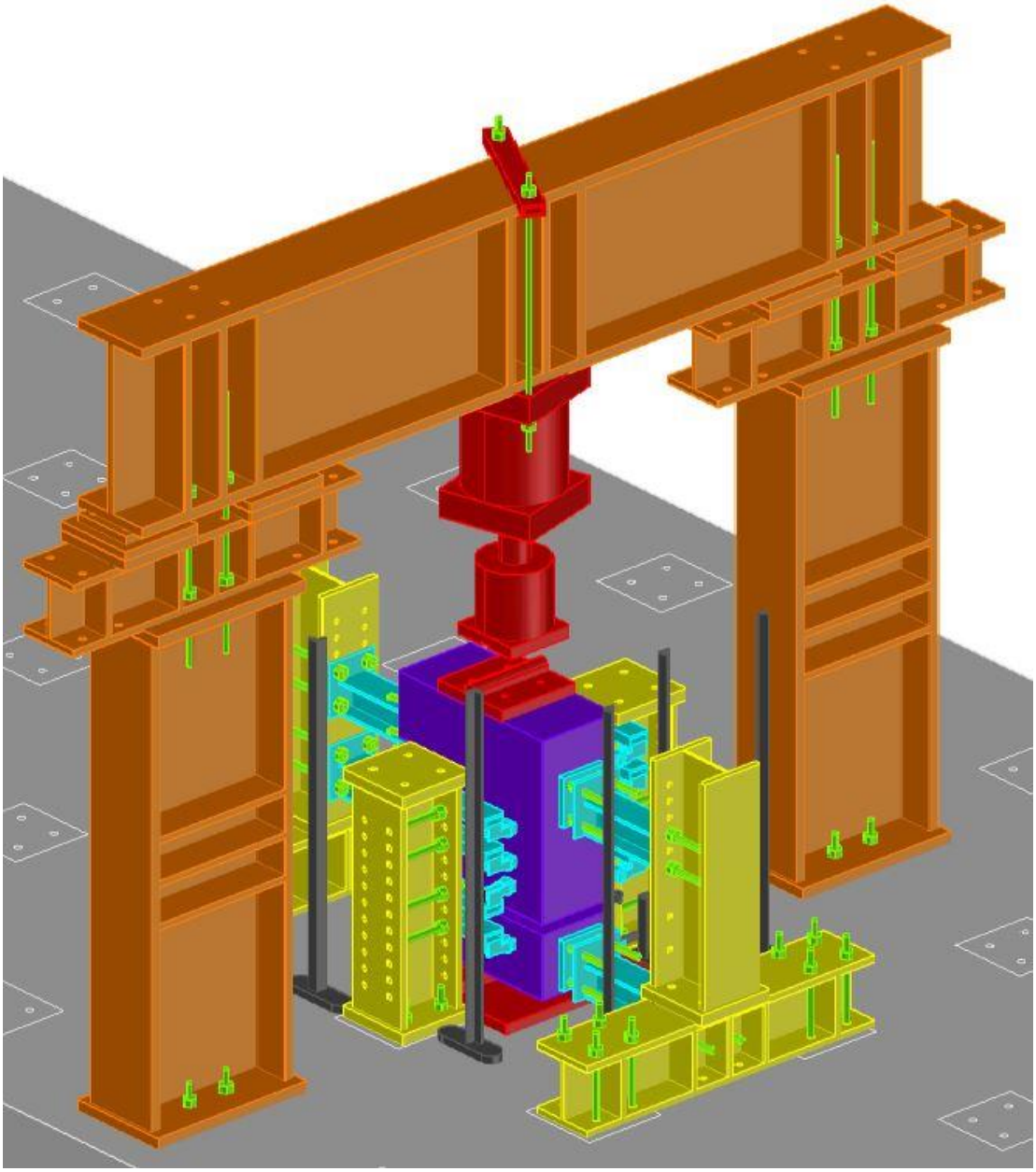

APPENDIX D

TESTING PARAMETERS

Testing Parameters

1. Initiation of cracking (Δ_{cr}, V_{cr})
2. Peak interface shear force, V_{ult}
3. Interface shear displacement at V_{ult}, Δ_{ult}
4. Minimum sustained interface shear force, $V_{sus,min}$
5. Maximum sustained interface shear force, $V_{sus,max}$
6. Interface shear force at first bar fracture, V_b
7. Interface shear displacement at V_b, Δ_b